Anthropogenic Fire and the Development of Neolithic Agricultural Landscapes: Connecting Archaeology, Paleoecology, and Fire Science to Evaluate Human Impacts on Fire Regimes

by

Grant Snitker

A Dissertation Presented in Partial Fulfillment
of the Requirements for the Degree
Doctor of Philosophy

Approved January 2019 by the
Graduate Supervisory Committee:

C. Michael Barton, Chair
Christopher Morehart
Janet Franklin

ARIZONA STATE UNIVERSITY

May 2019

ABSTRACT

The recent emergence of global ‘megafires’ has made it imperative to better understand the role of humans in altering the size, distribution, and seasonality of fires. The dynamic relationship between humans and fire is not a recent phenomenon; rather, fire has deep roots in our biological and cultural evolution. Because of its long-term perspective, archaeology is uniquely positioned to investigate the social and ecological drivers behind anthropogenic fire. However, the field faces challenges in creating solution-oriented research for managing fire in the future. In this dissertation, I originate new methods and approaches to archaeological data that enable us to interpret humans’ long-term influences on fire regimes. I weave together human niche construction theory and ecological resilience, creating connections between archaeology, paleoecology, and fire ecology. Three, stand-alone studies illustrate the usefulness of these methods and theories for charting changes in land-use, fire-regimes, and vegetation communities during the Neolithic Transition (7600 - 3800 cal. BP) in eastern Spain. In the first study (Ch. II), I analyze archaeological survey data using Bayesian methods to extract land-use intensities from mixed surface assemblages from a case study in the Canal de Navarrés. The second study (Ch. III) builds on the archaeological data collected computational model of landscape fire, charcoal dispersion, and deposition to test how multiple models of natural and anthropogenic fire activity contributed to the formation a single sedimentary charcoal dataset from the Canal de Navarrés. Finally, the third study (Ch. IV) incorporates the modeling and data generated in the previous chapters into sampling and analysis of sedimentary charcoal data from alluvial contexts in three study areas throughout eastern Spain. Results indicate that anthropogenic fire played a significant

role in the creation of agricultural landscapes during the Neolithic period, but sustained, low-intensity burning after the late Neolithic period maintained the human created niche for millennia beyond the arrival of agro-pastoral land-use. With global fire activity on the rise, it is vital to incorporate perspectives on the origins, development, and maintenance of human-fire relationships to effectively manage fire in today's coupled social-ecological landscapes.

ACKNOWLEDGMENTS

Many people have supported me during graduate school and the development of this dissertation research. First, I thank the chair of my dissertation committee, Michael Barton. Michael has been a constant source of support and enthusiasm for my ideas, plans, and passions. He also shares an appreciation for good brandy, which has facilitated many a productive late-night conversation during fieldwork in Spain. Michael continues to inspire me to dream 'big' in my research plans for the future. I am also very appreciative of Chris Morehart and Janet Franklin for their support as members of my committee. Chris generously provided me space in his ethnobiology lab to develop and conduct the analyses presented in this dissertation. Janet acted as my sounding board as I developed many of the concepts and coding decisions in the CharRec model—supporting me as I dove deeply into the world of fire ecology.

None of the work presented in this dissertation would have been possible without the generosity of my friends and fellow researchers at the Universitat de València. I am grateful for Agustín Diez Castillo, Oreto García Puchol, and Joan Bernabeu Auba for their willingness to host me in the field during four field seasons in València and during my residency during the Fall of 2017. Agustin, Oreto, and Joan are always willing collaborators, thoughtful teachers, and dear friends. I also thank Alfredo Cortell Nicolau, Salva Pardo-Gordo, Pilar Escriba, Paloma Vidal Matutano, and Joaquin Jimenez—my fellow PhD students and post-docs in Valencia. I will never forget the many laughter-filled evenings over cremaets in the little bars and cafes throughout Navarrés, Yátova, Dos Aguas, and València.

Many others have lent me support over the years. I am thankful for the SHESC archaeology and museum studies faculty who have provided me with opportunities to develop and grow as a scholar. Specifically, I extend my gratitude to Frank McManamon, Colleen Strawhacker, Ann Kinzig, Keith Kintigh, Peter Toon, Michelle Hegmon, Peggy Nelson, and Kostalena Michelaki for being advocates for both me and my research. Outside of ASU, I have encountered many generous archaeologists willing to invest their time and energy into helping me develop as a researcher. I would like to thank Marcos Llobera and Ben Fitzhugh for giving me a home away from home while I was in residency at the University of Washington in Seattle. Much of my work would not have been possible without the support of my Forest Service colleagues in Arizona and Washington who gave me the flexibility to leave for extended fieldwork trips to Spain in the middle of our survey season. I am particularly grateful for Mark Swift, Heather Davis, and Pete Cadena who also gave me the opportunity to pursue training as a fireline archaeologist on wildfires. Finally, I would not be the person or archaeologist I am today without the thoughtful guidance and long-lasting friendship of Dennis Jenkins at the University of Oregon. Dennis brought me on as a freshman field school student and has continued to support me and my endeavors in the years since.

I also thank my friends for their unwavering support. Together we have celebrated many good times and you have been a comfort to me during some of the worst. I am lucky to have journeyed through graduate school with Claudine Gravel-Miguel, Chris Caseldine, Sarah Klassen, and Tim Dennehy. I also thank Sean Bergin and Jon Paige for always being willing to take a break and play Nintendo 64 in the lab at the end of a long semester. Kent Simer, Taylor and Anne Vos (plus baby Arie and his little Silvie, who was

born on the morning of my defense), Scott Saline, Nohemi Montano, Mark Vetto, and Jessica Johnson brought me into their community and made me feel like I was not only family, but a native Arizonan.

I thank my family for their patience, support, and for never questioning why I wanted to be an archaeologist. I thank my mother, Holly, and father, Craig, for their love, sacrifice, and encouragement which enabled me to follow my passions. Mom, you gave everything that you could to help us succeed. There was love and selflessness behind your every action. None of this would be possible without you. I thank all of brothers and sisters including Giegs, Hassan, Adam, Emily, Kurt, Katie, and Luke, for camping trips, fly-fishing, and all of our adventures. Steve and Genelle, I cannot thank you enough for your support and for truly welcoming me as a member of your family. Most importantly, I thank my wife and partner, Kerice. You are my constant source of strength and encouragement. You inspire me to live fully (and feast!) through your incredible love and generosity. Thank you, dear.

This work was generously funded by the National Science Foundation (NSF) Dissertation Improvement Grant (Award # 1656342) and the NSF Coupled Natural and Human Systems Grant (Award # 1313727). Other support was provided through the NSF Graduate Research Fellowship (GRFP), the Arizona Archaeological and Historical Society Research Grant, ASU Graduate and Professional Student Association Travel and Research grants, the ASU Graduate Education Research Support Program Grant, ASU School of Human Evolution and Social Change Travel and Research grants, the Association for Fire Ecology TREE Grant, and the ASU School of Human Evolution and Social Change Dissertation Completion Fellowship.

TABLE OF CONTENTS

APPENDIX Page

LIST OF TABLES

Table Page

Table Page

LIST OF FIGURES

Figure Page

Figure Page

Figure Page

Figure Page

Figure Page

CHAPTER I

INTRODUCTION

As the scientific community grapples with our conception of the *Anthropocene* and the lasting impact humans have made on earth's systems, there is an emerging and urgent need to understand the origins and development of social-ecological systems and how they differ from natural processes (Braje, 2015; Chin et al., 2013; Smith and Zeder, 2013). Fire is one such topic that demands attention both as a product of our warming planet and as a process deeply related to human biological and cultural relationships with the environment (Glikson, 2013). Humans have intentionally set fires for millennia to transform the arrangement and diversity of resources within their landscapes, with long-term influences on global terrestrial and atmospheric systems (Boivin et al., 2016; Pyne, 2012, 1998; Pyne and Goldammer, 1997; Roos et al., 2014). Differentiation between natural and anthropogenic fire has long been debated, but it remains relatively poorly understood in the historical and ecological sciences (Bowman et al., 2009). Understanding the degree to which anthropogenic fire regimes have shaped ecological systems in the past, as well as the global diversity of culturally framed uses of fire, has significant implications for managing fire in today's social ecological systems (Bowman et al., 2011; Jackson and Hobbs, 2009; Pyne, 1997).

Archaeology is uniquely positioned to investigate anthropogenic fire in the past, while also offering perspectives on how future fire-human relationships may develop. As an example, prehistoric transitions to agriculture often coincided with increases in fire

frequency and changes in vegetation community composition and distribution (Ellis et al., 2010; Pyne, 1998). Archaeological research focused on this phenomenon can incorporate the spatial and temporal dimensions of anthropogenic fire with the dynamics of land-use change to inform discussions of the development and future maintenance of agricultural landscapes.

To this end, this dissertation integrates new field and laboratory methods, quantitative models of wildfire and its ecological effects, and an "off-site" archaeological perspective to study the impacts of anthropogenic fire on landscape dynamics and human socio-ecological systems during the Neolithic period (7600 – 3800 BP) in eastern Spain. This research is guided by three principal goals: 1) to identify the spatial and temporal attributes of Neolithic anthropogenic fire regimes from alluvial sedimentary charcoal records, 2) to determine spatial scale and intensity of land-use during the Neolithic period and assess how it may have related to anthropogenic burning practices, 3) to evaluate the role of anthropogenic fire during the Neolithic in the long-term development of agricultural landscapes. Through this work, I demonstrate how archaeology provides a unique perspective on the human dimensions of fire in the past and can help shape our understanding of the long-term role of human-fire relationships in fire-prone landscapes.

Much like an edited volume, this dissertation is composed of three, stand-alone research papers, which are organized as chapters and tied together by the research goals outlined above. As an introduction to these studies, in the following sections I outline the conceptual framework that guided their development, provide a brief summary of each study and its results, and describe how this work advances archaeological theories and methodologies for investigating long-term anthropogenic fire regimes. The studies

included in this dissertation have benefited from collaborations with colleagues at Arizona State University and the University of Valencia, as well as funding from the NSF-supported interdisciplinary Mediterranean Landscape Dynamics (MedLanD) Project. For this reason, several collaborators are listed as co-authors for Chapter III. Information about the publication status of each of chapter and the permission for use of published materials by all co-authors is included in Appendix VII.

Conceptual Framework Directing this Dissertation

Archaeological interest in anthropogenic fire has a long history in human-environmental research but has not benefited from specific theory-building. Research has focused on detecting signatures of anthropogenic burning in the past but often does not substantially engage with the long-term processes that constitute a human-fire relationship (Roos et al., 2014). With global fire activity on the rise, it is increasing necessary to understand the origins and development of human-fire relationships in order to effectively manage fire in today's coupled social-ecological landscapes. Given the ways human have impacted fire in the past, several key interdisciplinary concepts are the foundation for how I approach anthropogenic fire as an archaeologist.

Human niche construction and anthropogenic fire

Niche construction theory provides a framework to understand the bi-directional feedbacks between an organism and its environment. This paradigm emphasizes an organism's capacity to modify its environment and thus influence the drivers of natural

selection affecting itself and subsequent generations (Odling-Smee et al., 2003, 1996). Humans are extremely effective niche-constructing organisms and, unlike other niche-constructing organisms, use cultural practices to pass information regarding the environment to subsequent generations (Laland and O'Brien, 2012). Human niche construction (HNC) emphasizes the interconnection between 1) the evolution of environments created through human action, 2) an altered environment's impact on the evolution of both humans and all other organisms within the ecosystem, and 3) the evolution of cultural practices in response to changing ecological conditions. HNC provides basic insights into long-term human-fire relationships, but it falls short of explaining how or why humans might maintain a niche through fire, or what the cascading effects on the landscape may be if that niche is eventually abandoned.

Ecological resilience to understand landscape change

Ecological resilience describes an ecosystem's capacity to recover from perturbations (Holling, 1973). Although resilience theory can be used in the social sciences to explain many cultural processes, here I refer to resilience in its original ecological sense, especially in respect to an ecosystem's response to fire. In the context of fire, vegetation communities demonstrating a high degree of resilience maintain overall species composition and structure in the context of a consistent fire regime. A repeated change in the frequency, size, or seasonality of fire, such as the introduction of anthropogenic fire, may create conditions that extend beyond a vegetation community's resilience, attracting the system toward a transition into an alternative, stability domain Ecological resilience contributes a framework for understanding how HNC can transform

a landscape, while also suggesting that subsequent landscape maintenance must be performed in order to sustain a newly created human niche.

Connecting fire ecology to human behaviors in the past

Finally, interconnecting the principles of fire ecology and vegetation dynamics with archaeological approaches provides an enhanced framework to understand anthropogenic fire as a niche-constructing behavior. The fire regime is a central concept in fire ecology and describes the long-term role of the frequency, type, intensity, extent, and seasonality of fire disturbances within the ecology of a particular landscape (Keeley et al., 2012; Whelan, 1995; Whitlock et al., 2010). Fire regimes operate at multiple spatial and temporal scales and are the basis for interpreting how fire activity varies through time due to changes in climate, fuels, or ignition sources. Fire regimes also describe the potential impact of HNC on an ecosystem's response to long-term, iterative fire disturbances. Whitlock and colleagues suggest that prehistoric human land-use altered the sources and patterns of fires, often causing a "synchrony between fire ignitions, fire-weather and fuel conditions in time and space" (2010:15). During the Neolithic transition in the Western Mediterranean, HNC likely influenced the arrangement of fuels, ignition sources, and consequently local and regional fire regimes (Carrión et al., 2010; Vanniere et al., 2011).

In Mediterranean ecosystems, fire has a diverse set of influences on the evolutionary dynamics of vegetation communities and life history of individual species (Keeley et al., 2012; Moreno and Oechel, 1994). Plant species have evolved multiple strategies for coping with fire disturbance, including protective bark, post fire seed

dispersal, or re-sprouting (Pausas, 1999a; Pausas and Keeley, 2009). These strategies are influential drivers in vegetation succession, a process that shapes vegetation community structure and composition after a fire disturbance. Untangling the complex relationship between anthropogenic ecosystem disturbances and vegetation responses is integral to tracking the timing, extent, and nature of vegetation changes during the Neolithic period and the emergence of agricultural landscapes.

Data challenges facing an integrated approach to anthropogenic fire

By integrating these three concepts, I have created a theoretical framework that focuses on the social and ecological dynamics of creating, maintaining, and abandoning human-fire relationships over the long-term. These processes occur over multiple spatial and temporal scales, impacting local and regional fire regimes. This framework has been instrumental in how I developed my research questions, methods, and field sites over the last several years. But finding the right evidence to validate an integrated approach to human-fire relationships can be challenging using traditional archaeological and paleoecological data sources.

Connecting archaeological information on settlement pattern and land-use with paleoecological evidence for fire and vegetation change remains one of the biggest challenges limiting current research on long-term human-fire relationships. Often there is a mismatch of spatial scales between archaeological data and paleoenvironmental data. Landscape-scale survey data is not easily compared to pollen and charcoal data from a single terrestrial core. The temporal scales of archaeological periods, traditions, or cultures are too broad to adequately evaluate anthropogenic impacts on the year-by-year

variation in charcoal accumulation often seen in laminated lake core sequences. To compound these issues, both archaeological and paleoecological data are incomplete proxies because they are subject to degradation and taphonomic processes that make them difficult to identify and interpret. Finally, current paleoecological methods do not easily distinguish anthropogenic fire and landscape change from variation in natural fire regimes due to climate. Ultimately, new archaeological methods are needed to accommodate for these challenges.

The three stand-alone research papers that compose this dissertation attempt to resolve these issues by reevaluating the how archaeological and paleoecological data are collected and analyzed in the context of anthropogenic fire. The following chapters employ new techniques in archaeological survey and analysis, reinterpret previously published proxy data with the help of computational and agent-based models, and use watersheds as an analytical unit to evaluate the role of fire and land-use intensity in HNC at the same spatial scale. These new strategies for understanding long-term anthropogenic fire provide multiple avenues for expansion or redevelopment of traditional approaches to archaeological and paleoecological datasets.

Summaries of Stand-alone Research Papers

Each chapter is organized as a stand-alone paper, following the research arch of an introduction, methods, results, and discussion. Additional descriptions of the methods and data used to create these studies can be found in Appendices I-V.

Summary of Chapter II: Patch-based survey methods for studying prehistoric land-use in agriculturally modified landscapes: a case study from the Canal de Navarrés, eastern Spain

In landscapes whose surface has been modified by terracing and other agricultural practices, the spatial and temporal patterning of prehistoric settlement can be difficult to detect using traditional, site-orientated archaeological survey methods, especially for small-scale societies. Making specific connections between human behaviors, fire activity, and landscape change requires evaluating prehistoric land-use dynamics. In this chapter, we employ a stratified, randomly selected patch-based survey strategy to examine socio-ecological dynamics from the Middle Paleolithic through Bell Beaker (Chalcolithic) periods within the Canal de Navarrés, eastern Spain. We divide the study region into survey strata according to differences in topography and vegetation communities and use a random selection of demarcated, terraced fields as data collection patches. Surface artifact densities, estimated from sampled patches, are used to generate prehistoric land-use maps and empirical Bayesian methods allow us to track shifts in occupational patterns through time. Regional reference collections of well-dated lithic artifacts provide the "prior knowledge" required to make estimates of the probability of prehistoric occupation in each sampled patch. By utilizing these sampling and analytical strategies, archaeological surface collections can be used to develop chronologies of changing land-use intensities throughout the Canal de Navarrés, which helps to facilitate a direct comparison of land-use to evidence for changing fire regimes throughout the region. The results of this chapter are used to connect Neolithic land-use intensities to changes in fire activity and HNC in subsequent chapters.

Summary of Chapter III: Identifying natural and anthropogenic drivers of prehistoric fire regimes through simulated charcoal records

Differentiating between natural and anthropogenic ignitions is a primary goal for reconstructing the drivers of prehistoric fire regimes and has significant implications for how we conceptualize social-ecological systems of the past. While statistical methods for discriminating between fire intensity and spatial distribution provide promising steps forward, sedimentary charcoal accumulations alone provide only limited information about changes in fire regimes influenced by human-caused fires (Whitlock et al., 2010). Computational modeling offers a new approach to detecting anthropogenic fire that links social and biophysical processes in a "virtual laboratory" where long-term scenarios can be tested and then compared with empirical charcoal data. This chapter presents CharRec, a computational model of landscape fire, charcoal dispersion, and deposition that simulates charcoal records formed by multiple natural and anthropogenic fire regimes. Building on the distribution and intensity of Neolithic land-use identified in Chapter II, CharRec is applied to a case study in the Canal de Navarrés region in eastern Spain to reveal the role of human-driven fire regimes during the early and middle Holocene. Statistical comparisons of simulated charcoal records to empirical charcoal data from the Canal de Navarrés indicate that anthropogenic burning, following the Neolithic transition to agro-pastoral subsistence, was a primary driver of fire activity during the middle Holocene.

Summary of Chapter IV: Agro-pastoral niche construction and maintenance during the Neolithic period in eastern Spain

By expanding on the model results and data generated in chapters II and III, this chapter analyzes the social and ecological aspects of anthropogenic fire during the Neolithic period (7600–3800 cal. BP) in three study areas throughout eastern Spain. This work is informed by integrating human niche construction theory and ecological resilience to emphasize the processes of creating and maintaining agricultural landscapes over the long-term. Several methodological advances in sedimentary charcoal analysis are introduced, including a semi-automated method for quantifying charcoal fragments, a semi-supervised classification method for assigning charcoal morphotypes, and a predictive GIS and mathematical model of charcoal source areas. These methods are applied to sedimentary charcoal data collected from alluvial sediments in watersheds in the Canal de Navarrés, Hoya de Buñol, and Vall del Serpís study areas. These data are used to assess prehistoric landscape change in response to Neolithic anthropogenic fire in each study area. Results for each study area are then compared to identify changing regional relationships between ecological and cultural inheritance through time.

Goals for Advancing Archaeological Approaches to Anthropogenic Fire

The priority for this dissertation is to develop an understanding of the complexities of the relationship between sedimentary charcoal records and archaeological data. If creatively analyzed and interpreted, these data can offer much more than simple correlations between changing in land-use and increases in fire frequency. Framing a nuanced archaeological perspective on anthropogenic fire is challenging, with numerous data limitations currently facing this type of work. Consequently, I have focused the

majority of this dissertation on advancing field and laboratory methods so archaeology can more directly operationalize and measure the human dimensions of long-term fire regimes. I emphasize the impacts that creation, development, and maintenance of anthropogenic burning practices can have on ecosystems. Based on past socio-ecological patterns, I provide ways that we might conceptualize our own future human-fire relationships.

CHAPTER II

PATCH-BASED SURVEY METHODS FOR STUDYING PREHIRTORIC LAND-USE IN AGRICULTURALLY MODIFIED LANDSCAPES: A CASE STUDY FROM THE CANAL DE NAVARRÉS, EASTERN SPAIN

Grant Snitker, Agustín Diez Castillo, C. Michael Barton, Joan Bernabeu Auban, Oreto García Puchol, Salvador Pardo-Gordó

Introduction

For decades, archeological survey methods have focused on identifying sites through concentrations of artifacts on the surface of the landscape. But in recent years, research aims have widened beyond sites to include the spatial, temporal, and non-linear interactions between human and ecological systems (Arikan, 2012; Barton et al., 2004, 2002, 1999; Carey et al., 2006; Diez Castillo et al., 2016). New social-ecological systems science in archaeology now focuses on multiple types of landscape-scale data, including the continuous distribution of surface artifacts (Bevan and Conolly, 2006, 2002; Bintliff, 2005; Dunnell, 1992). This approach is particularly effective when examining the diachronic interactions between prehistoric land-use, ecological systems, and their influence on landscape evolution (Barton et al., 2004; C. M. Barton et al., 2010).

Such a perspective has played a primary role in driving our research over the last three decades in eastern Spain. Survey in the Mediterranean Basin is often stymied by

landscapes that have been modified through intensive agricultural land-use, resulting in complex palimpsests of archaeological material (Barton et al., 1999; Cherry, 1983; Llobera et al., 2010). We have worked to develop alternative field and analytical approaches that can overcome these challenges. Multiple seasons of fieldwork and experimental methods in the Serpís Valley have resulted in a suite of techniques that consider geomorphology, taphonomy, ground visibility, and relative chronology to evaluate changing patterns of prehistoric land-use (Barton et al., 1999, 2002, 2004; Bernabeu Auban et al., 2001a; Bernabeu Aubán et al., 2008; Bernabeu Auban et al., 1999; Pardo Gordó et al., 2009, 2015).

As part of *Mediterranean Landscape Dynamics Project (MedLanD)*, a collaborative project between Arizona State University, the University of Valencia, and other organizations, we are now applying the methods developed in the Serpís Valley to a new study area in the Canal de Navarrés, Valencia, Spain. This paper presents our initial results as a case study that examines the challenges and our solutions for evaluating prehistoric land-use in landscapes intensively modified by agricultural terracing. We incorporate patch-based survey methods, digital data collection, and Bayesian statistical methods to systematically evaluate the distribution and intensity prehistoric land-use in this study area.

Regional Setting

Environmental setting

The Canal de Navarrés (255 m.a.s.l., 39° 06’ N 0° 41’ W) is a flat-bottomed,

Fig. 1: Overview Map of the Canal de Navarrés, Valencia, Spain.

northwest-southeast oriented tectonic valley located at the intersection of the Iberian and Baetic systems in Valencia, eastern Spain (Fig. 1). The valley is circumscribed by three low-lying ranges: the Massís del Caroig to the west, the Serra de Sumacárcer to the east, and the Serra d'Enguera to the south. Tributaries of the Riu Xúquer actively drain this area from both the north and south. Due to tectonic influences and the formation of

transverse alluvial fans during the Quaternary, the valley is semiendorheic, resulting in the formation of lakes, peatlands, and travertines throughout the Holocene (La Roca et al., 1996). The modern lakes of Playamonte and l'Albufera d'Anna are evidence of these processes.

This region is situated in the Mesomediterranean belt, a transitional zone between coastal and inland climate zones in eastern Spain. The mean annual temperature is ~16 ºC and the region receives an average annual rainfall of 550 mm. The Mesomediterranean belt experiences typical Mediterranean seasonality, with hot, dry summers and mild, wet winters (Carrión and Van Geel, 1999). Modern vegetation communities consist primarily of *matorral* species (including *Quercus coccifera* and *Pistacia lentiscus*) with some *Pinus halepensis* in the uplands. In lowland areas, agriculture has replaced most endemic vegetation. Regional palynological studies have revealed multiple fluctuations in vegetation diversity over the last 30,000 years related to global changes in climate (Carrión et al., 2010; Dupré et al., 1998). But the modern distribution and diversity of matorral vegetation may have been influenced by the introduction of fire associated with Neolithic agricultural practices during the middle Holocene (Carrión and Van Geel, 1999), resulting in the replacement of Pinus dominated forests with more fire-tolerant genera such as *Quercus, Cistus, and Ulex*.

Previous archaeological research

The Canal de Navarrés

Archaeological research in the Canal de Navarrés is limited, but current evidence for occupations span from the Middle Paleolithic to the present. Previous work focused

on endorheic areas throughout the valley, targeting late Pleistocene and early Holocene occupations. Excavations in the vicinity of Las Fuentes revealed Mousterian lithics and preserved *Pinus nigra* trunks with radiocarbon dates of more than 40,000 years BP (Aparicio Perez, 1981). Excavations prior to development at another nearby lake, l'Albufera d'Anna, documented geometric lithic forms dating the late Mesolithic (Aparicio Perez, 1979, 1973). The subsequent recovery of pottery remains from l'Albufera d'Anna, indicates a possible Neolithic component (Martí Oliver et al., 2009). Additional evidence of Neolithic occupations is confined to an isolated occurrence of early Neolithic cardial pottery at Covacha de la Bellota (Fletcher Valls and Aparicio Perez, 1968) and the late Neolithic open-air site of Ereta del Pedregal.

Ereta del Pedregal is located within a peatland between the modern communities of Navarrés and Playamonte (Fletcher Valls et al., 1964; Pla Ballester et al., 1983; Juan Cabanilles, 1994, 2008). Initial investigations in the 1940's and later excavations in the 1980's revealed early examples of stone building construction, a circular stone enclosure, and numerous artifacts. These include lithics and decorated bone associated with Late Neolithic (6,000 – 4,500 BP), Chalcolithic (4,500 – 3,800 BP), and early Bronze Age (3,800 – 3,250 BP) (Pla Ballester et al., 1983). Ereta del Pedregal established the chronology of middle Holocene occupations for the Canal de Navarrés and has been used to interpret the context of other isolated finds throughout the valley.

Regional archaeological research

The Canal de Navarrés is comparatively under-studied in contrast to nearby valleys throughout southern Valencia. The regional chronology of Middle Paleolithic (approximately 100,000 – 30,000 BP) and Upper/Late Upper Paleolithic (30,000 –

10,000 BP) occupations is reconstructed through well-documented sites such as El Salt, Cova Beneito, Cova de Parpalló, and Cova de les Cendres (Barton, 1988; Riel-Salvatore and Barton, 2007; Villaverde Bonilla et al., 2012; Villaverde et al., 1998). Middle Paleolithic chronologies were developed at El Salt and Cova Beneito through a combination of radiocarbon dating and Uranium series dates from travertines underlying occupational contexts. Upper/Late Upper Paleolithic industries recovered from Cova Beneito, Cova de Parpalló, and Cova de les Cendres have shaped the interpretation of late Pleistocene occupations and chronologies throughout the region (Mallol et al., 2012; Villaverde Bonilla et al., 2012).

Regional Mesolithic and Neolithic chronologies have been built through several decades of systematic excavations in caves, rockshelters, and open-air contexts. Evidence of hunter-gatherer occupations during the Mesolithic (11,000 – 7,600 BP) has been primarily identified through diagnostic lithic technologies, including geometric, triangular/trapezoidal microburins and microliths. Regionally, the early Mesolithic is represented by burials and associated artifacts recovered from El Collado (Garcia Guixé et al., 2006; Gibaja et al., 2015). Important late Mesolithic sites identified throughout the region include Abric de la Falguera (García Puchol and Aura Tortosa, 2006) and Cueva de la Cocina (Fortea Perez, 1971; García Puchol et al., 2009; Bernabeu-Aubán and Martí-Oliver, 2014; García Puchol et al., 2017).

The earliest Neolithic occupations date to 7,600 - 7,500 cal. BP at multiple sites, including Mas d'Is (Bernabeu Auban et al., 2003), Abric de la Falguera (García Puchol and Aura Tortosa, 2006) and Cova de les Cendres (Bernabeu Auban, 1999; Bernabeu Aubán and Molina Balaguer, 2009). By 6,500 cal. BP, cardial ceramics and evidence of

domesticated plants and animals were widespread (Sites include Cova d'En Pardo: García Atiénzar 2009; Cova de l'Or: Martí-Oliver 2011; Cova de la Sarsa: Garcia Borja et al. 2011). Although excavations in caves and rockshelters have provided reliable ceramic and lithic chronologies for the Valencian Neolithic period, open-air sites such as Mas d'Is (Bernabeu Auban et al., 2003), Niuet (Bernabeu Aubán et al., 1994), Les Jovades (Bernabeu Auban and Badal Garcia, 1992), and Ereta del Pedregal (Fletcher Valls et al., 1964; Pla Ballester et al., 1983; Juan Cabanilles, 1994, 2008) offer insights into the changing land-use patterns and social organization that accompanies the Neolithic and Bell Beaker (Chalcolithic) periods.

Material and Methods

Off-site survey in the Canal de Navarrés

Survey objectives and background

The primary objective of the Canal de Navarrés archaeological survey is to establish the chronology and intensity of human land-use throughout the valley so we may better understand the changing interaction between social and ecological systems (Diez Castillo et al., 2016; García Puchol et al., 2014). Second, we aim to adapt innovative strategies and analytical techniques to deal with the difficulties of systematic archaeological survey in Mediterranean Basin. Survey projects in the Mediterranean are rare due to several methodological and practical obstacles (Barton et al., 1999; Cherry, 1983). Extensive landscape modification due to agricultural terracing, field delimitation, and water control features have redistributed contexts, making chronological

interpretations from artifacts difficult. Additionally, complex subdivisions of agricultural land have created a mosaic of walled and terraced fields that vary in ownership from parcel to parcel. Uncultivated areas are often overgrown with thick stands of shrubby vegetation, reducing ground visibility and access. Archaeological survey methods relying on continuous, long transects are often impractical in heavily terraced Mediterranean landscapes.

To address these issues, a series of strategies were developed over several decades of survey in the Serpís Valley, Alicante, Spain. That survey was designed with a patch-based, off-site methodology to evaluate the continuous distribution of human activities across the landscape, rather than focusing on identifying sites (Barton et al., 2002, 1999; Bernabeu Aubán et al., 2008). Agricultural terraces across the landscape were not seen as detrimental, but rather as a process through which buried artifacts are exposed on the surface through centuries of tilling, planting, and excavating sediment for terrace construction (Barton et al., 1999). This strategy was effective in evaluating the spatial dimensions of long-term interactions between humans and ecosystems through variations in artifact accumulation and distribution (Barton et al., 2004). Patches without artifacts provide insights into patterns of land-use just as much as those with dense artifact accumulations.

Adaptation for the Canal de Navarrés Survey

The strategies used in the Serpís Valley were updated and adapted for systematic archaeological survey in the Canal de Navarrés during the 2014 and 2015 field seasons. The project is designed as a stratified, randomly selected pedestrian survey, where the

Canal de Navarrés region is divided into survey zones based on topographical features, vegetation communities, and the degree of landscape modification due to agriculture. See Table 1 for descriptions of each zone, stratum designations, and survey coverage. Survey zones are subdivided into survey blocks ("sectors"), which are randomly selected to create sampling strata (Fig. 2). Within each sector, field and parcel boundaries are used

Fig. 2: Survey Zones and Sectors in the Canal de Navarrés.

Table 1: Survey Zone Descriptions.

Zone	Num. of Sectors	Topographic Landform	Dominant Modern Vegetation	Degree of Modern Agricultural Land-use	Sectors in Survey Stratum	Area of Stratum	Area Surveyed	Coverage
1	3	Lowland	Agricultural	High	1-1, 1-2	3.58 km^2	0.26 km^2	7%
2	3	Lowland	Agricultural	High	2-2	1.46 km^2	0.24 km^2	16%
3	6	Lowland	Agricultural	High	3-2, 3-3, 3-5	5.53 km^2	0.59 km^2	11%
4	2	Transitional	Mixed Agricultural & Pine Forest	Moderate	4-1, 4-2	3.90 km^2	0.73 km^2	19%
5	2	Transitional	Mixed Agricultural & Matorral	High	5-1, 5-2	3.10 km^2	0.49 km^2	16%
6	3	Upland	Mixed Agricultural & Matorral	Moderate	6-1	1.36 km^2	0.32 km^2	24%
7	4	Upland	Pine Forest	Low	7-2, 7-4	9.60 km^2	1.00 km^2	11%
8	3	Upland	Mixed Agricultural & Pine Forest	Moderate	--	--	--	--
9	6	Upland	Mixed Agricultural & Pine Forest	Moderate	9-6	3.25 km^2	0.71 km^2	22%
10	--	Transitional	Mixed Agricultural & Matorral	Moderate	10	0.09 km^2	0.09 km^2	100%

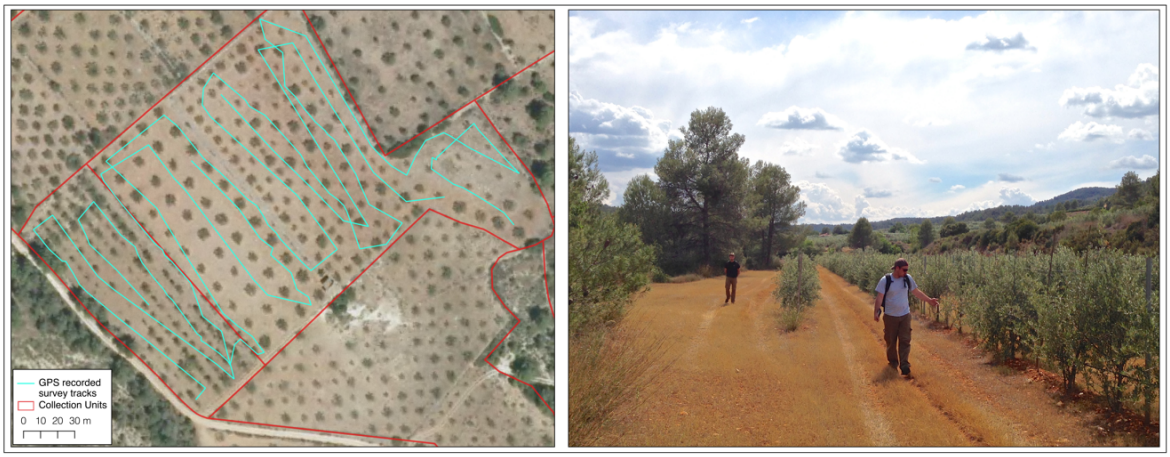

Fig. 3: Example of Survey Methodology in Collection Units.

to demarcate patches, which we refer to as collection units. Groups of 3-4 crewmembers walk in transects spaced at approximately 10-meter intervals, with some variation to accommodate for cultivated rows in each collection unit (Fig. 3). All encountered artifacts are collected and later washed, identified, and counted in the Department of Prehistory at the University of Valencia (Department of Prehistory, Archaeology, and Antiquity).

Overall, we sampled approximately 25 percent of collection units within each stratum. At the end of the 2014 and 2015 seasons, all zones were sampled with the exception of Zone 8, which was excluded due to its similarity in topography, vegetation, and modern agricultural land-use to Zone 9. A small series of collection units outside of the original survey zones were also targeted, non-randomly, in 2015 due to their close proximity to previously known Mesolithic or Neolithic sites. These collections units were labeled as Zone 10. Although not stratified or randomly selected, these collection units helped to pinpoint other areas likely to contain evidence of prehistoric land-use.

Digital data collection

All in-field data collection was recorded digitally on tablets, rather than paper forms or maps. Tablets greatly increase the ease and reliability of collecting archaeological data in the field by creating digital back-ups of site data and instantly connecting spatial attributes to field forms. Each survey team was assigned a tablet with custom digital forms created in CartoMobile®, a GIS data entry and visualization application for iOS mobile devices. The types of digital data recorded for each collection unit is shown in Table 2. In addition to tablets, each team recorded GPS tracks of survey transects, as required by the Valencian Directorate of Cultural Heritage and Museums.

Table 2: Description of Digital Data Recorded for Each Collection Unit.

Data field	Description
Date and time	Timestamp when each collection unit was recorded
Sector	Survey Sector (eg. Sector 5)
Subsector	Survey Subsector (eg. Subsector 1)
Collection Unit number	Field parcel number (eg. 100263)
Ground visibility	Good, Moderate, or Poor
Artifacts collected	Yes or No
Geospatial information for each collection unit	Digitized centroid if entire parcel is used as a collection unit; digitized polygon and centroid if only a partial parcel is used as a collection unit
Photographs of collection unit	Digital photographs detailing the collection unit, ground visibility, or notable artifacts
Additional Notes	Other notes related to the collection unit

Statistical "unmixing" through Bayesian age estimates of surface assemblages

One of the challenges facing any archaeological survey is building chronologies using surface assemblages that represent multiple occupational periods or intensities.

This problem is exacerbated in Mediterranean landscapes, which are typified by palimpsests of archaeological material created through dynamic erosional regimes and long histories of plowing and terracing. Artifacts spanning the last 100,000 years of human occupation may be found within the same surface contexts. Seriation techniques assume that each assemblage is deposited during a single temporal period and cannot readily accommodate for mixed assemblages.

Bayesian statistical concepts offer an alternative solution for relative chronology building using surface assemblages and explicitly address the palimpsest issue. This approach 'unmixes' surface collections by allowing multiple occupational periods to be simultaneously represented at different probabilities (Buck et al., 1996; Buck and Sahu, 2000; Fernández-López de Pablo and Barton, 2013; Ortman et al., 2007). Bayesian statistics are a branch of statistical theory developed from the work of Thomas Bayes, an eighteenth-century mathematician. Formally, Bayes' theorem is stated as the following:

$$P(H|D) \propto P(H) * P(D|H) \quad (1)$$

in such that the probability of some phenomenon (its *posterior probability*) *P(H|D)* is proportional to the *prior probability P(H)* multiplied by the *conditional probability P(D|H)*, also known as the likelihood. In other terms, Bayes' theorem provides a means of assessing the probability of an outcome based on the combination of new data and prior knowledge about the probability of that outcome. Practically, this perspective provides a systematic method for estimating the age of surface assemblages by incorporating previous knowledge about the association of certain artifact forms with

temporal periods. Relying on expert knowledge and experience in archaeology is commonly employed in archaeological projects, but a Bayesian approach allows us to formalize these methods by utilizing a wide variety of published data on regional sites to evaluate our confidence in assigning occupational chronologies to the landscape. See Fernández-López de Pablo and Barton 2013 and Ortman et al. 2007 for more details on Bayesian age estimates for archaeological surface assemblages.

Calibration dataset based on prior knowledge

Barton and colleagues (1999, 2002, 2004) developed a Temporal Index (TI) by assigning rank-order probability estimates for specific time periods based on the presence and absence of artifact forms collected during archaeological survey in the Serpís Valley. The present work expands their chronology-building framework by incorporating formalized Bayesian statistics to the presence/absence data for temporally sensitive artifact forms. We use this approach to estimate the probability that a surface assemblage from a collection unit is associated with one of nine occupational periods in the Canal de Navarrés (including the Middle Paleolithic, Upper Paleolithic, Late Upper Paleolithic, Early Mesolithic, Late Mesolithic, Early Neolithic, Middle Neolithic, Late Neolithic, and Bell Beaker periods). See Table 3 for details on each occupational period.

Other applications of Bayesian methods for dating surface assemblages have relied on independently dated artifact forms from excavated contexts to create calibration datasets and establish prior probabilities for temporal periods (Fernández-López de Pablo and Barton, 2013; Ortman et al., 2007). Unfortunately, few sites have been excavated in

Table 3: Details of Archaeological Periods and Lithic Forms Used in the Analysis.

Temporal Range	Duration (kyr)	Archaeological Period	Attributed Lithic Forms
4500 - 3800 BP	0.7	Bell Beaker	- Foliate/Bifacial projectile points - Invasive retouched blades - Denticulated sickle blades - Undifferentiated lithics (flakes, chunks, and shatter)
6000 - 4500 BP	1.5	Late Neolithic	- Foliate/Bifacial projectile points - Triangle microliths - Trapeze microliths - Invasive retouched blades - Retouched blades - Generic blade technology (blades, bladelets, and blade core preparation) - Undifferentiated lithics (flakes, chunks, and shatter).
6800 - 6000 BP	0.8	Middle Neolithic	- Triangle microliths - Trapeze microliths - Invasive retouched blades - Retouched blades - Generic blade technology (blades, bladelets, and blade core preparation) - Undifferentiated lithics (flakes, chunks, and shatter).
7600 - 6800 BP	0.8	Early Neolithic	- Truncated blades - Triangle microliths - Trapeze microliths - Retouched blades - End scrapers - Generic blade technology (blades, bladelets, and blade core preparation) - Undifferentiated lithics (flakes, chunks, and shatter).
8600 - 7600 BP	1	Late Mesolithic	- Truncated blades - Triangle microliths - Trapeze microliths - Backed blades - Microburins - End scrapers - Generic blade technology (blades, bladelets, and blade core preparation) - Undifferentiated lithics (flakes, chunks, and shatter).

Table 3: Continued.

Temporal Range	Duration (kyr)	Archaeological Period	Attributed Lithic Forms
11,000 - 8600 BP	2.4	Early Mesolithic	- Backed blades - End scrapers - Generic blade technology (blades, bladelets, and blade core preparation) - Notches/Denticulates microliths - Undifferentiated lithics (flakes, chunks, and shatter).
13,000 - 11,000 BP	3	Late Upper Paleolithic	- Backed blades - End scrapers - Generic blade technology (blades, bladelets, and blade core preparation) - Burins - Undifferentiated lithics (flakes, chunks, and shatter).
30,000 - 13,000 BP	17	Upper Paleolithic	- End scrapers - Generic blade technology (blades, bladelets, and blade core preparation) - Burins - Undifferentiated lithics (flakes, chunks, and shatter).
100,000 - 30,000 BP	70	Middle Paleolithic	- Discoidal/Levallois Flake Technology - Mousterian technology (projectile points and side scrapers) - Notches/Denticulates microliths - Undifferentiated lithics (flakes, chunks, and shatter).

the Canal de Navarrés, and those that have been excavated do not include dated materials that span the entire range of the occupation periods present in this region. Rather than artifacts counts assigned to each chronological period to estimate our prior probabilities, we rely a calibration dataset of presence/absence data developed from TI measurement of archaeological survey and excavation in the Serpís Valley (Barton et al., 2004, 1999). Presence and absence of 16 lithic forms in each of the nine periods were coded as 1s and 0s, respectively (Table 3). Prior probabilities were estimated by calculating the frequency of a particular lithic form relative to all other forms. This is then compared to the relative frequency of that form for each temporal period where it was present. Although ceramics

or other temporally sensitive artifact types could provide data for building a calibration dataset, only lithics were recovered from prehistoric contexts in the Canal de Navarrés survey area.

Posterior Probabilities for occupational periods

Posterior probabilities for each occupational period were calculated based on the frequency of temporally sensitive artifact forms identified in each collection unit from the Canal de Navarrés survey. Following the application of Bayes' theorem from Fernández-López de Pablo and Barton (2013), we calculate the probability that a collection unit dates to one of nine occupational periods, based on specific artifact forms, as follows:

$$P(m_i|type_j) = \frac{P(m_i) * \sum_{j=1}^{n} P(type_j|m_i)}{\sum_{l=1}^{k} P(m_l)) * \sum_{j=1}^{n} P(type_j|m_i)} \quad (2)$$

where i=1 to k are the nine occupational periods in the Canal de Navarrés and j=1 to n are the temporally sensitive artifact forms. $P(type_j \mid m_i)$ is the conditional probability for artifact form $type_j$ and occupational period m_i, and $P(m_i)$ is the prior probability of artifact form $type_j$ being represented in occupational period m_i.

Since prior probabilities for the Canal de Navarrés are based on presence/absence data for each occupational period, additional prior knowledge was introduced in the form of independent weighting of posterior probabilities. This allows us to rely on expert knowledge about artifact forms and their associated occupation periods rather than artifact frequencies from well-dated, excavated contexts. Assemblages from each collection unit were assigned a score between 0 and 6 for each of the nine occupational periods based on combinations of artifact forms, as illustrated in Table 4. Scores for each

Table 4: Weight Scores for Posterior Probabilities by Presence/Absence of Artifact Forms (Adapted from Barton et al. 1999): G1: Trapezes or Triangles; G2: Segments or Rectangles; Sickles: Sickle Blades/Bladelets; Dent. Sickles: Denticulated Sickles; Bif. drills: Bifacial Drill; Nch. and Dent: Notches and Denticulated Microliths; Blade Tech.: Blade Technology; Flake Tech.: Discoidal/Levallois flakes; Backed Blds.: Backed Blades/Bladelets; End Scrp.: End-Scrapers; Brn: Burins; Must.: Mousterian Technology (Bifaces and Side Scrapers); Proj. Points: Foliate/Bifacial Projectile Points; Ret. Blades: Retouched Blade; Inv. Ret.: Invasive Retouched Blade; Trc: Truncated Blades; M1: Microburins; Labs: Labios Engrosados Ceramics; BB Ceramics: Bell Beaker Campaniforme Ceramics; Cardial: Cardial Ceramics; Esgr.: Esgrafiada Ceramics; Peina: Peina Ceramics; Epi: Ceramics Decorated with Incisions or Impressions.

	6	5	4	3	2	1	0
Bell Beaker (Chalcolithic)	P: BB ceramics	P: Dent. sickles	P: Proj. points	P: Inv. Ret. + Labs.	P: Inv. Ret. or Labs.	P: Lithics, Ceramics	
							A: Artifacts
Late Neolithic	P: Proj. points + Labs. + Inv. Ret.	P: Proj. points + (Inv. Ret. or Labs.)	P: Proj. points or Inv. Ret. or Labs.	P: Blade tech. + (Ret. blades, Bif. drills, Sickles, Ceramics or G1)	P: Blade tech. + (Ret. blades, Bif. drills, Sickles, Ceramics or G1)	P: Lithics, Ceramics	
	A: BB ceramics or Dent. sickles	A: BB ceramics or Dent. sickles		A: BB ceramics, Dent. sickles, Esgr. or Card.			A: Artifacts
Middle Neolithic	P: Esgr.	P: (Inv. Ret or G2)+ (Epi. or Peina)	P: (Inv. Ret or G2)+ (Epi. or Peina)	P: Blade tech. + (Ret. blades, Sickles, Ceramics or G1)	P: Blade tech. + (Ret. blades, Bif. drills, Sickles, Ceramics or G1)	P: Lithics, Ceramics	
		A: BB ceramics, Dent. Sickles or Proj. points		A: BB ceramics, Dent. sickles, Proj. points or Card.			A: Artifacts
Early Neolithic	P: Card.	P: Epi + (G1 or Trc) + (Ret. blades, Bif. drills or Sickles) + (G1 or Trc) + Ceramics	P: Epi+ (G1 or Trc) + (Ret. blades, Bif. drills or Sickles) + (G1 or Trc)+ Ceramics	P: Blade tech. + (Ret. blades, Bif. Drills, Sickles, Ceramics or G1)	P: Blade tech. + (Ret. blades, Bif. Drills, Sickles, Ceramics or G1)	P: Lithics, Ceramics	
		A: BB ceramics, Dent. Sickles, Proj. points or Esgr,		A: BB ceramics, Dent. Sickles, Proj. points or Esgr,			A: Artifacts
Late Mesolithic	P: (G1 or M1) + Backed blds. + (End scrp. or Trc)	P: (G1 or M1) + End scrp. + (Backed blds. or Trc)	P: (G1 or M1) + End scrp. + (Backed blds. or Trc)	P: Blade tech. + (G1, Trc or End scrp.)	P: Blade tech. + (G1, Trc or End scrp.)	P: Lithics	
	A: Ceramics, G2, Sickles, Proj. points	A: Ceramics, G2, Sickles, Proj. points		A: Ceramics, G2, Sickles, Proj. points			A: Lithics

Table 4: Continued.

Early Mesolithic	P: Backed blds. + End scrp. + Nch. and Dent.	P: (Backed blds. or End scrp.) + Nch. and Dent.	P: (Backed blds. or End scrp.) + Nch. and Dent.	P: Blade tech., End scrp. or Backed blds.	P: Blade tech., End scrp. or Backed blds.	P: Lithics	
	A: G1, G2, Sickles, Bif. drills, Ceramics or Proj. points	A:G1, G2, Sickles, Bif. drills, Ceramics or Proj. points		A:G1, G2, Sickles, Bif. drills, Ceramics or Proj. points			A: Lithics
Late Upper Paleolithic	P: End scrp. + Brn + Backed blds.	P: Backed blds.+ (Brn or End scrp.)	P: Backed blds. + (Brn or End scrp.)	P: Blade tech., End scrp, Brn or Backed blds.	P: Blade tech., End scrp., Brn or Backed blds.	P: Lithics	
	A: G1, G2, Sickles, Bif. drills, Ceramics or Proj. points	A: G1, G2, Sickles, Bif. drills, Ceramics, Proj. points		A: G1, G2, Sickles, Bif. drills, Ceramics, Proj. points			A: Lithics
Upper Paleolithic	P: Blade tech. + End scrp. + Brn	P: Blade tech. + (End scrp. or Brn)	P: Blade tech. + (End scrp. or Brn)	P: Blade tech., End scrp. or Brn	P: Blade tech., End scrp. or Brn	P: Lithics	
	A: G1, G2, Sickles, Bif. drills, or Ceramics	A: G1, G2, Sickles, Bif. Drills, or Ceramics		A:G1,G2, Sickles, Bif. drills, or Ceramics			A: Lithics
Middle Paleolithic	P: Flake tech. + Nch. and Dent. + Must.	P: Flake tech.+ (Must. or Nch. and Dent.)	P: Flake tech.+ (Must or Nch. and Dent.)	P: Flake tech. or Must.	P: Flake tech. or Must.	P: Lithics	
	A: Ceramics, Blade tech., or Proj. points.	A: Ceramics, Blade tech., or Proj. points.		A: Ceramics, Blade tech., or Proj. points.			A: Lithics

collection unit where re-scaled to sum to 1 and were multiplied by the posterior probability for each collection unit and occupational period. See Fig. 4 for a conceptual map of this methodology.

Results

Summary of survey results

Zone 1

Zone 1 is located within the municipality of Navarrés and consists of lowland, endorheic areas such as the large karstic upwelling of Las Fuentes. This area is intensively cultivated and irrigated, but terracing remains somewhat limited due to the landscape's low slope. Ereta del Pedregal and Las Fuentes archaeological sites are both located in this zone (Diez Castillo et al., 2016).

Within zone 1, samples of both sectors 1-1 and 1-2 were surveyed during the 2014 and 2015 field seasons (Fig. 5A). Lithic artifacts were recovered in 22 of the 79 collection units surveyed in sector 1-1 and in 2 of the 4 collection units surveyed in sector 1-2. In collection unit 1100355, located adjacent to the site of the Ereta del Pedregal, multiple temporally sensitive artifacts were recovered including truncated and laminate blades.

Zone 2

Zone 2 is located within the municipality of Chella on the west bank of the Riu Bolbaite within the middle section of the valley. Only sector 2-2 was sampled, resulting

in lithic artifacts recovered in 24 of the 99 collection units surveyed. The distribution of artifacts recovered from this portion of the valley suggest that most of the prehistoric record is likely buried under alluvial sediments deposited throughout the Holocene by the Riu Bolbaite and its tributaries (Fig. 5A).

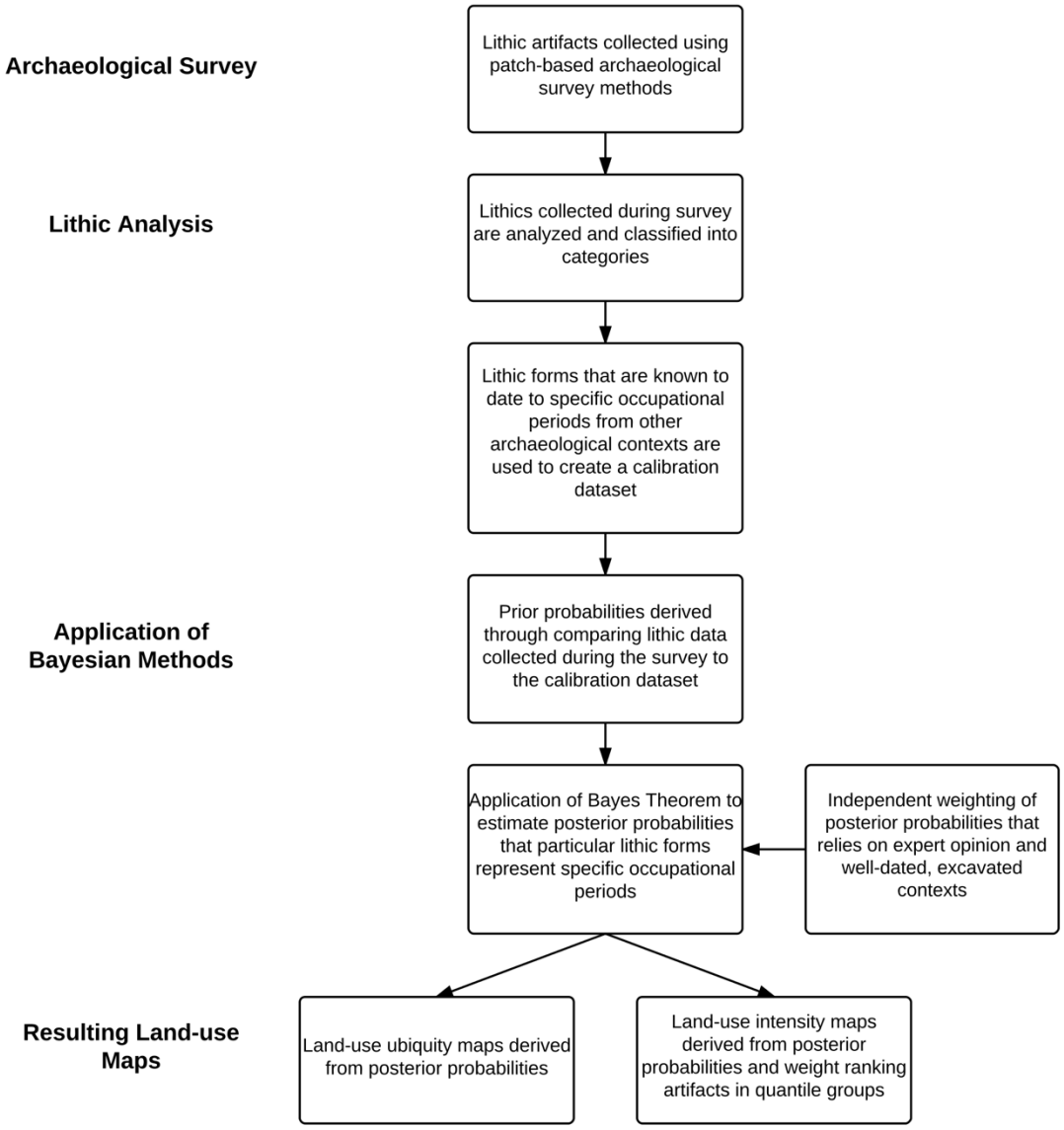

Fig. 4: Conceptual Map of Bayesian Methodology.

Zone 3

Zone 3 is located within the municipality of Anna and encompasses l'Albufera d'Anna, a small lake within the southern end of the endorheic basin that has been improved in recent years for use as a recreation site. This area has also undergone major agricultural and recreational development in the last several decades, resulting in increased erosion and denudation of Holocene sediments. During the 2014 and 2015 field seasons, crewmembers sampled sectors 3-2, 3-3, and 3-5, surveying a total of 113 collection units. Collections were made in 14 units, resulting in a total of 28 lithic artifacts from all of zone 3 (Diez Castillo et al., 2016).

Zone 4

Zone 4 is split between the municipalities of Bolbaite and Chella and sectors 4-1 and 4-2 near Chella were sampled for survey. This zone encompasses the western portion of a secondary, adjacent drainage (barranco del Matet) that flows south into the Riu Bolbaite and is positioned in a transitional area between other upland and lowland survey zones. Numerous smaller tributaries have downcut the adjacent limestone hills, creating small ravines and rockshelters. Zone 4 contains Covacha de la Bellota, a small rockshelter from which cardial ceramics were recovered during earlier investigations (Fletcher and Aparicio 1970). Lithics were recovered from 62 of the 100 collection units surveyed, with a maximum of 58 lithics collected from a single parcel (Diez Castillo et al., 2016).

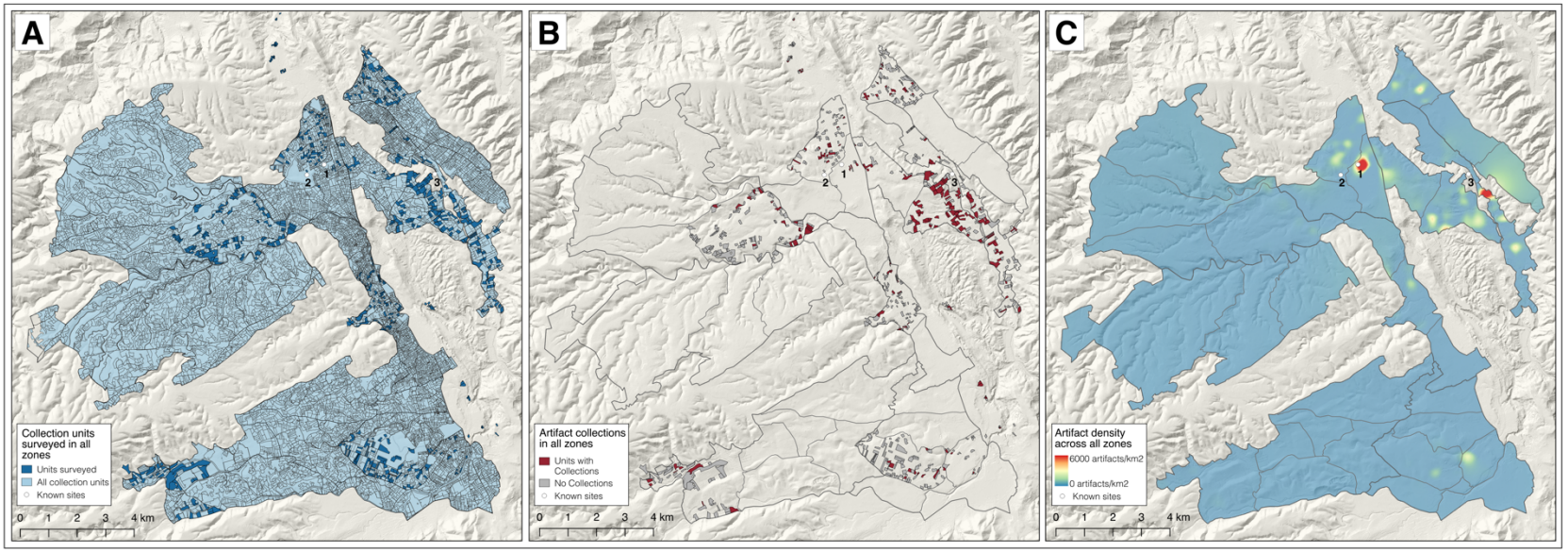

Fig. 5: A) Collection Units Surveyed During the 2014 and 2015 Field Seasons, B) Collection Units with Lithic Artifacts, and C) Interpolated Artifacts Densities for the Study Area. Previously Recorded Sites Are Labeled as 1. Las Fuentes, 2. Ereta del Pedrega

Zone 5

Zone 5 is located east of zone 4, and is composed of two sectors, 5-1 and 5-2, both of which were sampled. Both sectors encompass transitional areas between upland areas in Zone 6 and the adjacent valley bottom. Zone 5-1 is located at the southern end of the valley, near the confluence of el barranco del Matet and the Riu Bolbaite, and produced a high density of lithic artifacts. Lithics were recovered from 26 out of 57 collection units surveyed. Notably, 131 lithic artifacts (including retouched flakes and blades) were recovered from collection unit 5-1-100181. In stark contrast, very few lithics were collected in sector 5-2, located to the north of sector 5-1. Low densities of lithic artifacts were recorded in only 4 out of 29 collection units in this sector.

Zone 6

Zone 6 is located in an upland area within the municipality of Navarrés and is the only sector that drains north to the Riu Escalona, which joins the main Riu Xúquer upstream of Sumácarcer. In this zone, only sector 6-1 was sampled and surveyed, yielding lithics in 14 of 75 collection units (Diez Castillo et al., 2016). This area, along with sectors 2-2, 3-3, and 5-2, has one of the lowest densities of artifacts in the Canal de Navarrés survey area.

Zone 7

Zone 7 is located in the upland area at the western most edge of the Canal de Navarrés survey area. Sector 7-4 is located on the border between Navarrés to the north and Bolbaite to the south and encompasses the watershed that drains to Las Fuentes

(Playamonte) and the Riu Bolbaite. A total of 120 collection units were surveyed in sector 7-4 with lithic artifacts recovered from 22 fields.

Zone 9

Zone 9 is located within the municipality of Enguera and within a relatively high, upland area in the southern most portion of the survey area. Survey was concentrated in sector 9-6, located at the southeastern end of the Caroig massif, crossed by the Riajuelo rambla before it joins the Riu Sellent. Of the 40 collection units surveyed, artifacts were recovered from 21 fields, making this one of the more productive areas within the survey area. Most artifacts recovered in this zone are Iberian-Roman ceramics related to the nearby Iberian site of Cerro Lucena and are not included in the current analysis (Diez Castillo et al., 2016).

Zone 10

During the 2015 field season, additional parcels outside of the original survey zones were identified as areas that could potential yield more information regarding the spatial distribution of prehistoric land-use in the Canal de Navarrés (Fig 5A). These parcels were primarily located in transitional areas outside of the main valley. A total of 52 additional collection units were identified for survey and labeled as zone 10. A total of 17 of the 52 units surveyed contained lithic artifacts, including burins, retouched flakes, notches, and blades.

Spatial distribution and density of artifacts in the Canal de Navarrés

The spatial distribution of surveyed collection units in each zone, units where lithic artifacts were collected, and the density of artifacts across the survey area are illustrated in Figs. 5A-C. Artifact densities were calculated by dividing the frequency of lithic artifacts observed in each collection unit by its area (km^2). The resulting densities were interpolated using bilinear b-spine interpolation (directional steps = 150 m; smoothing parameter = 0.01; 30 m resolution) to create a continuous estimation of artifact density. All raster, vector, and interpolation calculations are conducted in GRASS GIS Version 7.0 (GRASS Development Team, 2016).

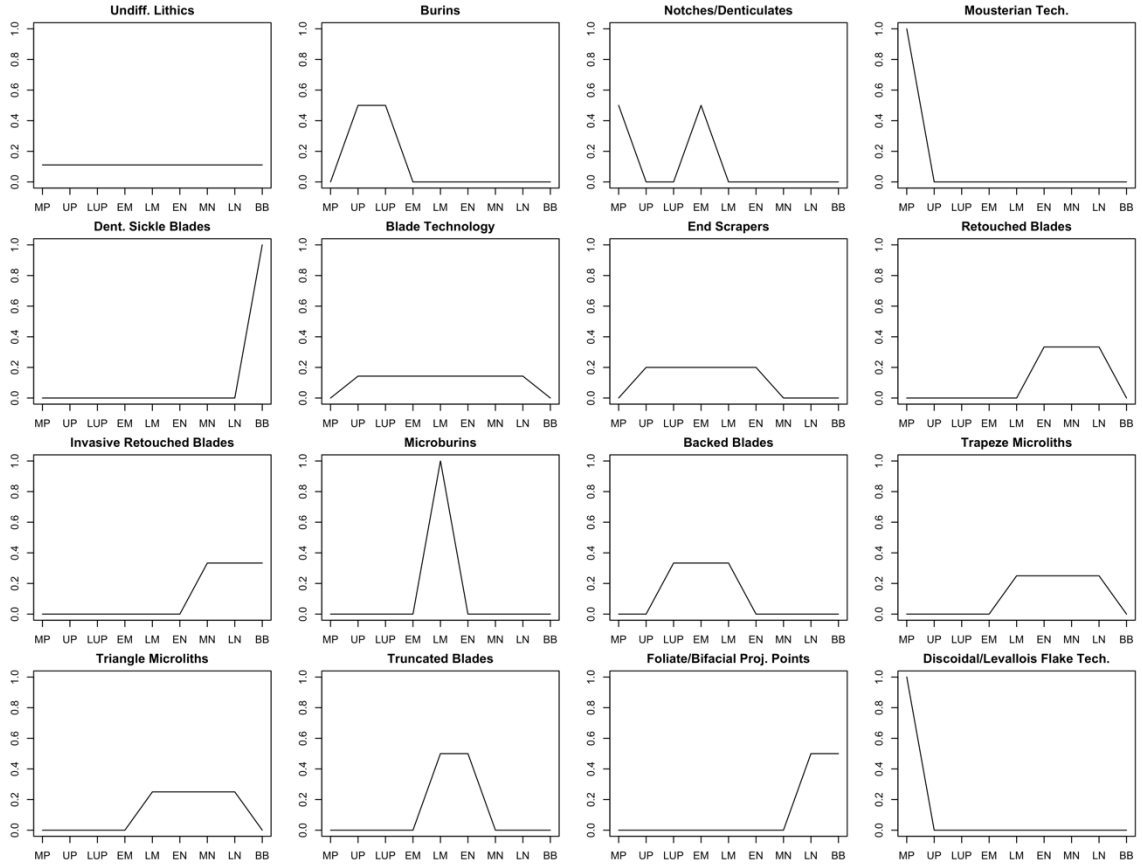

Fig. 6: Graphical Representation of Prior Probabilities Derived from the Calibration Dataset for the Canal de Navarrés.

Applying Bayesian age estimates to surface assemblages

Prior probabilities and collection unit weights

Prior probabilities of each artifact form, calculated from the calibration dataset, are graphically illustrated in Fig. 6. Artifact forms present in only one (25.0% of forms), two (25.0% of forms), or three (18.8% of forms) occupational periods are considered temporally sensitive indicators. These include burins, notches and denticulated flakes, Mousterian technology (bifaces and side scrapers), denticulated sickle blades, retouched blades, invasive retouched blades, microburins, backed blades, truncated blades, projectile points (foliate and other bifacial points), and discoidal/levallois flake technology. Trapeze microliths and triangle microliths occur in four occupation periods and are considered less temporally sensitive.

Three artifact forms are present in over half (≥ 5) of the occupational periods and are therefore general indicators of occupation. These include blade technology (blades, bladelets, and blade core preparation), end scrapers, and undifferentiated lithics (flakes, chunks, and shatter). Although the extended temporal range of these artifacts makes it difficult to identify the occupational period most closely associated with them, it does provide a means through which to identify the overall presence of prehistoric land-use. The weights applied the posterior probability of each occupation period for all collection units that contained artifacts (not including collection units with only undifferentiated lithics) are shown in Table 5. Collection units with only undifferentiated lithics were assigned equal weights (1/n occupational periods or 0.111).

Posterior probabilities and estimating the age of surface assemblages in the Canal de Navarrés

Table 6 shows the posterior probabilities that material recovered from collection units are associated with each occupational period. Units in which only undifferentiated lithics were collected have equal posterior probabilities for each occupational period and are not shown. These results illustrate the extensive mixing of surface assemblages in the Canal de Navarrés survey area, with very few collection units possessing a distinct, unimodal association. It is important to note that posterior probabilities are an expression of both prior knowledge and an assessment of our confidence in assigning occupational periods to artifacts on the landscape. For this reason, the *relative* strength of the posterior probabilities is most important, not the absolute value of any given collection unit. For example, a collection unit associated with a single occupation period would have a posterior probability of 1 for that period and 0 for all other periods. Similarly, a collection unit with three associated occupational periods would have posterior probabilities of 0.333 for each of the represented periods and 0 for all other periods. Although the absolute values of the posterior probabilities in these two examples differ by a factor of 3, they are of equal weight when assessing the likelihood of land-use during each occupational period.

Land-use Ubiquity in the Canal de Navarrés survey area

Posterior probabilities of lithic material associated with each occupational period provide an in-depth perspective on variation in land-use through time within the survey area. But posterior probabilities alone do not give a sense of how land-use is distributed

Table 5: Weights Calculated for All Collection Units with Artifacts Other than Undifferentiated Lithics.

Zone	Sector	Parcel	MP	UP	LUP	EM	LM	EN	MN	LN	BB
1	1	900568	0.067	0.200	0.200	0.200	0.067	0.067	0.067	0.067	0.067
		1100119	0.063	0.188	0.188	0.188	0.125	0.063	0.063	0.063	0.063
		1100140	0.111	0.111	0.111	0.111	0.111	0.111	0.111	0.111	0.111
		1100168	0.111	0.111	0.111	0.111	0.111	0.111	0.111	0.111	0.111
	2	1100355	0.053	0.158	0.158	0.158	0.158	0.105	0.053	0.105	0.053
2	2	600256	0.067	0.200	0.200	0.200	0.067	0.067	0.067	0.067	0.067
		900041	0.111	0.111	0.111	0.111	0.111	0.111	0.111	0.111	0.111
	7	1300156	0.250	0.083	0.083	0.167	0.083	0.083	0.083	0.083	0.083
		400173	0.111	0.111	0.111	0.111	0.111	0.111	0.111	0.111	0.111
3	2	2100131	0.067	0.200	0.200	0.200	0.067	0.067	0.067	0.067	0.067
	3	2200018	0.067	0.200	0.200	0.200	0.067	0.067	0.067	0.067	0.067
		2500013	0.067	0.067	0.067	0.067	0.067	0.067	0.067	0.267	0.267
		2200015	0.067	0.200	0.200	0.200	0.067	0.067	0.067	0.067	0.067
		2200016	0.273	0.091	0.091	0.091	0.091	0.091	0.091	0.091	0.091
	5	1000050	0.067	0.200	0.200	0.200	0.067	0.067	0.067	0.067	0.067
4	1	200087	0.048	0.095	0.095	0.095	0.143	0.095	0.095	0.095	0.238
		100392	0.067	0.200	0.200	0.200	0.067	0.067	0.067	0.067	0.067
		100312	0.067	0.200	0.200	0.200	0.067	0.067	0.067	0.067	0.067
		100307	0.059	0.294	0.177	0.177	0.059	0.059	0.059	0.059	0.059
		100279	0.059	0.177	0.177	0.177	0.177	0.059	0.059	0.059	0.059
		100168	0.046	0.091	0.091	0.091	0.091	0.091	0.091	0.182	0.227
		0200089B	0.067	0.200	0.200	0.200	0.067	0.067	0.067	0.067	0.067
		200073	0.059	0.118	0.118	0.118	0.059	0.177	0.177	0.118	0.059
		100276	0.188	0.125	0.125	0.250	0.063	0.063	0.063	0.063	0.063
		100283	0.056	0.222	0.167	0.167	0.167	0.056	0.056	0.056	0.056
		100277	0.071	0.143	0.214	0.214	0.071	0.071	0.071	0.071	0.071
		100319	0.059	0.118	0.118	0.118	0.059	0.177	0.177	0.118	0.059
		100164	0.059	0.118	0.118	0.118	0.059	0.177	0.177	0.118	0.059
		100137	0.067	0.200	0.200	0.200	0.067	0.067	0.067	0.067	0.067
		0100109B	0.188	0.125	0.125	0.250	0.063	0.063	0.063	0.063	0.063
		0100109C	0.063	0.125	0.125	0.125	0.063	0.063	0.063	0.063	0.313
		200076	0.067	0.200	0.200	0.200	0.067	0.067	0.067	0.067	0.067
		200074	0.067	0.200	0.200	0.200	0.067	0.067	0.067	0.067	0.067
		200086	0.273	0.091	0.091	0.091	0.091	0.091	0.091	0.091	0.091
		200075	0.067	0.200	0.200	0.200	0.067	0.067	0.067	0.067	0.067

Table 5: Continued.

Zone	Sector	Parcel	MP	UP	LUP	EM	LM	EN	MN	LN	BB
4	1	100221	0.214	0.071	0.071	0.286	0.071	0.071	0.071	0.071	0.071
		100252	0.067	0.200	0.200	0.200	0.067	0.067	0.067	0.067	0.067
		100245	0.067	0.200	0.200	0.200	0.067	0.067	0.067	0.067	0.067
		100353	0.067	0.200	0.200	0.200	0.067	0.067	0.067	0.067	0.067
		100147	0.067	0.200	0.200	0.200	0.067	0.067	0.067	0.067	0.067
		100155	0.273	0.091	0.091	0.091	0.091	0.091	0.091	0.091	0.091
		0100109A	0.111	0.111	0.111	0.111	0.111	0.111	0.111	0.111	0.111
	2	1000508	0.048	0.143	0.143	0.143	0.143	0.143	0.095	0.095	0.048
5	1	100181	0.074	0.222	0.222	0.222	0.111	0.037	0.037	0.037	0.037
		100288	0.059	0.177	0.177	0.177	0.177	0.059	0.059	0.059	0.059
		100372	0.040	0.200	0.120	0.120	0.120	0.120	0.120	0.120	0.040
		400003	0.046	0.136	0.136	0.136	0.046	0.046	0.046	0.227	0.182
		200018	0.048	0.143	0.095	0.095	0.095	0.048	0.048	0.238	0.191
		100263	0.071	0.214	0.214	0.143	0.071	0.071	0.071	0.071	0.071
		100292	0.125	0.125	0.125	0.313	0.063	0.063	0.063	0.063	0.063
		400004	0.067	0.200	0.200	0.200	0.067	0.067	0.067	0.067	0.067
		200012	0.077	0.077	0.077	0.077	0.077	0.077	0.077	0.077	0.385
		300018	0.067	0.200	0.200	0.200	0.067	0.067	0.067	0.067	0.067
		100180	0.067	0.200	0.200	0.200	0.067	0.067	0.067	0.067	0.067
		100199	0.067	0.200	0.200	0.200	0.067	0.067	0.067	0.067	0.067
		500045	0.077	0.077	0.077	0.077	0.077	0.077	0.077	0.077	0.385
	2	100028	0.067	0.200	0.200	0.200	0.067	0.067	0.067	0.067	0.067
6	1	300362	0.063	0.125	0.125	0.125	0.063	0.063	0.063	0.063	0.313
		300361	0.063	0.125	0.188	0.188	0.188	0.063	0.063	0.063	0.063
		300204	0.067	0.200	0.200	0.200	0.067	0.067	0.067	0.067	0.067
7	4	1300198	0.071	0.071	0.214	0.214	0.143	0.071	0.071	0.071	0.071
		500313	0.056	0.167	0.167	0.167	0.056	0.056	0.056	0.167	0.111
		500317	0.067	0.200	0.200	0.200	0.067	0.067	0.067	0.067	0.067
		1300166	0.067	0.200	0.200	0.200	0.067	0.067	0.067	0.067	0.067

spatially in each occupational period. A simple method for evaluating both spatial and temporal dimensions is through a measure of land-use ubiquity (Barton et al., 2004) for each occupational period.

Land-use ubiquity is assessed by first extracting the locations of centroids from all collection units surveyed during the 2014 and 2015 field seasons. These spatial data are then merged with the posterior probabilities for each occupational period, while units with no observed artifacts are assigned probabilities of 0. The resulting spatial points contain three dimensions: *x* and *y* locational information, and z, the posterior probability that a given collection unit is associated with each occupational period. Using b-spline interpolation (directional steps = 150 m; smoothing parameter = 0.01; 30 m resolution), a probability surface for each occupational period is created between all collection unit centroids at the scale of the entire survey area. Values are then rescaled from 0 to 1 to facilitate comparison between occupational periods. This method allows us to use the presence/absence of artifacts included in our original sample to estimate the posterior probability of each occupation period in additional areas. The resulting land-use ubiquity maps for each occupational period are shown in Fig. 7.

Land-use Intensity in the Canal de Navarrés survey area

Land-use ubiquity alone does not account for the intensity of land-use through time. For example, a collection unit may contain only a single artifact that is uniquely associated with a single occupation period, while another collection unit has 100 artifacts uniquely associated with a single occupation period. Both of these collection units would be assigned a high posterior probability for the associated occupational period, even though the intensity of land-use in those two collection units is likely very different. Estimations of artifact abundance and accumulation rates are incorporated into land-use

Table 6: Posterior Probabilities for All Collection Units with Artifacts Other than Undifferentiated Lithics.

Zone	Sector	Parcel	MP	UP	LUP	EM	LM	EN	MN	LN	BB
1	1	900568	0.036	0.214	0.214	0.214	0.071	0.071	0.071	0.071	0.036
		1100119	0.033	0.200	0.200	0.200	0.133	0.067	0.067	0.067	0.033
		1100140	0.182	0.091	0.091	0.182	0.091	0.091	0.091	0.091	0.091
		1100168	0.063	0.125	0.125	0.125	0.125	0.125	0.125	0.125	0.063
	2	1100355	0.024	0.146	0.146	0.146	0.220	0.146	0.049	0.098	0.024
2	2	600256	0.036	0.214	0.214	0.214	0.071	0.071	0.071	0.071	0.036
		900041	0.200	0.100	0.100	0.100	0.100	0.100	0.100	0.100	0.100
	7	1300156	0.353	0.059	0.059	0.235	0.059	0.059	0.059	0.059	0.059
		400173	0.077	0.077	0.077	0.077	0.154	0.154	0.154	0.154	0.077
3	2	2100131	0.036	0.214	0.214	0.214	0.071	0.071	0.071	0.071	0.036
	3	2200018	0.036	0.214	0.214	0.214	0.071	0.071	0.071	0.071	0.036
		2500013	0.043	0.043	0.043	0.043	0.043	0.043	0.043	0.348	0.348
		2200015	0.036	0.214	0.214	0.214	0.071	0.071	0.071	0.071	0.036
		2200016	0.429	0.071	0.071	0.071	0.071	0.071	0.071	0.071	0.071
	5	1000050	0.036	0.214	0.214	0.214	0.071	0.071	0.071	0.071	0.036
4	1	200087	0.020	0.080	0.080	0.080	0.180	0.120	0.120	0.120	0.200
		100392	0.036	0.214	0.214	0.214	0.071	0.071	0.071	0.071	0.036
		100312	0.036	0.214	0.214	0.214	0.071	0.071	0.071	0.071	0.036
		100307	0.045	0.341	0.205	0.205	0.045	0.045	0.045	0.045	0.023
		100279	0.029	0.171	0.171	0.171	0.257	0.057	0.057	0.057	0.029
		100168	0.019	0.077	0.077	0.077	0.077	0.077	0.077	0.231	0.289
		0200089B	0.036	0.214	0.214	0.214	0.071	0.071	0.071	0.071	0.036
		200073	0.025	0.100	0.100	0.100	0.050	0.225	0.225	0.150	0.025
		100276	0.171	0.114	0.114	0.343	0.057	0.057	0.057	0.057	0.029
		100283	0.021	0.250	0.187	0.187	0.187	0.063	0.042	0.042	0.021
		100277	0.030	0.121	0.273	0.273	0.091	0.061	0.061	0.061	0.030
		100319	0.025	0.100	0.100	0.100	0.050	0.225	0.225	0.150	0.025
		100164	0.025	0.100	0.100	0.100	0.050	0.225	0.225	0.150	0.025
		100137	0.036	0.214	0.214	0.214	0.071	0.071	0.071	0.071	0.036
		0100109B	0.171	0.114	0.114	0.343	0.057	0.057	0.057	0.057	0.029
		0100109C	0.032	0.129	0.129	0.129	0.065	0.065	0.065	0.065	0.323
		200076	0.036	0.214	0.214	0.214	0.071	0.071	0.071	0.071	0.036
		200074	0.036	0.214	0.214	0.214	0.071	0.071	0.071	0.071	0.036
		200086	0.429	0.071	0.071	0.071	0.071	0.071	0.071	0.071	0.071
		200075	0.036	0.214	0.214	0.214	0.071	0.071	0.071	0.071	0.036

Table 6: Continued

Zone	Sector	Parcel	MP	UP	LUP	EM	LM	EN	MN	LN	BB
4	1	100221	0.286	0.048	0.048	0.381	0.048	0.048	0.048	0.048	0.048
		100252	0.036	0.214	0.214	0.214	0.071	0.071	0.071	0.071	0.036
		100245	0.036	0.214	0.214	0.214	0.071	0.071	0.071	0.071	0.036
		100353	0.036	0.214	0.214	0.214	0.071	0.071	0.071	0.071	0.036
		100147	0.036	0.214	0.214	0.214	0.071	0.071	0.071	0.071	0.036
		100155	0.429	0.071	0.071	0.071	0.071	0.071	0.071	0.071	0.071
		0100109A	0.200	0.100	0.100	0.100	0.100	0.100	0.100	0.100	0.100
	2	1000508	0.022	0.130	0.130	0.130	0.196	0.196	0.087	0.087	0.022
5	1	100181	0.055	0.218	0.273	0.273	0.109	0.027	0.018	0.018	0.009
		100288	0.020	0.184	0.184	0.184	0.245	0.082	0.041	0.041	0.020
		100372	0.014	0.203	0.122	0.122	0.122	0.162	0.122	0.122	0.014
		400003	0.021	0.125	0.125	0.125	0.042	0.042	0.042	0.312	0.167
		200018	0.022	0.130	0.087	0.087	0.087	0.043	0.043	0.326	0.174
		100263	0.069	0.207	0.207	0.207	0.069	0.069	0.069	0.069	0.034
		100292	0.118	0.118	0.118	0.441	0.059	0.059	0.029	0.029	0.029
		400004	0.063	0.187	0.187	0.281	0.063	0.063	0.063	0.063	0.031
		200012	0.056	0.056	0.056	0.056	0.056	0.056	0.056	0.056	0.556
		300018	0.036	0.214	0.214	0.214	0.071	0.071	0.071	0.071	0.036
		100180	0.036	0.214	0.214	0.214	0.071	0.071	0.071	0.071	0.036
		100199	0.036	0.214	0.214	0.214	0.071	0.071	0.071	0.071	0.036
		500045	0.056	0.056	0.056	0.056	0.056	0.056	0.056	0.056	0.556
	2	100028	0.036	0.214	0.214	0.214	0.071	0.071	0.071	0.071	0.036
6	1	300362	0.059	0.118	0.118	0.176	0.059	0.059	0.059	0.059	0.294
		300361	0.026	0.103	0.231	0.231	0.231	0.051	0.051	0.051	0.026
		300204	0.036	0.214	0.214	0.214	0.071	0.071	0.071	0.071	0.036
7	4	1300198	0.029	0.059	0.265	0.265	0.177	0.059	0.059	0.059	0.029
		500313	0.026	0.154	0.154	0.154	0.051	0.051	0.077	0.231	0.103
		500317	0.036	0.214	0.214	0.214	0.071	0.071	0.071	0.071	0.036
		1300166	0.036	0.214	0.214	0.214	0.071	0.071	0.071	0.071	0.036

ubiquity to assess the overall land-use intensity (Barton et al., 2004, 1999) throughout the survey area.

Artifact abundances are weighted by ranking artifacts in each collection unit by artifact density (lithic pieces per square kilometer) into five quantile groups (Barton et al., 2004, 1999). Each group is assigned a weight, which is then multiplied by the posterior

probabilities for that collection unit. Weights are as follows: 1.00 for collection units with densities in the 91st–100th percentile, 0.90 for collection units in the 75th–90th percentile, 0.75 for collection units in the 51st–75th percentile, 0.50 for collection units in the 26th–50th percentile, 0.25 for collection units in the 1st–25th percentile, and 0 for collection units with no artifacts. The resulting index accounts for the density of artifacts in assessing the intensity of land-use across the study area. See Barton et al. (2004) for more details on this methodology.

Artifact accumulation rates through time can also influence the interpretation of land-use intensity for each occupation period. This is particularly relevant as the chronological sequence for the Canal de Navarrés contains highly variable accumulation times (e.g. Middle Paleolithic encompasses 70 millennia and Bell Beaker encompasses 0.7 millennia). The intensity index developed for artifact densities is scaled by the number of years in each occupational period (in kyr) to account for differences in artifact accumulation rates (Barton et al., 2004). All values are then rescaled from 0 to 1 and b-spline interpolation (directional steps = 150 m; smoothing parameter = 0.01; 30 m resolution) is used to generate a settlement intensity surface at the scale of the survey area. The resulting land-use intensity maps for each occupational period are shown in Fig. 8.

Discussion

Artifact Densities and Spatial Distribution

Our off-site survey methodology, adapted for surveying in agriculturally modified landscapes, resulted in a spatially and temporally explicit evaluation of prehistoric land-

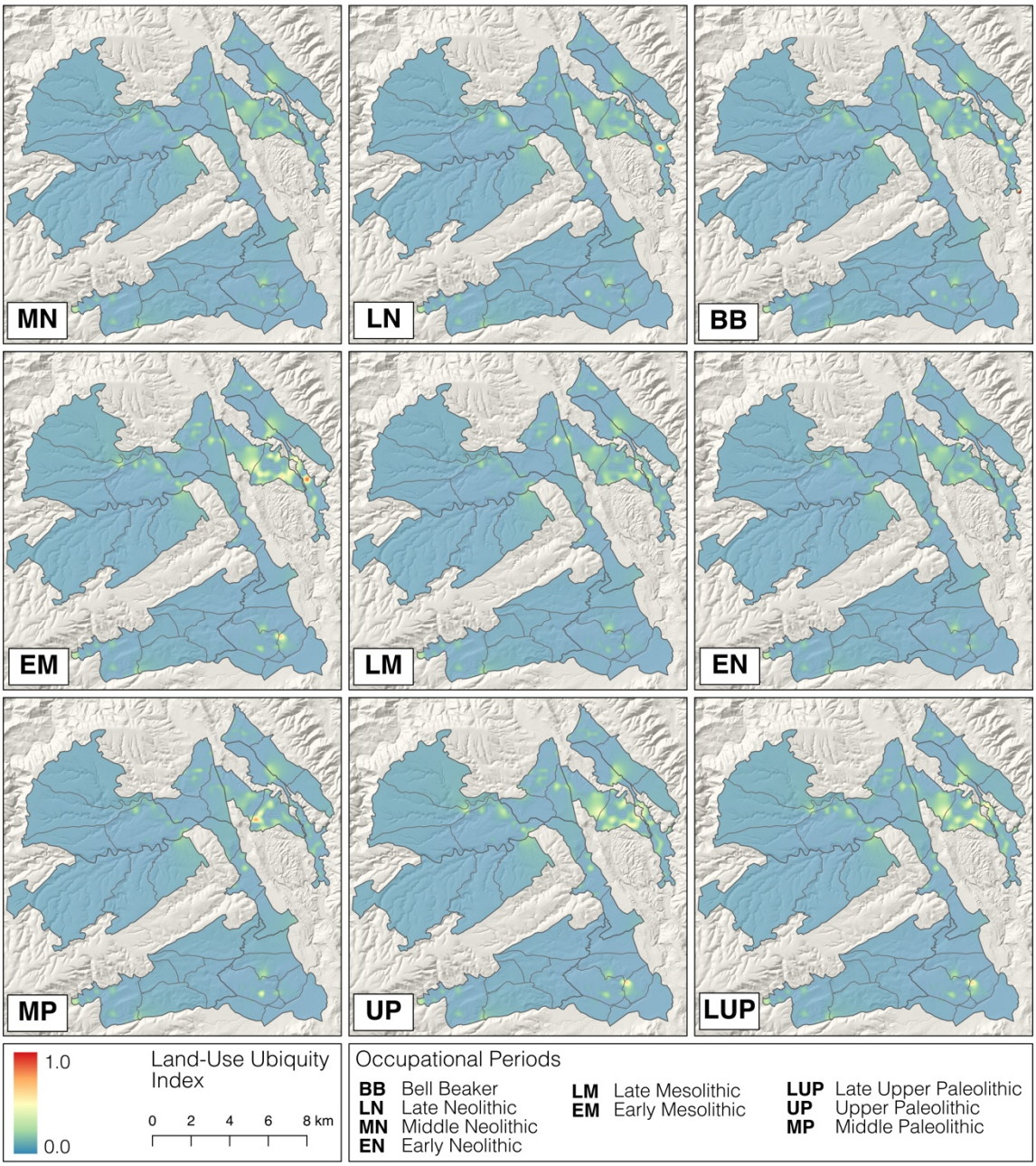

Fig. 7: B-spline Interpolated Surface (Spline Step = 150 m, Smoothing Parameter = 0.01) of Land-use Ubiquity by Occupational Period.

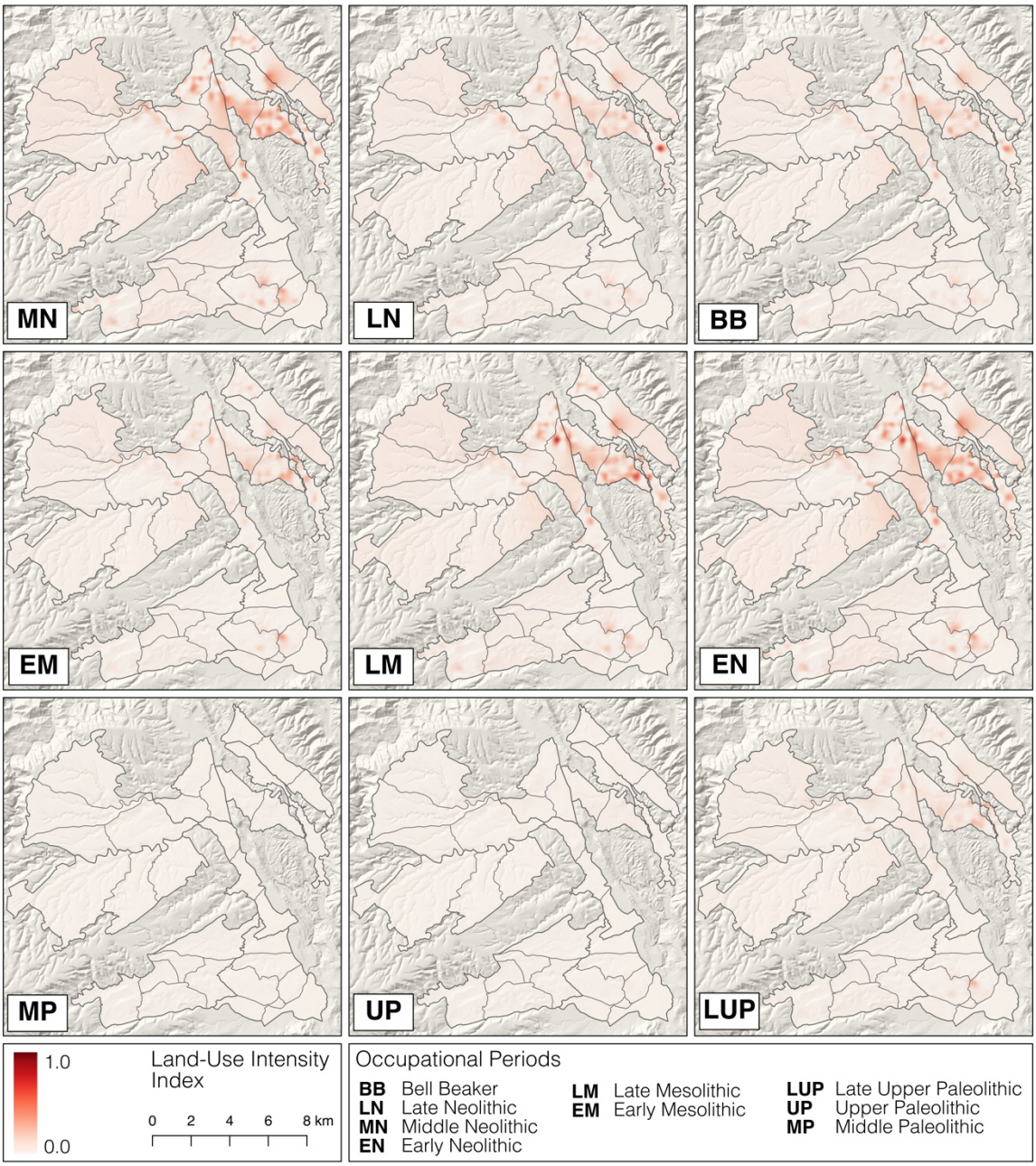

Fig. 8: B-spline Interpolated Surface (Spline Step = 150 m, Smoothing Parameter = 0.01) of Land-use Intensity by Occupational Period.

use in the Canal de Navarrés. Artifact densities demonstrated spatial variation throughout the study area, with zones 1, 2, 4 and 5 yielding highest concentrations of artifacts. Upland areas in zones 3, 6, 7, 8, and 9, have relatively low concentrations of lithic artifacts. This distribution suggests that lowland and transitional areas were preferentially used for prehistoric land-use activities resulting in relatively high artifact accumulations (i.e. encampments, resources processing, villages, small-scale agricultural activities, etc.).

These results fit well with previous local and regional archaeological research, which has identified late Pleistocene and the Holocene occupations in and around lakes or upwellings in valley bottoms (Barton et al., 2012; C. M. Barton et al., 2010). Concentrations of lithic artifacts correspond with the previously known prehistoric sites, such as Ereta del Pedregal, Las Fuentes, and l'Albufera d'Anna. Several previously uninvestigated areas, such as the northern portion of sector 5-1 almost the entirety of sector 4-1, and several collection units in Zone 10 near the small lake of Gorgo del Catalan, contain high densities of lithic artifacts and likely represent unrecorded prehistoric occupational areas.

Upland areas demonstrating low densities of artifacts also fit with our expectations regarding the distribution of prehistoric land-use in the survey area. These areas were likely less important for prehistoric land-use or were used for hunting or pastoralism, activities that that may result in low-density artifact accumulations. It should be noted that erosion in upland areas and on hillslopes might have also contributed to low artifact densities. Portions of zones 3 and 9 are severely deflated with exposed bedrock between cultivated pockets of sediment. If surface artifact assemblages existed in these areas, they were likely re-deposited on the surface downslope.

To accommodate for the potential of redistributed artifacts due to erosion, we sampled upland fields with both highly deflated fields and fields with relatively stable, intact sediments. Both contexts yielded few prehistoric artifacts. Additionally, if artifacts were moving downslope due to sheet wash or other erosional processes, we would expect to find high concentrations of artifacts in terraces located at mid-slope or at the bases of hills. Even if artifacts were buried, repetitive plowing would have exposed some re-deposited artifacts in this zone. This is not the case, as the highest densities of artifacts are found near perennial, mid-valley seeps and springs. We are confident that fields surveyed in zones 3, 6, 8, and 9 adequately represent low-density artifact accumulations and evidence for low-intensity upland prehistoric land-use.

Paleolithic and Early Mesolithic Land-use in the Canal de Navarrés

Late Pleistocene and Early Holocene occupational periods (including the Middle Paleolithic, Upper Paleolithic, Late Upper Paleolithic, and Early Mesolithic periods) shared similar spatial ubiquities and intensities throughout survey area with particular abundance in zones 3, 4, 5, 6, and 8. Boxplots of posterior probabilities for lithics recovered from all collection units (Fig. 9) indicate high average posterior probabilities for Upper Paleolithic, Late Upper Paleolithic periods and Early Mesolithic, as well as abundant, high value outliers for the Middle Paleolithic. The statistical distribution of posterior probabilities for the Middle Paleolithic is explained by a combination of two artifact types with unimodal associations with this period (Mousterian technology and discoidal/levallois flake technology) and their presence in collection units where only these artifacts are observed. These two factors result in very high posterior probabilities

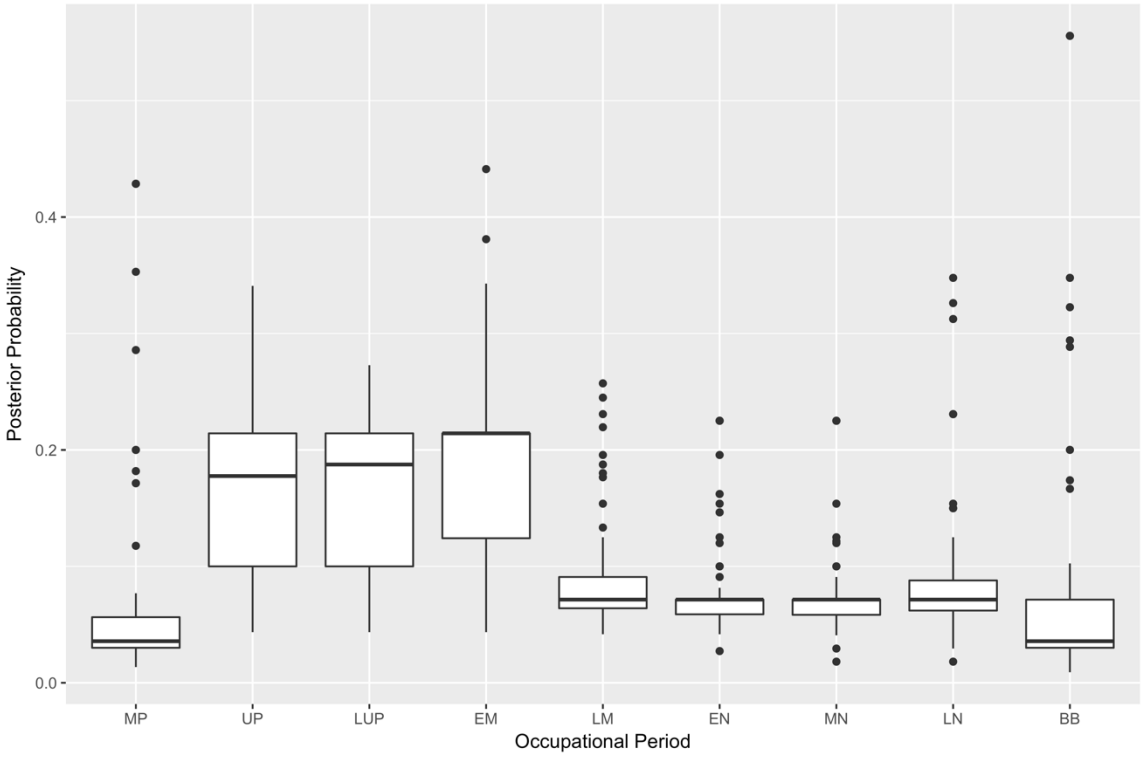

Fig. 9: Boxplots of Posterior Probabilities for Lithics Recovered from All Collection Units.

and ubiquity values in spatially precise places on the landscape. Such is the case in sector 4-1, where Middle Paleolithic associated artifacts have high ubiquity values due to their presence in a small number of collection units.

Upper Paleolithic, Late Upper Paleolithic, and early Mesolithic periods have the highest average ubiquity values and are widely distributed through the survey area. Ubiquity values indicate that these lithic forms are consistently located either near the previously identified prehistoric sites of Las Fuentes and l'Albufera d'Anna, as well as in the newly identified high-artifact density areas in sectors 4-1 and 5-1. The spatial distributions of these two periods are very similar and cannot be easily differentiated with the data collected.

Although ubiquity values during the late Pleistocene and early Holocene periods are relatively high, accumulation rates are very low due to the extended length of these periods (Table 3). As illustrated in Fig. 8, settlement intensity during the Paleolithic and early Mesolithic is consequently low when compared to the middle Holocene. Paleolithic land-use in the Canal de Navarrés was either at a consistent low-intensity, or episodic, with periods of high-intensity followed by extended hiatuses.

Late Mesolithic and Early-Middle Neolithic Land-use in the Canal de Navarrés

Undifferentiated lithics and blade technology represent the majority of the artifact forms associated with middle Holocene periods. The overall pattern of ubiquity and intensity follows closely with the general distribution of artifact densities across the study area, with concentrations of artifacts in lowland areas and near previously recorded sites. This is not to say that prehistoric land-use did not occurring during these periods, but rather we cannot confidently identify specific markers of Late Mesolithic or Neolithic occupations from the surface assemblages. Due to the short duration of each of these occupational periods, potential settlement intensity is relatively high across each of these periods.

It should be noted that it is during these periods that previous paleoecological research within the Canal de Navarrés identified substantial transition from pine to oak-dominated vegetation communities during the middle Holocene. Carrion and Van Geel (1999) remarked that this shift was independent of regional climate variation and co-occurred with an increase in regional charcoal concentrations associated with the arrival of early Neolithic. The lack of surface artifacts highly associated with the late Mesolithic

and early-middle Neolithic occupational periods complicates this assertion. Further investigations into the social and ecological processes behind the co-occurrence of anthropogenic fire and this vegetation transition are needed.

Late Neolithic and Bell Beaker (Chalcolithic) Land-use in the Canal de Navarrés

Estimates for the Late Neolithic and Bell Beaker land-use ubiquity and intensity maintain much of the same spatial structure as previous middle Holocene occupational periods. The pattern deviates in zones 4, 5, and 7 where lithic forms particularly associated with the Late Neolithic or Bell Beaker periods (denticulated sickle blades and foliate/bifacial projectile points) are present along with undifferentiated lithics. These areas are represented as 'hot-spots' of late prehistoric land-use (Fig. 7). Average posterior probabilities for the Late Neolithic and Bell Beaker periods are low, with the exception of a series of high value outliers caused by these artifact forms.

Although surface assemblages associated with Late Neolithic and Bell Beaker occupations do occur in same sector as the site of Ereta del Pedregal, it is notable that no high probability 'hot-spots' are located adjacent to the site. Potentially high rates of late Holocene erosion and deposition may have resulted in deeply buried assemblages that are not well represented on the surface. Late Neolithic and Chalcolithic artifacts were recovered at depths of over two meters during previous excavations—well outside the plow zone and influence of most agricultural land-use (Fletcher Valls, 1964; Pla Ballester et al., 1983). Ereta del Pedregal is positioned within the valley bottom in a location susceptible to high rates of deposition from nearby drainages and active alluvial fans. Subsurface testing planned for the future field seasons will hopefully confirm that

additional buried deposits closely associated with the Late Neolithic and Early Bell beaker periods are present.

Future directions for evaluating archaeological surface assemblages in agricultural modified landscapes

While the Bayesian approach applied to the Canal de Navarrés survey allows us to make interpretations about the changing spatial patterns and intensity of land-use through time, we believe future work can continue to improve these methods. One of the primary drivers of our results is the diversity of temporally sensitive lithic artifact forms assigned to each occupational period. Although only lithic artifacts were included in this project due to their abundance on the surface in the Canal de Navarrés, we could increase the diversity of temporally sensitive artifact forms by incorporating ceramic or groundstone artifacts (Fernández-López de Pablo and Barton, 2013). Since very few non-lithic artifacts we recovered in the Canal de Navarrés, increasing survey coverage or extending the bounds of the survey area to include surrounding valleys could result in a more diverse selection of artifact forms to create the calibration dataset for this analysis, as well as increase the spatial representativeness of our sample.

Additionally, the extensive modification of the survey area by modern agriculture played a critical role in the design of our survey methods, application of Bayesian methods, and the interpretation of the complex palimpsests of archaeological material in the Canal de Navarrés. Plowing, terrace building, and other ground disturbing agricultural activities provided a mechanism for moving artifacts from multiple occupational periods to the surface. We sampled zones with differing intensities of modern land-use in an

effort to evaluate its effects on our survey results (see Table 1). Zones with high or moderate intensities of land-use yielded the highest densities of artifacts, but future work is required to determine to what degree these results are due to modern agriculture, patterns of prehistoric settlement, or both.

Conclusions

This paper presents the results of off-site, patch-based survey methods for agricultural modified landscapes in the Canal de Navarrés, Valencia, Spain. Digital data collection and a focus on evaluating artifact densities across the landscape allowed us to move away from attempting to identify sites and instead focus on recording spatial information pertaining to the prehistoric and modern land-use. This approach allows us to interpret the distribution and intensity of prehistoric artifacts, as well as evaluate the impact of modern agriculture, surface visibility, and geomorphic processes on our interpretations.

Bayesian methods for estimating ages of surface assemblages allow us to derive more robust chronologies from our data than would be otherwise possible. By formalizing how we incorporate prior knowledge about archaeological assemblages from throughout the Valencian region into our survey results, we can begin to address the interpretive problems associated with palimpsests. Combining Bayesian posterior probabilities, with GIS spatial analysis techniques, allows us to track diachronic change in the Canal de Navarrés through measurements of land-use ubiquity and intensity. These two measures provide a more complete picture of changing land-use that incorporates the

influence of artifact density and accumulation rates through time. We are able to evaluate the chronology and intensity of prehistoric land-use with the goal of identifying changing interactions between long-term social and ecological systems. This work would not be possible without a suite of analytical tools that can accommodate intensively modified landscapes and derive conclusions without relying on site-based investigations.

CHAPTER III

IDENTIFYING NATURAL AND ANTHROPOGENIC DRIVERS OF PREHISTORIC FIRE REGIMES THROUGH SIMULATED CHARCOAL RECORDS

Grant Snitker

Introduction

Humans are uniquely able to take advantage of the ecological impacts of fire and use it as a tool to create and sustain changes to their environments (Boivin et al., 2016; Bowman et al., 2011; Ellis, 2015; Roos et al., 2014; Scott et al., 2016). Regular and controlled use of fire by hominins dates to the Middle Pleistocene, but measurable impacts of anthropogenic fire on terrestrial and atmospheric systems are most evident during the last several millennia (Bowman et al., 2011; Roebroeks and Villa, 2011; Shimelmitz et al., 2014). Multiple global syntheses of archaeological and ethnographic case studies identify fire's role in political, religious, and ecological realms, including burning practices associated with land clearing, warfare, game driving, propagating beneficial plant and animal species, and fire prevention (Bliege Bird et al., 2008; Bowman et al., 2011; Pyne, 2012; Scherjon et al., 2015; Trauernicht et al., 2015). Diversity in anthropogenic fire can create variation in regional fire regimes; however, evidence of human-driven ignitions is not readily observable in sedimentary charcoal

records, particularly when these fires co-occur with large-scale changes in climate and fuels.

This paper presents the Charcoal Record Simulation Model (CharRec), a computational model that simulates the formation of a sedimentary charcoal record based on varying fire regime components, including fire frequency, intensity, size, and spatial distribution. Within the model, fire regimes can be modified to represent differing human and climate drivers. Following a pattern-oriented modeling approach, CharRec is built using a bottom-up strategy where observable patterns within target datasets inform programming decisions (Grimm et al., 2005). This strategy allows CharRec to function as a "virtual laboratory," where multiple model outputs are compared to patterns within empirical charcoal data to identify which combinations of fire regime components mostly likely contributed to the formation of the empirical record through time (Bankes et al., 2002).

Formation and interpretation of sedimentary charcoal records

Variation in the concentration of charcoal particles from lacustrine cores or terrestrial sediment samples is commonly used to identify paleoenvironmental trends in landscape fire (Bowman et al., 2011, 2009; Whitlock and Anderson, 2003; Whitlock and Larsen, 2001). Bridging the interpretive gap between charcoal abundance and fire history has remained at the forefront of paleoecological research for several decades. The theoretical relationships between charcoal transport and accumulation were first proposed by Clark (1988) and have since been expanded and tested in experimental contexts (Clark et al., 1998; Clark and Royall, 1996, 1995; Lynch et al., 2004; Peters and Higuera, 2007).

Fire history interpretations from these models rely on two major underlying assumptions: 1) the physics of primary charcoal transport result in spatially discernable differences in the distribution of charcoal particles following a fire; and 2) secondary charcoal transport is minimal and does not obfuscate patterns of primary deposition and fire occurrence (Higuera et al., 2007).

The spatial distribution and abundance of primary charcoal dispersed via aerial transport during a fire is assumed to be a function of charcoal attributes related to fuel combustion, such as particle size, morphology, shape, and density, as well as combustion conditions, including wind velocity and plume injection height (Clark, 1988a; Clark et al., 1998; Enache and Cumming, 2007, 2006; Lynch et al., 2004; Peters and Higuera, 2007; Vachula and Richter, 2018). Generally, the relationship between these variables results in spatially differentiated dispersion, where macroscopic charcoal particles (typically >100 μm) are dispersed close to their source and are interpreted as local in origin; microscopic charcoal particles (typically <100 μm) can be dispersed greater distances and are typically interpreted as representing regional fires (Clark, 1988b; Clark et al., 1998; Ohlson and Tryterud, 2000). Although this relationship assumes that atmospheric and combustion conditions remain constant throughout the duration of a fire, transport distances based on charcoal size have been validated in multiple empirical studies (Clark and Royall, 1996; Gardner and Whitlock, 2001; Lynch et al., 2004; Ohlson and Tryterud, 2000; Pisaric, 2002; Tinner et al., 2006; Whitlock and Millspaugh, 1996).

Secondary charcoal refers to charcoal introduced into the sedimentary record during non-fire years and can include geomorphological processes such as run-off, post-depositional sediment mixing, or other landscape reservoir effects. Empirical studies of

post-fire slope-wash estimate that the contribution of additional charcoal from non-fire years can continue for upwards of a decade, but in quantities small enough not to mask primary deposition (Carcaillet et al., 2006; Clark, 1988a; Clark et al., 1998; Lynch et al., 2004; Patterson et al., 1987; Whitlock and Millspaugh, 1996). Mixing within the sediment column can further blur, but not entirely obscure primary charcoal. Statistical methods for peak detection and sampling strategies targeting on return intervals help to account for these processes (Clark, 1988b; Higuera et al., 2010; Kelly et al., 2011).

Peak detection methods rely on separating a charcoal series into its background and peak components. Background charcoal refers to low-frequency variations in macro-charcoal accumulation, as well as the contributions from secondary charcoal transport (Higuera et al., 2010; Kelly et al., 2011) . When background charcoal is statistically removed, peak charcoal related to primary transport and deposition is easily distinguishable. The distinction between background and peak charcoal components may be unclear in landscapes with both natural and anthropogenic ignition sources. Ethnographic examples of managed fire indicate that ignitions are often spatially circumscribed, frequent, and at low intensities (Scherjon et al. 2015), hence it is possible that local anthropogenic burning may contribute to low-frequency accumulations of macro-charcoal without clear and discernible peaks. Thus, the anthropogenic signal may be misidentified or obscured, particularly if a sampling strategy is not designed to accommodate for short fire return intervals.

Anthropogenic fire in the archaeological record

Humans have intentionally set fires for millennia to transform the arrangement or

diversity of resources within their landscape (Boivin et al., 2016; Pyne, 2012). Identifying prehistoric human influences on fire regimes remains difficult due to a mismatch between available archaeological data on human activities and paleoecological data on fire and vegetation change (Bowman et al., 2011). Prominent archaeological approaches to fire have centered on detecting evidence of landscape burning in relation to food production and hunter-gatherer impacts on ancient environments. Low-level food production (Smith, 2001), "fire-stick" farming (Bird et al., 2005; Bliege Bird et al., 2013, 2008), swidden agriculture (Levin and Ayres, 2017; Roos, 2008; Roos et al., 2016; Schier et al., 2013), and mitigating resource vulnerability (Freeman and Anderies, 2012) suggest that fire was an important tool for creating predictable resource mosaics within landscapes across the globe (*North America:* (Liebmann et al., 2016; Roos, 2015; Roos et al., 2010; Sullivan et al., 2015; Sullivan and Forste, 2014; Swetnam et al., 2016; Taylor et al., 2016; Van de Water and Safford, 2011; Walsh et al., 2010); *Europe:* Doyen et al. 2012; Innes et al. 2013; *Southeast Asia/Oceania:* (Maxwell, 2004; McGlone, 2001; McWethy et al., 2010, 2009; Roos et al., 2016); *Neotropics:* Dull 2004; Nevle et al. 2011).

Human-caused ignitions can also drive fire regimes in regions with long-term histories of agricultural land-use (Carrión et al., 2010, 2001; Colombaroli et al., 2008; Vannière et al., 2008). For instance, Pitkänen et al. examined two lacustrine sediment cores from Lake Pönttölampi in eastern Finland to evaluate the formation of the local charcoal record and its association with documented "slash and burn" agricultural practices (Pitkänen et al., 1999; Pitkänen and Huttunen, 1999). By examining charcoal data in conjunction with historical maps of land-use and fire-scarred trees, Pitkänen and colleagues (1999) concluded that frequent, low-intensity fires associated with

maintaining open woodlands contributed significantly to the sedimentary charcoal record and were the primary driver of local fire history. Unfortunately, the patterns reported by this study would be difficult to observe in prehistoric contexts that predate historic documents and living, fire-scarred trees. Simulation models provide an opportunity to examine multiple patterns of burning in prehistory while accommodating complex patterns of both natural and anthropogenic ignition sources. Evaluating simulations against empirical charcoal data allows multiple, alternative interpretations of prehistoric fire regimes to be tested, adapted, and improved.

Materials and Methods

Introduction to CharRec and model design considerations

CharRec is a spatially explicit computational model that simulates the formation of long-term charcoal records based on empirically supported models of primary charcoal transport (Fig. 10). The model is an exploratory tool that assists researchers in interpreting how natural and anthropogenic fire regime components contribute to the formation a sedimentary charcoal record. One of the most challenging aspects of developing computer simulations of social-ecological systems is including enough complexity to address specific research questions while reducing the amount of uncertainty in the model structure and parameters. Pattern-oriented modeling offers a strategy for optimizing the relationship between complexity and uncertainty by focusing on multiple patterns observed in real systems at differing scales (Grimm et al., 2005). Such models focus on a small number of underlying processes that can be calibrated

independently to influence the overall pattern of the system (2005:989). CharRec does not attempt to capture the extensive complexity of charcoal production, dispersion, and deposition. Instead, it utilizes four specific components that contribute to the overall patterning of primary charcoal in sedimentary records. These include fire spatial distribution, frequency, size, and intensity. These characteristics are most susceptible to manipulation by humans, thus providing a means for testing the influence of burning practices related to land-use on the formation of charcoal records.

The following section provides details regarding the specific modules that comprise CharRec and presents a statistical method for systematically comparing CharRec simulated charcoal data to empirical datasets. CharRec is built in Netlogo Version 6.0.2, an agent-based programming language and open-access modeling environment (Wilensky, 1999). Netlogo is ideal for this modeling application because it is easily programmed and customized, has a user-friendly interface, and the ability to couple with other open-access GIS and statistical software. The model and ODD documentation are publically available through the CoMSES Net Computational Model Library (https://www.openabm.org/model/4795).

CharRec modules and main components

CharRec is composed of five modules, which include the 1) Landscape, 2) Ignition Scenario, 3) Burn, Disperse, and Deposit, 4) Form record, and 5) Export modules; together these simulate the formation of a sedimentary charcoal record on an annual time scale. In a simulation run, fires disperse micro- and macro-charcoal

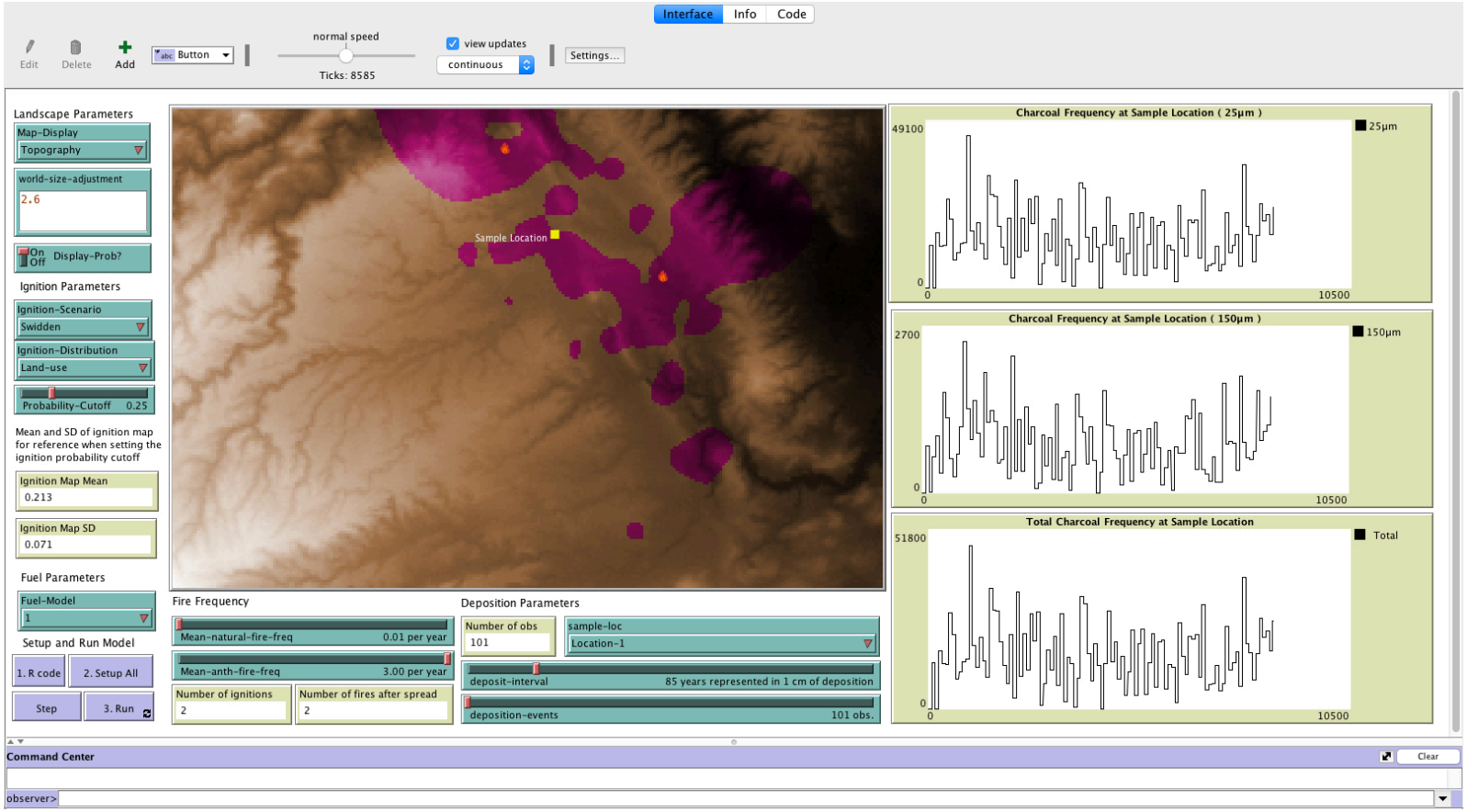

Fig. 10: CharRec Interface, Showing a Landscape Map, Sample Location, Fires, and Various User-defined Ignition Scenario Parameters and Outputs.

throughout the landscape, which is aggregated at a designated sampling point according to a set deposition interval (e.g., 100 years cm^{-2}). At the end of each deposition interval, charcoal counts are exported as a single observation in the charcoal record series. A diagrammatic representation of the relationship between CharRec modules is illustrated in Fig. 11.

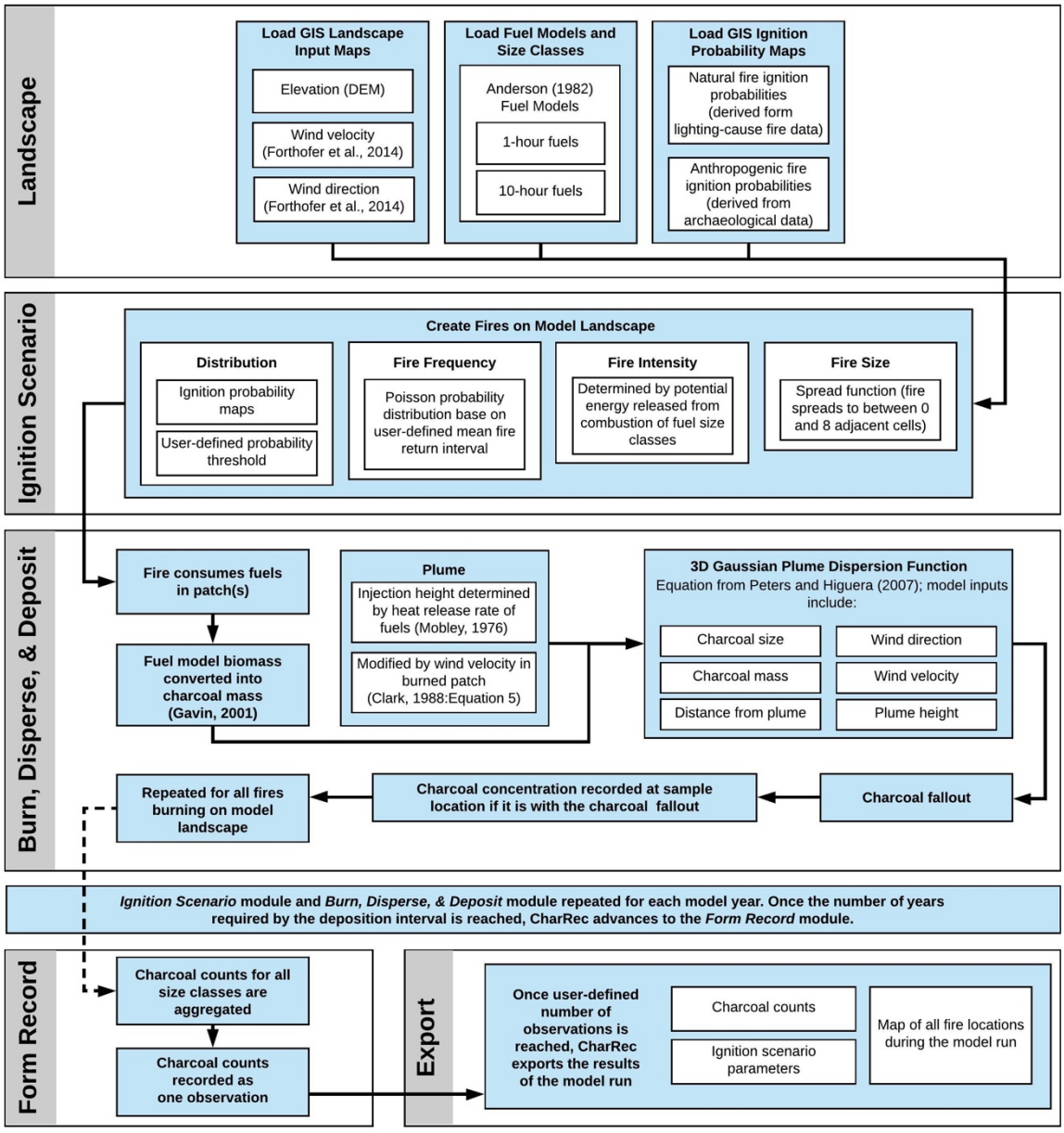

Fig. 11: Diagrammatic Representation of CharRec Modules and Data Inputs.

Landscape module

The CharRec model landscape is a geo-referenced representation of a user-defined study area and is composed of rasters representing topographic, atmospheric, and fuel conditions. The physical terrain of the model landscape is represented by a raster digital elevation model (DEM) applied to each landscape patch. Atmospheric input rasters are created from modern local weather station measurements of wind velocity and direction (IVIA, 2015). These data are interpolated across the model landscape using WindNinja, a free software program developed by the U.S Forest Service Rocky Mountain Research Station's Fire, Fuel, Smoke Science Program (Forthofer et al., 2014). WindNinja creates patch-specific, spatially varying wind fields based on topographic variation.

Fuels in CharRec are based on the 13 fuel models developed by Anderson (1982) for predicting wildfire behavior. Although updated models have improved accuracy in North American ecosystems (see Scott and Burgan, 2005), the original 13 models have been adapted to describe a diverse range of international ecosystems. For broad usability, CharRec uses these original models. Available dead and live biomass approximations for 1-hour and 10-hour fuel size classes are assigned to each landscape patch. For each simulation, a single fuel model is distributed homogenously across all patch. Potential heat release rates from combustion are calculated for all fuel model size classes (Johansen et al., 1976: Equation 1) and used to approximate plume injection heights resulting from convective uplift (Clark, 1988a: Equation 5). These calculations are done assuming a wind velocity of 0 meters sec^{-1}, thus producing the maximum potential plume

injection height for each fuel class. These data are saved in CharRec as global variables for later use in the Burn, Disperse, and Deposit module.

Ignition Scenario module

The Ignition Scenario module determines the fire regime components (fire spatial distribution, frequency, size, and intensity) used each model run. These variables are set by the user to simulate natural or anthropogenic ignitions and influence charcoal production, dispersion, and deposition in subsequent modules. To begin the module, fire frequency is determined annually by a Poisson probability distribution based on a user-defined mean-ignitions-per-year value (see Higuera et al., 2007 for a similar method). A low mean-ignitions-per-year value may result in many model years that do not have any fires burning on the landscape, while a higher value will allow for multiple fires to burn simultaneously.

Fire spatial distribution is determined by the ignition probability of each landscape patch. A random-number algorithm is used to determine a fire's potential location; this algorithm is weighted to favor areas with high ignition probabilities over those with low probabilities. The range of probability values available to the random-number algorithm is set by a user-defined probability cutoff. In practice, if the probability cutoff is set at 0, all landscape patches within the model landscape have the potential to ignite. If the probability cutoff is set at 0.5, a subset of landscape patches with ignition probabilities above or equal to 0.5 have the potential to ignite. The probability cutoff parameter allows for a range of spatial configurations to be tested.

Changes in fire size are modeled through a spread function that randomly selects the number of directly adjacent patches that a fire will spread to. The number of adjacent patches ranges from 0 to 8; a value of 0 indicates that a fire will remain in its original patch (0.09 ha), while a value of 8 indicates the fire will spread to all adjacent patches via a shared edge or a shared vertex (0.81 ha). Fire intensity of the original fire is assigned to all additional fires as it spreads.

Within CharRec, fire intensity refers to the amount of energy released from the combustion of fuels at each landscape patch (Keeley, 2009). Fuel size classes and plume injection heights calculated in the Landscape module are used to differentiate between fire intensities. For example, when an ignition scenario includes low-intensity fires, only plume injection heights calculated from the heat release rate of 1-hour fuels are used. Ignition scenarios with high-intensity fires use plume injection heights calculated from the heat release rate of both 1-hour and 10-hour fuels. Although there is variation within fuel models, generally a fire consuming 1-hour fuels results in a shorter plume injection height than a fire consuming both 1-hour and 10-hour fuels.

Burn, Disperse, and Deposit module

Once a fire ignites on a landscape patch, its intensity determines the size class of available biomass that is consumed and the injection height of the resulting plume. Available biomass is converted into charcoal mass using the conversion rate published by Gavin (2001:32). Charcoal mass is then transformed into micro- and macro-charcoal particle counts based on experimental charcoal particle size distribution data published by Pitkänen et al. (1999). Plume injection height for each fire is modified by wind velocity

at the fire's patch following the empirical relationship illustrated by Clark (1988a: Equation 5). Finally, the amount of micro- and macro-charcoal dispersed at a given x and y distance from a fire's patch is calculated using a three-dimensional form of Clark's (1988a) Gaussian aerial transport model adapted by Peters and Higuera (2007: Equations 1 and 2). The equations are reproduced below (see Table 7 for equation inputs and Higuera et al., 2007 and Peters and Higuera, 2007 for more details regarding the Gaussian aerial transport model):

$$\chi(x,y) = \frac{2\nu Q(x)}{u\pi C_y C_z x^{2-n}} \exp\left(\frac{-y^2}{C_y^2 x^{2-n}}\right) \exp\left(\frac{-h^2}{C_y^2 x^{2-n}}\right) \quad (1)$$

$$Q(x) = Q_0 \exp\left\{\frac{4v_g}{nuC_z\sqrt{\pi}} \left[\left[-x^{n/2}e^{-\xi} + \left(\frac{h}{C_z}\right)^{2m} \times \left(\Gamma(-m+1) - \Gamma_\xi(-m+1)\right)\right]\right\}\right. \quad (2)$$

Micro- and macro-charcoal fallout occurs according to wind direction at the fire's origin. Counts of micro- and macro-charcoal are recorded only when fallout reaches and deposits charcoal at the user-designated sampling site. The Burn, Disperse, and Deposit module operates for every fire that burns on the model landscape during a model year.

Form Record and Export modules

Sediment accumulation rates in CharRec are determined by a user-defined deposition interval, which sets how many years represent one cubic centimeter of deposition. Once the number of model years in the deposit interval is reached, the Form Record module aggregates charcoal counts at the sample location into single observations of micro- and macro-charcoal. A complete CharRec simulation is run for a user-defined number of deposit interval observations. At the end of the simulation, the Export module

collates all charcoal count observations created by the Form Record module, as well as ignition scenario variables used during the simulation, and exports them as a spreadsheet. A map of all fire locations created during the simulation is also exported in raster format.

Table 7: Parameters Used in Equations 1 and 2. Reproduced from Peters and Higuera (2007).

Parameter	Description
x	Distance downwind (m)
y	Distance crosswind (m)
v_g	Deposition velocity (m s^{-1})
Q_0	Source strength ($m^2 \times 100$)
u	Mean wind speed (see Sutton, 1947) (m s^{-1})
C_y, C_z	Diffusion constants ($C_y = 0.21$, $C_z = 0.12$; see Sutton, 1947) ($m^{1/8}$)
h	Source height (m)
n	Measure of turbulence near ground (1/4; see Sutton, 1947) (dimensionless)
m	$n/(4 - 2n)$ (dimensionless)
ξ	$h^2/(x^{2-n} C_z^2)$ (dimensionless)
$(\Gamma(-m+1) - \Gamma_\xi(-m+1))$	$= -m\int_\xi^\infty e^{-t} t^{-m-1} dt$ (dimensionless)

Statistical comparison of model outputs to an empirical charcoal record using LDA

Linear discriminant analysis (LDA) is a statistical method for classification that reduces a dataset into a lower dimensional space while maximizing the separation between multiple classes (Duda et al., 2001). LDA is a flexible and robust classification technique that does not require data standardization (i.e. z-score transformation) or normal distributions, making it an ideal candidate for comparing CharRec outputs to empirical sedimentary charcoal data. LDA uses an initial dataset to form linear combinations of predictor variables that emphasize differences between classification groups. The resulting linear discriminants can then be used to classify new data,

generating posterior probabilities of classification group membership for each observation in the new dataset. The best-fit classification for each new observation is determined by the highest posterior probability. The distribution of posterior probabilities for other classification groups provides insight into the quality of the best-fit classification.

When comparing CharRec simulated charcoal data to an empirical charcoal record, the unique ignition scenario parameters from each complete simulation constitutes a classification group. Linear discriminants for charcoal data created by CharRec are used to predict ignition scenario membership for each micro- and macro-charcoal observation in the empirical dataset. The ignition scenario with the highest

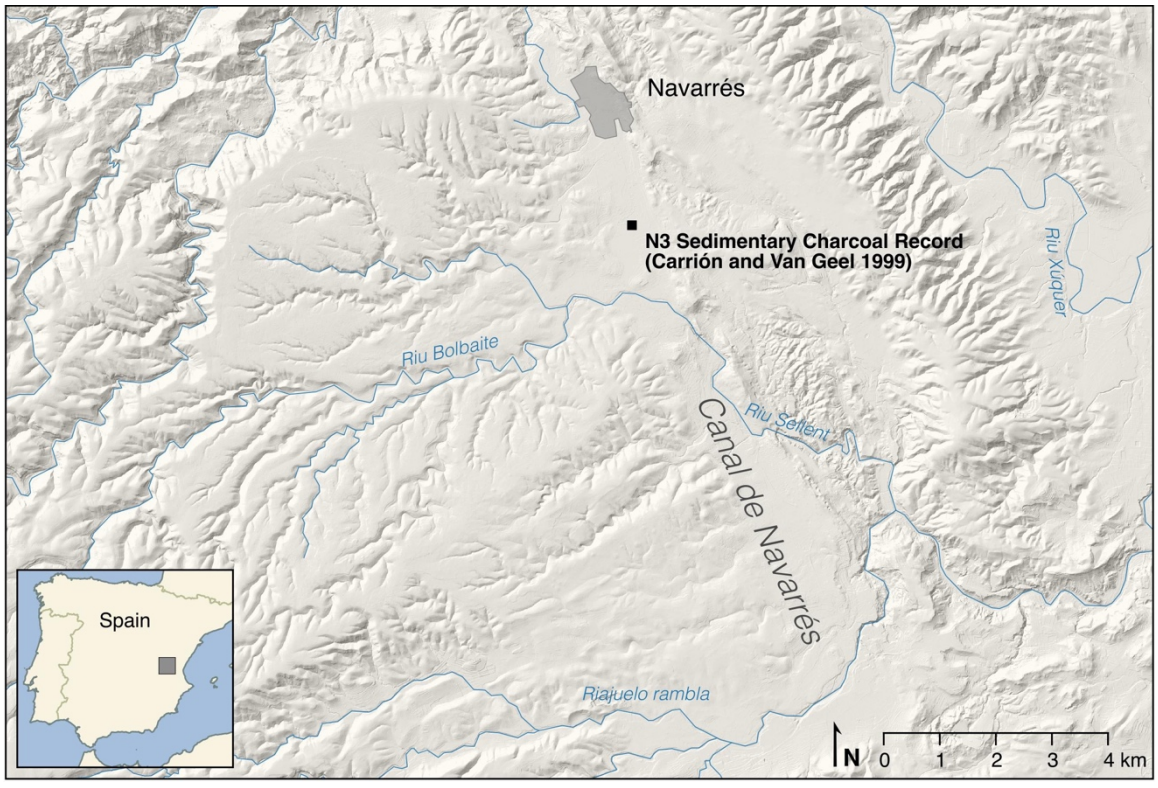

Fig. 12: Canal de Navarrés Study Area and Location of the N3 Sedimentary Charcoal Record Collected by Carrión and Van Geel (1999).

posterior probability is considered a 'best-fit' for a given observation in the empirical dataset. Prediction quality for the best-fit ignition scenario is assessed by comparing its posterior probability to the mean probability of all classification groups in the original dataset; the greater a best-fit ignition scenario's deviation from the mean posterior probability, the higher its prediction quality.

Evaluating the Canal de Navarrés sedimentary charcoal record with CharRec

To demonstrate the utility of CharRec and evaluate potential natural or anthropogenic drivers of fire regimes in an empirical test case, a series of simulated records were generated for comparison with a terrestrial sedimentary charcoal record from the Canal de Navarrés, Valencia, Spain (Fig. 12). The Canal de Navarrés (39° 06' N, 0° 41' W) is a flat-bottomed valley located at the intersection of the Iberian and Baetic mountain systems. The area is semi-endorheic due to tectonic activity, creating small lakes, peatlands, and travertines throughout the region (La Roca et al., 1996). The valley and much of surrounding uplands are currently intensively cultivated, but abandoned areas support *matorral* species such as *Quercus coccifera*, *Erica sp., Ulex europaeus,* and occasional stands of *Pinus halepensis.*

Previous archaeological research in the Canal de Navarrés has identified occupations dating as far back as the Middle Paleolithic, but for the purposes of this case study, only archaeological periods during the late Pleistocene and early/middle Holocene are addressed (see Table 8). Investigations into the early agricultural history in Canal de Navarrés began in the 1940s with the excavation of Ereta de Pedregal (Fletcher Valls, 1964; Menéndez Amor and Florschütz, 1961; Pla Ballester et al., 1983), an open-air site

located in the center of the valley. Initial testing and later excavations revealed structures and artifacts dating to the late Neolithic and Bell Beaker periods. In the decades since, the Canal de Navarrés has been studied extensively as part of a multi-year, joint research program by Arizona State University and the University of Valencia to systematically collect archaeological and paleoecological data in an effort to better understand the evolution of agro-pastoral landscapes (Diez Castillo et al., 2016; García Puchol et al., 2014; Snitker et al., 2018b). Recent archaeological survey results indicate relatively ephemeral land-use during the late Pleistocene and early Holocene, including the early (7600 – 6800 BP) and middle (6800 – 6000 BP) Neolithic periods. This trend is interrupted with a marked increase in artifact densities during the late Neolithic (6000 – 4500 BP) and Bell Beaker periods (4500 – 3800 BP), suggesting agricultural land-use intensification (Snitker et al., 2018b).

Table 8: Temporal Ranges for Archaeological Periods During the Late Pleistocene and Early/Middle Holocene in the Canal de Navarrés.

Occupational Period	Temporal Range
Bell Beaker	4500 – 3800 BP
Late Neolithic	6000 – 4500 BP
Middle Neolithic	6800 – 6000 BP
Early Neolithic	7600 – 6800 BP
Late Mesolithic	8600 – 7600 BP
Early Mesolithic	11,000 – 8600 BP
Late Upper Paleolithic	13,000 – 11,000 BP

Three terrestrial sedimentary cores (referred to as N1, N2, and N3) were collected and analyzed from peat deposits near Ereta del Pedregal to track long-term changes in vegetation, fire, and climate (Carrión and Dupré, 1996; Carrión and Van Geel, 1999). These records indicated a substantial increase in charcoal concentrations and shift from

pine- to oak-dominated vegetation communities at approximately 7000 BP (Fig. 13A-B). The introduction of agricultural burning by Neolithic farmers likely precipitated these changes, but it is difficult to determine how this process may have occurred, as well as the relative importance of anthropogenic and natural ignitions, from charcoal and pollen data alone.

To evaluate the extent to which Neolithic anthropogenic burning or natural ignitions shaped the fire regimes in the Canal de Navarrés, a series of simulated charcoal records were produced using CharRec and compared to N3, the most detailed charcoal record collected and analyzed by Carríon and Van Geel (1999). Multiple ignition scenarios were designed with combinations of fire spatial distribution, frequency, size, and intensity to emulate occasional mixed-intensity natural fires, frequent low-intensity broadcast burning associated with pastoral land-use, and frequent high-intensity, spatially confined fires related to land clearing and swidden agriculture. Ignition probability maps (Fig. 14) for natural and anthropogenic ignition scenarios were generated using available data on lightning-caused fire locations (EFFIS, 2014) and archaeological survey data from the Canal de Navarrés (Diez Castillo et al., 2016; García Puchol et al., 2014; Snitker et al., 2018b). The N3 sedimentary charcoal record contains dated deposits spanning the last 25,000 years, but only charcoal concentrations from the late Pleistocene and early/middle Holocene (13,000 – 3800 BP) and two size classes (micro-charcoal: 25 – 150 μm; macro-charcoal: > 150 μm) were simulated to evaluate fire regimes before, during, and after the transition to agro-pastoral economies. Fuel models adapted for the Canal de Navarrés by the *Instituto para la Conservación de la Naturaleza* were used in

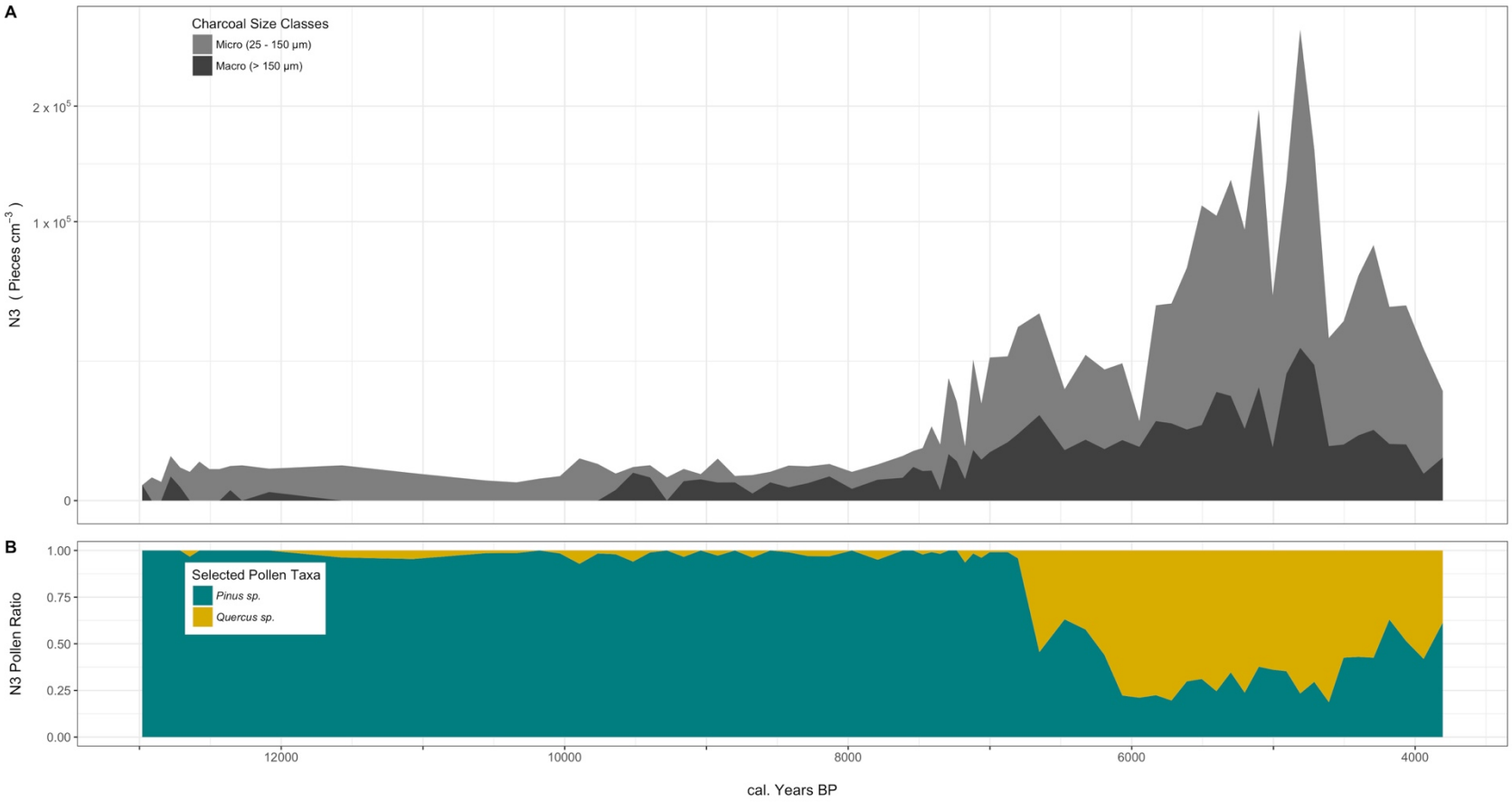

Fig. 13: Summary of N3 Sedimentary Charcoal Record Empirical Data; A) Micro- and Macro-charcoal Counts (Note Square Root Transformation of Y-axis to Highlight Low Charcoal Counts from 13000 – 8000 BP); B) Ratio of *Pinus sp.* and *Quercus sp.* Pollen Counts from the N3 Record.

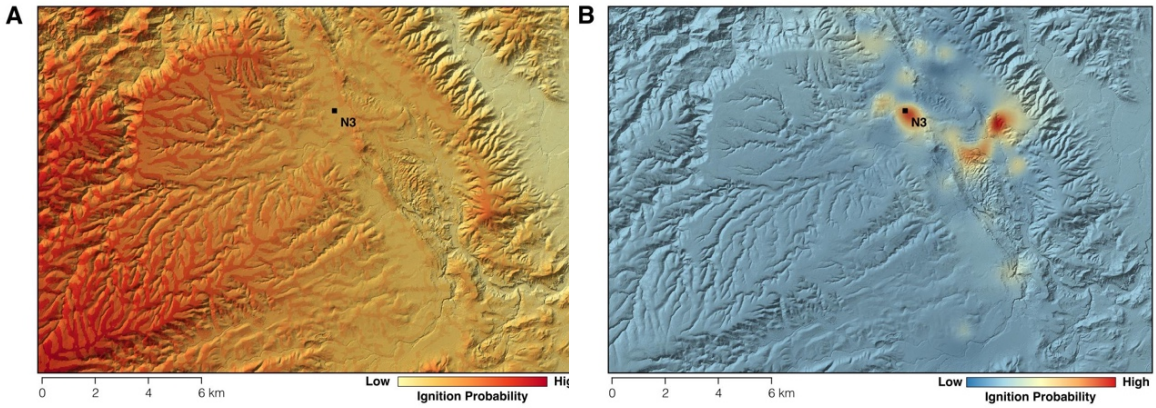

Fig. 14: Ignition Probability Maps for A) Lightning-Caused Fires and B) Anthropogenic Fires in the Canal de Navarrés.

this simulation (MAPA, 1989). Details about ignition scenarios and data inputs are shown in Table 9.

Results

Sensitivity Analysis

To evaluate the sensitivity of CharRec to changes in the ignition scenario variables (fire spatial distribution, frequency, size, and intensity), a series of sensitivity tests were conducted on a randomly generated model landscape (see Table 10 for sensitivity parameters). To identify the minimum number of charcoal observations needed to build a representative sample for each ignition scenario, a sample of low-intensity, high-intensity, and mixed-intensity scenarios were modeled to simulate 1000 observations each. The variance within a random sample of 100, 200, 300, 400, 500, 600, 700, 800, 900, and 1000 observations of each scenario was calculated and compared across ignition scenarios. Results indicated that 300 observations are the fewest needed to

Table 9: CharRec Model Parameters Used to Simulate N3, an Empirical Sedimentary Charcoal Record from the Canal de Navarrés (Carrión and Van Geel, 1999).

CharRec Module	Variable Description	Input(s)	Units	Data Source / Citation
Model Landscape	Elevation	30m resolution elevation raster	m	NASA, 2011
	Wind velocity	30m resolution wind velocity raster	m sec^{-1}	IVIA, 2015; Forthofer et al., 2014
	Wind direction	30m resolution wind direction raster	degrees	IVIA, 2015; Forthofer et al., 2014
	Fuels (1-hour and 10-hour)	Fuel Models 1, 4, and 6 adapted to Spanish ecosystems	--	MAPA, 1989
	Natural ignition probability	30m resolution probability raster generated from regional lightning-caused fires during 1990-2010	--	EFFIS, 2014
	Anthropogenic ignition probability	30m resolution probability raster generated from Neolithic artifact density in Canal de Navarrés	--	Snitker et al., 2018
Ignition Scenario	*Pastoral*			
	Frequency	0.1 - 3.0 by 0.1; mean annual fire frequency	fires yr^{-1}	--
	Size	1 - 9 patches; depends on size function	--	--
	Intensity	Low-intensity; 1-hour fuels	--	--
	Spatial distribution	0 - 0.9 by 0.1; probability thresholds for anthropogenic ignition probability raster	--	--

Table 9: Continued.

CharRec Module	Variable Description	Input(s)	Units	Data Source / Citation
Ignition Scenario	*Swidden*			
	Frequency	0.1 - 3.0 by 0.1; mean annual fire frequency	fires yr^{-1}	--
	Size	1 patch	--	--
	Intensity	High-intensity; 1- and 10-hour fuels	--	--
	Spatial distribution	0 - 0.9 by 0.1; probability thresholds for anthropogenic ignition probability raster	--	--
	Natural (lightning)			
	Frequency	0.1 - 2.0 by 0.1; mean annual fire frequency	fires yr^{-1}	--
	Size	1 - 9 patches; depends on size function	--	--
	Intensity	Mixed-intensity; variable fuel size classes	--	--
	Spatial distribution	0 - 0.9 by 0.1; probability thresholds for natural ignition probability raster	--	--
Form Record	Deposition interval	85; Average sedimentation rate for N3 charcoal record from 13,000 – 3000 cal. BP	yr cm^{-1}	Carrión and Van Geel, 1999

Table 10: CharRec Model Parameters Used in Sensitivity Testing.

CharRec Module	Variable Description	Input(s)	Units
Model Landscape	Elevation	Randomly generated 30m resolution elevation raster	m
	Wind velocity	Randomly generated 30m resolution wind velocity raster	m sec^{-1}
	Wind direction	Randomly generated 30m resolution wind direction raster	degrees
	Fuels (1-hour and 10-hour)	Fuel Models 1, 4, and 6 adapted to Spanish ecosystems	--
Ignition Scenario	*High-intensity*		
	Frequency	0.5 - 3.0 by 0.5; mean annual fire frequency	fires yr^{-1}
	Size	1 patch	--
	Intensity	10-hour fuels	--
	Spatial distribution	0.1- 0.9 by 0.2; probability thresholds	--
	Low-intensity		
	Frequency	0.1 - 3.0 by 0.1; mean annual fire frequency	fires yr^{-1}
	Size	1 patch	--
	Intensity	1-hour fuels	--
	Spatial distribution	0.1- 0.9 by 0.2; probability thresholds	--
	Mixed-intensity		
	Frequency	0.1 - 3.0 by 0.1; mean annual fire frequency	fires yr^{-1}
	Size	1 patch	--
	Intensity	Mixed intensity; variable fuel size classes	--
	Spatial distribution	0.1- 0.9 by 0.2; probability thresholds	--
Form Record	Deposition interval	85	yr cm^{-1}

capture most variance within each ignition scenario. This number of observations was used in sensitivity analyses and all further model experiments (see Bernabeu Aubán et al., 2015 for more details on this approach).

Model sensitivity was evaluated using a one-factor-at-a-time (OFAT) methodology, where one ignition scenario parameter is changed at a time, while keeping all others at baseline values. Charcoal counts generated from all sensitivity tests were z-score transformed and described by a linear regression model. Figs. 15A-C present linear model coefficients and their 95% confidence intervals for each test. CharRec charcoal counts are most sensitive to changes in fuel model and fire intensity in all parameter combinations that were tested. Fuel models are readily distinguishable within the tests, but intensity does cause some overlap between confidence intervals for low-intensity and mixed-intensity fires (Fig. 15). Differences between fire frequency and spatial distribution (Figs. 15B-C) are very stable and are primarily differentiated by fire intensity. With only a few exceptions, linear model coefficients and their confidence intervals for these ignition scenario parameters do not overlap, suggesting that simulated charcoal records can be discerned based on their inputs.

Comparison to the N3 charcoal record from the Canal de Navarrés

Ignition Scenarios

A total of 2,400 simulated charcoal records were modeled in CharRec to represent a diverse set of natural pastoral, and swidden ignition scenarios (see Table 9), resulting in 720,000 individual observations of micro- and macro-charcoal. LDA was applied to all

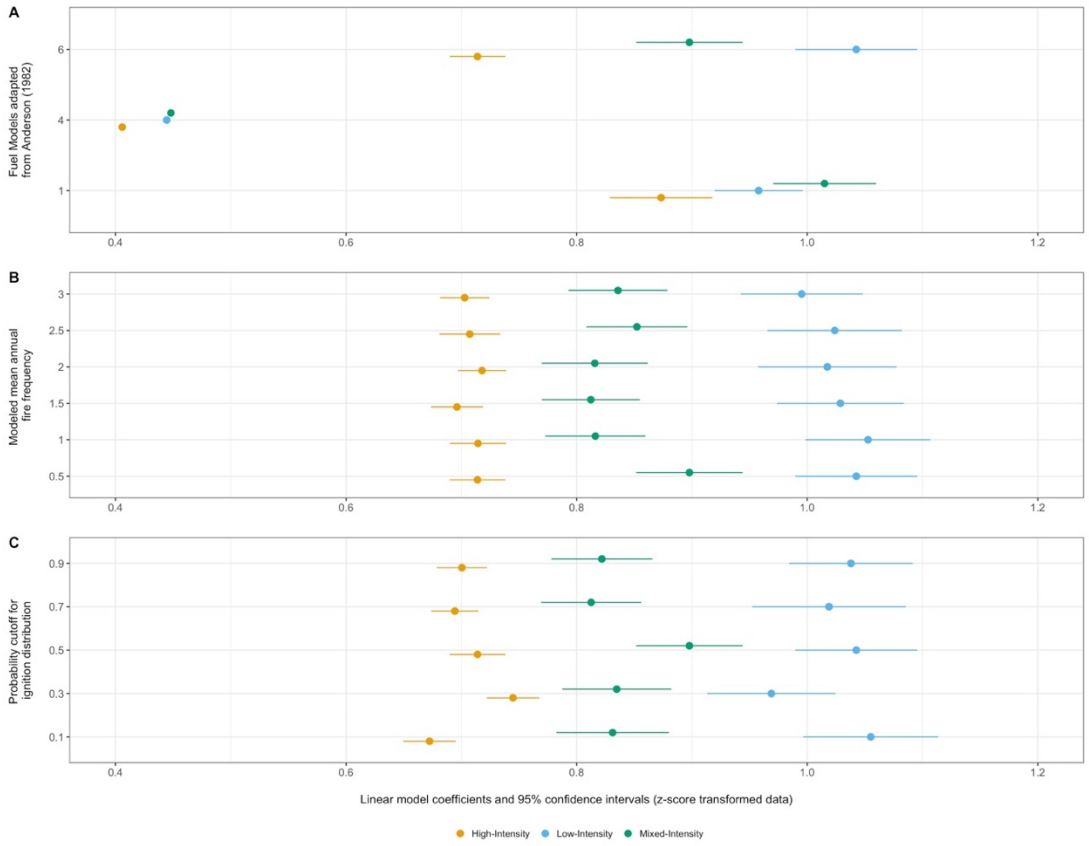

Fig. 15: Linear Coefficients and 95% Confidence Intervals Describing CharRec Outputs from Sensitivity Runs; A) Sensitivity of CharRec Ignition Scenarios to Changes in Fuel Model; B) Sensitivity of CharRec Ignition Scenarios to Changes in Mean Annual Fire Frequency; C) Sensitivity of CharRec Ignition Scenarios to Changes in Probability Cutoff for Ignition Distribution.

2,400 simulated records, generating linear discriminants for each ignition scenario. Linear discriminants were used to classify the empirical micro- and macro-charcoal counts from N3 into best-fit ignition scenarios based on the posterior probability of group membership. Best-fit ignition scenarios were assembled chronologically to create a composite simulated charcoal record that reflects changes in fire regime components through time. A comparison of the empirical charcoal data from N3 and the composite simulated record generated by CharRec is illustrated in Figs. 16A-B.

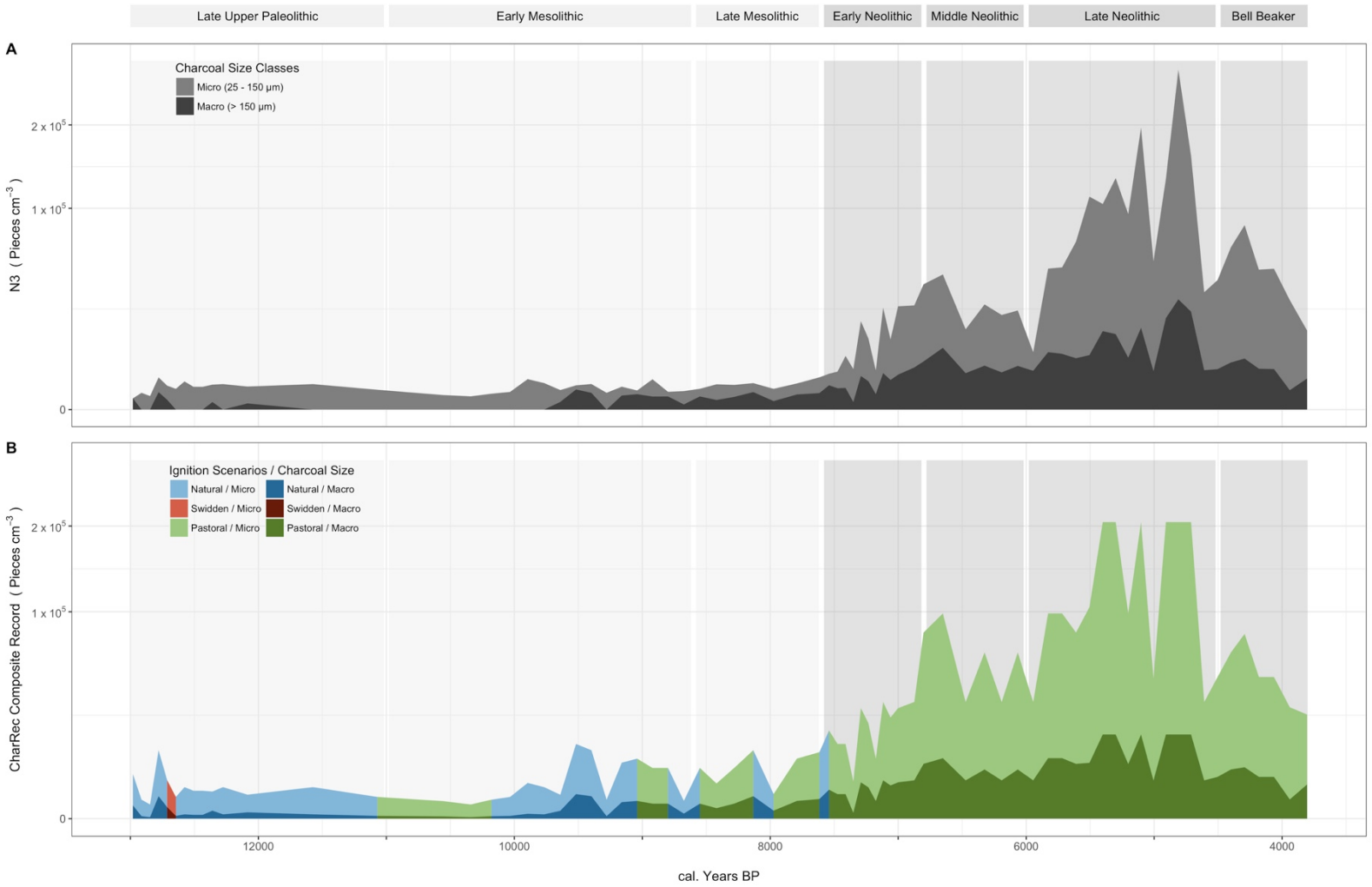

Fig. 16: Comparison of A) N3 Micro- and Macro-charcoal Counts; B) Composite, Simulated CharRec Charcoal Counts (Note Square Root Transformation of Y-axis to Highlight Low Charcoal Counts from 13,000 – 8000 BP). Late Pleistocene and Early Holocene Archaeological Periods Highlighted in Light Grey and Neolithic Periods Highlighted in Dark Grey.

CharRec simulations indicate that the N3 charcoal record is best described by a range of natural ignition scenarios leading up to the transition to Neolithic agro-pastoral land-use. During the transition between the late Mesolithic and early Neolithic periods, charcoal counts increase, and best-fit scenarios fluctuate between natural and pastoral ignitions. At approximately 7400 BP, ignitions stabilize with pastoral as the dominant scenario throughout the remainder of the early and middle Neolithic periods. Both micro- and macro-charcoal counts in both the N3 charcoal record and the simulated composite record significantly increase during the late Neolithic period and continue at elevated accumulation rates through the Bell Beaker Period.

Fire regime parameters

The fire regime parameters contributing to each of the best-fit ignition scenarios are described in Figs. 17A-D. The most striking patterns in these data are the sudden constriction in spatial distribution throughout the entirety of the Neolithic period and the transition to low- intensity fires in fuel model 6 (Figs. 17C-D). These trends are complimented by a slight increase in fire frequency during the early, middle and late Neolithic periods (Fig. 17A). Finally, it is worth noting that fires are consistently small throughout the entire composite simulated charcoal record, with most fires below 0.1 hectares in size (Fig. 17B). Mean fire size does increase during the Neolithic period, but still remains relatively small with values fluctuating between approximately 0.05 and 0.1 hectares.

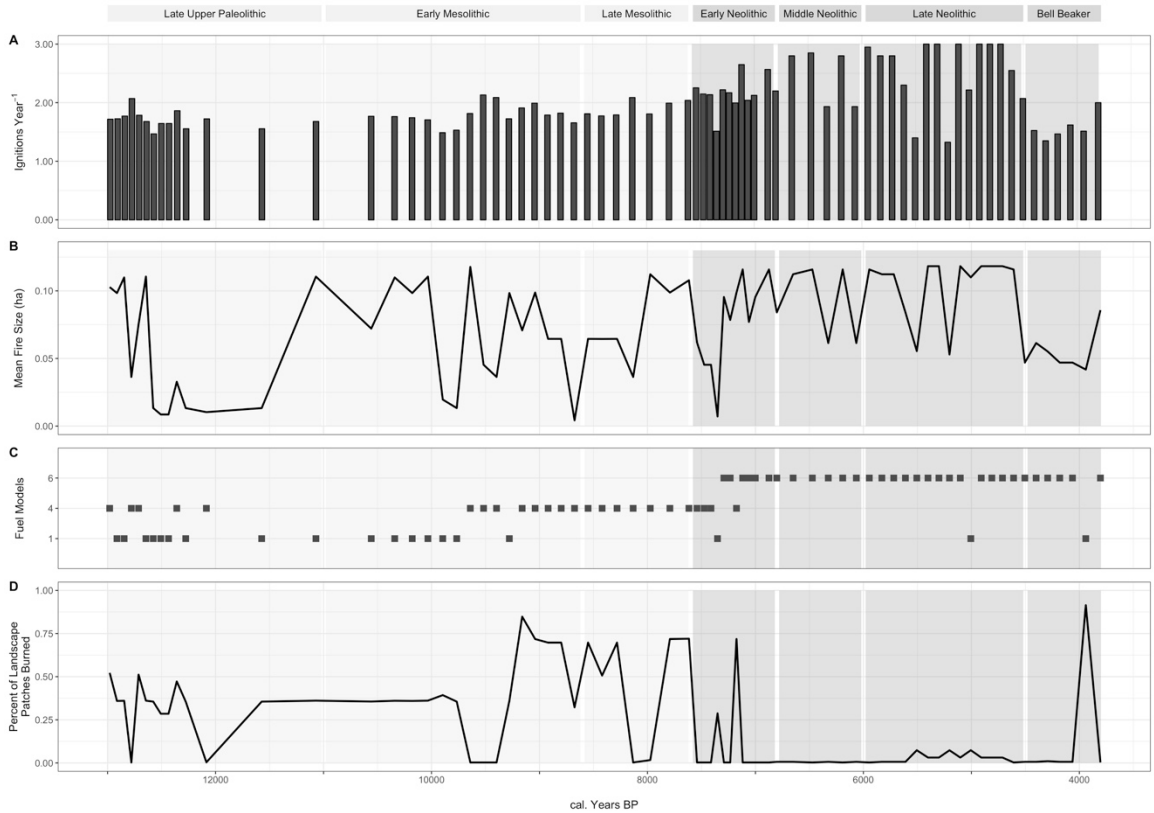

Fig. 17: Fire Regime Parameters from Best-fit CharRec Ignition scenarios through time; A) Simulated Ignitions per Year; B) Simulated Mean Fire Size; C) Fuel Models Used by Best-fit Ignition Scenarios; D) Spatial Distribution of Simulated Fires as Measured by the Percent of the Model Landscape Burned during All 300 Repetitions of the Best-Fit CharRec Ignition Scenario. Late Pleistocene and Early Holocene Archaeological Periods Are Highlighted in Light Grey and Neolithic Periods Highlighted in Dark Grey.

Discussion

Drivers of early and middle Holocene fire regimes in the Canal de Navarrés

The composite simulated charcoal record generated through CharRec provides a robust tool for interpreting the N3 charcoal record in terms of the anthropogenic and natural fire regime components that contributed to its formation. Variations in fire regime parameters through time provide specific insights the spatial and temporal dimensions of fire on the landscape and how they relate to human land-use decisions. The following

discussion of the model results is interpreted in the context of the archaeological and paleoecological data from the Canal de Navarrés.

Broadly, the CharRec simulated charcoal record indicates that increased charcoal accumulations in the Canal de Navarrés during the early and middle Holocene was driven by intensifying Neolithic land-use, not climate. Simulated records during late Pleistocene and early Holocene (13,000 – 7600 BP) demonstrated that fires were primarily natural and caused by regional lightning strikes across a wide geographic area, resulting in the accumulation of background charcoal. The presence of some variation during this period in the N3 charcoal record may be accounted for by the ephemeral occupations by Mesolithic hunter-gatherers (Innes et al., 2013; Innes and Blackford, 2003; Zvelebil, 1994) or fluctuations in climate (Carrión et al., 2010). The Younger Dryas and other aridity events documented through regional pollen sequences are not easily distinguishable in the simulated or empirical charcoal accumulations (López de Pablo and Gómez Puche, 2009). However, changes in best-fit ignition scenarios from 9600 – 9400 BP and 8200 – 7900 BP do correspond with increased aridity and lower temperatures observed in other records, suggesting fires were still natural (Burjachs et al., 2016).

At the beginning of the early Neolithic, fires were likely still regional, with some indications that anthropogenic fire was emerging as a presence on the landscape. Fire intensity, spatial distribution, and fuels reflect a similar pattern suggesting pastoral fire was present, but not a driving force in shaping the regional fire regime. Archaeological survey results from the Canal de Navarrés support this conclusion, indicating that early Neolithic occupations were not specifically identifiable from surface assemblages.

Occupations were likely episodic, with periods of low-intensity land-use followed by extended hiatuses (Snitker et al., 2018b).

At the end of the early Neolithic (7200 – 6800 BP) and throughout the middle Neolithic (6800 – 6000 BP), simulations suggest that fires became consistently larger and more frequent. Fires are also restricted to areas with the highest densities of Neolithic artifacts, implying the establishment of regular, patterned anthropogenic burning related to Neolithic pastoral practices in the region. Fuel models represented in the simulated records also transitioned from closed communities in model 4, to more open woodland in model 6. Patterns of regular, low-intensity burning were likely intentionally used to create open, matorral vegetation communities, amenable to grazing. Post-fire resprouting genera, such *Quercus*, are able to outcompete reseeding genera such as *Pinus*, resulting in a sudden reduction in pine pollen like that observed between approximately 7000-6000 BP by Carrión and Van Geel (1999) (see Pausas, 1999 for a discussion of Mediteranean plant responses to fire).

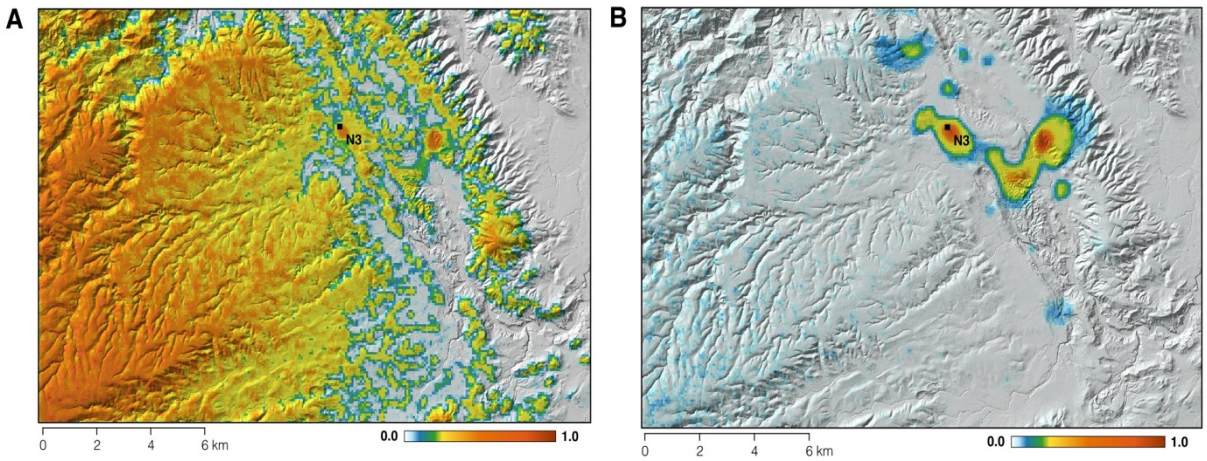

Fig. 18: Aggregated Distribution of Fires for All 300 repetitions of Best-fit Ignition Scenarios During the A) Late Pleistocene and Early Holocene Interval; B) Late Neolithic and Bell Beaker Interval. Indexed Values Range from 0 to 1 and Represent the Frequency a Patch was Burned for Each Period.

Finally, the N3 and simulated charcoal record both show a substantial increase in charcoal accumulations during the late Neolithic (6000 – 4500 BP) and Bell Beaker (4500 – 3800 BP) periods. CharRec model runs also indicate that fire frequencies were highest during this period and low-intensity pastoral fires were spatially constrained to lowland and transitional areas in the valley bottom and margins. Figs. 18A-B illustrate the extent of the spatial differentiation between simulated fires from the late Neolithic and Bell Beaker periods as compared to the late Pleistocene and early Holocene. The degree of spatial constriction during later periods, coupled with increased fire frequency and charcoal accumulation, points to patterns of land-use intensification and permanent settlement. The establishment of the nearby site of Ereta del Pedregal during the late Neolithic and its continued use through the Bell Beaker period supports this conclusion (Pla Ballester et al., 1983). Additionally, data from surface artifact assemblages point to increased diagnostic artifact density during these periods in areas of transitional elevation on the valley margins, like those highlighted in Fig. 18B. Although the N3 charcoal record does not extend beyond 3800 BP, the anthropogenic burning patterns that intensified during the late Neolithic and Bell Beaker periods likely played a role in establishing and maintaining an enduring agricultural landscape, whose legacy is apparent in the Canal de Navarrés today.

Future CharRec developments and applications

Improving CharRec simulations of the N3 charcoal record

Figs. 19A-B illustrate a moving window Pearson's r between CharRec and N3 data, as well as posterior probabilities of best-fit ignition scenarios through time. These

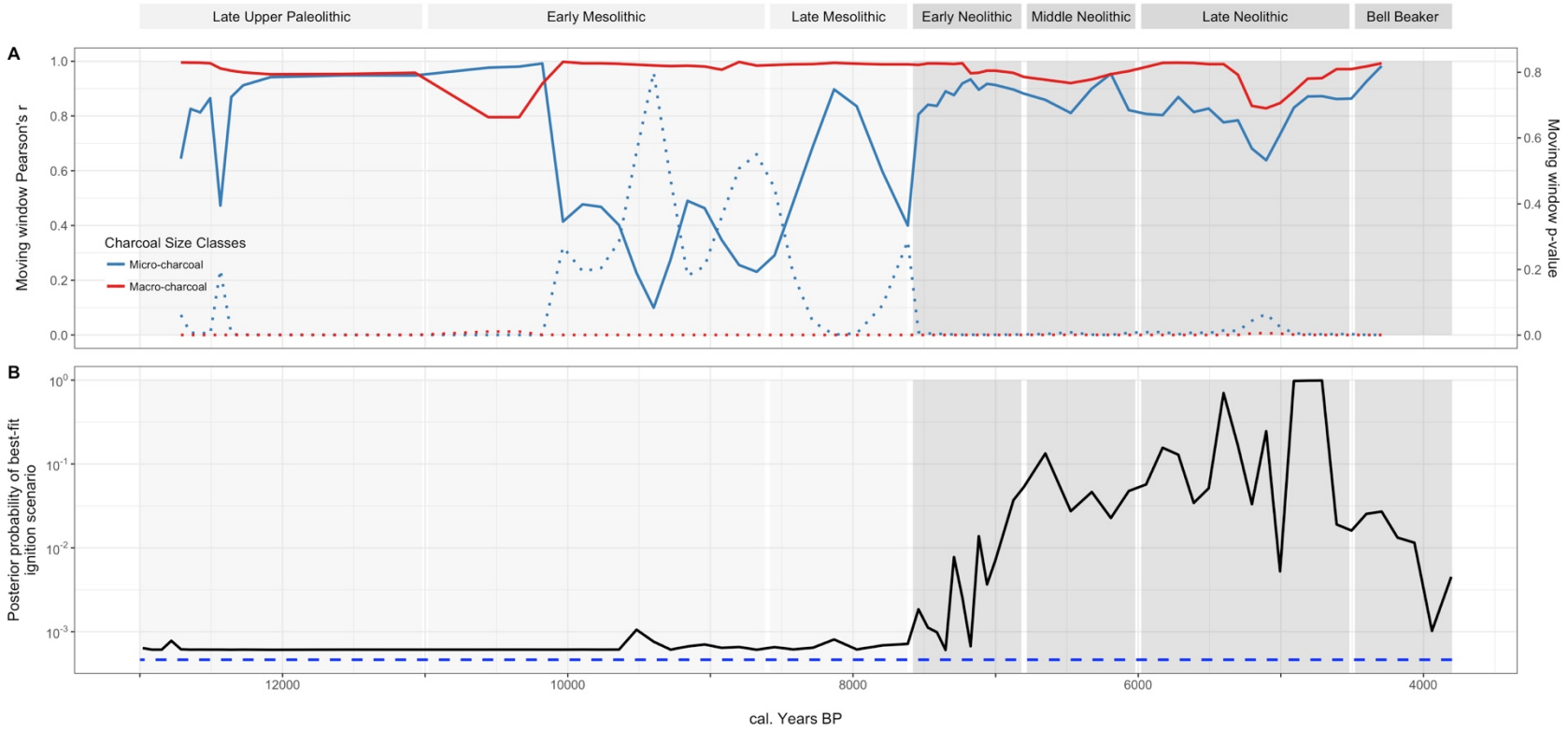

Fig. 19: Evaluation of CharRec Model Performance in Simulating the N3 Sedimentary Charcoal Record from the Canal De Navarrés. A) Solid Lines Indicate Moving Window Pearson's R Correlation Coefficient Calculated Between Empirical and Simulated Charcoal Counts (Window Size Is 9 Observations) and Dotted Lines Indicate Moving Window P-values; B) Posterior Probabilities for Best-fit Ignition Scenarios Shown in Black, While the Mean Posterior Probability for All 2,400 Ignition Scenario Models Is Indicated by the Blue, Dashed Line. Deviation from the Mean Posterior Probability Is an Indicator of Good Model Performance (Note Log10 Transformation of Y-axis).

two measures are used to evaluate the quality of the CharRec simulated charcoal record and its ability to describing the N3 empirical charcoal data. CharRec simulated charcoal records correlate well with the empirical data from N3, with the exception of approximately 10,000 – 7800 BP (Fig. 19A). Classification group probabilities are also low throughout the entirety of the pre-Neolithic periods, with relatively little distinction between the likelihood of the best-fit ignition scenario and the probability of all other ignition scenarios (Fig. 19B). Diminished model performance from 13,000 – 7800 BP is likely due to low charcoal counts, making the variation in the record difficult to accurately replicate. This limitation will need to be addressed before CharRec can be applied to other sedimentary charcoal records where the empirical data is less robust.

At present, two potential methods for improving CharRec's ability to replicate low charcoal counts include: 1) to increase the diversity of ignition scenarios to capture the subtle variation in the low-frequency, micro-charcoal accumulation; and 2) to add more nuance to the relationship between micro- and macro-charcoal production and dispersion in CharRec. Rather than diversifying the existing ignition scenarios, additional fire intensities and spatial configurations that facilitate the slow accumulation of micro-charcoal are needed. Possible ignition scenarios could include larger, more intense (consuming 100-hour or 1000-hour fuels) regional fires or a combination of multiple intensities, possibly emulating the intermittent occupation of the Canal de Navarrés by Mesolithic hunter-gatherers. Finally, the relationship between micro- and macro-charcoal production and dispersion could be improved by drawing from a wider range of published size-distribution data from experimental fires in other regions. Charcoal particle size-distribution, density, and other metrics are currently not well understood and

likely fluctuate substantially during the duration of a fire (Scott, 2010). Continued work on these processes is needed to advance modeling efforts such as CharRec.

Future applications

CharRec is a flexible modeling tool and "virtual laboratory" designed to explore the relationship between natural and anthropogenic drivers of fire regimes. Future applications are not limited to the emergence of agro-pastoral fire regimes or the landscape used in the comparison with the Canal de Navarrés. CharRec relies on fundamental relationships between fire regime components and charcoal dispersion, as well as a user-defined model landscape and ignition scenario inputs, meaning it can be customized to operate in any landscape. Using many of the same parameters, other nearby empirical charcoal records could be simulated and compared to the results observed in the Canal de Navarrés to evaluate the consistency of Neolithic land-use impacts across the region. Other applications in the Mediterranean could include examining historical changes in fire regimes related to documented land-use transitions, such as changes in land tenure during the Medieval Islamic period (AD 711 – 1238) in Valencia or rural re-organization after the Black Death (AD 1348 –1351) in the rest of western Mediterranean (Claramunt Rodríguez et al., 2014). CharRec can be employed to identify fire regime drivers outside of Mediterranean ecosystems by adapting the fuel models and landscapes the local specifics. New World applications may include identifying the degree to which Native American burning practices have shaped pre-contact fire regimes in the currently fire-prone western United States.

Simulating charcoal record formation through CharRec provides a reliable method for identifying anthropogenic fire in empirical sedimentary charcoal records and connecting the spatial and temporal dimensions of land-use to their formation. This work has implications for understanding the pace and scale of human influence on fire regimes and landscape transformation in prehistory. With the emerging interest in tracing the prehistoric roots of the Anthropocene, models like CharRec are becoming increasing more important in answering the difficult and often tangled questions regarding the feedbacks between humans and their environments in long-term-social ecological systems.

CHAPTER IV

AGRO-PASTORAL NICHE CONSTRUCTION AND MAINTENANCE DURING THE NEOLITHIC PERIOD IN EASTERN SPAIN

Grant Snitker

Introduction

The global transition to agro-pastoral subsistence inarguably created unprecedented changes in how humans related to plants and animals within their landscapes. In Europe, the spread of agro-pastoral subsistence from the Near East during the early and middle Holocene saw systematic biogeographic rearrangements of plants and animals leading to the development of agricultural landscapes (Ellis et al., 2013). An extensive literature exists on agricultural landscapes, much of which points to large-scale social and economic investments in built environments, such as terracing hill slopes, irrigation canals, or systems of raised fields (Bevan et al., 2012; Ellis, 2015; Erickson, 2003; Fisher, 2005; McKey et al., 2010; Morehart, 2012; Sheridan, 2014). Recent work in the Mediterranean Basin suggests that agricultural landscapes also can be created and maintained through less intensive human interventions (Coughlan, 2014; Leigh et al., 2015). Anthropogenic fire associated with agricultural practices is one such human intervention that, when iterated over the long-term, acts as driver in vegetation change and landscape morphology (Barton et al., 2015; Bond and Keeley, 2005; Bowman et al.,

2011, 2009; Glikson, 2013; Pausas, 1999b; Roos et al., 2014; Valese et al., 2014). Agricultural tasks, such as clearing land with fire for field placements, can create fragmented patterns of fuel within vegetation communities, change selection pressures on particular plant species, or facilitate the transition from forest to shrub-dominated *matorral* ecosystems (Pausas and Paula, 2012). Although these interactions are long-term and dynamic, most research on early agricultural landscapes and fire in the Mediterranean Basin involves comparing synchronic snapshots at different times rather than on the complex spatial/temporal interactions between social and ecological systems (Asouti and Fuller, 2011; Dennell, 1985; Garcia Atienzar and Jover Maestre, 2011; Guilaine and Manen, 2007a; Oosterbeek, 2001; Zeder, 2008; Zilhão, 2001).

Evaluating the socio-ecological processes that drove the pace and scale of the development Neolithic agricultural landscapes in the western Mediterranean remains difficult due to variability in the spatial and temporal scope of prior research. Although numerous Neolithic cave and open-air sites have been systematically analyzed in conjunction with Middle Holocene pollen and charcoal records across the region, only speculative linkages have been made between archaeological and paleoecological data to explain why Neolithic land-use coincides with landscape transformation in some locations, but not others. Ultimately this disconnection is derived from a lack of evidence-based approaches that can address how indirect investments in landscape creation, such as anthropogenic fire, are connected to agricultural practices at a landscape scale.

This study examines the drivers behind the creation and long-term maintenance of agricultural landscapes during the Neolithic period (7600–3800 cal. BP) in eastern Spain,

employing concepts from human niche construction theory (HNC) and ecological resilience. These concepts are critically evaluated using charcoal and archaeological land-use data collected from three study areas. This study applies a series of methodological advances in charcoal analysis with the goal of creating more direct connections between charcoal data and the social, biological, and taphonomic processes that created them. Ultimately, this approach will assist in understanding the scale and speed of the creation and development of agricultural landscapes, as well as in evaluating the role of anthropogenic fire in long-term landscape maintenance in fire-prone Mediterranean ecosystems.

Human niche construction theory, ecological resilience, and landscape change

Niche construction theory (Fig. 20A) provides a framework to understand the feedbacks inherent within social-ecological systems by emphasizing an organism's capacity to modify its environment and thus influence the drivers of natural selection affecting it and subsequent generations (Laland, 1999; Laland and O'Brien, 2010; Odling-Smee et al., 2003). Also referred to as ecosystem engineering (Jones et al., 1997), this approach considers the structure and distribution of species relationships, the role of keystone species, and overall ecosystem resilience as the result of persistent, long-term modifications by niche-constructing organisms (Laland, 1999). Many organisms exhibit niche-constructing behaviors. For example, beavers create and maintain dams that alter the long-term biotic and abiotic attributes of their ecosystem, including stream flow dynamics and nutrient transport and cycling, which in turn influence beaver evolution (Laland and O'Brien, 2010). Niche construction theory recognizes a dual system of

inheritance in which species not only inherit genes but also inherit modified, selective environments created by their ancestors (i.e., their niches)—a process termed ecological inheritance. Niche-constructing behaviors occur over a wide range of spatial and temporal scales. Removing, adding, or changing the behaviors of niche-constructing organisms can have substantial effects on ecosystems at multiple trophic levels (Bliege Bird et al., 2013; Smith, 2012, 2011).

Odling-Smee, Laland, and colleagues (Ellis, 2015; Kendal et al., 2011; Laland and O'Brien, 2010; Odling-Smee et al., 2003) have proposed that humans are extremely effective niche-constructing organisms and possess an amplified potential for creating, destroying, or modifying niches within ecosystems. Unlike other niche-constructing organisms, humans pass information to subsequent generations through cultural, as well as genetic and ecological inheritance (Fig. 20B). Cultural inheritance provides an additional pathway for conveying information across multiple generations (Laland and O'Brien, 2012). Cultural decisions, such as land-use strategies, taboos on consumption, or territorial arrangements, can create persistent impacts on the structures of the social and ecological landscape. Such impacts will influence the subsequent success of human

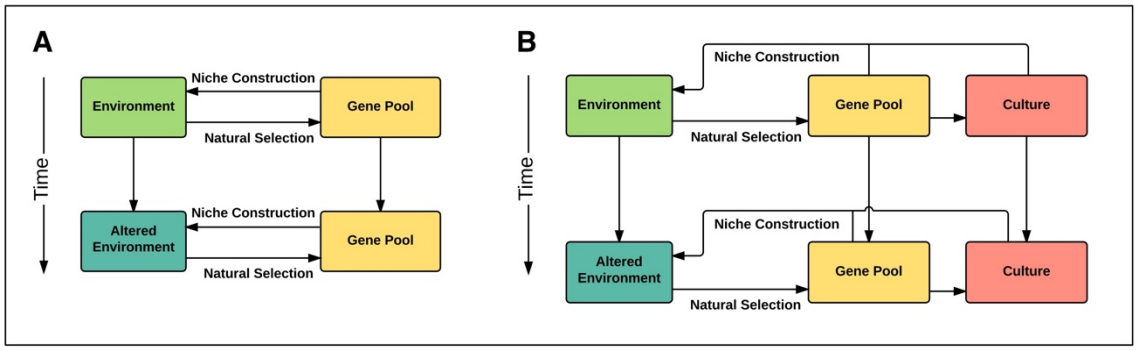

Fig. 20: A) Process of Natural Selection Where Only Genetics Are Inherited Between Generations, B) Niche Construction Theory Emphasizes Evolutionary Processes Where Both Genetic and Ecological Inheritances Are Passed to Subsequent Generations (Laland and O'Brien, 2012).

populations and other organisms, as well as subsequent niche-constructing behavior (Odling-Smee and Turner, 2011; Smith, 2011). Niche construction in human societies manifests in a wide spectrum of activities, including both intentional manipulation and inadvertent disruption or of biotic and abiotic systems.

Human niche construction (HNC) systems are not equally influenced by all three types of inheritance, especially in the relatively short timescale of the middle Holocene. During the Neolithic period in eastern Spain, cultural and ecological inheritance were especially significant for creating a complex set of interactions between cultural behaviors, their impacts on ecological arrangements, and long-term feedbacks that influenced both systems. Characterizing these relationships through time can provide new insights into long-term human adaptive strategies, ecological stability domains, or thresholds that might not be as apparent from archaeological interpretations of material culture alone.

A complementary approach to HNC is ecological resilience, which considers the effects of long-term disturbance regimes in ecological systems. Resilience describes an ecosystem's ability to absorb and recover from a disturbance while still maintaining its overall structure and function (Holling, 1973, 1996). Resilience is measured by the magnitude or duration of a disturbance that is required to flip an ecosystem out of its current stability domain into another (Gunderson and Holling, 2002). In the context of fire disturbance, vegetation communities demonstrating a high degree of resilience maintain overall species composition and structure in the context of a consistent fire regime. Variation in fire disturbances may create conditions that extend beyond a vegetation community's resilience, attracting the system toward a transition into a

different stable state (Berkes and Folke, 1998; Folke, 2006; Holling, 1996). For example, humans clearing land with fire can facilitate the transition of woodlands to grasslands, thus creating a new human-driven niche (Whitlock et al., 2010).

Ecological resilience provides insights into co-evolutionary dynamics between ecosystems and niche-constructing organisms, such as humans. Species that have a long history of coexistence and dependence on human niche-constructing activities are adapted to and therefore reliant on moderate levels of anthropogenic disturbance (Bliege Bird et al., 2013; Codding et al., 2014). In the western Mediterranean, vegetation communities that are dependent on anthropogenic burning should be resilient to structural and functional changes within a consistent fire regime resulting from subsistence strategies and land-use. Co-evolutionary relationships can be interrupted when the scale, scope, or intensity of anthropogenic disturbance changes rapidly, resulting in an ecological regime shift from one stability domain to another. This process can be driven by sudden changes in human behaviors, such as colonization, changes in mobility, or new subsistence strategies (Codding et al. 2014:660). Shifts in co-evolutionary relationships and low levels of ecological resilience can result in changes in species distributions and ecosystem structure, or species extinctions.

Reframing HNC in archaeology to understand long-term agricultural landscapes

Human niche construction has been used as an analytical framework in archaeology to examine abroad range of human-environmental interactions, including both intentional and inadvertent changes to landscapes brought on by human action (Smith, 2015a). One of the most notable, if at least not the most cited, example of niche

construction is transition to agro-pastoral subsistence in multiple regions across the globe (see Smith 2007, 2015b, 2012; Zeder 2016; O'Brien and Laland 2012; Bleed and Matsui 2010). But other archaeological studies have ventured beyond plant and animal domestication and applied niche construction as a framework to understand a variety of human-environmental interactions, including selective hunting and regional megafauna extinctions (Braje and Erlandson, 2014; Grayson, 2001; Malhi et al., 2016; Sandom et al., 2014), nutrient cycling in terrestrial and aquatic systems (Ekdahl et al., 2007, 2004), and translocation of plants and animals (Fitzpatrick and Keegan, 2007; Gremillion, 2011; Kirch, 1997; Vigne et al., 2012).

Although human niche construction theory is a powerful explanatory framework for investigating the origins of anthropogenic landscapes, it suffers from two major limitations that have been highlighted in the literature (Riel-Salvatore, 2010; Smith, 2015a): 1) difficulty in quantifying HNC behaviors and outcomes using traditional archaeological approaches to material culture, and 2) use as an explanatory framework without clear ways to operationalize it in terms of long-term processes. Advances in paleoecological analyses have started to isolate human influences on particular ecological systems (Balch et al., 2017; Cattau et al., 2016; Roos et al., 2018), but often it is difficult to distinguish the human signature of change from other earth system processes, such as climate. These limitations are compounded by many archaeological questions that do not seek to engage the inherent evolutionary underpinnings of niche construction theory and rely on the theory to explain synchronic events rather than processes.

This study addresses these limitations by building on current efforts to identify human-impacts on fire regimes by bridging the interpretative gap between archaeological

and paleoecological data. I present series of new methods in charcoal analysis that help differentiate variation in the distribution and intensity of fire related to agro-pastoral practices from natural caused fires. This approach positions both archaeological and paleoecological data on the same spatial and temporal scales and facilitates comparison across multiple study areas. Finally, these new data sources aid in interpreting niche construction as a long-term, diachronic process involving both the creation and maintenance of a niche through time.

Research Setting

Study areas within the Comunitat Valenciana, eastern Spain

The Canal de Navarrés, Hoya de Buñol, and Vall del Serpís study areas are located in a semi-mountainous region approximately 40km inland of the Mediterranean coast within the Comunitat Valenciana in eastern Spain (Fig. 21). This region has been the center of archaeological and paleoecological research by for the last several decades, making it uniquely suited to investigate the influence on anthropogenic fire on the creation of long-term agricultural landscapes (Barton et al., 2004, 1999; Bernabeu Aubán et al., 2008; Diez-Castillo et al., 2008; Diez Castillo et al., 2016; García Puchol et al., 2014; García Puchol and Aura Tortosa, 2006). Comparable climates, geology, and natural fire frequency make these three areas ideal for comparing the impact of variable Neolithic land-use histories on the anthropogenic fire regimes and agro-pastoral niche construction. The following section outlines the regional environmental and

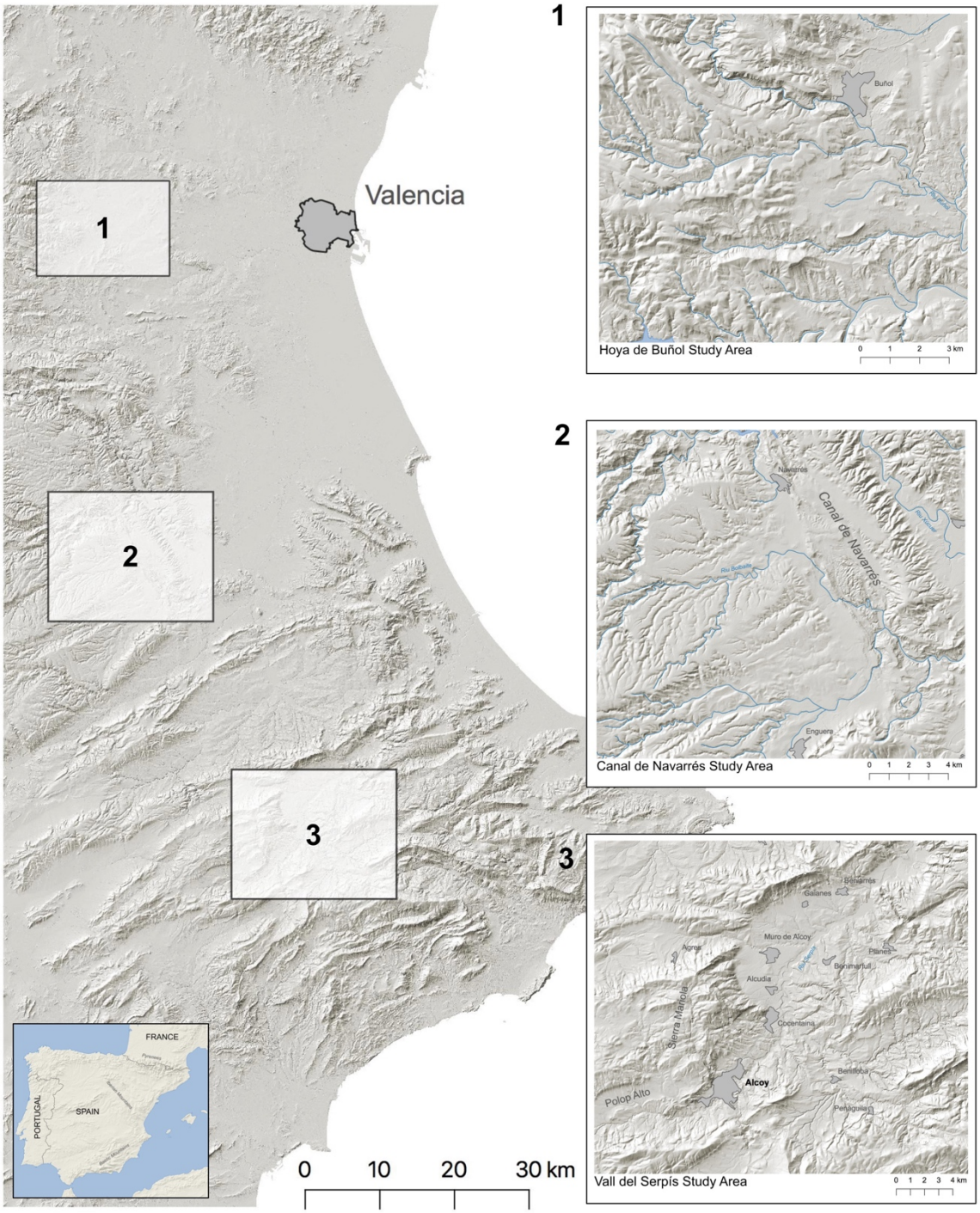

Fig. 21: Study Areas in Eastern Spain Mentioned in This Dissertation. 1) Hoya de Buñol Study Area, 2) Canal de Navarrés Study Area, and 3) Vall de Serpís Study Area.

archaeological background, then provides details on the specific previous archaeological and paleoecological research conducted in each study area.

Regional environmental background

The study region is characterized by topographic variability created by the intersection of the Iberian and Baetic mountain ranges, with high limestones ridges extending to approximately 1300 meters above sea level and wide, flat-bottomed valleys at approximately 200 - 500 meters above sea level (Bernabeu Aubán et al., 2008; La Roca et al., 1996). Major rivers in this area include the Riu Serpís, Riu Xúcar, and the Riu Magre, all of which drain east to the Mediterranean. Both perennial and intermittent tributaries of these rivers have deeply incised the landscape, exposing sedimentary sequences in channel walls.

The regional climate is classified as Meso-mediterranean, experiencing hot, dry summers and mild, wet winters, but due to elevation, has greater seasonality than nearby coastal areas (Carrión et al., 2010). Vegetation communities throughout the Holocene are composed primarily of maqui shrublands species, with the most common being *Quercus coccifera*, *Pistacia lentiscus*, *Rosmarinus sp., Erica arborea, Cistus albidas,* and *Ulex europaeus.* Upland areas include arboreal species such as *Quercus ilex* and *Pinus halepensis* and occasional *Pinus nigra* at higher elevations. From the late Pleistocene through the late Holocene, local climate reflected global trends experiencing multiple fluctuations between colder/arid and warmer/wetter conditions (Bernabeu Aubán et al., 2015b; Carrión and Dupré, 1996; Carrión and Van Geel, 1999; Jalut et al., 2000; McClure et al., 2009). Throughout eastern Spain, several paleoecological studies of

pollen and charcoal point to transitions in vegetation communities that are primarily linked to changing climate trends (Pantaléon-Cano et al., 2003; Yll et al., 1997). But in some inland valleys and throughout the Balearic Islands, this trend is interrupted by an increase in regional fire activity (Fig. 22) and the transition of vegetation communities into oak-dominated matorral (Carrión et al., 2010; Carrión and Dupré, 1996; Carrión and Van Geel, 1999; López-Sáez et al., 2009; Yll et al., 1997). This pattern is often attributed to mid-Holocene changes in fire regimes due to the introduction of Neolithic land-use, but this conclusion has yet to be systematically tested in a regional context.

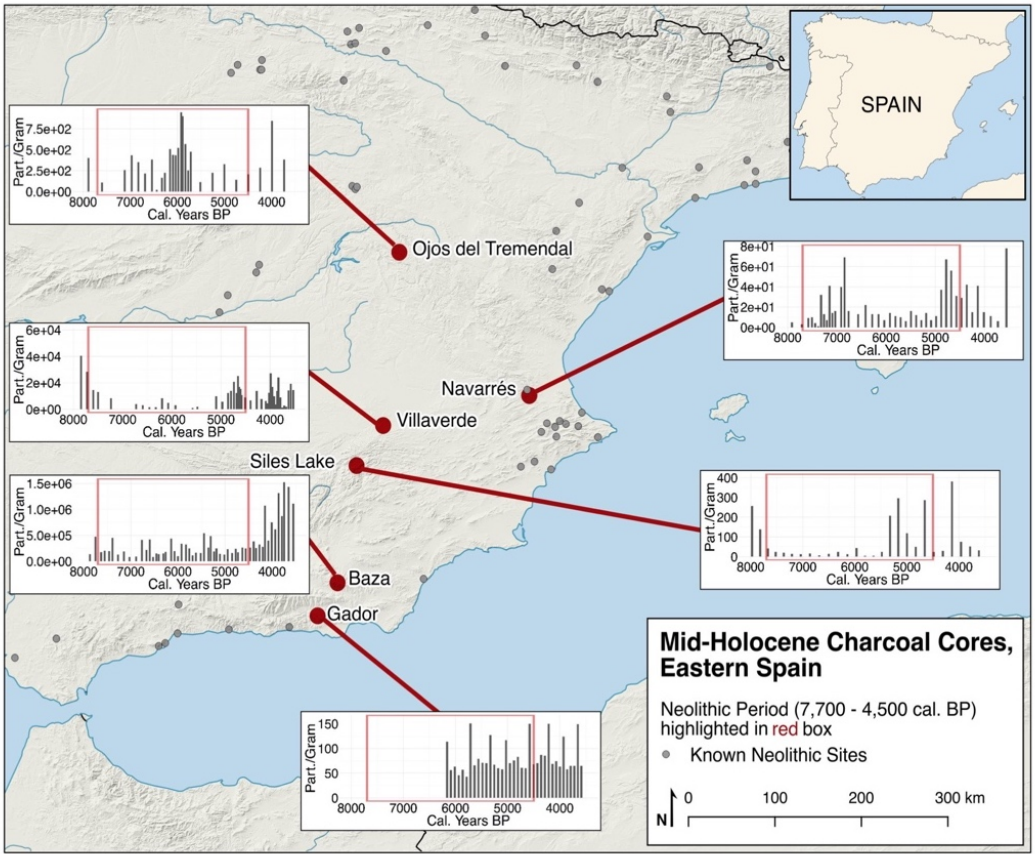

Fig. 22: Regional Variability in Charcoal Accumulation During the Middle Holocene in Eastern Spain. The Neolithic Period (7700–4500 BP) Is Highlighted in the Red Box. Known Neolithic Sites Shown as Grey Points on the Map. While Some Charcoal Records Indicate an Increase in Fire Activity During the Middle Holocene, Other Do Not. There Is Not a Clear Relationship Between the Presence of Neolithic Land-use and Changes in Fire Activity at This Regional Scale. Charcoal Data Accessed Through the Global Charcoal Database (Blarquez et al., 2014).

Regional archaeological background

The Neolithic period (7600 – 3800 BP) in Spain begins between 2,000 to 2,500 years after the earliest evidence of agriculture in the Near East. Multiple geographic and social pathways have been proposed for agriculture reaching the Iberian Peninsula (see Ackland et al., 2007; Bergin, 2016; Conolly et al., 2008; Lemmen et al., 2011; Zeder, 2008; Zilhão, 2001), but by approximately 7600 BP, floral and faunal evidence from excavated contexts indicate a subsistence shift to herding and cultivating domesticates (Barton et al., 1999; Bernabeu Auban, 2004; Bernabeu Auban et al., 2001b; Bernabeu Aubán et al., 2008; Chapman, 2008; Zeder, 2011, 2008). The Early Neolithic (also referred to as Neolithic I) spans from 7600 – 6800 B.P. and is characterized by a transition from hunting and gathering (Late Mesolithic period: 8600 – 7600 BP) to agricultural subsistence, including both shifting cultivation and pastoralism. During this phase, there is clear evidence for domesticated sheep, goats, wheat, barley, and the introduction of cardial ceramics, a distinct ceramic form in which vessels are impressed with cardium shells to create a decorative pattern (Barton et al., 1999; Bernabeu Auban et al., 2001b; Oosterbeek, 2001). Subsequent periods, including the Middle Neolithic (6800 – 6000 BP), the Late Neolithic (6000 – 4500 BP) and the Bell Beaker or Eneolithic (4500-3800 BP) are often referred to collectively as the Neolithic II period and are characterized by both local and regional sites that demonstrate general trends of land-use intensification, population growth and consolidation, and increased social complexity (Marti Oliver, 1988; McClure, 2004; McClure et al., 2009).

The Late Mesolithic and Neolithic periods in the Comunitat Valenciana have been reconstructed through several decades of systematic excavations in caves, rockshelters,

and open-air contexts. Evidence of hunter-gatherer occupations during the Late Mesolithic have been primarily identified in caves and rockshelters through diagnostic lithic technologies, including geometric, triangular/trapezoidal microburins and microliths (Bernabeu Auban et al., 2002). Major Late Mesolithic sites identified in the region include Abric de la Falguera (García Puchol and Aura Tortosa, 2006), Cueva de la Cocina (Bernabeu Aubán and Martí Oliver, 2014; Fortea Perez, 1971; García-Puchol et al., 2018; García Puchol et al., 2009), and El Collado (Arias Cabal and Alvarez Fernández, 2004; Garcia Guixé et al., 2006; Guilaine and Manen, 2007b).

The earliest Neolithic occupations are dated to 7700 – 7500 BP at multiple sites throughout the region, including Mas d'Is (Bernabeu Auban et al., 2003), Abric de la Falguera (García Puchol and Aura Tortosa, 2006), and Cova de les Cendres (Bernabeu Auban et al., 2001c; García Puchol et al., 2009; Llobregat et al., 1981). By 6500 BP, cardial ceramics and evidence of domesticated plants and animals were widespread (Sites include Cova d'En Pardo: García Atiénzar 2009; Cova de l'Or: Martí 2011; Cova de la Sarsa: García Borja et al. 2012). Although excavations in caves and rockshelters have provided reliable ceramic and lithic chronologies for the Valencian Neolithic period, open-air sites such as Mas d'Is (Bernabeu Auban et al., 2003; Gallello et al., 2013), El Barranquet (de Pablo and Gomez Puche, 2009), Niuet (Bernabeu Aubán et al., 1994), Les Jovades (Bernabeu Auban and Badal Garcia, 1992), and La Ereta del Pedregal (Fletcher Valls, 1964; Juan Cabanilles, 1994; Pla Ballester et al., 1983), offer insights into the changing land-use patterns and social organization that accompanies the Neolithic period. These sites are located in valley bottoms with access to arable land and feature communal earthworks, such as concentric ditches, walls, or community storage pits and silos

(Bernabeu Auban et al., 2009; Bernabeu Aubán and Martí Oliver, 2014; Pla Ballester et al., 1983).

The Canal de Navarrés Study Area

The Canal de Navarrés is a flat-bottomed valley located approximately 50 km southwest of the city of Valencia (Fig. 21) and is circumscribed by a series of low-lying ridgelines (see chapters II and III for detailed descriptions of the geographic and geomorphic background of the Canal de Navarrés). The presence of La Ereta del Pedregal, an open-air site dated to the Late Neolithic through Bell Beaker cultural periods, has inspired multiple archaeological and paleoecological research endeavors in the lowland and transitional areas of this valley since the 1940s (Aparicio Perez, 1974; Carrión and Dupré, 1996; Carrión and Van Geel, 1999; Diez Castillo et al., 2016; Fletcher Valls, 1964; García Puchol et al., 2014; Juan Cabanilles, 1994; La Roca et al., 1996; Snitker, 2018; Snitker et al., 2018a). A series of terrestrial sedimentary cores taken from peat deposits adjacent to Ereta del Pedregal have identified increases in fire frequency and large-scale shifts in local vegetation from pine to oak-dominated woodlands that corresponds to the arrival of Neolithic land-use to the region at approximately 7000 BP (Carrión and Dupré, 1996; Carrión and Van Geel, 1999; Menéndez Amor and Florschütz, 1961). The combination of previous archaeological investigations and detailed chronologies of Holocene vegetation dynamics and fire make this Canal de Navarrés an important test case for examining niche construction and maintenance via anthropogenic fire during the Neolithic period.

The Vall del Serpís Study Area

Located within the Riu Serpís watershed in the province of Alicante, the Vall del Serpís is composed of several small valleys surrounded by the mountains and ridgelines within the northern most portion of the Baetic system (Fig. 21). The valley was deeply incised during the middle and late Holocene, exposing Neolithic-aged sediments and fertile valley fill perched high above modern drainages. Over a decade of systematic survey and excavation in this area has identified extensive evidence of intensive prehistoric land-use throughout the early and middle Holocene (Barton et al., 2004, 2002, 1999, Bernabeu Auban et al., 2001b, 2000; Diez-Castillo et al., 2008; García Puchol and Aura Tortosa, 2006). Multiple cave and open-air sites identified in the Vall del Serpís have been used to build the regional chronology for the process of neolithization in eastern Spain (Bernabeu Auban, 2004, 2002). Regional paleoecological research primarily consists anthracological analyses of archeological charcoal assemblages from Late Pleistocene and Early Holocene contexts, but has some limited pollen studies in cave sites. Neolithic sites such as Cova de l'Or (Badal Garcia, 1995, 1994; Dupré, 1988), El Abric de la Falguera (García Puchol and Aura Tortosa, 2006), Niuet (Badal Garcia, 1994), and Cova d'En Pardo (González Sampériz, 1998) indicate changes in their pollen and charcoal sequences during the Neolithic period that transition from pine- to oak-dominated woodland. While this trend is more pronounced in some sequences than other, it is indicative of landscape-scale vegetation change that may be related to Neolithic land-use practices and fire.

The Hoya de Buñol Study Area

The Hoya de Buñol study area is located approximately 30 km east of the city of Valencia and is circumscribed by a series of low mountains (Fig. 21). This area drains via a series of small perennial streams into the Riu Magre, one of the main tributaries of the Riu Xúcar. Multiple, large travertine deposits are associated with waterfalls, caves, and rockshelters in this area, few of which have been evaluated for evidence of prehistoric occupation. Two cursory archaeological evaluations of this area during the first half of the twentieth century (Jiménez, 1935; Jiménez Navarro and San Valero, 1943) identified surface artifacts in Cueva de las Palomas and in the Cueva Turche, two travertine formed caves along the Charca de las Palomas. Otherwise, previous archaeological and paleoecological research in this area is extremely limited.

In 2017, a joint research team from Arizona State University and the University of Valencia began a systematic, archaeological survey project this this area to compare methods and interpretations of Neolithic settlement patterns and land-use to previously recorded data in the Canal de Navarrés and the Vall del Serpís. Preliminary results indicate the presence of Neolithic occupations throughout this area, with intensifying artifact densities throughout the local Bronze (3800 – 2800 BP) and Iberian (2800 – 2200 BP) cultural periods. The lack of information on prehistoric agro-pastoral land-use in this the Hoya de Buñol make it an appropriate case study against which to test models of the development and maintenance of agricultural landscapes developed in the Canal de Navarrés and the Vall de Serpís study areas.

Methods

To evaluate how anthropogenic fire is connected to the emergence and persistence of Neolithic agricultural landscapes in all three study areas, integrated methods are needed to examine changing patterns of fire, land-use, and the resulting landscape response. The following multi-proxy methods are used to evaluate anthropogenic fire and agro-pastoral niche construction and maintenance during the Neolithic period in eastern Spain. Additional information on the methods presented here can be found in Appendices I-V.

Archaeological survey data to evaluate changing land-use intensities through time

Archaeological survey methods

The spatial distribution of land-use intensity was evaluated through an analysis of diagnostic ceramic and lithic artifacts collected during a series of systematic, intensive surveys of all study areas. The archaeological survey strategy employed in all study areas is outlined in Barton et al. (1999; 2002) and Bernabeu Auban et al. (2008) and is adapted in Snitker et al. (2018). These methods are designed as stratified, randomly selected pedestrian surveys, where each study region is divided into survey strata based on geography and vegetation communities. Strata are subdivided into survey blocks (randomly sampled within each stratum) and individual agricultural fields serve as collection units within each block. Chapter II presents the details of this strategy, as well as the results from the Canal de Navarrés case study, so they will not be reiterated here. See Fig. 23 and Table 11 a summary of survey coverage for the Canal de Navarrés.

The Hoya de Buñol study area was surveyed in 2017 using these same methods by a combined Arizona State University and University of Valencia research team. Survey locations were selected to be spatially representative, as well as capture variation in topography, vegetation, and modern landscape modifications. Survey coverage and descriptions of survey zones for the Hoya de Buñol study area are illustrated in Fig. 24 and Table 11.

The Vall de Serpís study area has been a part of a collaborative research program between Arizona State university and the University of Valencia since 1990. Over the past three decades, this area has been intensively surveyed through numerous grant-funded projects, resulting in a distribution of surveyed parcels which cover much of the Middle Serpís Valley, as well as the adjacent Polop Alto and Gorgos valleys (Barton et al. 1999, 2002, 2004; Bernabeu et al. 2000, 2001, 2008; Castillo et al. 2014; García and Aura 2006). Data was collected here using the same methods that would be eventually employed in the other two study areas, making them comparable even though they were collected several decades apart. Survey coverage and descriptions of survey zones for the Vall de Serpís study area are illustrated in Fig. 25 and Table 11.

Table 11: Archaeological Surveys and Spatial Coverage Used to Evaluate Prehistoric Land-use in Each Study Area.

Study Area	Archaeological Survey	Size (sq. km)
Canal de Navarrés	Navarrés	82.0
Hoya de Buñol	Hoya de Buñol	23.0
Vall del Serpís	Alcala	2.6
	Muro de Alocy	11.7
	Penàguila	10.0
	Polop Alto	8.8

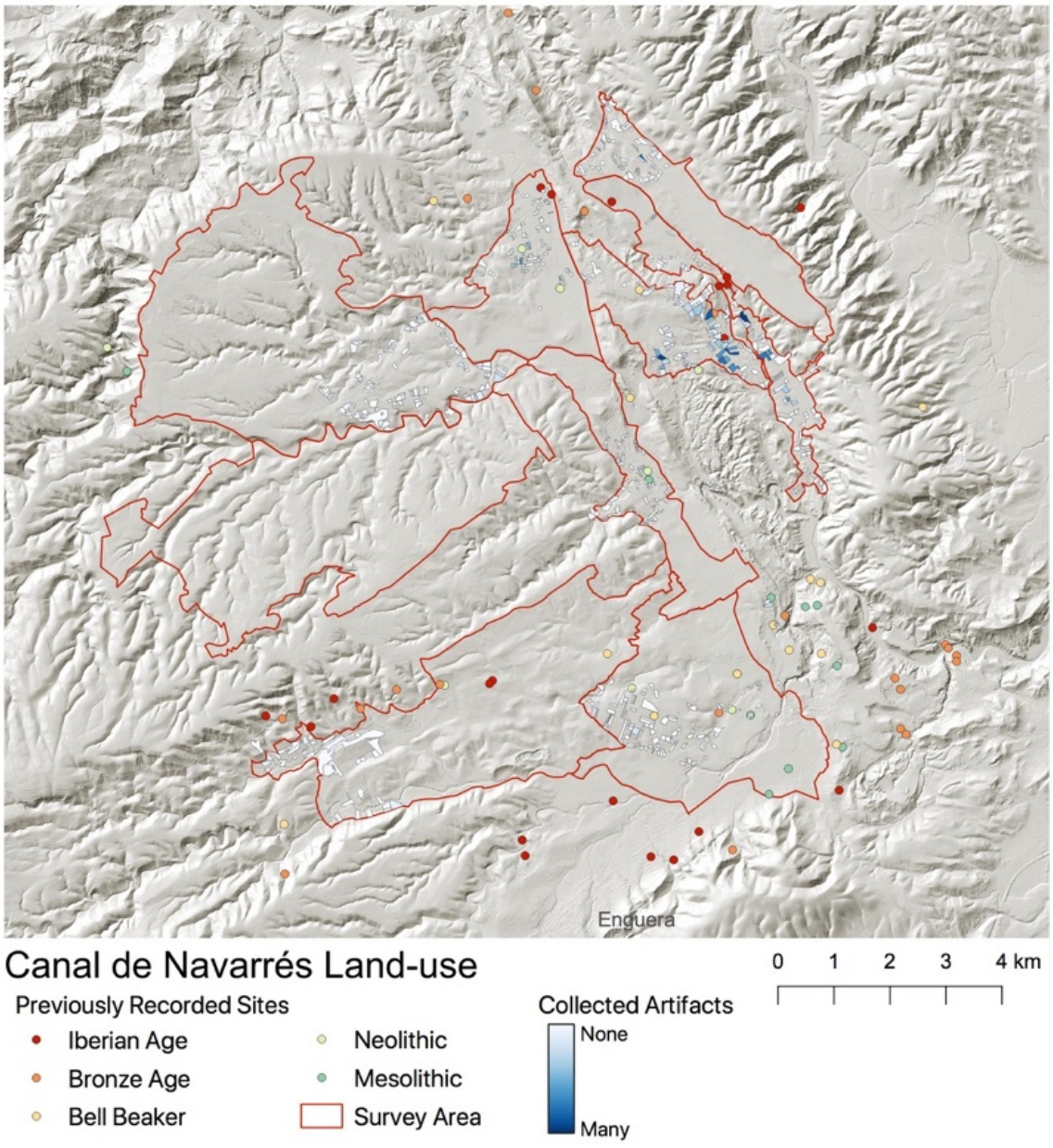

Fig. 23: Survey Area, Locations of Collections, and Previously Recorded Sites From the Canal de Navarrés Study Area.

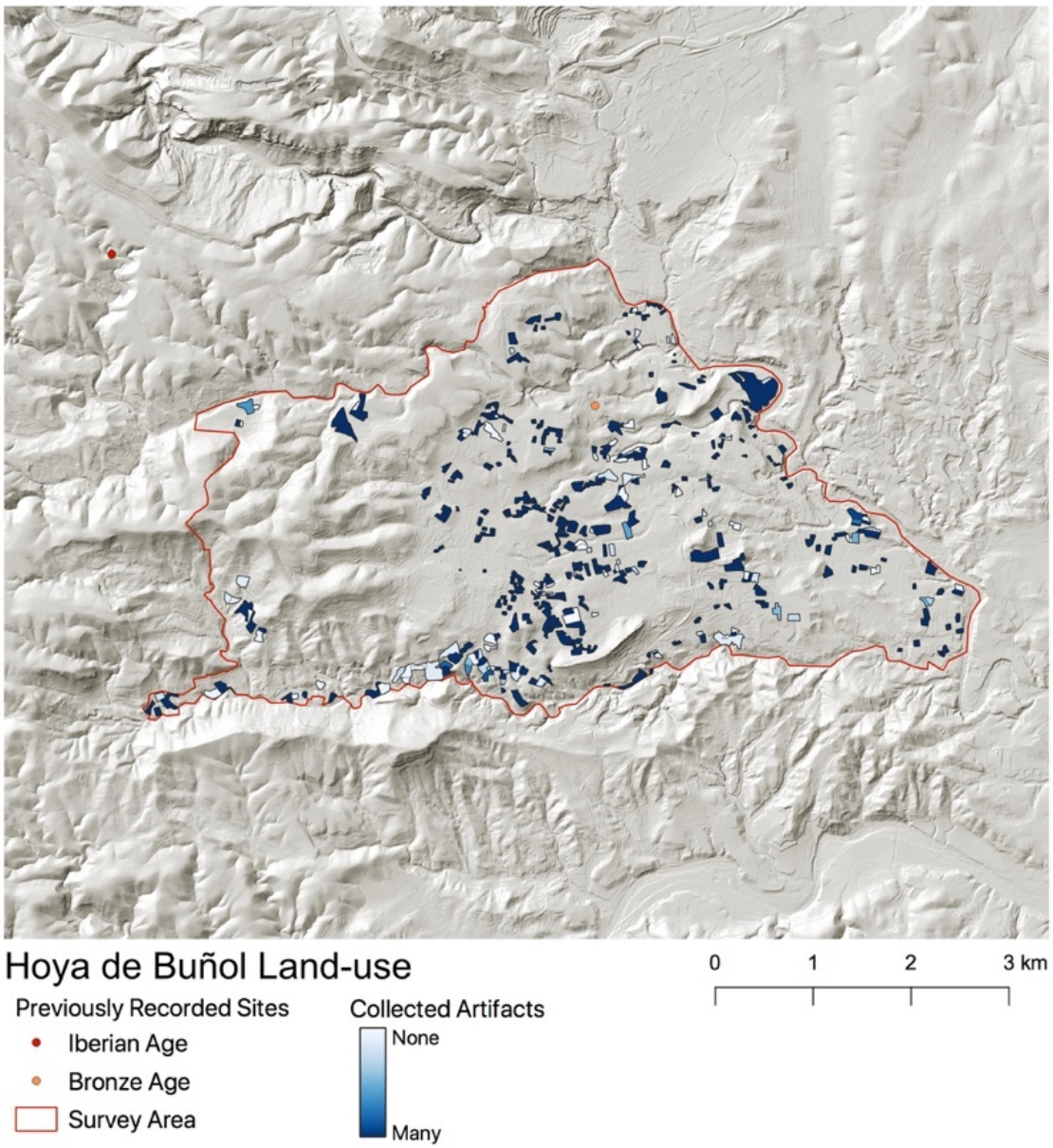

Fig. 24: Survey Area, Locations of Collections, and Previously Recorded Sites From the Hoya de Buñol Study Area.

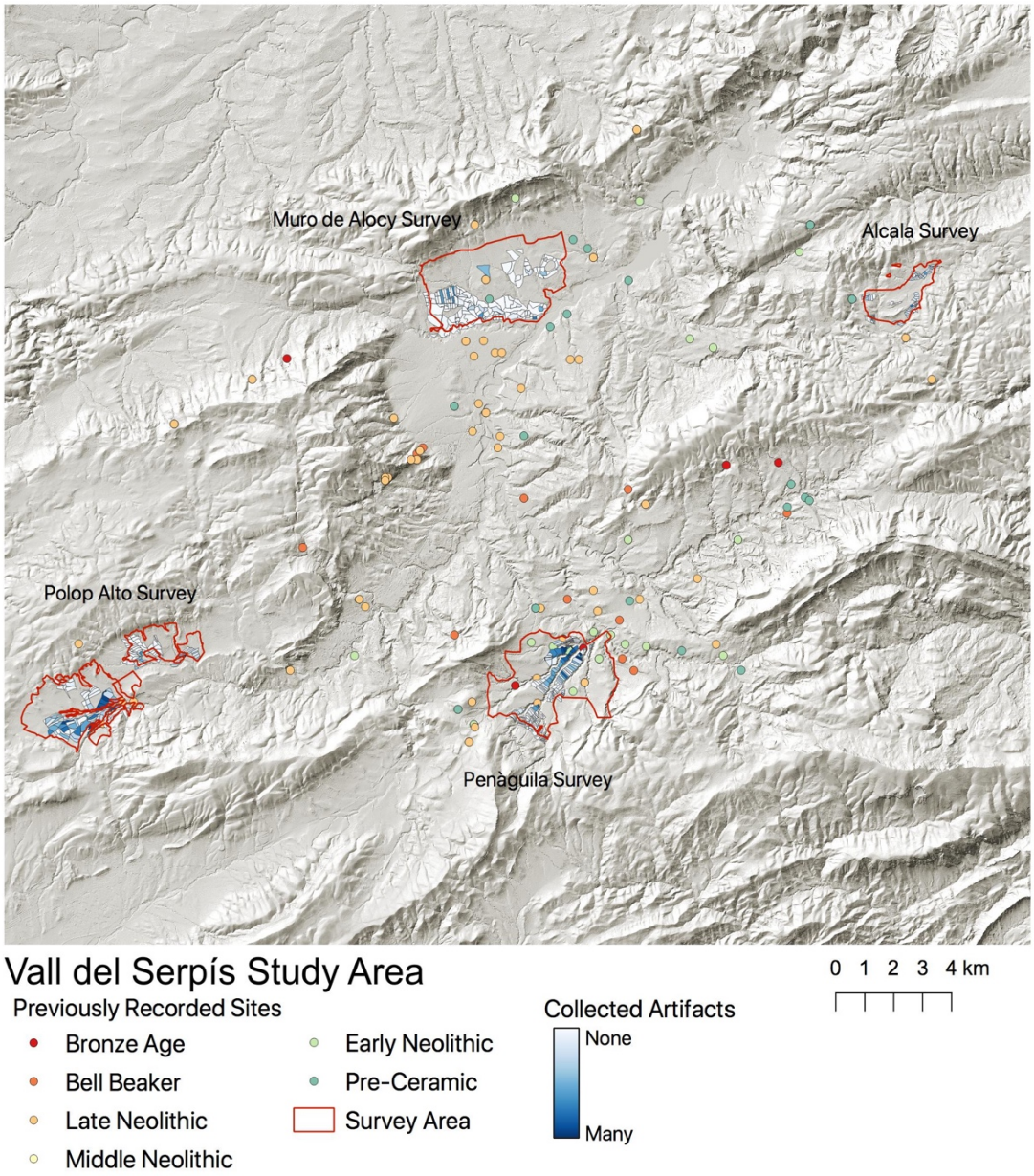

Fig. 25: Survey Area, Locations of Collections, and Previously Recorded Sites From the Vall de Serpís Study Area.

Bayesian approaches to archaeological survey data

Bayesian statistical methods were employed to connect surface collections identified through pedestrian survey to evidence for changes land-use intensity. Regional reference collections of well-dated lithic and ceramic artifacts will provide the "prior knowledge" required in Bayesian statistics to make estimates of probability of land-use intensity during specific cultural-temporal periods (Fernández-López de Pablo and Barton, 2013; Ortman et al., 2007; Ortman, 2016; Snitker et al., 2018a). See Chapter II for details about this approach.

In addition to survey data for each study area, all previously recorded sites with ascribed cultural-temporal periods were incorporated into the final results of the Bayesian analysis. Sites with only one ascribed cultural-temporal period are given a posterior probability of 1.0 for that period. Site with two or more ascribed periods have the probability of occupation distributed equally across each period. For example, a site with Bronze Age and Iberian cultural-temporal periods have a posterior probability of 0.5 assigned to the Bronze Age and Iberian periods respectively.

In order to understand the emergence of anthropogenic burning and HNC related to creation of agricultural landscapes, the cultural-temporal periods for this study are limited to the Late Mesolithic, Early Neolithic, Middle Neolithic, Late Neolithic, and Bell Beaker, Bronze Age, and Iberian periods (see Table 12 for temporal ranges). Although these are relatively coarse-grained temporal units, they are reliably identified from survey collections and provide sufficient chronological resolution to identify changing spatial and temporal patterns of land-use with the study area landscapes.

Table 12: Archaeological Periods Used in This Study.

Archaeological Period	Temporal Range
Bell Beaker	4500 – 3800 BP
Late Neolithic	6000 – 4500 BP
Middle Neolithic	6800 – 6000 BP
Early Neolithic	7600 – 6800 BP
Late Mesolithic	8600 – 7600 BP
Early Mesolithic	11,000 – 8600 BP
Late Upper Paleolithic	13,000 – 11,000 BP

Sedimentary charcoal data to evaluate anthropogenic fire regimes

Sedimentary charcoal sampling and processing

Sedimentary charcoal was collected in column samples in the lower reaches of watersheds from exposed banks of barrancos (the Spanish term for intermittent watercourses). Watersheds offer a convenient means of exposing sediments that can be sampled systematically without the need of coring or intensive excavation. Materials collected from alluvial contexts represent cumulative fire activity and vegetation located upstream of the sample location, having moved material downstream due to channel flow, sheet wash, and other fluvial processes. Finally, previous archaeological research in this region has indicated that most Prehistoric occupations occurred in valley bottoms and near drainages or rivers, making watersheds an ideal candidate for identifying evidence of past land-use (Barton et al., 2010; 2012).

Watersheds were limited to small catchment areas (< 40 sq. km) with priority given to areas that were surveyed for archaeological material. Samples were excavated in continuous, 5 cm levels where possible. Sediments near the top of each exposure were sampled in 10 cm levels due to an increased likelihood that they are young and impact by modern agricultural activities (tilling, fertilizing, filling, etc.). The top 30 cm of sediment

was excluded entirely due to the assumption that it represents the modern plow zone. A minimum of 10 samples were collected from each column, with a focus on alluvial sediments positioned above *terra rossa* sediments associated with the Pleistocene in this region. In the Vall de Serpís, samples were taken in locations identified by Gallello et al. (2017) as containing Neolithic aged sediments and associated artifacts.

Sedimentary charcoal samples collected from alluvial contexts in watersheds were processed for quantification using standard protocols outlined in Roos (2008) and Whitlock and Anderson (2003) and are escribed in detail in Appendix I. Briefly, these protocols involve deflocculating and lightening organic materials within the sample to isolate charcoal fragments. Samples are then wet-screened through 250 μm sedimentology sieves to separate meso-charcoal fragments from smaller clasts. Samples are moved to petri dishes and allowed to dry at room temperature before they are analyzed.

Semi-automated charcoal quantification

Once dried, petri dishes are analyzed using CharTool, a semi-automated image analysis macro built for ImageJ. ImageJ an open-access software program for image analysis developed by the National Institutes for Health, making it easily programable and adaptable to wide variety of research objectives (Schneider et al., 2012). CharTool was built specifically to increase the accuracy and productivity of quantifying charcoal under low magnification by using a live video-microscope feed to identify charcoal fragments through an on-the-fly color thresholding procedure. CharTool quantifies 20 individual metrics for each identified charcoal fragment (see Table 17 in Appendix II for descriptions of each metric). Charcoal is analyzed using a Dino-Lite Pro II 1.3-megapixel

digital microscope at 50x magnification. All charcoal fragments encountered are quantified and exported as a comma separated values file. See Appendix II for details about the design and use of CharTool.

Morphological analysis using machine-learning methods

Charcoal fragment morphology has recently been established as a reliable method in paleoecology for determining the extent of burn areas, primary charcoal transport processes, or taphonomic factors influencing preservation (Enache and Cumming, 2007, 2006). But charcoal morphotypes are also often used to estimate fuel sources and fire intensities of landscape fires. Many studies have suggested that the temperature reached by fire determines the response of a fuel and consequently the morphology and structure of charred fragments (Jensen et al., 2007; Leys et al., 2015; Vachula and Richter, 2018).

Although charcoal morphotypes provide a promising step forward in connecting fire characteristics with the charcoal record, there are several limitations to current classification methods. They include: 1) current methods are developed for fuels in temperate, North American forests with species specific to only that ecoregion; 2) they are intended for application in lacustrine depositional environments, where charcoal preservation is less impacted by high energy stream flow; and 3) the potential for inter-observer error and subjectivity of classification based on visual representations. To address these limitations, I designed a series of methodological enhancements developed for quantifying and classifying charcoal from alluvial sedimentary contexts. The first is the creation of a dataset of modern charcoal samples from fuels present during the Holocene in eastern Spain. This collection of modern charcoal acted as a training set for

the machine-learning statistical classifier. Second, all modern charcoal samples were exposed to artificial mechanical weathering/rounding associated with alluvial deposition, following published protocols. Alluvial transport has been shown to alter the morphological characteristics of charcoal fragments, making common classification typologies unsuitable (Crawford and Belcher, 2014; Umbanhowar Jr. and McGrath, 1998). By creating new classification training sets from mechanical weathered charcoal fragments, classifications of charcoal from Mediterranean alluvial contexts can be made more accurately. Finally, to standardize charcoal fragment measures, reduce inter-observer error, and increase replicability in morphological classifications, all charcoal metrics were collected using CharTool.

A detailed description of the methods used to classify charcoal particles from each sediment column is outlined in Appendix II. In brief, experimental assemblages of charcoal particles were created from woody, herbaceous, and grassy plant taxa collected from the study areas. Together, these fuels represent a variety of geometric/blocky morphotypes corresponding to charcoal derived from woody fuels at higher intensities, irregular morphotypes created from finer fuels, such as leafy or small diameter fuels burned at lower intensities, and elongated morphotypes created during low-intensity burning of fine fuels such as from grasses, stems, or pine needles. These species are common to all three study areas and appear throughout the paleo-pollen record in multiple regional cores (Carrión, 2012; Carrión et al., 2010). Samples were stirred for two hours in a solution of water and silica gravels to simulated mechanical weathering associated with alluvial transport. After weathering, experimental charcoal assemblages were then quantified using CharTool.

A subset known fuels were then used as a training set to generate classification models using a K-nearest neighbors (K-NN) semi-supervised classifying algorithm. These models are then applied to the empirical charcoal data collected from all the column samples in each study area to assign a probability that each fragment fits into each morphotype category. Charcoal fragments that are bi- or multi-modal in their classification probabilities are assigned an "indeterminate" designation, meaning their variation cannot be captured by the existing fuel types. Although some fragments cannot be classified, these methods still offer a reliable and reproducible method for classification that eliminates many of the ambiguities of other methods.

Charcoal Source Areas

Watersheds provide an excellent analytical unit for examining landscape-scale evidence of land-use and fire, but only account for secondary, post-fire transport processes acting on charcoal fragments such as such as sheet wash or channel flow. During combustion, micro-charcoal particles can be transported great distances due to aerial dispersion, contributing regional charcoal to local watersheds and obscuring the patterns observed in the charcoal record (Whitlock and Larsen, 2001). To directly tie anthropogenic burning to land-use practices, a new spatial analytical unit must be defined to account for the source areas of both archaeological and charcoal data.

To address this issue, I developed CharSource, a mathematical and GIS-based model of transport processes and charcoal source areas. CharSource accounts for both primary and secondary charcoal transport, thus providing a spatial representation of

charcoal source areas that can be directly related to archaeological measures of land-use. This model was applied to each individual charcoal particle from each sample location to estimate the spatial distribution of fires within the landscape that could have created it (Clark, 1988a; Higuera et al., 2007; Peters and Higuera, 2007). The model combines a Gaussian model of plume injection, topographic elevation and slope, prevailing winds, charcoal fragment size, and vegetation types to estimate where fires mostly likely occurred on the surrounding landscape given ignition and transport conditions. The charcoal source areas created for all fragments in a sample interval are aggregated to identify the total areas on the landscape that contributed to the formation of that charcoal assemblage (Fig. 26). Source areas change throughout the column based on the size distribution of charcoal particles in each sampling interval. By expanding the source area for charcoal beyond the watershed, I can now identify how archaeological data beyond the watershed may have contributed to the formation of a particular record.

Other geoarchaeological data

Categorical assessment of grain size

To evaluate the degree to which episodes of intense sedimentation may influence charcoal frequency and preservation, clasts contained in each sample are categorized based on size. This method relies on the assumption that settling velocity and threshold velocity for clast traction increase with clast size and provides an expedient, yet low-resolution analysis of sedimentation conditions. Using the Wentworth scale, sediments were divided into three categories based on clast diameter size: sands and fine sediments

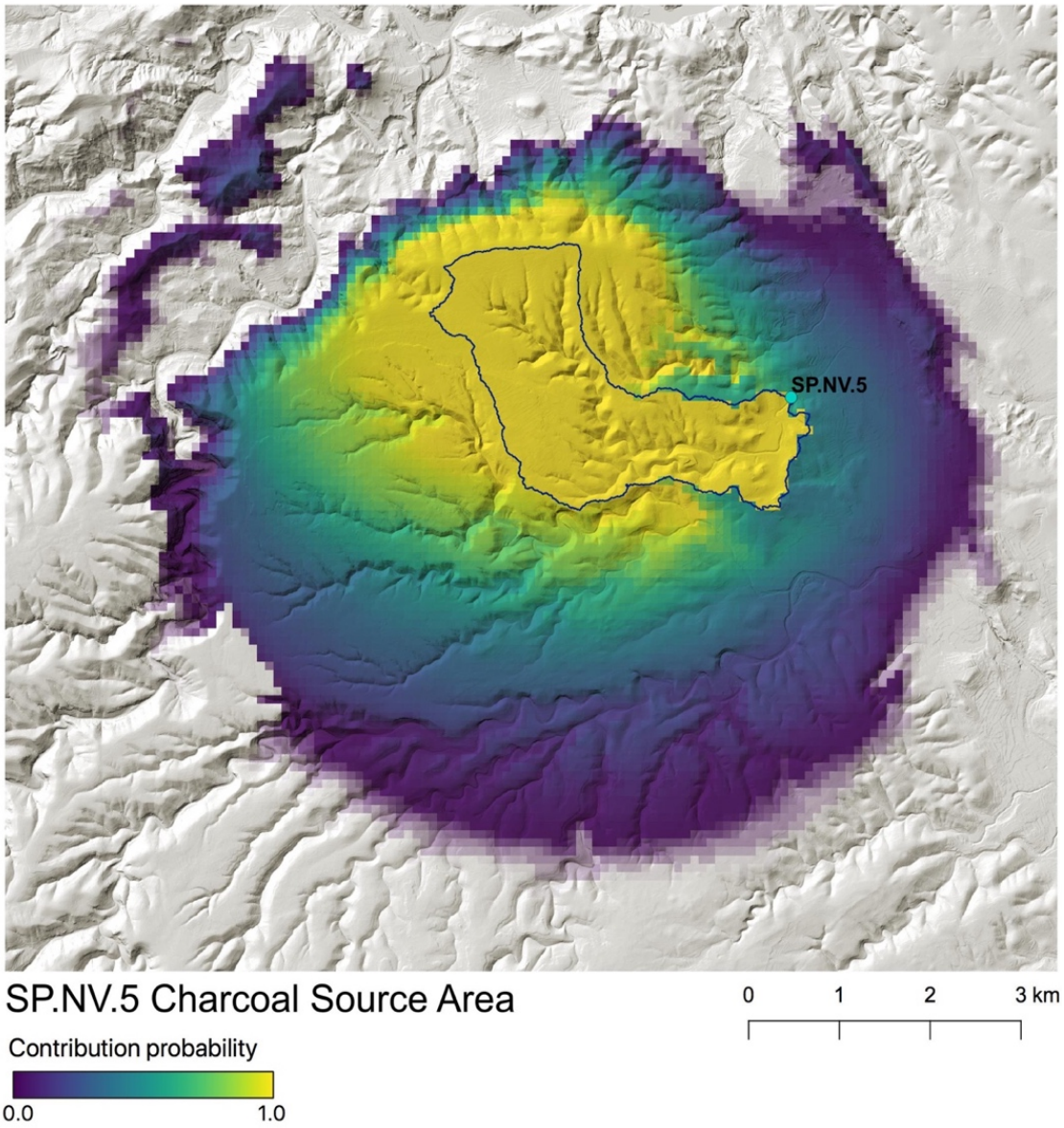

Fig. 26: Example of a Charcoal Source Area Created for Column SP.NV.5 in the Canal de Navarrés Study Area. Conditional Probability Refers to the Likelihood That a Fire Burning on a Given Cell Will Contribute Charcoal to the Watershed of SP.NV.5 Under the Prevailing Wind, Fire Intensity, and Topographic Parameters Set in the CharSource Model.

(< 2mm), fine and medium gravels (2 – 8 mm), and coarse gravels (8 – 64 mm) (Wentworth, 1922). These categories correspond to periods of low energy sedimentation (sands and fine sediments), moderate energy sedimentation (fine and medium gravels), and high energy sedimentation (coarse gravels).

Age-depth models for selected column samples

Large charcoal fragments were selected from column samples throughout all three study areas for AMS C^{14} dating. Unfortunately, the number of radiocarbon samples that could be successfully and reliably dated from these study areas is limited due to the small size of charcoal fragments. This is likely due to the mechanical weathering and fragmentation that occurs during alluvial transport.

Columns with multiple charcoal fragments suitable for radiocarbon dating were processed and dated at the Accelerator Mass Spectrometry Laboratory at the University of Arizona. Resulting C^{14} ages occurred in stratigraphic order, supporting regular deposition within each watershed. An age-depth model was applied to all to non-dated samples within each column using the R package Bchron. Statistical age-depth models are being used more frequently in archaeological and geological sciences and employ either linear and non-linear models to estimate the relationship between depth and age of stratigraphically positioned samples based on known ages and depths of dated materials. This information is then used to estimate the age of non-dated samples within a sampling column or excavated context. Age-depth models derived from these dates are illustrated in Appendix VI. The amount of carbon extracted from small charcoal fragment sizes, especially those from the Vall del Serpís study area, is at the lower limits of reliable AMS C^{14} age measurement. The resulting radiocarbon dates have high measurements of error, which should be considered when interpreting their significance. See Table 13 for radiocarbon dates used in this study.

Table 13: AMS Radiocarbon Dates Used in This Study.

Study Area	Column	Sample	Depth (cmbs)	Cal. BP	AMS Sample #
Canal de	SP.NV.2	03	190	3498 ± 131	AA110528
Navarrés		01	200	3417 ± 303	AA111219
	SP.NV.5	16	50	1854 ± 268	AA111221
		09	110	4741 ± 88	AA109273
		02	145	6998 ± 192	AA110529
	SP.NV.7	24	76	666 ± 7	AA107775
		14	170	5266 ± 158	AA109784
		01	235	8377 ± 27	AA110530
	SP.NV.11	32	56	143 ± 95	AA109274
		19	240	4463 ± 44	AA111976
		04	315	7521 ± 34	AA111975
Hoya de	SP.BN.1	03	205	5195 ± 99	AA110526
Buñol	SP.BN.2	15	150	1920 ± 25	AA111973
		C14	160	2370 ± 154	AA111972
Vall del	PB.RE	09	60	5710 ± 91	AA111969
Serpís		06	90	7049 ± 82	AA111222
		05	100	14575 ± 1545	AA111968
	AC8.RE	06	120	34276 ± 985	AA111220
	BK5.RE	13	80	17617 ± 1909	AA111224
	LP.RE	01	400	41096 ± 3549	AA111223

Results

The results of each of the analysis outlined above are presented as stratigraphic plots for each columns sample. Charcoal data is reported as the frequency of charcoal fragments, as well as the size fraction skewness of the total assemblage of charcoal within each sample. Large skewness values correspond to charcoal assemblages dominated by larger fragments while small values correspond to a greater abundance of small fragments. Charcoal morphologies are presented as percentages of the morphotype represented within each sample's charcoal assemblage. Charcoal source areas, as

calculated by CharSource, are averaged for each sample and present as a ratio of the charcoal source are to the watershed area to capture variation in the spatial distribution of fires. Low source area to watershed ratios indicate that the fires contributing charcoal observed in a column sample were mostly likely located within or near the watershed. High ratios indicate that fires were distant and likely outside of the watershed.

Archaeological data are presented as indices of local archaeological land-use intensity and regional archaeological land-use intensity. Local land-use refers to the sum of all land-use intensity values that occur within the charcoal source area during an archaeological period. This measure of land-use is assumed to be most directly related to the accumulation of charcoal within the watershed. Regional land-use refers to the sum of all land-use intensity values for the entire survey area. See Fig. 27 for an illustration of local verses regional land-use in the Canal de Navarrés case study. The relationship between these two measures can help to identify spatial homogeneity or heterogeneity of human activities related to fire across the landscape.

Finally, to statistically identify zones of changing fire activity, a constrained incremental sum of squares cluster analysis (CONISS) was performed on all variables from each column sample. CONISS is a stratigraphically constrained clustering algorithm in that it considers both the stratigraphic position and the Euclidian distance between each set of variables (Grimm, 1987). Clusters of stratigraphically adjacent, similar observations assigned zone designations, indicating they are statistically different from samples above and below them. This method is very common in palynology and is used to identify changing vegetation communities through time (see Burjachs et al., 2016; Jones et al., 2018; or López-Merino et al., 2009 for examples of CONISS in palyology).

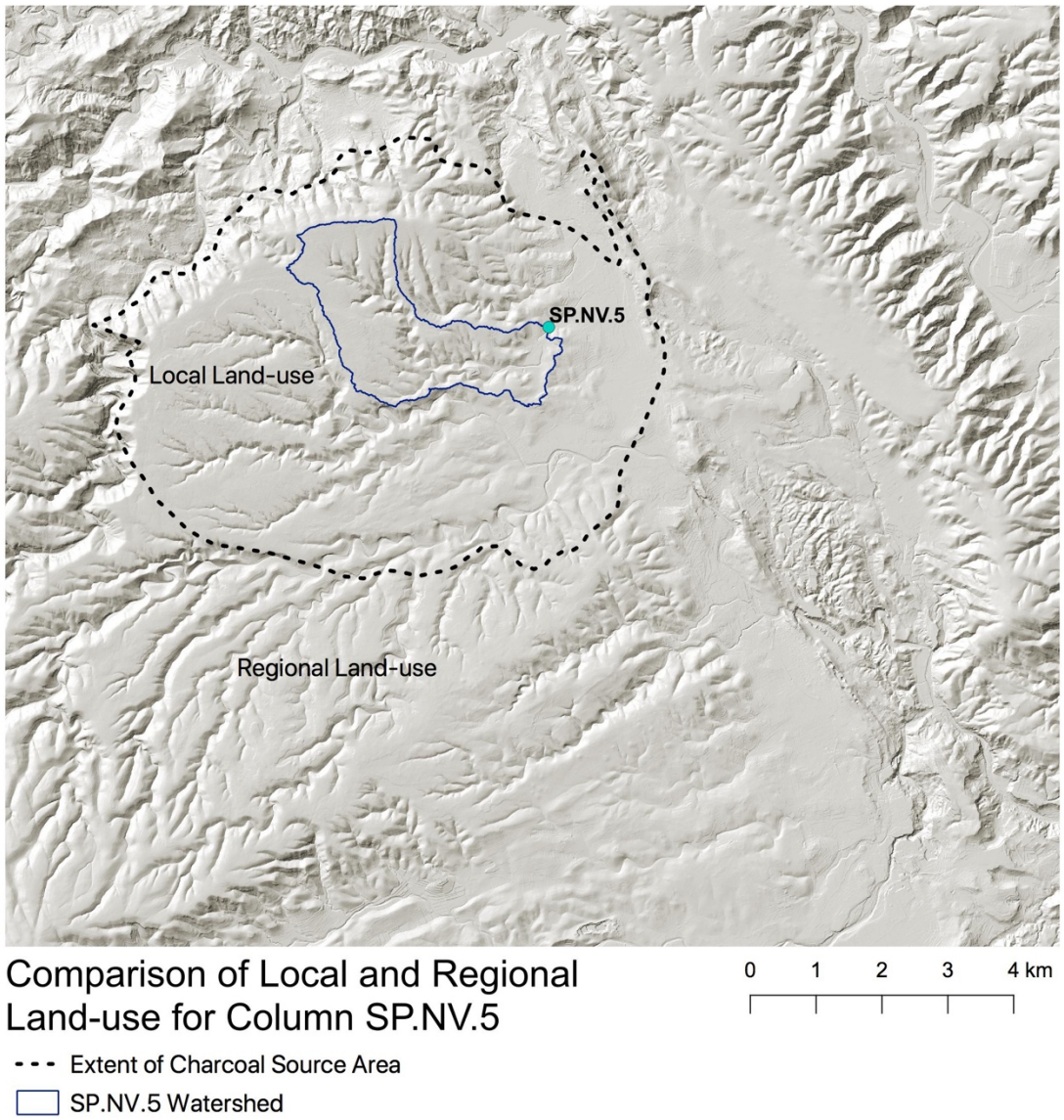

Fig. 27: Illustration of Areas Used in Calculating Local and Regional Land-use. Local Land-use Refers to the Sum of All Land-use Intensity Values That Occur Within the Charcoal Source Area During an Archaeological Period. Regional Land-use Refers to the Sum of All Land-use Intensity Values for the Entire Survey Area.

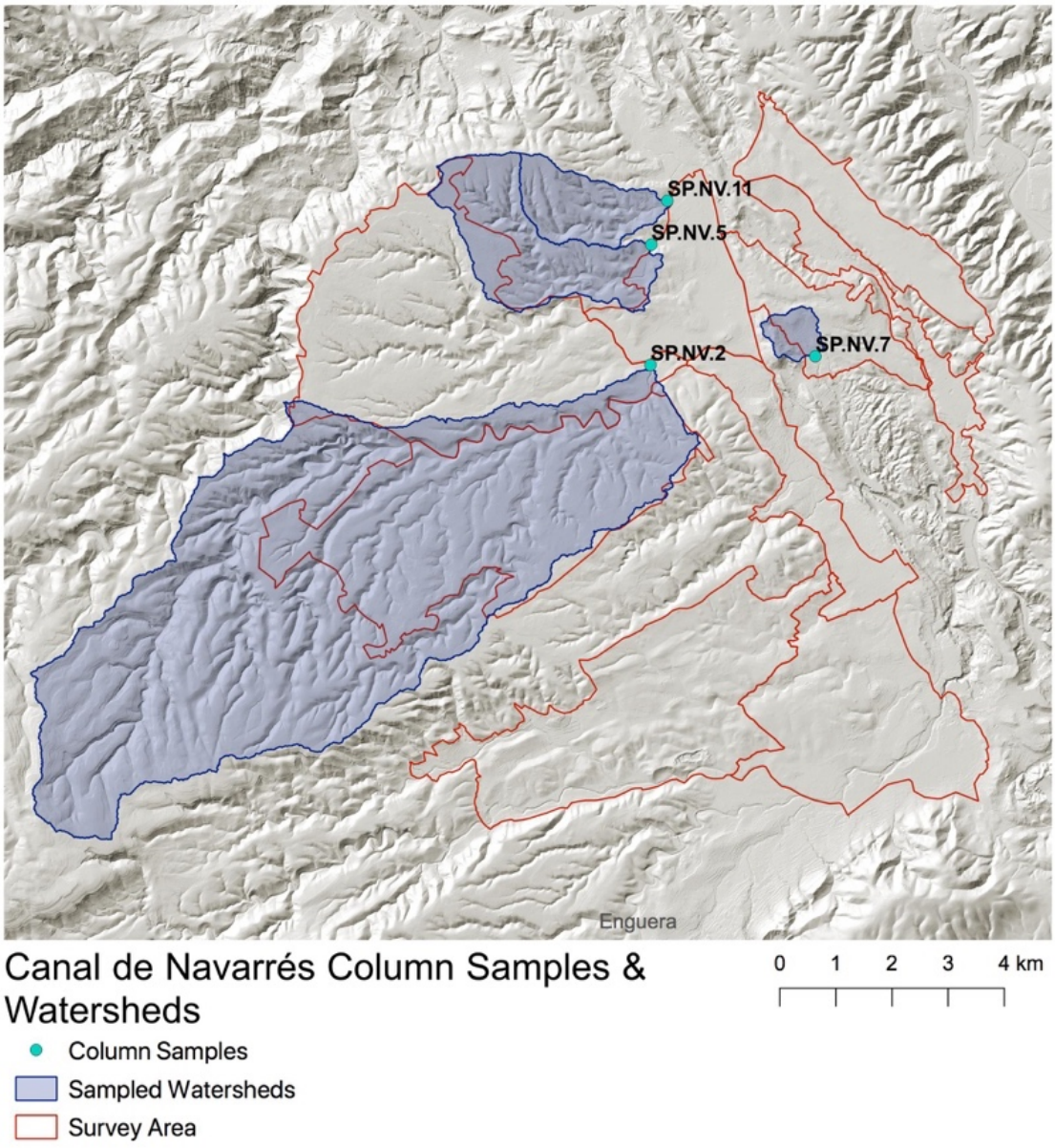

Fig. 28: Column Sample Locations and Watersheds Within the Canal de Navarrés Study Area.

In the context of this study, CONISS is a useful tool for identifying zones of changing fire activity that can be linked to changes niche construction through the Neolithic period.

Canal de Navarrés Study Area

Column samples within the Canal de Navarrés include SP.NV.2, SP.NV.5, SP.NV.7, and SP.NV.11 and were excavated from Neolithic sediments exposed through fluvial incision over the last several hundred years. Despite being limited to exposed sediments, the spatial distribution of the columns samples is fairly representative, spanning a range of watershed sizes, upland and lowland drainages, and distances from archaeologically measured areas of middle and late Holocene occupations (Fig. 28). Age-depth models were calculated from multiple radiocarbon dated charcoal fragments in each column sample, indicating that deposition spans the late Mesolithic to Iberian periods (Table 14).

The general trends within the Canal de Navarrés point to punctuated phases of increased fire activity during the Neolithic period (Figs. 29-32). The first phase occurs during the early Neolithic and is accompanied by larger charcoal fragments, an increase in regional and local land-use intensity, and a transition from geometric morphotypes associated with woody fuels and high intensity fires to irregular morphotypes associated with finer fuels and lower intensity fires. This pattern is observed in column samples SP.NV.7 and SP.NV.11 during zones B. A second phase of increase charcoal accumulation occurs at the beginning of the Late Neolithic period and is visible in zone B in SP.NV.5 and zone D in SP.NV.7. This phase is similar to the Early Neolithic zone, in

that charcoal assemblages are skewed toward larger particles and higher intensity fires, but they differ in that local and regional land-use does not increase. Finally, a third phase of increase charcoal frequency occurs in zone E in SP.NV.7 and zone D in SP.NV.11 at the end of the Late Neolithic and at the beginning of the Bell Beaker periods. All three phases correspond to peaks in micro- and macro-charcoal accumulation rates observed in the N3 pollen and charcoal dataset published by Carrión and van Geel (1999) (See Chapter III and Fig. 33).

Matching phases of Neolithic charcoal accumulation from alluvial deposits with variation within the original N3 dataset confirms that the sampling strategy for this study is effective at capturing major trends in local fire activity within the Canal de Navarrés. These results also indicate that spatial scale plays a significant role in detecting fire activity, as some column samples identify particular zones of changing charcoal metrics while others do not. Finally, elevated charcoal accumulation rates and the dominance of irregular morphotypes during the Neolithic in all of the Canal de Navarrés column samples support the modeling results presented in Chapter III where low-intensity fire associated with pastoralism drove local fire activity and vegetation change.

All four column samples indicate an increase in charcoal source area to watershed area ratios throughout the Bell Beaker, Bronze Age and Iberian periods indicating a reduction in watershed level fire activity. See Fig. 26 for an illustration of the charcoal source area calculated for SP.NV.5 during the Late Neolithic period. SP.NV.2, which spans a temporal range later than the other three column samples, indicates late period zones of punctuated charcoal accumulation in zones A and C. This pattern is likely

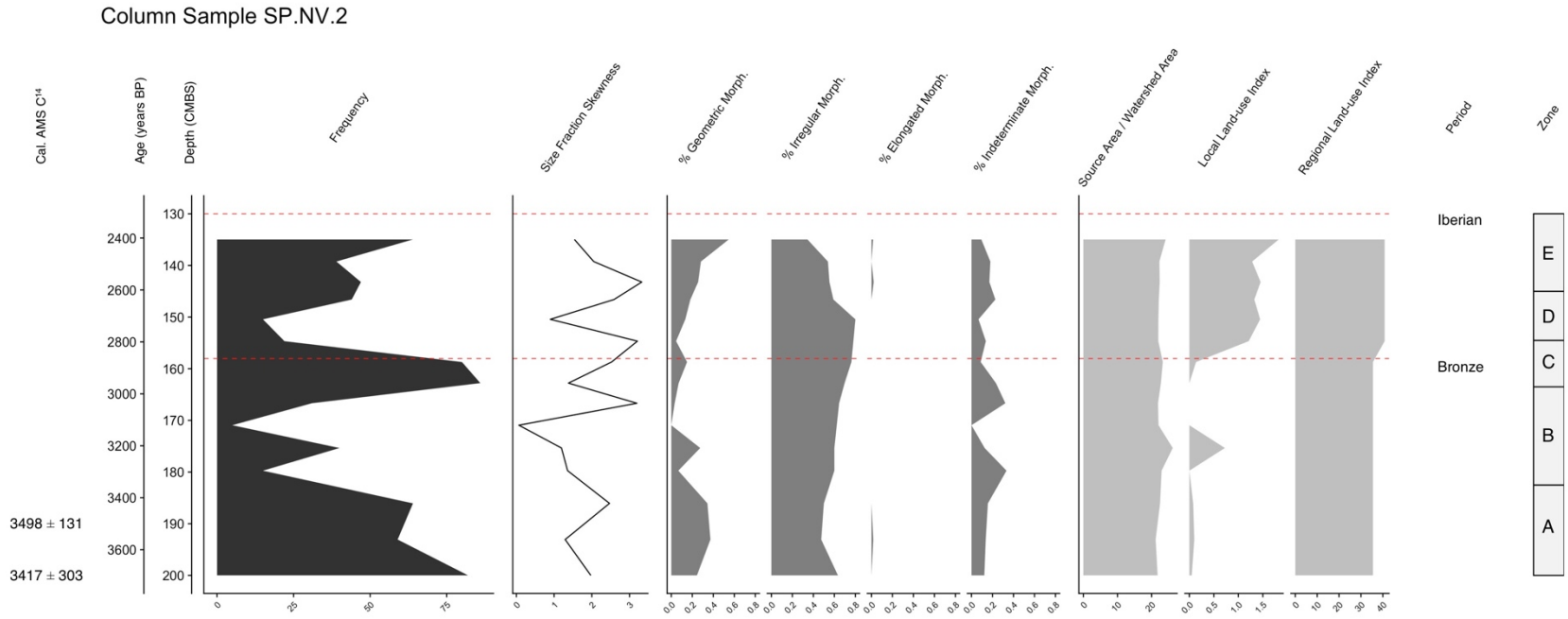

Fig. 29: Column SP.NV.2 Charcoal and Archaeological Data.

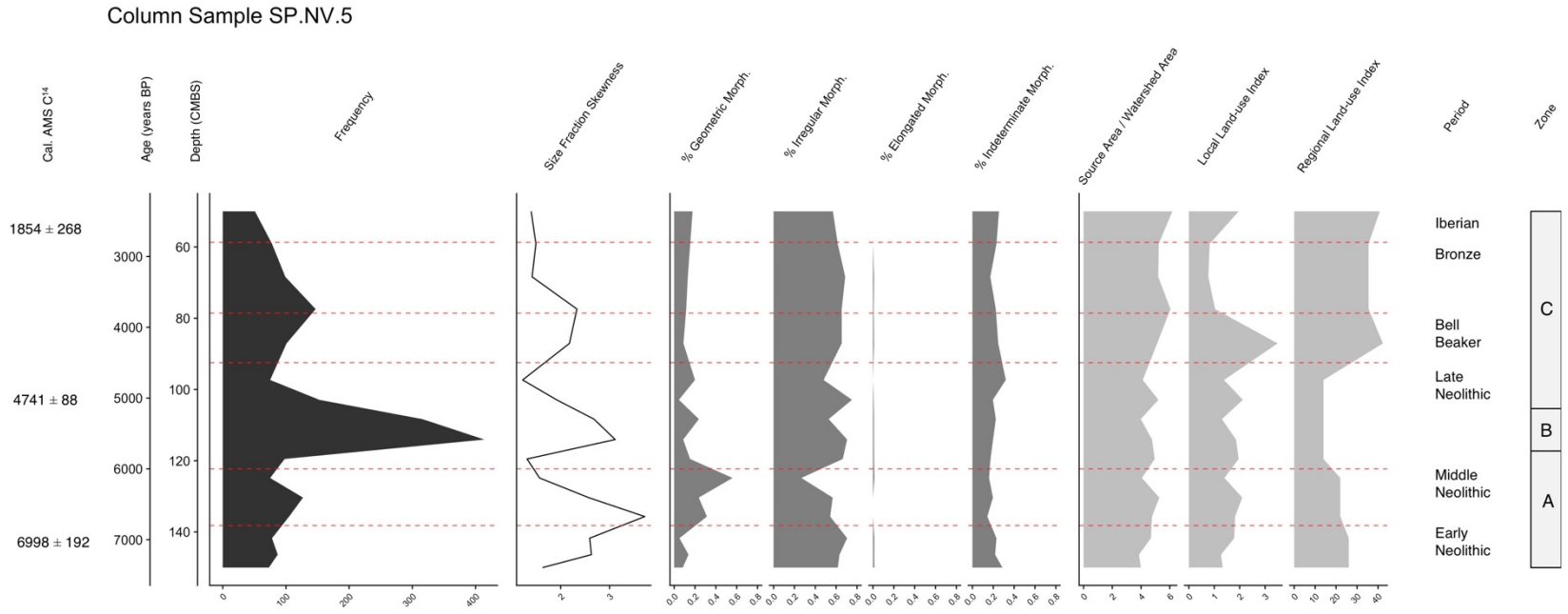

Fig. 30: Column SP.NV.5 Charcoal and Archaeological Data.

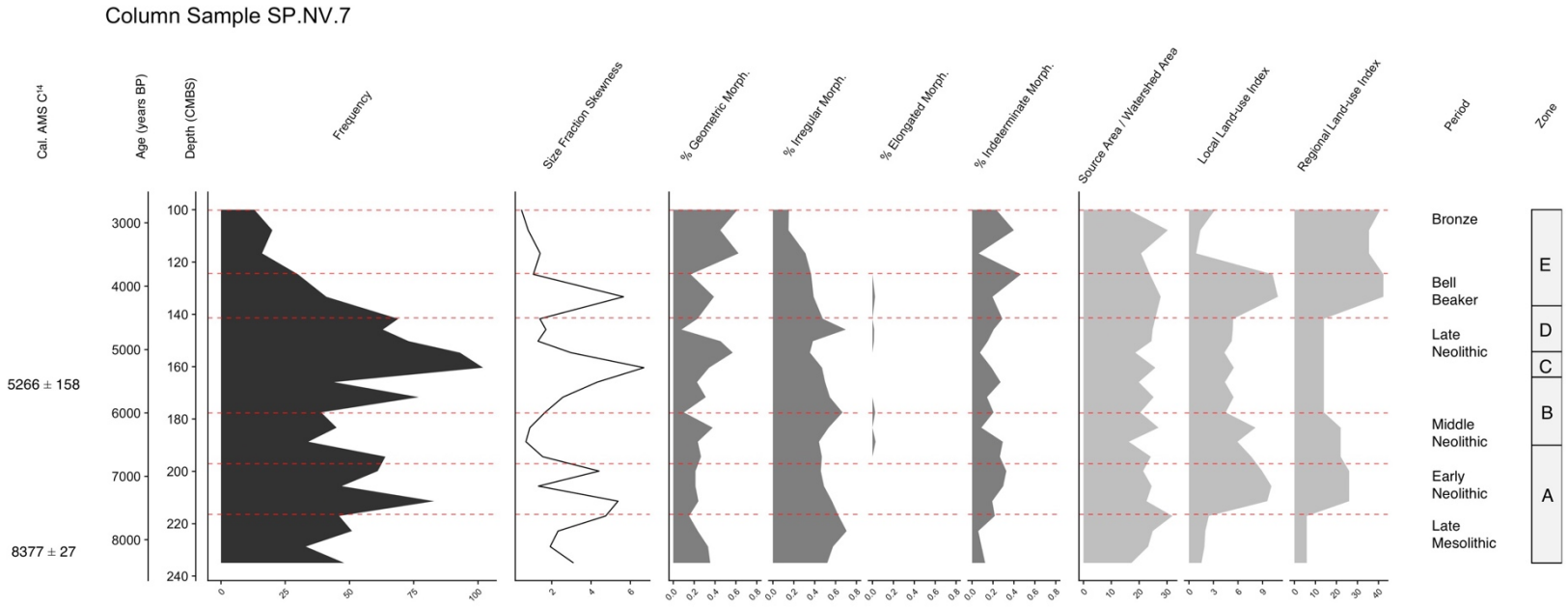

Fig. 31: Column SP.NV.7 Charcoal and Archaeological Data.

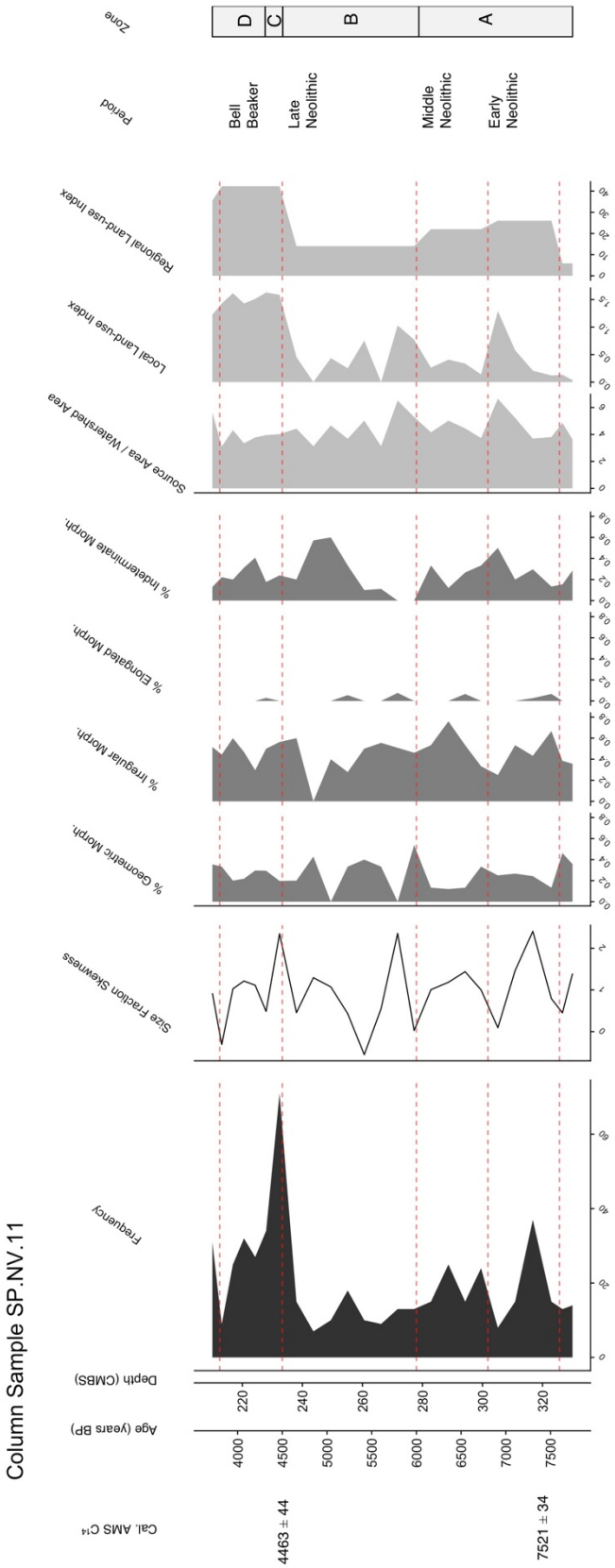

Fig. 32: Column SP.NV.11 Charcoal and Archaeological Data.

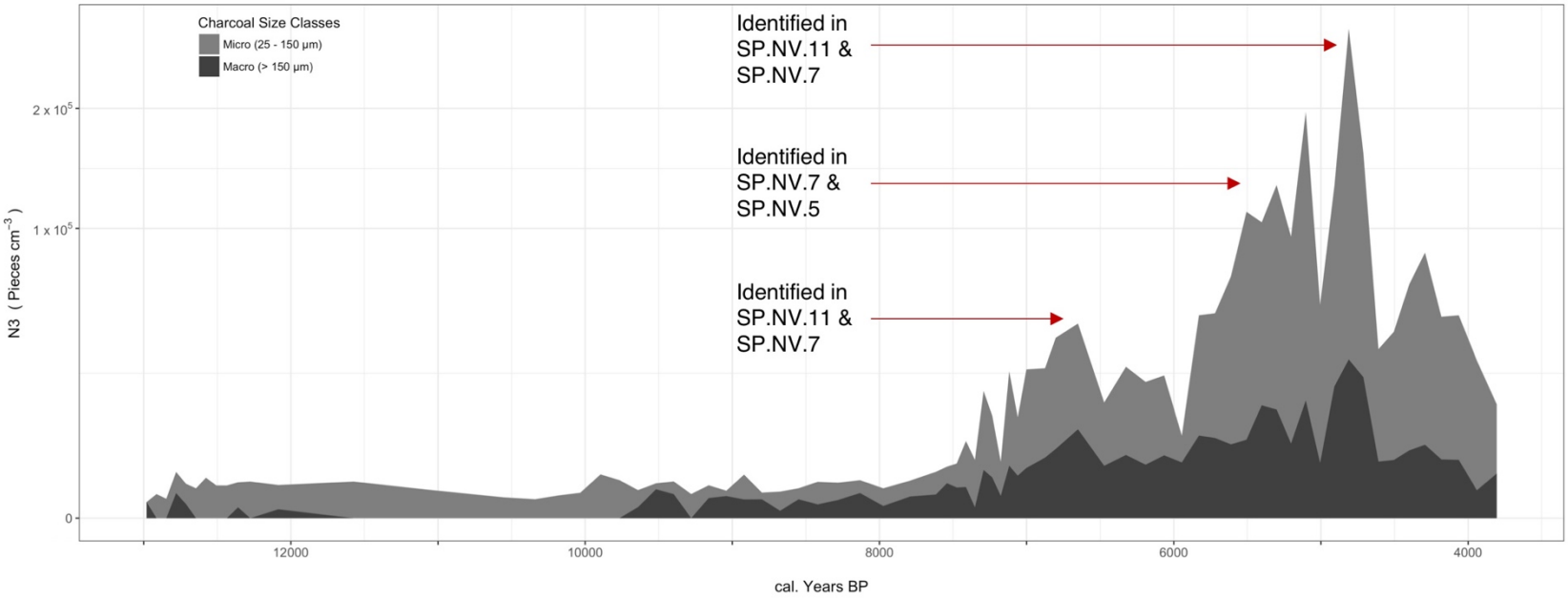

Fig. 33: Summary of N3 Sedimentary Charcoal Record Empirical Data from Carrion and Van Geel, 1999. Fire Activity Observed in Canal de Navarrés Column Samples Correspond to Peaks in Charcoal Concentration in the N3 Core and Are Highlighted with Red Arrows.

related to the establishment of multiple, nearby hilltop occupations during the Bronze Age and Iberian periods.

Hoya de Buñol Study Area

Column samples within the Hoya de Buñol study area include SP.BN.1 and SP.BN.2, which together provide spatial coverage for the western half of the Buñol survey area (Fig. 34). Exposure of these sediments appears to have occurred at a similar timescale as those in the Canal de Navarrés. An age-depth model was generated from multiple radiocarbon dates for SP.BN.2, but only a single radiocarbon date was obtained for SP.BN.1 (Table 13). SP.BN.2 spans the Bronze Age and Iberian periods, while a sample from the bottom of the SP.BN.1 column dates to the Late Neolithic period, suggesting the upper samples represent Bell Beaker, Bronze Age, Iberian, or later occupations. CONISS performed on each column sample identified distinct zones relate to changes in fire and land-use (Figs. 35-36).

SP.BN.2 is characterized by two zones of high charcoal frequency which correspond to the Bronze Age (zone A) and Iberian periods (zone C). Zone A exhibits low charcoal size fraction skewness and a relatively large charcoal source area to watershed area ratio, suggesting a regional increase in fire activity. This interpretation is supported by a low local land-use index compared to a higher regional land-use index during that zone. Zone C represents a reversed pattern during the Iberian period, with high charcoal frequencies, slightly more large charcoal fragments, and elevated levels of local land use indicated more local fire activity.

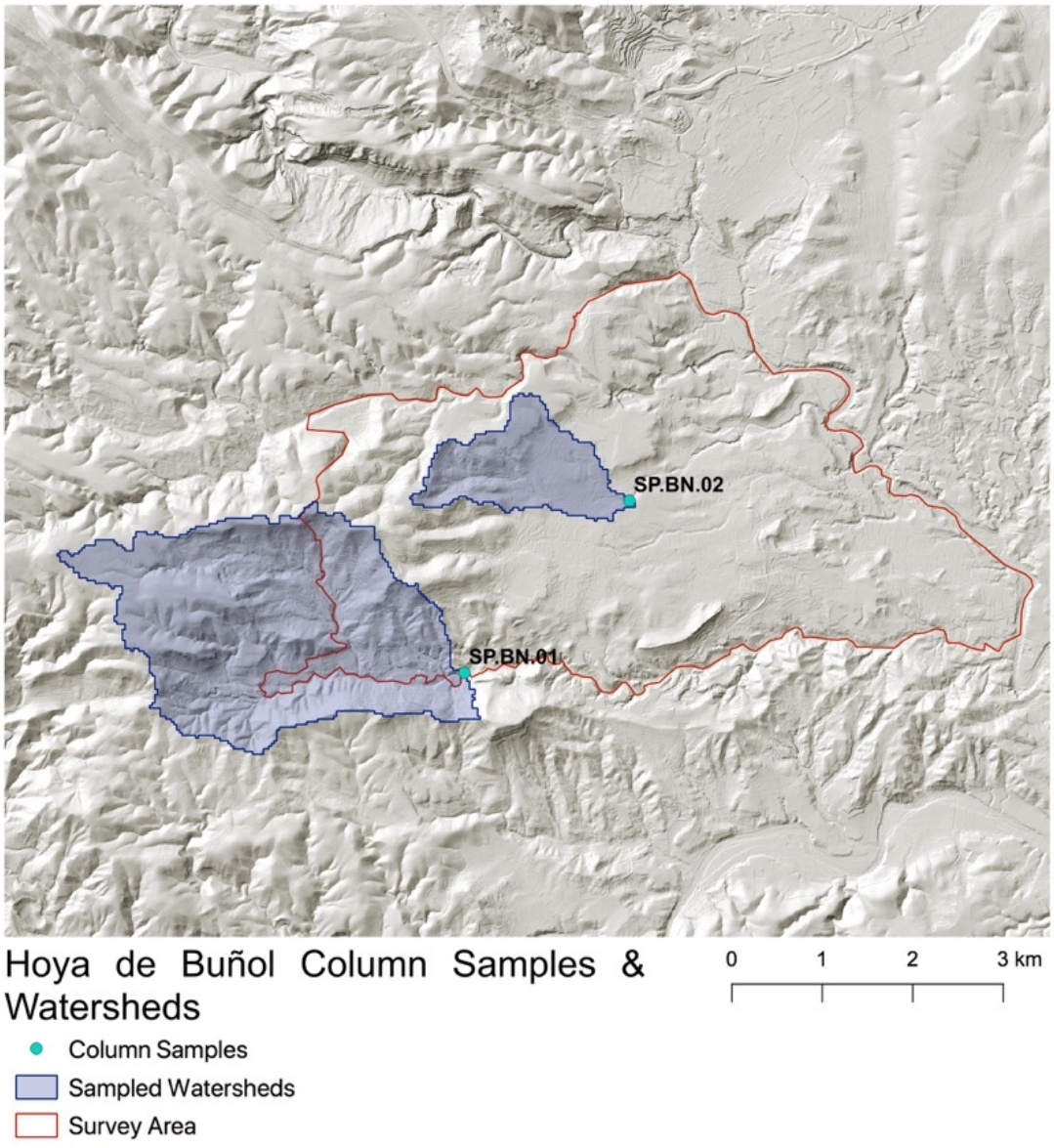

Fig. 34: Column Sample Locations and Watersheds Within the Hoya de Buñol Study Area.

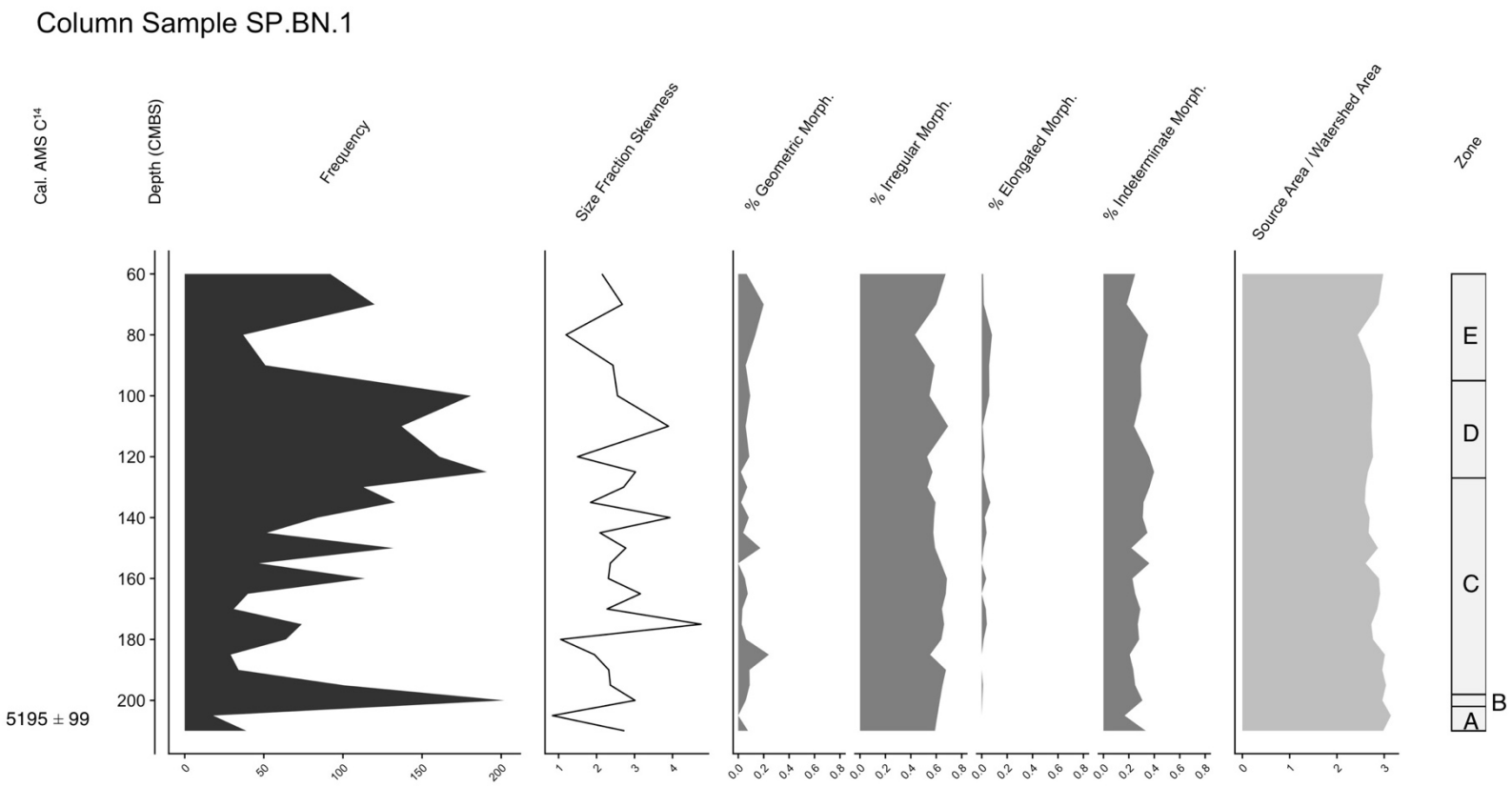

Fig. 35: Column SP.BN.1 Charcoal and Archaeological Data.

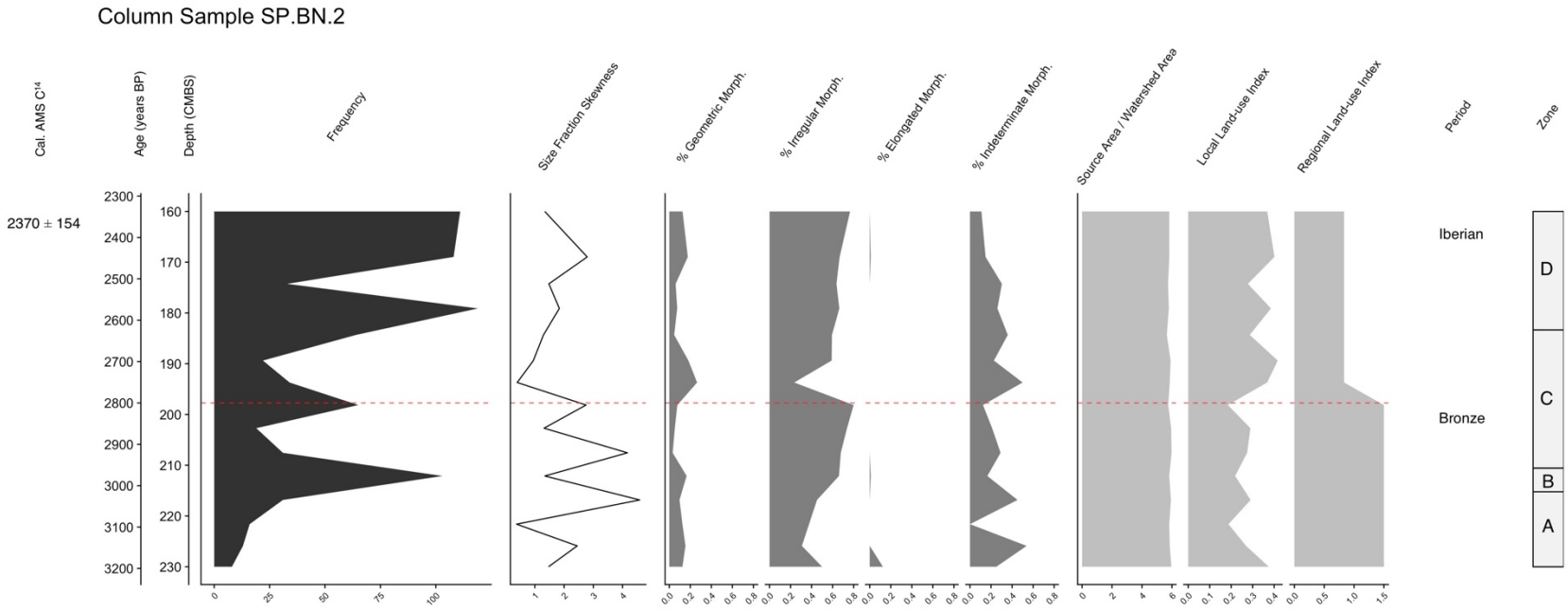

Fig. 36: Column SP.BN.2 Charcoal and Archaeological Data.

Although an age-depth model cannot be generated for SP.BN.1, this column also demonstrates two zones of fire activity at 200 cmbs (zone B) and 120 – 110 cmbs (zone D). Zone B occurs during the Late Neolithic and shows a pattern similar to Neolithic fire activity in the Canal de Navarrés with high frequencies of large charcoal fragments and an increase in the percentage of irregular morphotypes. The charcoal size and irregular morphotype percentage in Zone D shows similarity to Zone D in SP.BN.2. This, in combination with its stratigraphic position, it is reasonable to assume that Zone D in both SP.BN1 and SP.BN.2 represent the same Iberian period fire activity. It is noteworthy that elongated morphotypes, related to fine fuels such as grasses, are present in relative high abundance in post Neolithic samples in SP.BN.1. This suggests either a change in available fuels within SP.BN.1 charcoal source area as a response to changing ecological conditions or the introduction of agro-pastoral practices, such as post-harvest agricultural field burning.

Vall del Serpís Study Area

Column samples collected from the Vall del Serpís include PB.RE, AC8.RE, BK5.RE, LP.RE and BK.RE and represent a wide spatial distribution throughout the valley (Fig. 37). Previous geomorphological studies and landscape modeling in the Vall del Serpís indicate that erosion and incision occurred much earlier than the other study areas, leaving Neolithic aged sediments perched high above the modern watercourses. Due to these conditions, columns samples were excavated from modern road cuts though remaining alluvial deposits.

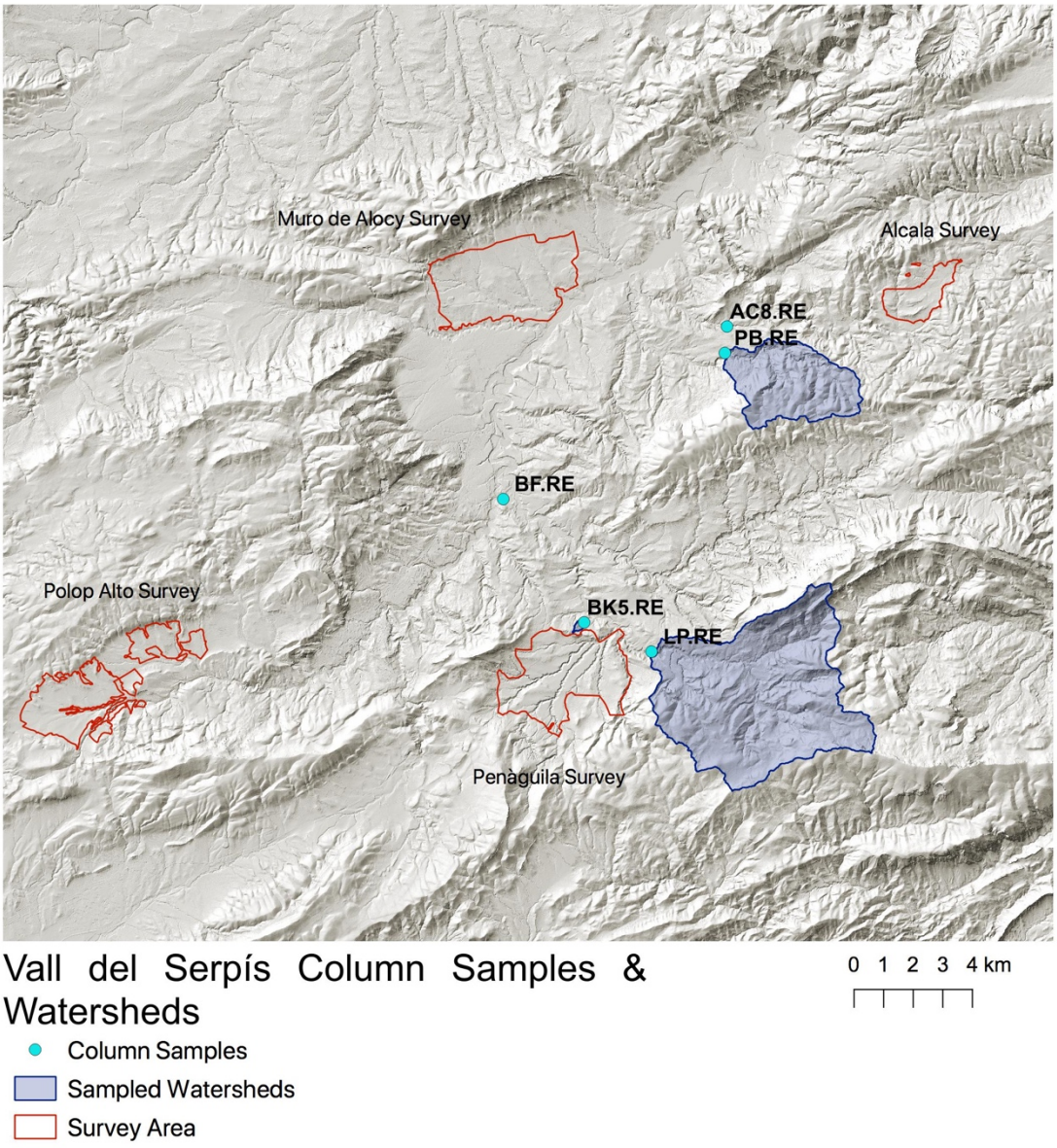

Fig. 37: Column Sample Locations and Watersheds Within the Vall de Serpís Study Area.

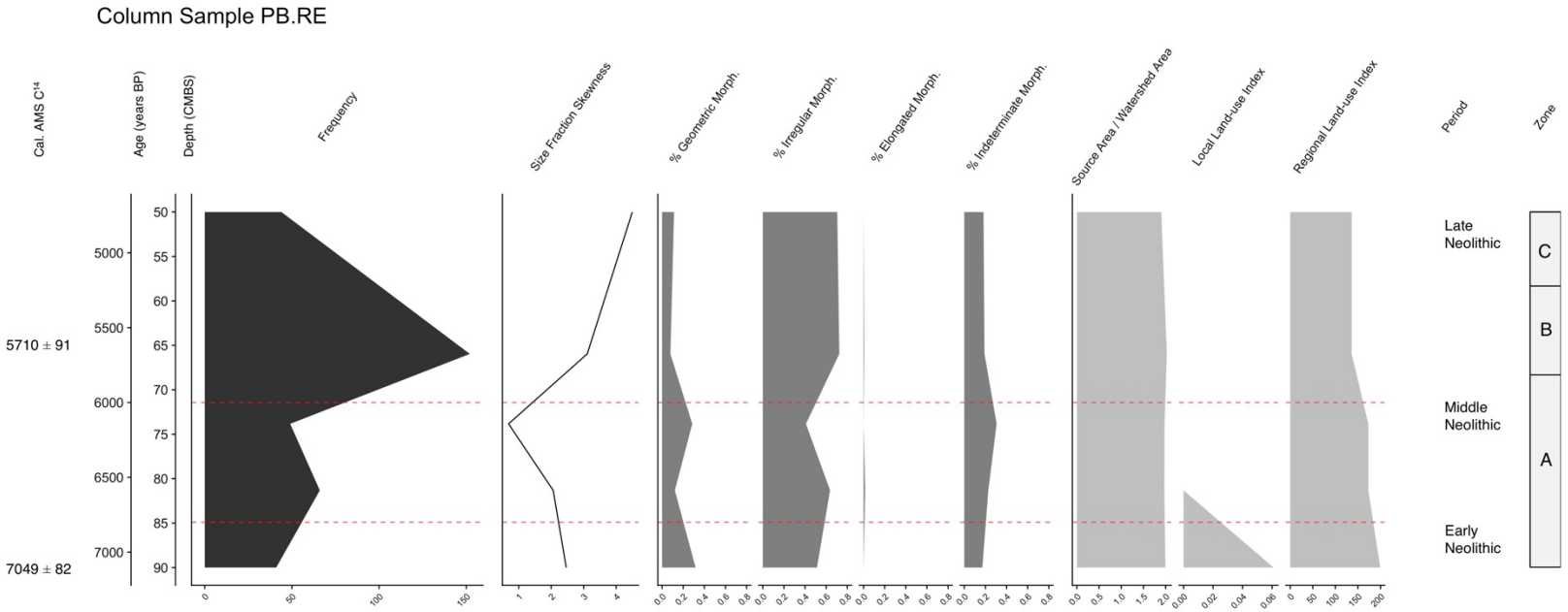

Fig. 38: Column PB.RE Charcoal and Archaeological Data.

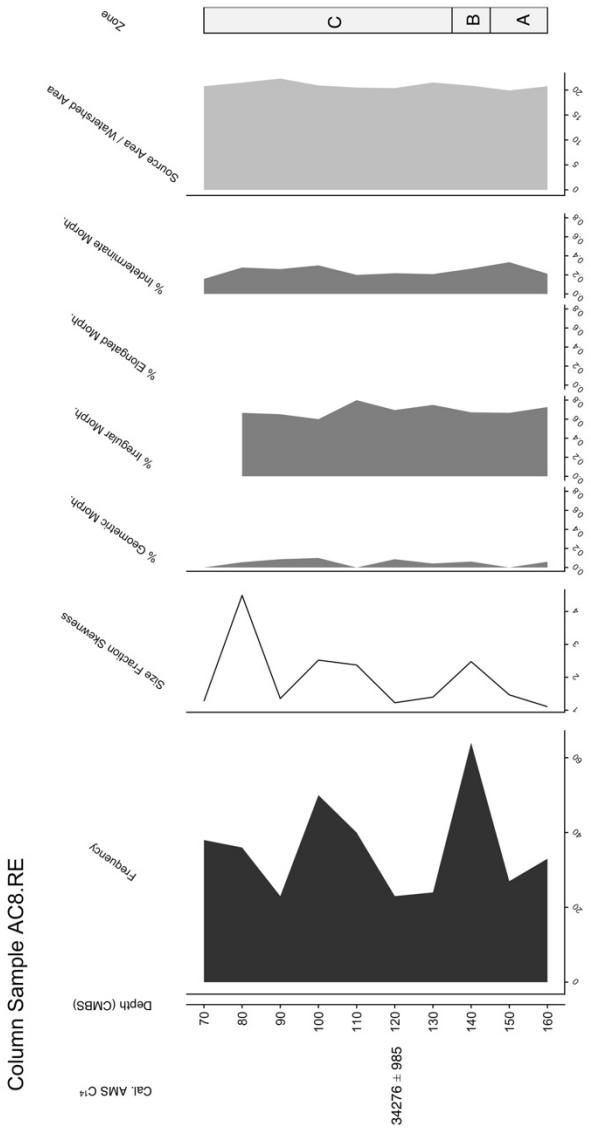

Fig. 39: Column AC8.RE Charcoal and Archaeological Data.

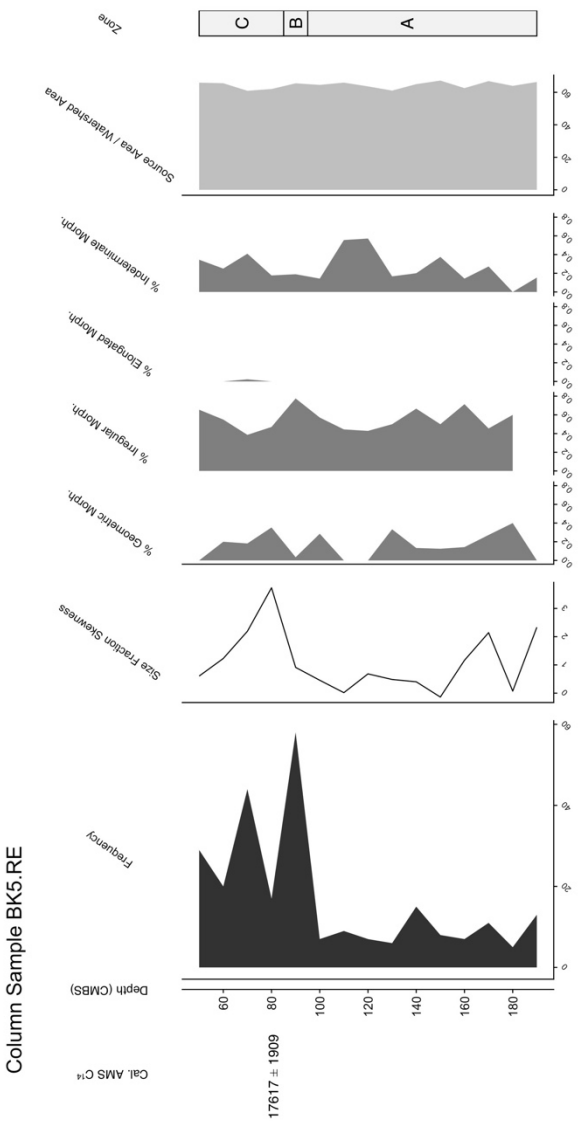

Fig. 40: Column BK5.RE Charcoal and Archaeological Data.

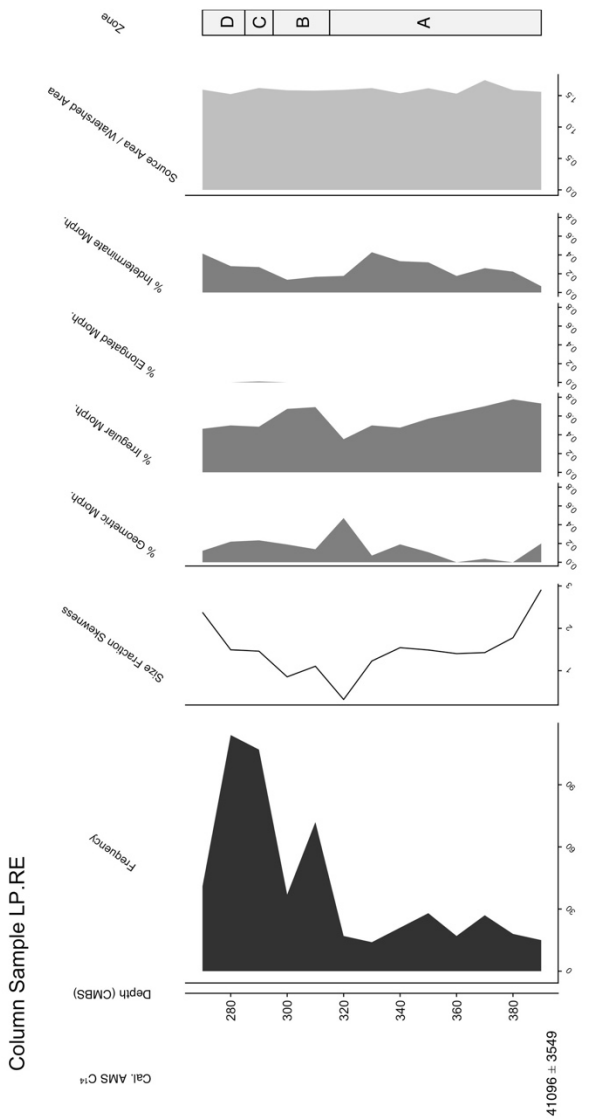

Fig. 41: Column LP.RE Charcoal and Archaeological Data.

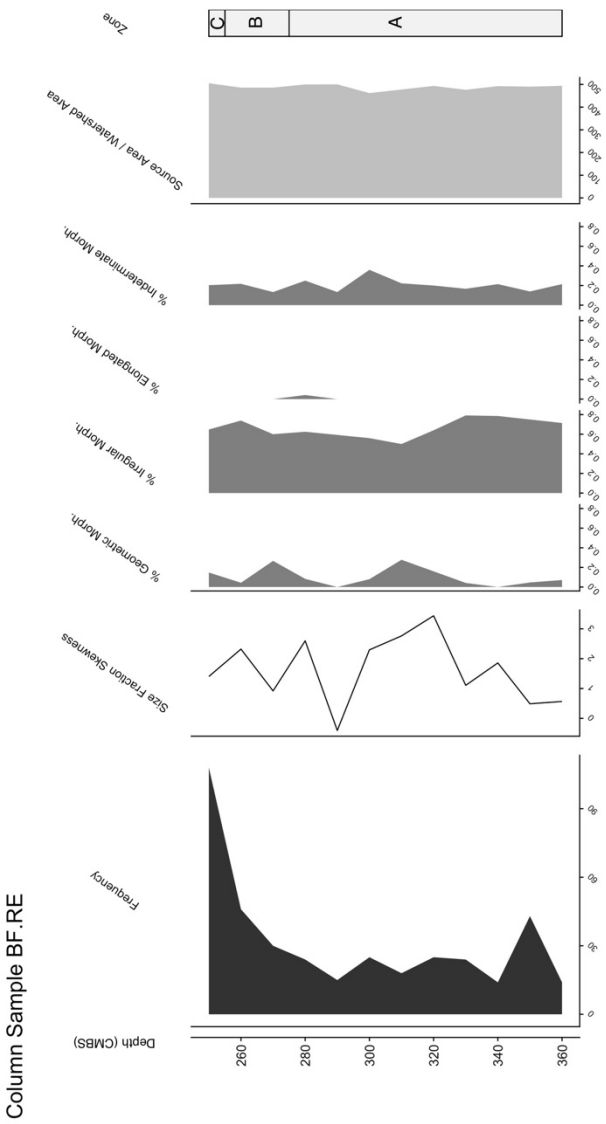

Fig. 42: Column BF.RE Charcoal and Archaeological Data. Note That No AMS C14 Dates Are Associated with This Column.

Due to the unavailability of dateable charcoal fragments in the Vall del Serpís, an age-depth model could only be generated for the three radiocarbon dates from PB.RE (Fig. 38). Although this column sample only contains five observations that date to between the Late Mesolithic and Iberian periods, it nonetheless contains a zone of increased fire activity during the Late Neolithic (zone B). Charcoal and archaeological data in this zone are similar to patterns observed in the Canal de Navarrés and Hoya de Buñol study areas, including an increase in charcoal frequency, charcoal size, and the percentage of irregular morphotypes.

The other column samples within this study area (Figs. 39-42) are difficult to evaluate due to their wide-ranging radiocarbon dates with large errors (Table 13). Even though these sediments were identified as Neolithic in age by Gallello et al. (2017), radiocarbon ages for charcoal fragments from these column samples date to the late Pleistocene (30,000 – 17,000 cal. BP). All of the remaining column samples (AC8.RE, BF. RE, BK5.RE, LP.RE) demonstrate variation in charcoal frequency, size fraction skewness, and morphotypes that could be related to Neolithic anthropogenic fire. For example, it is plausible that LP.RE contains a zone of increased charcoal frequency (290 – 280 cmbs) that could correspond to anthropogenic fire during the Neolithic period, but more evidence would be needed. Making reliable interpretations from the stratigraphic plots alone is not feasible.

Discussion

Multivariate Analysis to identify HNC during the Neolithic Period

Stratigraphic plots and CONISS zonation of charcoal and archaeological data provide a basic framework for identifying fire during the Neolithic period, but making interpretation regarding the drivers of local and regional fire regimes is difficult from these figures alone. Evaluating the co-variance between column samples through time is necessary to identify variables that contribute most to similarities or dissimilarities between each case and can ultimately provide insights into the behaviors that create and maintain agricultural landscape through fire. Principle components analysis (PCA) is a multivariate statistical method that summarizes the variation of datasets with multiple variables by using orthogonal transformations to create a set of variables called principal components. The first principle component describes the largest amount of variance within the dataset, the second principle component describes the second largest amount of variance, and so on and so forth. By interpreting the adjusted loadings of each original variable within the new set of principle components, as well as the spatial location of each observation within a PCA biplot, the overall influence of multiple of variables can be observed in two-dimensional space (Gallello et al., 2013; Servera-Vives et al., 2018).

PCA was performed on all of the observations from all three study areas using a subset of variables that are common across both dated and undated column samples and most related to changes in fire frequency, intensity, and spatial distribution through time. These variables include charcoal frequency, average size of charcoal fragments, charcoal size fraction skewness, morphotype classification, and charcoal source area to watershed area ratio. The zones identified in each column sample through CONISS zonation were classified into periods of high fire activity, moderate fire activity, and low fire activity based on the relative frequency of fire in each zone.

Charcoal metric comparisons within the Canal de Navarrés

PCA biplots with adjusted loadings for the column samples SP.NV.2, SP.NV.5, SP.NV.7, and SP.NV.11 from the Canal de Navarrés are displayed in Figs. 43-45. Although no distinct clusters emerge from a visual examination within the PCA plots, the patterns within the influence of specific variables (eigenvectors) on the structure of charcoal data through time does provide a basis for interpreting distinct phases of niche construction and niche maintenance related to agricultural landscapes in the Canal de Navarrés (Table 14). These trends are likely diminished by the complicated changing spatial scales and preservation challenges associated with comparing multiple alluvial column samples from dispersed locations across the study area, but nonetheless, patterns do emerge from this analysis.

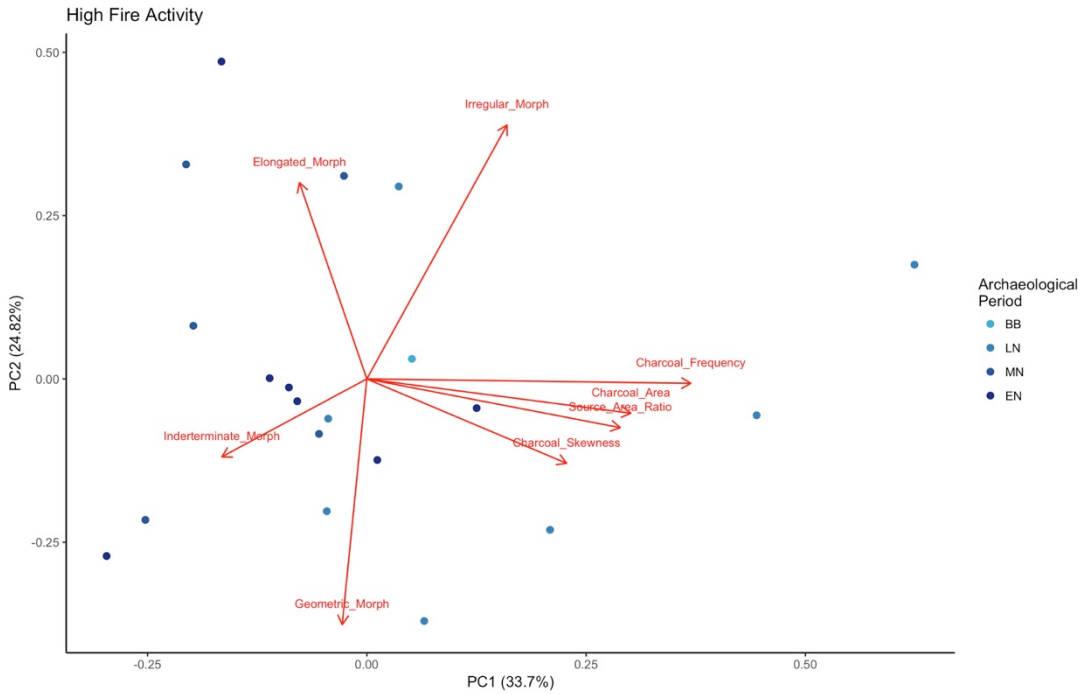

Fig. 43: PCA Biplot of High Fire Activity Zones Within All Column Samples from the Canal de Navarrés Study Area.

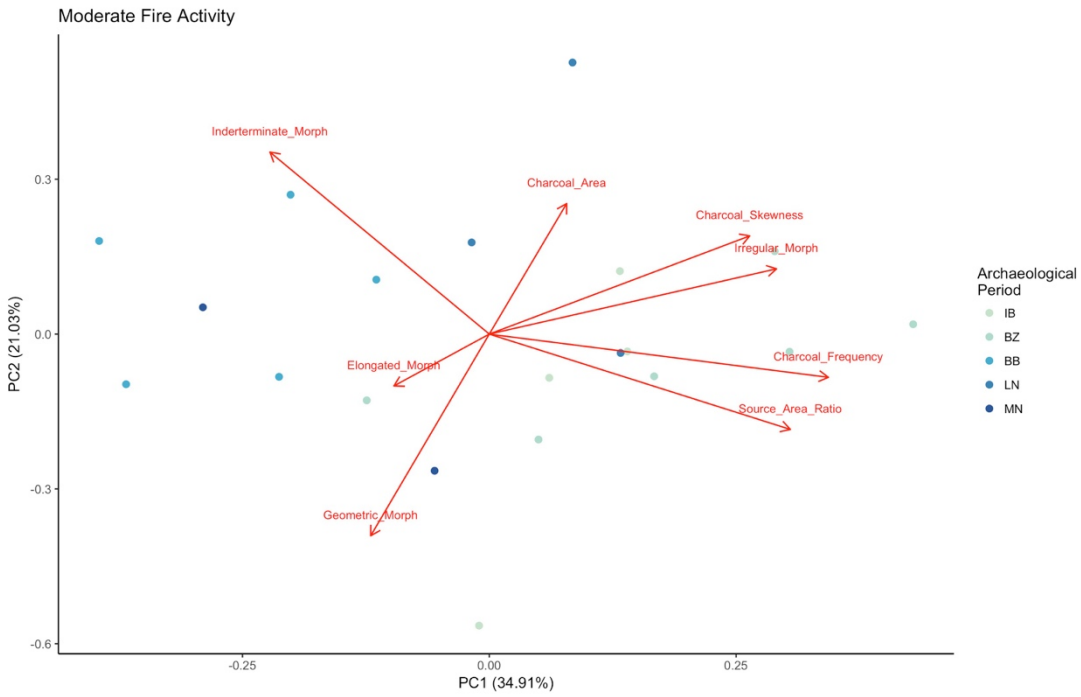

Fig. 44: PCA Biplot of Moderate Fire Activity Within All Column Samples from the Canal de Navarrés Study Area.

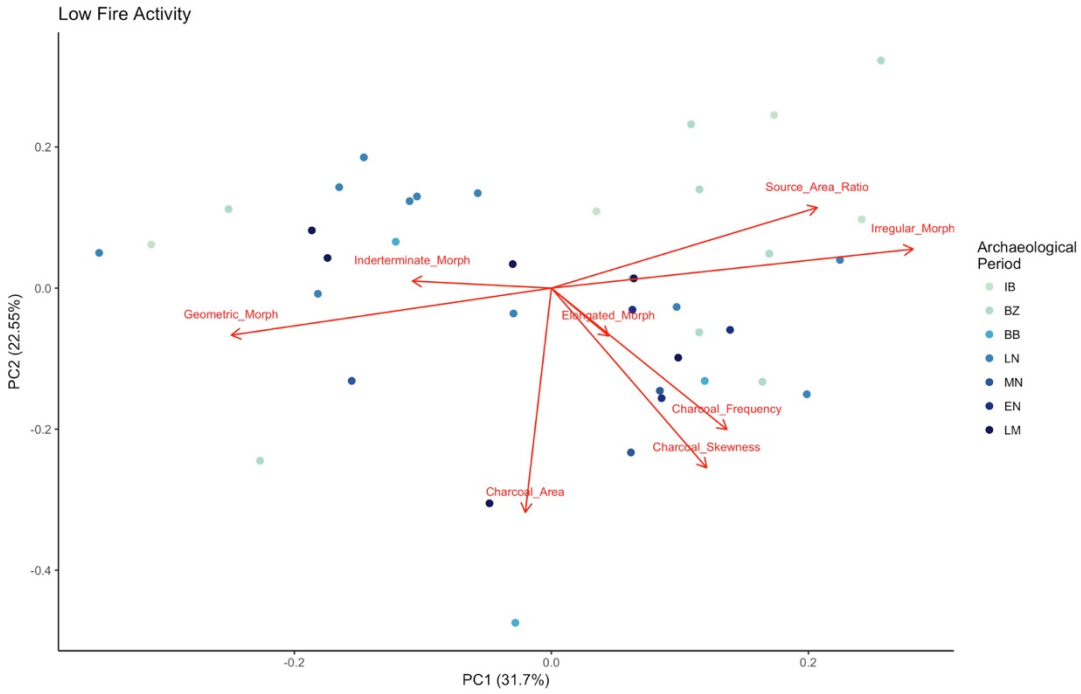

Fig. 45: PCA Biplot of Low Fire Activity Within All Column Samples from the Canal de Navarrés Study Area.

Table 14: Eigenvectors for PCA of All Fire Activity Types in the Canal de Navarrés Study Area.

Fire Activity	Variable	PC1	PC2	PC3	PC4	PC5	PC6	PC7	PC8
High	Charcoal Frequency	0.569	-0.010	-0.178	0.245	-0.163	0.022	-0.747	0.000
	Charcoal Area	0.463	-0.081	0.019	0.561	0.252	-0.428	0.466	0.000
	Charcoal Skewness	0.351	-0.199	0.294	-0.319	0.710	0.379	-0.048	0.000
	Geometric Morphotype	-0.043	-0.579	0.446	0.132	-0.298	0.058	-0.021	-0.595
	Irregular Morphotype	0.246	0.598	0.070	-0.331	-0.006	-0.229	0.048	-0.642
	Elongated Morphotype	-0.118	0.462	0.223	0.573	0.027	0.617	0.051	-0.102
	Indeterminate Morphotype	-0.254	-0.183	-0.704	0.160	0.378	0.105	-0.050	-0.473
	Source Area Ratio	0.445	-0.115	-0.364	-0.207	-0.416	0.475	0.464	0.000
Moderate	Charcoal Frequency	0.515	-0.126	0.069	-0.042	0.131	0.693	-0.463	0.000
	Charcoal Area	0.118	0.379	0.608	-0.174	-0.380	0.291	0.462	0.000
	Charcoal Skewness	0.396	0.285	0.401	-0.128	0.091	-0.609	-0.453	0.000
	Geometric Morphotype	-0.180	-0.586	0.464	0.107	-0.102	-0.055	-0.093	-0.612
	Irregular Morphotype	0.436	0.190	-0.480	-0.018	-0.342	-0.090	0.133	-0.633
	Elongated Morphotype	-0.145	-0.151	-0.106	-0.969	0.036	0.001	-0.036	-0.064
	Indeterminate Morphotype	-0.333	0.529	0.056	0.017	0.588	0.192	-0.054	-0.470
	Source Area Ratio	0.457	-0.277	0.067	-0.032	0.597	-0.124	0.580	0.000
Low	Charcoal Frequency	0.284	-0.417	-0.240	-0.096	0.718	-0.230	-0.332	0.000
	Charcoal Area	-0.042	-0.661	0.077	-0.173	-0.135	-0.247	0.668	0.000
	Charcoal Skewness	0.251	-0.529	-0.143	0.026	-0.528	0.399	-0.444	0.000
	Geometric Morphotype	-0.518	-0.139	0.316	-0.315	-0.046	-0.197	-0.370	0.580
	Irregular Morphotype	0.585	0.115	0.214	-0.015	0.102	0.266	0.241	0.678
	Elongated Morphotype	0.092	-0.141	0.387	0.801	-0.068	-0.395	-0.130	0.050
	Indeterminate Morphotype	-0.225	0.021	-0.773	0.339	-0.086	-0.102	0.128	0.449
	Source Area Ratio	0.430	0.237	-0.149	-0.323	-0.403	-0.672	-0.134	0.000

Early Neolithic fire activity (7600–6800 BP) is characterized by frequent, low-intensity fires as evident by small charcoal fragments sizes and the almost equal influence of irregular morphotypes, geometric morphotypes, and indeterminate morphotypes in the PCA biplot and adjusted loadings (highlighted in Figs. 43 and 45). Fires were not strictly local to the watersheds but appear to be spatially discrete and in areas only captured by charcoal source areas for SP.NV.11 and SP.NV.7. As indicated by the modeling in chapter III and confirmed through this analysis, this process likely constitutes the initial HNC phase within the Canal de Navarrés, where the introduction of frequent low-intensity fire related to pastoral burning and the initial settlement of the valley by Neolithic agro-pastoralists, caused a transition in vegetation and available fuels.

Following initial niche construction to create the Neolithic agricultural landscape, fire activity remained relatively moderate. The spatial scale of fire increased, indicating an expansion of pastoral burning to different portions of the landscape. This effect can be seen with the distribution of Middle and Late Neolithic samples along the axis related to the ratio between charcoal source area to watershed area. Column samples SP.NV.7 and SP.NV.11 experience greater ratio values, indicating less local fire. During this same period, SP.NV.5 experiences an increase in fire frequency, a constriction of source area to watershed area ratio values, and larger charcoal fragments, indicating frequent burning was introduced into that watershed during the Middle and Late Neolithic. This behavior can be interpreted as an expansion of niche-constructing behavior, likely with the goal of maintaining a larger portion of the landscape for grazing by domesticated sheep and goats.

This pattern is disrupted with a phase of increased fire activity that spans the late Neolithic and Bell Beaker periods (from approximately 5200 – 4500 BP). Charcoal metrics here point to a greater influence of charcoal frequency, size, and size fraction skewness within the PCA biplot suggesting that more burning occurred within the landscape during this phase. No substantial differences appear within the PCA biplot or adjusted loadings in terms of charcoal morphology or source area to watershed area ratio when compared to the initial phase of HNC during the Early Neolithic, indicating an overall intensification of earlier pastoral burning practices. Archaeological survey data support this interpretation, with local a regional land-use increasing throughout the Late Neolithic and Bell Beaker periods, suggesting population growth in the Canal de Navarrés. Post-Neolithic fire activity, as observed in SP.NV.2 and the upper portions of SP.NV.5, is more influenced by irregular morphotypes and larger variation in source area to watershed area ratios. These data likely represent less frequent, low-intensity fires distributed widely across the landscape to maintain a well-established agricultural landscape.

Charcoal metric comparisons between all study areas

The PCA biplots with adjusted loadings for the column samples from the Canal de Navarrés, as well as column samples from the Hoya de Buñol and the Vall del Serpís with age-depth models (SP.BN.2 and PB.RE) are displayed in Figs. 46-47 and table 15. Only high and low fire activity was observed in SP.BN.2 and PB.RE. The drivers of fire activity in the Hoya de Buñol and the Vall del Serpís correspond well with the trends in charcoal metrics identified in the PCA for the Canal de Navarrés, with frequent, spatially

dispersed low-intensity fires characterizing HNC during the late Neolithic and Bell Beaker periods. Low fire activity samples also follow a similar pattern to those observed in the later periods within the Canal de Navarrés, with a spectrum of irregular and indeterminate morphotypes associated with less frequent, spatially dispersed, low-intensity fires related to landscape maintenance.

Figs. 48-50 and table 16 demonstrate the effect of adding all the remaining column samples from the Hoya de Buñol and Vall del Serpís study areas, regardless of their limited or unreliable dates. Interestingly, distinct patterns of difference do not occur between samples that are assumed to much older than the Neolithic period—in fact they fit well with the variation observed in the Neolithic. Additionally, the influence of elongated charcoal morphologies on the distribution of high and moderate fire activity

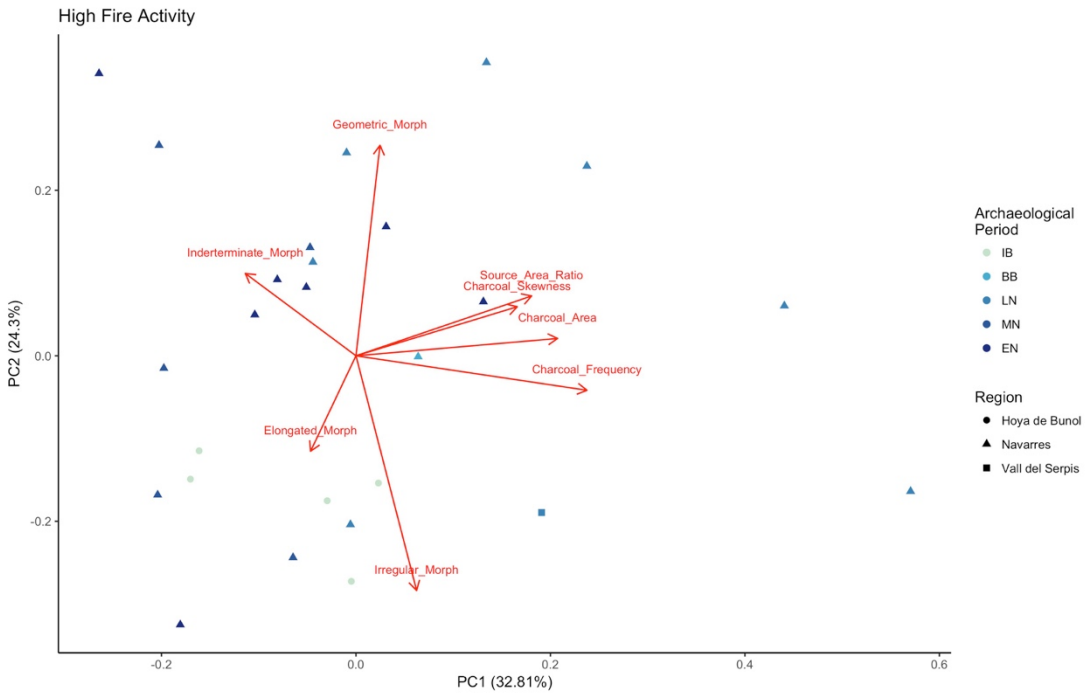

Fig. 46: Biplot of High Fire Activity Within All Column Samples from the Canal De Navarrés Study Area, as Well as Samples with Age-depth Models from the Other Two Study Areas (SP.BN.2 and PB.RE).

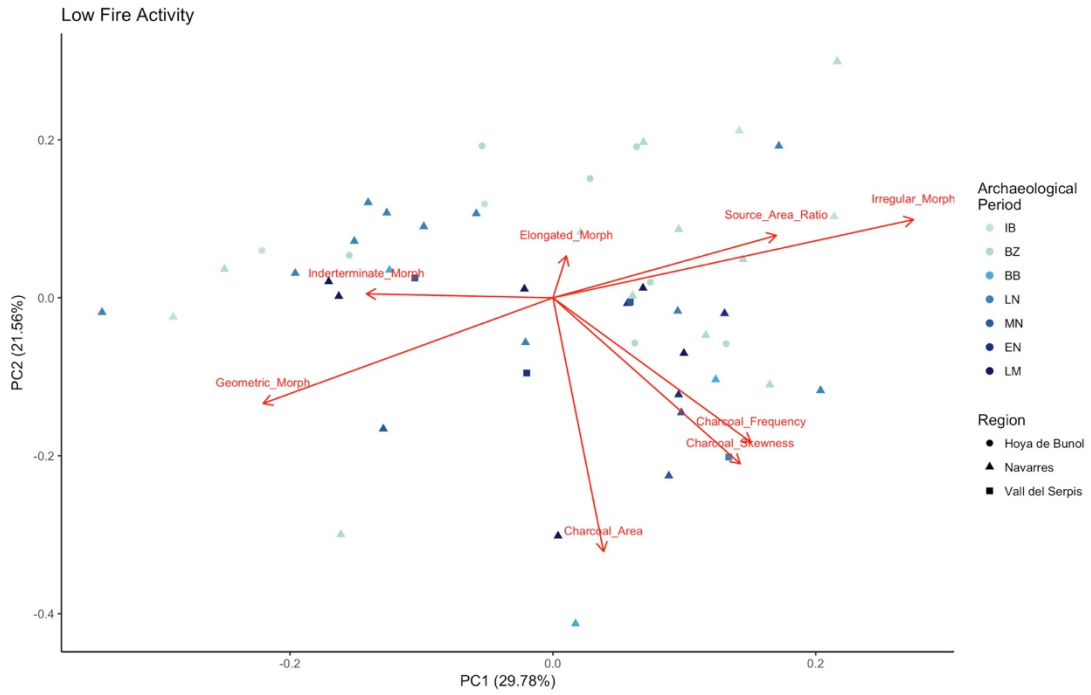

Fig. 47: Biplot of Low Fire Activity Within All Column Samples from the Canal De Navarrés Study Area, as Well as Samples with Age-depth Models from the Other Two Study Areas (SP.BN.2 and PB.RE).

substantially increases with the addition of these samples. This effect could be interpreted as the presence of additional types of burning or land clearance unique to the Hoya de Buñol and Vall de Serpís study areas. These results indicate that additional dates are needed to establish reliable chronologies for the remainder of the Hoya de Buñol and Vall de Serpís samples so variation in land-use practices between the study areas during the Neolithic can be more thoroughly explored.

Current limitations and directions for future research

This work has expanded the ways in which charcoal can be used to reconstruct the specific drivers of anthropogenic fire and niche construction, but it is currently limited by several factors. First, as highlighted in the interpretation of the Vall del Serpís datasets,

Table 15: Eigenvectors for PCA of All Fire Activity Types in the Canal De Navarrés Study Area, as Well as Samples with Age-depth Models from the Other Two Study Areas (SP.BN.2 and PB.RE).

Fire Activity	Variable	PC1	PC2	PC3	PC4	PC5	PC6	PC7	PC8
High	Charcoal Frequency	0.561	-0.098	0.215	-0.174	0.002	-0.198	-0.748	0.000
	Charcoal Area	0.490	0.049	0.045	-0.319	-0.597	-0.213	0.502	0.000
	Charcoal Skewness	0.392	0.140	-0.224	0.352	-0.212	0.776	-0.076	0.000
	Geometric Morphotype	0.058	0.601	-0.454	-0.033	0.087	-0.240	-0.094	-0.596
	Irregular Morphotype	0.147	-0.670	-0.017	0.265	0.061	-0.048	0.145	-0.657
	Elongated Morphotype	-0.110	-0.272	-0.368	-0.786	0.089	0.373	-0.069	-0.088
	Indeterminate Morphotype	-0.269	0.235	0.693	-0.188	-0.221	0.312	-0.073	-0.453
	Source Area Ratio	0.427	0.171	0.282	-0.138	0.728	0.134	0.376	0.000
Low	Charcoal Frequency	0.323	-0.392	0.148	-0.135	-0.696	0.351	0.305	0.000
	Charcoal Area	0.083	-0.689	-0.120	0.072	0.133	0.094	-0.688	0.000
	Charcoal Skewness	0.306	-0.450	0.309	0.106	0.497	-0.319	0.498	0.000
	Geometric Morphotype	-0.473	-0.287	-0.473	-0.014	0.090	0.180	0.353	0.553
	Irregular Morphotype	0.588	0.212	-0.157	0.101	-0.102	-0.264	-0.160	0.684
	Elongated Morphotype	0.022	0.114	0.190	0.836	0.082	0.489	0.026	0.072
	Indeterminate Morphotype	-0.304	0.011	0.758	-0.260	0.031	0.097	-0.187	0.469
	Source Area Ratio	0.364	0.169	-0.101	-0.434	0.473	0.645	0.025	0.000

more reliably radiocarbon dated charcoal fragments samples are needed to establish a more accurate chronologies for each study area. By placing finer chronological controls on the timing of increases in fire frequency, intensity, and distribution, a more detailed picture of the impacts of settlement, aggregation, and demography may emerge from these data. Additionally, charcoal data with high temporal resolution can be tied to well-dated excavated archaeological contexts within each study area, allowing more precise measures of land-use intensity to be evaluated in the contexts of changing fire regimes.

Second, with a better understanding of the temporal variation within each column sample, the relationship between local anthropogenic fire and clast size can be explored in greater detail. As shown in Fig. 51, the current low-resolution method for assessing clast size shows very little connection between deposition processes and the amount of

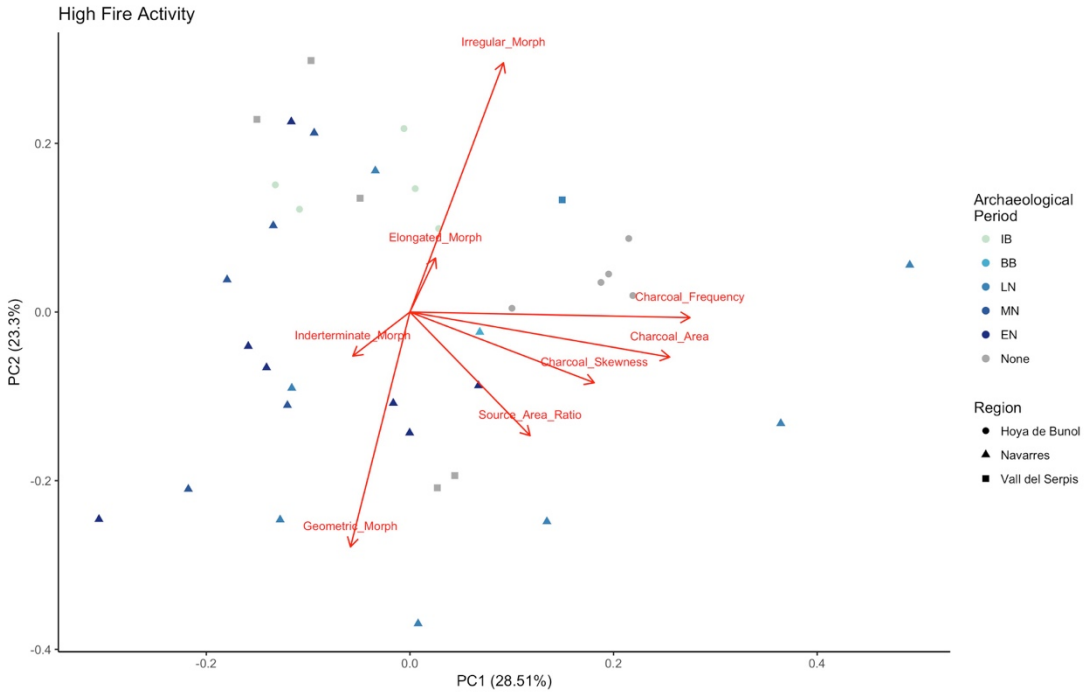

Fig. 48: PCA Biplot of High Fire Activity Within All Dated and Undated Column Samples from All Three Study Areas.

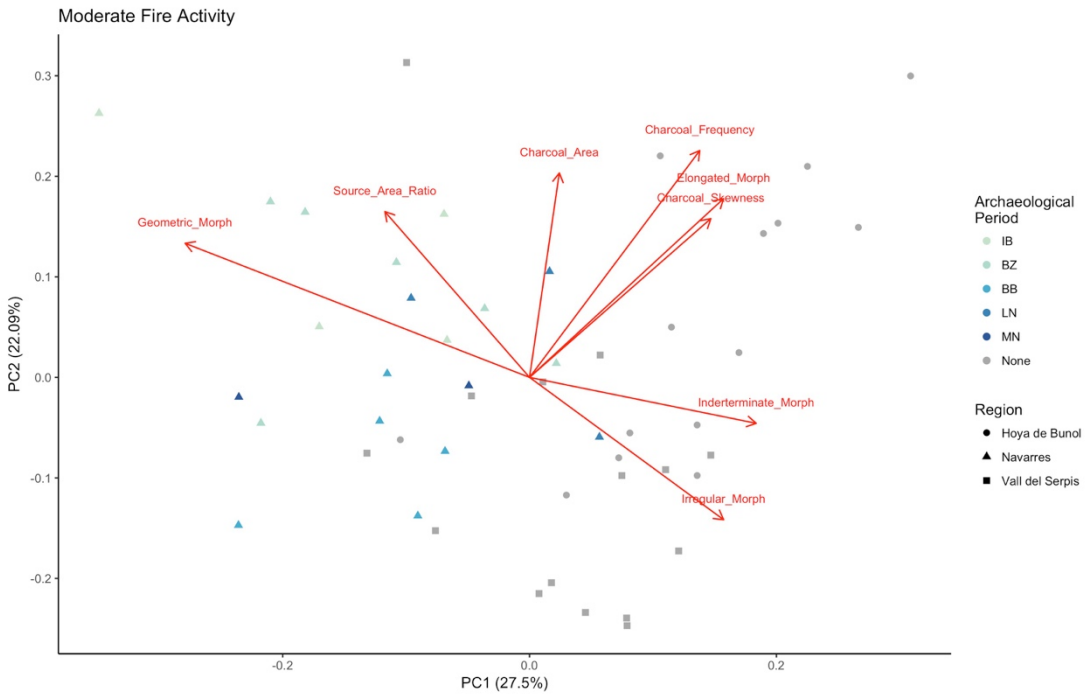

Fig. 49: PCA Biplot of Moderate Fire Activity Within All Dated and Undated Column Samples from All Three Study Areas.

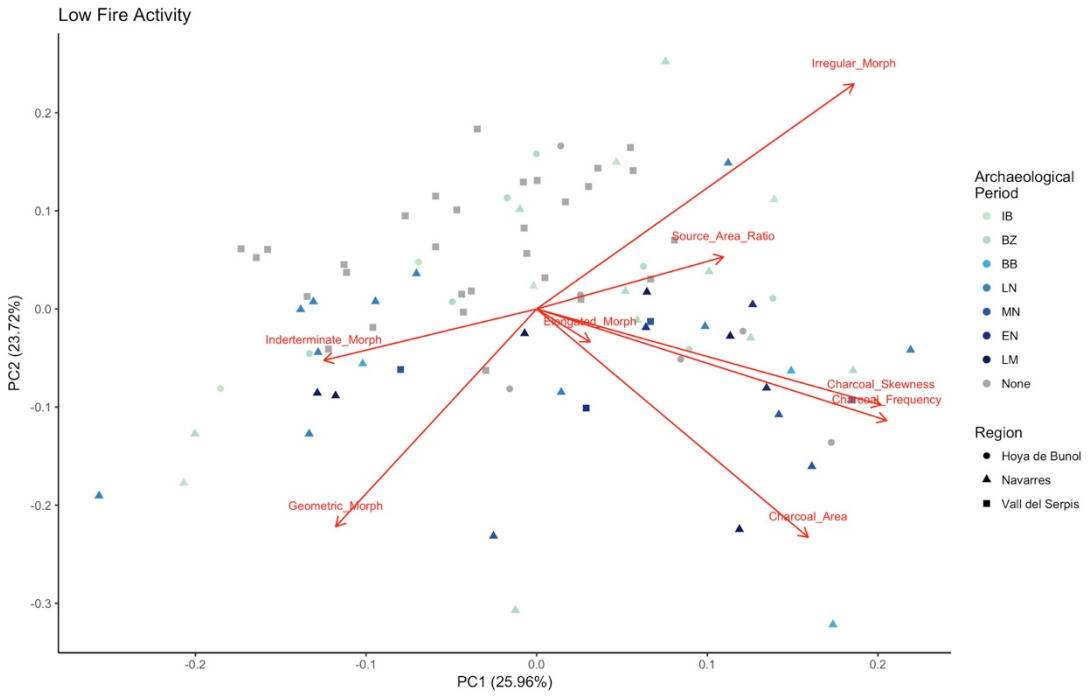

Fig. 50: PCA Biplot of Low Fire Activity Within All Dated and Undated Column Samples from All Three Study Areas.

Table 16: Eigenvectors for PCA of All Fire Activity Types in All Study Areas.

Fire Activity	Variable	PC1	PC2	PC3	PC4	PC5	PC6	PC7	PC8
High	Charcoal Frequency	0.610	-0.015	-0.103	0.048	-0.096	0.334	-0.703	0.000
	Charcoal Area	0.566	-0.119	-0.114	-0.106	0.332	0.364	0.631	0.000
	Charcoal Skewness	0.402	-0.186	0.318	0.153	0.368	-0.733	-0.082	0.000
	Geometric Morphotype	-0.130	-0.618	0.383	-0.160	-0.031	0.210	-0.063	0.617
	Irregular Morphotype	0.204	0.656	0.190	0.125	-0.206	-0.065	0.141	0.640
	Elongated Morphotype	0.056	0.142	-0.175	-0.931	0.064	-0.232	-0.111	0.092
	Indeterminate Morphotype	-0.124	-0.116	-0.762	0.232	0.323	-0.148	-0.093	0.448
	Source Area Ratio	0.262	-0.325	-0.285	0.015	-0.771	-0.307	0.237	0.000
Moderate	Charcoal Frequency	0.297	0.486	-0.303	0.259	-0.093	-0.413	0.581	0.000
	Charcoal Area	0.052	0.438	0.260	-0.567	-0.384	-0.390	-0.343	0.000
	Charcoal Skewness	0.316	0.340	-0.043	-0.511	0.517	0.473	0.178	0.000
	Geometric Morphotype	-0.600	0.287	0.144	0.000	-0.039	0.158	0.248	0.670
	Irregular Morphotype	0.338	-0.305	-0.563	-0.224	-0.235	0.010	-0.142	0.592
	Elongated Morphotype	0.338	0.383	0.137	0.463	-0.360	0.522	-0.313	0.082
	Indeterminate Morphotype	0.395	-0.098	0.511	0.214	0.440	-0.350	-0.127	0.441
	Source Area Ratio	-0.252	0.355	-0.470	0.202	0.444	-0.184	-0.563	0.000
Low	Charcoal Frequency	0.477	-0.264	0.086	-0.118	0.143	-0.698	-0.417	0.000
	Charcoal Area	0.370	-0.541	-0.057	0.041	0.055	0.006	0.750	0.000
	Charcoal Skewness	0.469	-0.227	0.243	-0.031	0.139	0.704	-0.391	0.000
	Geometric Morphotype	-0.274	-0.515	-0.489	0.004	-0.161	0.071	-0.263	0.566
	Irregular Morphotype	0.432	0.533	-0.153	0.143	0.140	-0.005	0.142	0.667
	Elongated Morphotype	0.073	-0.078	0.344	0.722	-0.577	-0.082	-0.063	0.073
	Indeterminate Morphotype	-0.290	-0.122	0.740	-0.315	0.083	-0.064	0.123	0.479
	Source Area Ratio	0.254	0.123	-0.048	-0.586	-0.756	0.037	0.047	0.000

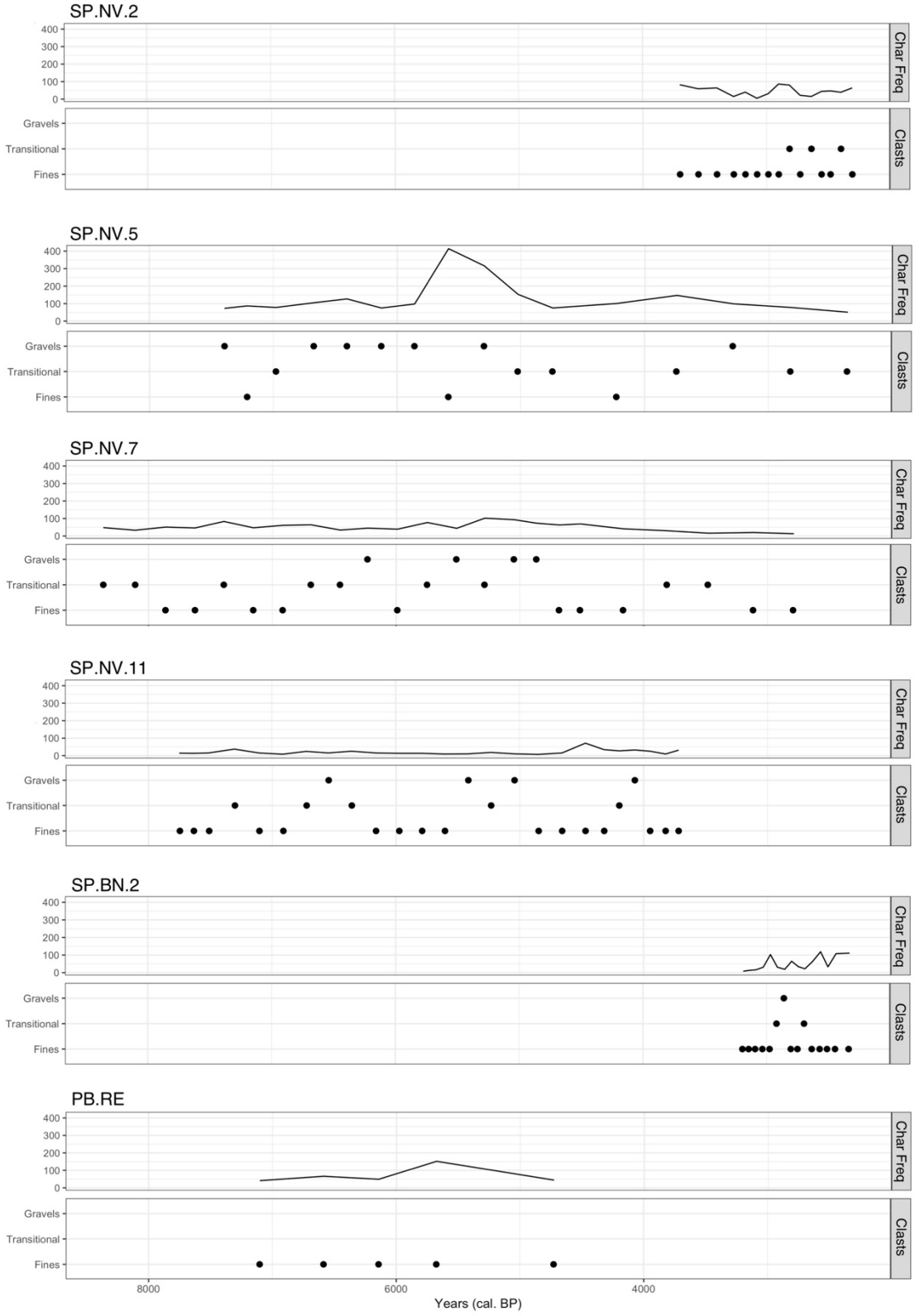

Fig. 51: Comparison of Clast Category and Charcoal Frequency in All Dated Column Samples from All Study Areas.

burning observed in each watershed. While it would be expected that in-watershed burning would increase the sedimentation rate and the accumulation of gravels, this relationship does not appear to be the case. Gaining a better understanding of the timing of sedimentation and clast size in relation to anthropogenic fire is vital in interpreting the impacts of frequent fire on land-cover and erosion through time. Both are factors that likely influenced the intensity of Neolithic land-use in a watershed.

Finally, the PCA results for all three study areas indicate that indeterminate morphotypes are related to the types of fire used during both niche construction and niche maintenance phases during the Neolithic. Additional experimental fuels from local plant species are needed to be generated more specific models for morphotype identification. Specifically, monocots such as palms are well represented in the regional pollen sequences from the Canal de Navarrés (Carrión and van Geel 1999; Dupre et al. 1996) and should be included in an effort to reduce the prevalence of unidentifiable morphotypes.

Conclusions

This study evaluates the drivers of anthropogenic fire during the Neolithic period in eastern Spain and the emergence of agricultural landscapes. By reframing human niche construction to consider the processes of both creating and maintaining agro-pastoral niches, new phases of landscape transformation are identified. Advances in charcoal analysis presented in this study make more direct connections between charcoal data and the social, biological, and taphonomic processes that influence their interpretation in the

archaeological record. Combining new techniques in charcoal analysis, such as semi-automated quantification and machine-learning approaches, with experimental charcoal datasets allows this study to extract more information regarding anthropogenic influences on fire and landscapes.

This approach has identified high frequency, low-intensity burning, resulting in niche-constructing behavior during the Early and Late Neolithic throughout eastern Spain. After landscapes were transformed, consistent patterns of anthropogenic fire related to landscape maintenance where identified from the end of the Bell Beaker and through the Iberian periods. The contributions of these new methods, and their ability to interpret human specific impacts on fire regimes, have creating led to detailed interpretations of the origins of agricultural landscape in eastern Spain, with implications for understanding the nature of long-term human-fire relationships in Mediterranean ecosystems more broadly.

CHAPTER V

CONCLUSIONS

The Importance of a Long-term Perspective on Human-Fire Relationships

Experts agree that climate change is creating conditions where wildfires are burning more frequently, over larger areas, and with more intensity than ever previously recorded in the United States (Abatzoglou and Williams, 2016; Balch et al., 2017) and around the world. The 2018 fire season is set to become one of the most destructive and costly in recent history. The Camp Fire alone is estimated to cost billions of dollars in mitigation and rebuilding efforts, not to mention the immeasurable impact of the immense destruction of property and loss of life in the community of Paradise, California (Elias, 2018). The Fourth National Climate Assessment (Reidmiller et al., 2018) predicts that increases in fire activity in the United States will threaten the safety and property of communities throughout the country, while also degrading air quality, recreation, and the economic and ecosystem services of forested areas. Unprecedent recent fire seasons in Europe, South America, Africa, and Australia have been more destructive and more costly than ever before (Hughes and Alexander, 2017; San-Miguel-Ayanz et al., 2018). Research-driven policy can help in ameliorating some of the potential wildfire-related effects of a warming world on our communities.

The paleoecological research community has suggested that specific linkages between past reconstructions and forecasting are vital in future landscape management,

conservation, and restoration efforts (Brown et al., 2018; Lestienne et al., 2018). This moves current policy in a direction that engages with long-term variability in fire and ecosystem change. However, an in-depth consideration of anthropogenic influences on ecological systems, particularly the contribution of human-caused fires, is being neglected.

Archaeological research is crucial in connecting paleoecological data and to the cultural practices that drive how landscapes are envisioned, valued, and altered in the past. But there is little utility in archaeological interpretations that consist of ecological cautionary tales or results that are hyper-specific to a single site or archeological culture and cannot be broadly applied. As a discipline, we need to develop methods and explanations that allow us to create flexible and adaptable information which casts humans as active agents of both change and stability in ancient and modern ecosystems.

Archaeological Contributions to Anthropogenic Fire Research

The work presented in this dissertation has attempted to engage with these limitations by advancing archaeological methods and theoretical perspectives on anthropogenic fire. Each of the individual studies is guided by the theme of adapting paleoecological measures to be interpreted alongside archaeological data. One of the biggest hurdles in connecting these two types of information is a mismatch in their spatial and temporal scales. This dissertation offers solutions to this problem though a combination of alternative statistical approaches and augmented data collection. On the

theory side, I demonstrate that human niche construction (HNC) situates land-use and burning practices as primary drivers of landscape change and fire regimes at multiple scales.

Multiple methodological contributions developed through this dissertation project enabled more direct comparisons between archaeological and paleoecological data. Reinterpreting archaeological surface collections through Bayesian statistical methods enabled me to evaluate these data as subsets of archaeological periods, aligning the temporal scales of land-use change and changing fire activity. By untangling the timing of land-use intensification I was able to identify specific periods of human niche construction and maintenance, particularly in the Canal de Navarrés study area. Perhaps more importantly, resolving the spatial scales of these data helped to tie fire activity in the past to specific agricultural practices, such as pastoralism. Targeted sampling of alluvial sediments from archaeologically surveyed watersheds provided one step forward in connecting these two phenomena. Expanded measures helped to reveal spatial variability in landscape fires that could not have been evaluated using traditional paleoecological measures alone. These measures included charcoal sources areas used to differentiate between local and regional land-use and charcoal morphotypes related to specific fire intensities and fuel sources. By incorporating new technologies and open-source software into the development of these new methodologies, they are accessible and transportable to regions and questions beyond the Neolithic period in eastern Spain.

Human niche construction helps to explain how agricultural landscapes are created and maintained through fire while also shedding light on the consequences of abandoning human-created niches. An important illustration of this point is the

connection between the pattern of modern wildfire in eastern Spain and the historical legacies of regional agricultural niche construction. Increased frequency and intensity of wildfire in eastern Spain in the last half century has been clearly documented (Brotons et al., 2013; Pausas and Fernández-Muñoz, 2012; Santana et al., 2014). While this trend is certainly exacerbated by increased temperatures and drought conditions related to global climate change, it is also likely driven by a relatively recent change in landscape-scale anthropogenic fire. Pausas and Fernández-Muñoz (2012) argue that abandonment of traditional rural land-use, including burning practices, have accelerated biomass accumulation and connectivity between vegetated areas within the landscape resulting in increased fire activity. In the language of HNC, the abandonment of traditional burning practices is a divergence from the niche-maintaining behaviors that rural populations have used to some degree since they were developed during the Neolithic period. In this example, the cost of abandonment has economic, ecological, and social ramifications for remaining rural communities in eastern Spain. While archaeological interpretations cannot be compared one-to-one with current wildfire risks in Spain, they do help us to frame this transition in terms of HNC, revealing the potential pace, scale, and intensity of fire activity in the future.

Future Directions

The studies compiled for this dissertation provide the groundwork for future methodological developments and theory building for studying anthropogenic fire in the past. The underlying goal of future work should be to make substantive and relevant

connections between archaeological perspectives and contemporary human-fire relationships. Land-use practices shaped by cultural values have and will continue to structure how we apply fire to the land. The research in this dissertation illustrates that sound and sustainable fire policy must take the long-term legacies of anthropogenic environments into consideration when planning for the future.

There are several avenues for the work presented here to move forward. First, to bolster the results presented in Chapter IV, additional AMS C^{14} dates are needed for all three study areas. This is especially important in the Vall del Serpís and Hoya de Buñol study areas, where too few dates and dates with large errors make it difficult to identify fire activity related to Neolithic HNC. Charcoal fragments from these sampling areas have proven too small to date reliably; bulk sediments or other organic materials may provide more appropriate quantities of carbon for AMS samples.

The new methods for analyzing sedimentary charcoal would also benefit from continued evaluation and testing in multiple contexts beyond those presented in this dissertation. K-NN methods for classifying morphotypes can also be expanded to include more species from the eastern Spain, as well as a wider range of combustion temperatures and durations of artificial mechanical weathering. An expanded experimental dataset could then be compared to charcoal produced during recent wildfires in the region to determine if variation in charcoal morphology produced under real combustion conditions can be captures through experimental methods.

The CharRec modeling laboratory should also be adapted for ecosystems beyond the Mediterranean Basin. The introduction of new types of fire associated with intensive land-use are prevalent throughout the world, particular in other fire-prone ecosystems in

the Americas, Asia, and Africa. The methods used in eastern Spain were purposely designed to be flexible and adaptable to accommodate wide variation in fire frequency, intensity, fuels, and spatial patterning. This also includes the contribution of a wider range of human-fire relationships, particularly the pattern and intensity of broadcast burning associated with hunter-gatherer groups. A recent study by Coughlan and colleagues (2018) compiled ethnographic accounts of hunter-gather burning practices indicates that forager food-ways are often highly dependent on fire. Assessing the cumulative hunter-gatherer contribution to vegetation change and global fire regimes could alter current perceptions of the origins of the Anthropocene.

Conclusions

Archaeological investigations of long-term anthropogenic fire regimes have the potential inform the ways contemporary scientific and policy-making entities think about our future with wildfire. Through a combination of non-traditional archaeological approaches to survey data, computational proxy record modeling, and new methods in charcoal analysis, this dissertation outlines the specific ways anthropogenic fire generated new fire regimes and the creation of agricultural landscapes in eastern Spain. Periods of intensive fire activity associated with subsistence change and intensification, followed by low-intensity fires to maintain agricultural landscapes, resulted in fire regimes that were dependent on anthropogenic inputs. Ultimately, this work advances our current

understanding of human-fire relationships and can be used to create research-driven policy that will hopefully aid in building future fire-resilient communities.

REFERENCES

Abatzoglou, J.T., Williams, A.P., 2016. The impact of anthropogenic climate change on wildfire across western US forests. Proc. Natl. Acad. Sci. 113, 11770–11775. https://doi.org/10.1073/pnas.1607171113

Ackland, G., Signitzer, M., Stratford, K., Cohen, M., 2007. Cultural hitchhiking on the wave of advance of beneficial technologies. Proc. Natl. Acad. Sci. 104, 8714–8719.

Anderson, H.E., 1982. Aids to Determining Fuel Models For Estimating Fire Behavior. Ogden, UT.

Aparicio Perez, J., 1981. Primeras dataciones de C14 para el Musteriense Valenciano. Arch. Prehist. Levantina XVI, 9–38.

Aparicio Perez, J., 1979. El Mesolítico en Valencia y en el Mediterraneo occidental. Servico de Investigacion Prehistorica, Diputacion Provincial de Valencia, Valencia, Spain.

Aparicio Perez, J., 1974. Un nuevo yacimiento musteriense en la provincia de Valencia: Las Fuentes (Navarrés). Zephyrus 25, 43–51.

Aparicio Perez, J., 1973. Los yacimientos prehistóricos de la Albufera de Anna (Valencia), in: XIII Congreso Nacional de Arqueología. Zaragoza, pp. 191–198.

Arias Cabal, P., Alvarez Fernández, E., 2004. Les chasseurs-cueilleurs de la Péninsule ibérique face à la mort : une révision des données sur les contextes funéraires du Paléolithique supérieur et du Mésolithique, in: La Spiritualité : Actes Du Colloque International de Liège (10-12 Décembre 2003). pp. 221–236.

Arikan, B., 2012. Don't abhor your neighbor for he is a pastoralist: The GIS-based modeling of the past human-environment interactions and landscape changes in the Wadi el-Hasa, west-central Jordan. J. Archaeol. Sci. 39, 2908–2920. https://doi.org/10.1016/j.jas.2012.04.051

Asouti, E., Fuller, D.Q., 2011. From foraging to farming in the southern Levant: the development of Epipalaeolithic and Pre-pottery Neolithic plant management strategies. Veg. Hist. Archaeobot. 21, 149–162. https://doi.org/10.1007/s00334-011-0332-0

Badal Garcia, E., 1995. La vegetación carbonizada. Resultados antracológicos del País Valenciano, in: El Cuaternario Del País Valenciano. Asociación Española para el Estudio del Cuaternario, Valencia, pp. 217–226.

Badal Garcia, E., 1994. Vegetation changes and human action from the Neolithic to the

Bronze Age (7000-4000 BP) in Alicante, Spain, based on charcoal analysis. Veg. Hist. Archaeobot. 155–166.

Balch, J.K., Bradley, B.A., Abatzoglou, J.T., Nagy, R.C., Fusco, E.J., Mahood, A.L., 2017. Human-started wildfires expand the fire niche across the United States. Proc. Natl. Acad. Sci. 114, 2946–2951. https://doi.org/10.1073/pnas.1617394114

Bankes, S., Lempert, R., Popper, S., 2002. Making Computational Social Science Effective: Epistemology, Methodology, and Technology. Soc. Sci. Comput. Rev. 20, 377–388.

Barton, C., Ullah, I., Mitasova, H., 2010. Computational Modeling And Neolithic Socioecological Dynamics : A Case Study From Southwest Asia. Am. Antiq. 75, 364–386.

Barton, C.M., 1988. Lithic variability and middle paleolithic behavior : new evidence from the Iberian peninsula, British archaeological Reports - International Series ; 408. British Archaeological Reports, Oxford.

Barton, C.M., Bernabeu, J., Aura, J.E., García, O., 1999. Land-use Dynamics and Socioeconomic Change: An example from the Polop Alto Valley. Am. Antiq. 64, 609–634.

Barton, C.M., Bernabeu, J., Aura, J.E., Garcia, O., Roca, N. La, 2002. Dynamic Landscapes, Artifact Taphonomy, and Landuse Modeling in the Western Mediterranean. Geoarchaeology 17, 155–190.

Barton, C.M., Bernabeu, J., Aura, J.E., Garcia, O., Schmich, S., Molina, L., 2004. Long-Term Socioecology and Contingent Landscapes. J. Archaeol. Method Theory 11, 253–295. https://doi.org/10.1023/B:JARM.0000047315.57162.b7

Barton, C.M., Ullah, I., Bergin, S., 2010. Land-Use, Water and Mediterranean Landscapes: Modeling Long-Term Dynamics of Complex Socioecological Systems. Proc. R. Soc. A 368, 5275–5297.

Barton, C.M., Ullah, I., Heimsath, A., 2015. How to Make a Barranco: Modeling Erosion and Land-Use in Mediterranean Landscapes. Land 4, 578–606. https://doi.org/10.3390/land4030578

Barton, C.M., Ullah, I.I.T., Bergin, S.M., Mitasova, H., Sarjoughian, H., 2012. Looking for the future in the past: long-term change in socioecological systems. Ecol. Modell. 241, 42–53. https://doi.org/10.1016/j.ecolmodel.2012.02.010

Bergin, S.M., 2016. Mechanisms and Models of Agropastoral Spread During the Neolithic in the West Mediterranean: The Cardial Spread Model. Arizona State

University.PhD Dissertation.

Berkes, F., Folke, C., 1998. Linking Social and Ecological Systems for Resilience and Sustainability. Beijer Discuss. Pap. Ser. https://doi.org/10.1016/S0014-5793(97)01160-5

Bernabeu Auban, J., 2004. Indigenism and Migrationism. The Neolithization of the Iberian Peninsula. Doc. Praehist. XXIV, 1–17.

Bernabeu Auban, J., 2002. The social and symbolic context of neolithization. Saguntum papeles del Lab. Arqueol. Val. Extra-5, 209–233.

Bernabeu Auban, J., 1999. Pots, Symbols and Territories: the Archaeological Context of Neolithisation in Mediterranean Spain. Doc. Praehistoria 26, 101–118.

Bernabeu Auban, J., Badal Garcia, E., 1992. A view of the vegetation and economic exploitation of the forest in the late neolithic sites of Les Jovades and Niuet (Alicante, Spain). Bull. la Soc. Bot. Fr. (Actualites Bot.) 139, 697–714.

Bernabeu Aubán, J., Balaguer, L.M., Orozco Köhler, T., Diez Castillo, A., Barton, C.M., 2008. Early Neolithic at the Serpis Valley, Alicante, Spain, in: Diniz, M. (Ed.), Early Neolithic in the Iberian Peninsula, {BAR} International Series. Archaeopress, Oxford, pp. 53–59.

Bernabeu Auban, J., Barton, C.M., García Puchol, O., Roca, N. La, 2000. Systematic Survey in Alicante Spain, First Results. Turkish Acad. Sci. J. Archaeol. III, 55–83.

Bernabeu Auban, J., Barton, C.M., Perez Ripoll, M., 2001a. A Taphonomic Perspective on Neolithic Beginnings: Theory, Interpretation, and Empirical Data in the Western Mediterranean. J. Archaeol. Sci. 28, 597–612. https://doi.org/10.1006/jasc.2000.0591

Bernabeu Auban, J., Barton, C.M., Perez Ripoll, M., 2001b. A Taphonomic Perspective on Neolithic Beginnings: Theory, Interpretation, and Empirical Data in the Western Mediterranean. J. Archaeol. Sci. 28, 597–612. https://doi.org/06/jasc.2000.0591

Bernabeu Aubán, J., Barton, M.C., Pardo Gordó, S., Bergin, S.M., 2015a. Modeling initial Neolithic dispersal. The first agricultural groups in West Mediterranean. Ecol. Modell. 307, 22–31. https://doi.org/10.1016/J.ECOLMODEL.2015.03.015

Bernabeu Aubán, J., García Puchol, O., Barton, M., McClure, S., Pardo Gordó, S., 2015b. Radiocarbon dates, climatic events, and social dynamics during the Early Neolithic in Mediterranean Iberia. Quat. Int. 1–10. https://doi.org/10.1016/j.quaint.2015.09.020

Bernabeu Aubán, J., Martí Oliver, B., 2014. The first agricultural groups in the Iberian Peninsula, in: La Transition Néolitique En Méditerranée. pp. 419–438.

Bernabeu Aubán, J., Molina Balaguer, L. (Eds.), 2009. La Cova de les Cendres, Serie Mayo. ed. Fundación MARQ, Alicante.

Bernabeu Auban, J., Molina Balaguer, L., García Puchol, O., 2001c. El mundo funerario en el horizonte cardial valenciano. Un registro oculto. Saguntum papeles del Lab. Arqueol. Val. 33, 27–36.

Bernabeu Auban, J., Molina, L., Esquembre, M.A., Ortega, J.R., Boronat, J.D., 2009. La cerámica impresa mediterránea en el origen del Neolítico de la Península Ibérica, in: De Méditerranée et d'ailleurs... Mélanges Offerts À Jean Guilaine. Archives d'Écologie Préhistorique, Toulouse, pp. 83–95.

Bernabeu Auban, J., Orozco Köhler, T., Diez Castillo, A., 2002. El poblamiento neolitico: desarollo de paisaje agrario en Les Valls de l'Alcoi, in: Hernandez, M.S. (Ed.), La Sarga. Arte Rupestre y Territorio. Ayuntamiento de Alcoy y Caja de Ahorras del Mediterraneo, Alcoi, pp. 171–184.

Bernabeu Auban, J., Orozco Köhler, T., Diez Castillo, A., Gómez Puche, M., Molina Hernández, F.J., 2003. Mas d'Is (Penàguila, Alicante): Aldeas y recintos monumentales del Neolítico inicial en el valle del Serpis. Trab. Prehist. 60, 39–59. https://doi.org/10.3989/tp.2003.v60.i2.80

Bernabeu Aubán, J., Pascual Benito, J.L., Orozco Köhler, T., Badal Garcia, E., Fumanal García, P., García, O., 1994. Niuet (L' Alqueria d' Asnar): Poblado del III Milenio A.C. Recer. del Mus. d'Alcoi 3, 9–74.

Bernabeu Auban, J., Perez Ripoll, M., Martinez Valle, R., 1999. Huesos Neolitizacion y Contextos Arqueologicos Aparentes, in: Bernabeu Auban, J., Orozco Köhler, T. (Eds.), Actes Del II Congres Del Neolitic a La Peninsula Iberica. Universitat de Valencia. 7-9 d'Abril, 1999. Universitat de Valencia, Valencia, Spain, pp. 589–596.

Bevan, a., Conolly, J., Colledge, S., Frederick, C., Palmer, C., Siddall, R., Stellatou, a., 2012. The Long-Term Ecology of Agricultural Terraces and Enclosed Fields from Antikythera, Greece. Hum. Ecol. 41, 255–272. https://doi.org/10.1007/s10745-012-9552-x

Bevan, A., Conolly, J., 2006. Confronting scale in archaeology: Issues of theory and practice, in: Lock, G., Molyneaux, B.L. (Eds.), Confronting Scale in Archaeology: Issues of Theory and Practice. Springer, New York, pp. 217–234. https://doi.org/10.1007/0-387-32773-8

Bevan, A., Conolly, J., 2002. GIS, Archaeological Survey, and Landscape Archaeology

on the Island of Kythera, Greece. J. F. Archaeol. 29, 123. https://doi.org/10.2307/3181488

Bintliff, J., 2005. Human impact, land-use history, and the surface archaeological record: a case study from Greece. Geoarchaeology 20, 135–147. https://doi.org/10.1002/gea.20040

Bird, D.W., Bliege Bird, R., Parker, C.H., 2005. Aboriginal Burning Regimes and Hunting Strategies in Australia's Western Desert. Hum. Ecol. 33, 443–464. https://doi.org/10.1007/s10745-005-5155-0

Blarquez, O., Vannière, B., Marlon, J.R., Daniau, A.L., Power, M.J., Brewer, S., Bartlein, P.J., 2014. Paleofire: An R package to analyse sedimentary charcoal records from the Global Charcoal Database to reconstruct past biomass burning. Comput. Geosci. 72, 255–261. https://doi.org/10.1016/j.cageo.2014.07.020

Bleed, P., Matsui, A., 2010. Why Didn't Agriculture Develop in Japan? A Consideration of Jomon Ecological Style, Niche Construction, and the Origins of Domestication. J. Archaeol. Method Theory 17, 356–370. https://doi.org/10.1007/s10816-010-9094-8

Bliege Bird, R., Bird, D.W., Codding, B.F., Parker, C.H., Jones, J.H., 2008. The "fire stick farming" hypothesis: Australian Aboriginal foraging strategies, biodiversity, and anthropogenic fire mosaics. Proc. Natl. Acad. Sci. U. S. A. 105, 14796–14801.

Bliege Bird, R., Tayor, N., Codding, B.F., Bird, D.W., 2013. Niche construction and Dreaming logic : aboriginal patch mosaic burning and varanid lizards (Varanus gouldii) in Australia. Proc. R. Soc. B 280, 1–7.

Boivin, N.L., Zeder, M.A., Fuller, D.Q., Crowther, A., Larson, G., Erlandson, J.M., Denham, T., Petraglia, M.D., 2016. Ecological consequences of human niche construction: Examining long-term anthropogenic shaping of global species distributions. Proc. Natl. Acad. Sci. 113, 6388–6396. https://doi.org/10.1073/pnas.1525200113

Bond, W.J., Keeley, J.E., 2005. Fire as a global "herbivore": the ecology and evolution of flammable ecosystems. Trends Ecol. Evol. 20, 387–94. https://doi.org/10.1016/j.tree.2005.04.025

Bowman, D.M.J.S., Balch, J., Artaxo, P., Bond, W.J., Cochrane, M.A., D'Antonio, C.M., DeFries, R., Johnston, F.H., Keeley, J.E., Krawchuk, M.A., Kull, C.A., Mack, M., Moritz, M.A., Pyne, S., Roos, C.I., Scott, A.C., Sodhi, N.S., Swetnam, T.W., Whittaker, R., 2011. The human dimension of fire regimes on Earth. J. Biogeogr. 38, 2223–2236. https://doi.org/10.1111/j.1365-2699.2011.02595.x

Bowman, D.M.J.S., Balch, J.K., Artaxo, P., Bond, W.J., Carlson, J.M., Cochrane, M.A.,

D'Antonio, C.M., DeFries, R.S., Doyle, J.C., Harrison, S.P., Johnston, F.H., Keeley, J.E., Krawchuk, M.A., Kull, C.A., Marston, J.B., Moritz, M.A., Prentice, I.C., Roos, C.I., Scott, A.C., Swetnam, T.W., van der Werf, G.R., Pyne, S.J., 2009. Fire in the Earth System. Science (80-.). 324, 481–484. https://doi.org/DOI 10.1126/science.1163886

Braje, T.J., 2015. Earth Systems, Human Agency, and the Anthropocene: Planet Earth in the Human Age. J. Archaeol. Res. 23, 369–396. https://doi.org/10.1007/s10814-015-9087-y

Braje, T.J., Erlandson, J.M., 2014. Looking forward, looking back: Humans, anthropogenic change, and the Anthropocene. Anthropocene 4, 116–121. https://doi.org/10.1016/j.ancene.2014.05.002

Brotons, L., Aquilué, N., de Cáceres, M., Fortin, M.J., Fall, A., 2013. How Fire History, Fire Suppression Practices and Climate Change Affect Wildfire Regimes in Mediterranean Landscapes. PLoS One 8. https://doi.org/10.1371/journal.pone.0062392

Brown, K.J., Power, M.J., Słowiński, M., Aardt, A.C. Van, Blarquez, O., Grondin, P., 2018. Workshop Report: Applying paleofire records in ecological management. Wildfire Mag.

Buck, C.E., Cavanagh, W.G., Litton, C.D., 1996. Bayesian approach to interpreting archaeological data. Stat. Pract. xix + 382.

Buck, C.E., Sahu, S.K., 2000. Bayesian Models for Relative Archaeological Chronology Building. J. R. Stat. Soc. Ser. C 49, 423–440. https://doi.org/10.1111/1467-9876.00203

Burjachs, F., Jones, S.E., Giralt, S., Fernández-López de Pablo, J., 2016. Lateglacial to Early Holocene recursive aridity events in the SE Mediterranean Iberian Peninsula: The Salines playa lake case study. Quat. Int. 403, 187–200. https://doi.org/10.1016/j.quaint.2015.10.117

Carcaillet, C., Richard, P.J.H., Asnong, H., Capece, L., Bergeron, Y., 2006. Fire and soil erosion history in East Canadian boreal and temperate forests. Quat. Sci. Rev. 25, 1489–1500. https://doi.org/10.1016/j.quascirev.2006.01.004

Carey, C.J., Brown, T.G., Challis, K.C., Howard, A.J., Cooper, L., 2006. Predictive Modelling of Multiperiod Geoarchaeological Resources at a River Confluence: a Case Study from the Trent-Soar, UK. Archaeol. Prospect. 13, 241–250. https://doi.org/10.1002/arp

Carrión, J., 2012. Paleoflora y paleovegitacion de la Pensinsula Iberica e Islas Baleares:

Plioceno-cuaternario, 1st Editio. ed. Murcia.

Carrión, J.S., Dupré, M., 1996. Late Quaternary vegetational history at Navarrés, Eastern Spain. A two core approach. New Phytol. 134, 177–191. https://doi.org/10.1111/j.1469-8137.1996.tb01157.x

Carrión, J.S., Fernández, S., González-Sampériz, P., Gil-Romera, G., Badal, E., Carrión Marco, Y., López-Merino, L., López-Sáez, J.A., Fierro, E., Burjachs, F., 2010. Expected trends and surprises in the Lateglacial and Holocene vegetation history of the Iberian Peninsula and Balearic Islands. Rev. Palaeobot. Palynol. 162, 458–475. https://doi.org/10.1016/j.revpalbo.2009.12.007

Carrión, J.S., Munuera, M., Dupré, M., Andrade, A., 2001. Abrupt vegetation changes in the Segura Mountains of the Holocene southern Spain throughout the holocene. J. Ecol. 89, 783–797.

Carrión, J.S., Van Geel, B., 1999. Fine-resolution Upper Weichselian and Holocene palynological record from Navarres (Valencia, Spain) and a discussion about factors of Mediterranean forest succession. Rev. Palaeobot. Palynol. 106, 209–236.

Cattau, M.E., Harrison, M.E., Shinyo, I., Tungau, S., Uriarte, M., DeFries, R., 2016. Sources of anthropogenic fire ignitions on the peat-swamp landscape in Kalimantan, Indonesia. Glob. Environ. Chang. 39, 205–219. https://doi.org/10.1016/j.gloenvcha.2016.05.005

Chapman, R., 2008. Producing Inequalities: Regional Sequences in Later Prehistoric Southern Spain. J. World Prehistory 21, 195–260.

Cherry, J.F., 1983. Frogs round the pond: perspectives on current archaeological survey projects in the Mediterranean region, in: Archaeological Survey in the Mediterranean Area. pp. 375–416.

Chin, A., Fu, R., Harbor, J., Taylor, M.P., Vanacker, V., 2013. Anthropocene: Human interactions with earth systems. Anthropocene 1, 1–2. https://doi.org/10.1016/j.ancene.2013.10.001

Claramunt Rodríguez, S., Portela Silva, E., González Jiménez, M., Mitre, E., 2014. Historia de la Edad Media, 1st ed. Ariel Publishing.

Clark, J.S., 1988a. Particle motion and the theory of charcoal analysis: Source area, transport, deposition, and sampling. Quat. Res. 30, 67–80. https://doi.org/10.1016/0033-5894(88)90088-9

Clark, J.S., 1988b. Stratigraphic charcoal analysis on petrographic thin sections: Application to fire history in northwestern Minnesota. Quat. Res. 30, 81–91.

https://doi.org/10.1016/0033-5894(88)90089-0

Clark, J.S., Lynch, J., Stocks, B.J., Goldammer, J.G., 1998. Relationships between charcoal particles in air and sediments in west-central Siberia. The Holocene 8, 19–29. https://doi.org/10.1191/095968398672501165

Clark, J.S., Royall, P.D., 1996. Local and regional sediment charcoal evidence for fire regimes in presettlement north-eastern North America. J. Ecol. 84, 365–382.

Clark, J.S., Royall, P.D., 1995. Particle-Size Evidence for Source Areas of Charcoal Accumulation in Late Holocene Sediments of Eastern North American Lakes. Quat. Res. 43, 80–89.

Codding, B.F., Bliege Bird, R., Kauhanen, P.G., Bird, D.W., 2014. Conservation or Co-evolution? Intermediate Levels of Aboriginal Burning and Hunting Have Positive Effects on Kangaroo Populations in Western Australia. Hum. Ecol. 42, 659–669. https://doi.org/10.1007/s10745-014-9682-4

Colombaroli, D., Vannière, B., Emmanuel, C., Magny, M., Tinner, W., 2008. Fire-vegetation interactions during the Mesolithic-Neolithic transition at Lago dell'Accesa, Tuscany, Italy. The Holocene 18, 679–692. https://doi.org/10.1177/0959683608091779

Conolly, J., Colledge, S., Shennan, S., 2008. Founder effect, drift, and adaptive change in domestic crop use in early Neolithic Europe. J. Archaeol. Sci. 35, 2797–2804. https://doi.org/10.1016/j.jas.2008.05.006

Coughlan, M.R., 2014. Farmers, flames, and forests: Historical ecology of pastoral fire use and landscape change in the French Western Pyrenees, 1830–2011. For. Ecol. Manage. 312, 55–66. https://doi.org/10.1016/j.foreco.2013.10.021

Coughlan, M.R., Magi, B.I., Derr, K.M., 2018. A Global Analysis of Hunter-Gatherers , Broadcast Fire Use , and Lightning-Fire-Prone Landscapes. Fire 1–13. https://doi.org/10.3390/fire1030041

Crawford, A.J., Belcher, C.M., 2014. Charcoal Morphometry for Paleoecological Analysis: The Effects of Fuel Type and Transportation on Morphological Parameters. Appl. Plant Sci. 2, 1400004. https://doi.org/10.3732/apps.1400004

de Pablo, J., Gomez Puche, M., 2009. Climate change and population dynamics during the Late Mesolithic and the Neolithic transition in Iberia. Doc. Praehist. 36, 67–96.

Dennell, R., 1985. The hunter-gatherer/agricultural frontier in prehistoric temperate Europe, in: The Archaeology of Frontiers and Boundaries. Academic Press, pp. 113–135.

Diez-Castillo, A., Barton, C.M., Roca-Cervigón, N. La, Bernabeu-Auban, J., 2008. Landscape Socioecology in the Serpis Valley (10,000 - 4000 {BP}), in: Posluschny, A., Lambers, K., Aguilera, I. (Eds.), Layers of Perception: Proceedings of the 35th International Conference on Computer Applications and Quantitative Methods in Archaeology ({CAA}), Berlin, Germany, April 2–6, 2007.

Diez Castillo, A., García-Puchol, O., Bernabeu, J., Barton, C.M., Pardo-Gordó, S., Snitker, G., Cegielski, W., Bergin, S., 2016. Resiliencia y cambio durante el Holoceno en La Canal de Navarrés (Valencia): recientes trabajos de prospección. Arch. Prehist. Levantina XXXI, 169–185.

Doyen, E., Vannière, B., Bichet, V., Gauthier, E., Richard, H., Petit, C., 2013. Vegetation history and landscape management from 6500 to 1500 cal. B.P. at Lac d'Antre, Gallo-Roman sanctuary of Villards d'Héria, Jura, France. Veg. Hist. Archaeobot. 22, 83–97. https://doi.org/10.1007/s00334-012-0364-0

Duda, R.O., Hart, P.E. (Peter E., Stork, D.G., 2001. Pattern classification 654.

Dull, R.A., 2004. A Holocene record of Neotropical savanna dynamics from El Salvador. J. Paleolimnol. 32, 219–231.

Dunnell, R., 1992. The notion of site. Space, time, Archaeol. landscapes.

Dupré, M., 1988. Apports de la palynologie à la connaissance du paléoenvironne- ment végétal holocène de la région de Valence (Espagne). Work Sci. Tech. Sect. French Inst. Pondicherry 25, 55–63.

Dupré, M., Carrion, J.S., Fumanal, M.P., La Roca, N., Martinez, J., Usera, J., 1998. Evolution and palaeoenvironmental conditions of an interfan area in eastern Spain (Navarrés, Valencia). Ital. J. Quat. Sci. 11, 97–105.

EFFIS, 2014. Lightning-caused fire locations in Spain: 1990-2010. European Forest Fire Information System, Brussels.

Ekdahl, E.J., Teranes, J.L., Guilderson, T.P., Turton, C.L., McAndrews, J.H., Wittkop, C.A., Stoermer, E.F., 2004. Prehistorical record of cultural eutrophication from Crawford Lake, Canada. Geology 32, 745. https://doi.org/10.1130/G20496.1

Ekdahl, E.J., Teranes, J.L., Wittkop, C.A., Stoermer, E.F., Reavie, E.D., Smol, J.P., 2007. Diatom assemblage response to Iroquoian and Euro-Canadian eutrophication of Crawford Lake, Ontario, Canada. J. Paleolimnol. 37, 233–246. https://doi.org/10.1007/s10933-006-9016-7

Elias, P., 2018. Interior Secretary Ryan Zinke says California's Camp Fire costs likley in

billions. Assoc. Press.

Ellis, E.C., 2015. Ecology in an anthropogenic biosphere. Ecol. Monogr. 85, 287–331. https://doi.org/10.1890/14-2274.1

Ellis, E.C., Goldewijk, K.K., Siebert, S., Lightman, D., Ramankutty, N., 2010. Anthropogenic transformation of the biomes, 1700 to 2000. Glob. Ecol. Biogeogr. 19, 589–606. https://doi.org/10.1111/j.1466-8238.2010.00540.x

Ellis, E.C., Kaplan, J.O., Fuller, D.Q., Vavrus, S., Klein Goldewijk, K., Verburg, P.H., 2013. Used planet: a global history. Proc. Natl. Acad. Sci. U. S. A. 110, 7978–85. https://doi.org/10.1073/pnas.1217241110

Enache, M.D., Cumming, B.F., 2007. Charcoal morphotypes in lake sediments from British Columbia (Canada): An assessment of their utility for the reconstruction of past fire and precipitation. J. Paleolimnol. 38, 347–363. https://doi.org/10.1007/s10933-006-9084-8

Enache, M.D., Cumming, B.F., 2006. Tracking recorded fires using charcoal morphology from the sedimentary sequence of Prosser Lake, British Columbia (Canada). Quat. Res. 65, 282–292. https://doi.org/10.1016/j.yqres.2005.09.003

Erickson, C.L., 2003. Agricultural landscapes as world heritage: raised field agriculture in Bolivia and Peru. Manag. Chang. Sustain. approaches to Conserv. built Environ. 4th Annu. US/ICOMOS Int. Symp. Organ. by US/ICOMOS, Progr. Hist. Preserv. Univ. Pennsylvania, Getty Conserv. Insti 181–204.

Fernández-López de Pablo, J., Barton, C.M., 2013. Bayesian estimation dating of lithic surface collections. J. Archaeol. Method Theory 559–583. https://doi.org/10.1007/s10816-013-9198-z

Fisher, C., 2005. Demographic and Landscape Change in the Lake Patzcuaro Basin, Mexico: Abandoning the Garden. Am. Anthropol. 107, 87–95.

Fitzpatrick, S.M., Keegan, W.F., 2007. Human impacts and adaptations in the Caribbean Islands: An historical ecology approach. Earth Environ. Sci. Trans. R. Soc. Edinburgh 98, 29–45. https://doi.org/10.1017/S1755691007000096

Fletcher Valls, D., 1964. La Ereta del Pedregal (Navarrés, Valencia). Excavaciones Arqueol. en España 42, 1–21.

Fletcher Valls, D., Aparicio Perez, J., 1968. Exploraciones arqueológicas en el Barranco del Lobo, Chella (Valencia). Actas del XI C.A.N. 265–270.

Folke, C., 2006. Resilience: The emergence of a perspective for social–ecological

systems analyses. Glob. Environ. Chang. 16, 253–267. https://doi.org/10.1016/j.gloenvcha.2006.04.002

Fortea Perez, J., 1971. La Cueva de la Cocina: Ensayo de Cronología del Epipaleolitico. Serv. Investig. Prehist. Núm. 40.

Forthofer, J.M., Butler, B.W., Wagenbrenner, N.S., 2014. A comparison of three approaches for simulating fine-scale surface winds in support of wildland fire management. Part I. Model formulation and comparison against measurements. Int. J. Wildl. Fire 23, 969–981. https://doi.org/10.1071/WF12089

Freeman, J., Anderies, J.M., 2012. Intensification, Tipping Points, and Social Change in a Coupled Forager-Resource System. Hum. Nat. 23, 419–446. https://doi.org/10.1007/s12110-012-9154-8

Gallello, G., Bernabeu, J., Diez, A., Escriba, P., Pastor, A., Lezzerini, M., Hodson, M.E., Stump, D., 2017. Rare Earth Elements analysis to identify anthropogenic signatures at Valle del Serpis (Spain) Neolithic settlements, in: Corozzi, A. (Ed.), Abstract Book CSI XL PISA 2017, EMSLIBS 2017.

Gallello, G., Pastor, A., Diez, A., La Roca, N., Bernabeu, J., 2013. Anthropogenic units fingerprinted by REE in archaeological stratigraphy: Mas d'Is (Spain) case. J. Archaeol. Sci. 40, 799–809. https://doi.org/10.1016/j.jas.2012.10.005

García-Puchol, O., McClure, S.B., Juan-Cabanilles, J., Diez-Castillo, A.A., Bernabeu-Aubán, J., Martí-Oliver, B., Pardo-Gordó, S., Pascual-Benito, J.L., Pérez-Ripoll, M., Molina-Balaguer, L., Kennett, D.J., 2018. Cocina cave revisited: Bayesian radiocarbon chronology for the last hunter-gatherers and first farmers in Eastern Iberia. Quat. Int. 472, 259–271. https://doi.org/10.1016/j.quaint.2016.10.037

García Atiénzar, G., 2009. Territorio Neolítico. Las primeras comunidades campesinas en la fachada oriental de la península Ibérica (ca. 5600-2800 cal BC). BAR Int. Ser. 2021.

Garcia Atienzar, G., Jover Maestre, F.J., 2011. The Introduction of the First Farming Communities in the Western Mediterranean: The Valencian Region in Spain as Example. Arqueol. Iberoam. 10, 17–29.

Garcia Borja, P., Salazar-García, D.C., Perez Fernandes, Á., Pardo Gordó, S., Casanova Vañó, V., 2011. El Neolítico antiguo cardial y la Cova de la Sarsa (Bocairent, Valencia): Nuevas perspectivas a partir de su registro funerario (antiguo neolítico Cardial y La Cova de la Sarsa cueva (Bocairent, Valencia). Munibe Antropol. y Arqueol. 62, 175–195.

Garcia Guixé, E., Richards, M.P., Eulàlia Subirà, M., 2006. Palaeodiets of Humans and

Fauna at the Spanish Mesolithic Site of El Collado. Curr. Anthropol. 47, 549–557.

García Puchol, O., Aura Tortosa, J.E., 2006. El Abric de la Falguera (Alcoí, Alacant). Diputación Provincial, Alicante.

García Puchol, O., Barton, C.M., Bernabeu Aubán, J., Diez Castillo, A., Pardo Gordó, S., 2014. De la prospección sistemática al laboratorio GIS en la Canal de Navarrés (Valencia). Saguntum 46, 209–214. https://doi.org/10.7203/SAGVNTVM.46.4239

García Puchol, O., McClure, S.B., Juan Cabanilles, J., Diez Castillo, A.A., Bernabeu Aubán, J., Martí Oliver, B., Pardo-Gordó, S., Pascual Benito, J.L., Pérez-Ripoll, M., Molina Balaguer, L., Kennett, D.J., 2017. Cocina cave revisited: Bayesian radiocarbon chronology for the last hunter-gatherers and first farmers in Eastern Iberia. Quat. Int. 1–13. https://doi.org/10.1016/j.quaint.2016.10.037

García Puchol, O., Molina Balaguer, L., Aura Tortosa, J.E., Bernabeu Aubán, J., 2009. From the Mesolithic ot the Neolithic on the Mediterranean Coast of the Iberian Peninsula. J. Anthrolpological Res. 65, 237–251.

Gardner, J.J., Whitlock, C., 2001. Charcoal accumulation following a recent fire in the Cascade Range, northwestern USA, and its relevance for fire-history studies. The Holocene 11, 541–549.

Gavin, D.G., 2001. Estimation of inbuilt age in radiocarbon ages of soil charcoal for fire history studies. Radiocarbon 43, 27–44. https://doi.org/10.2458/azu_js_rc.43.3995

Gibaja, J.F., Subirà, M.E., Terradas, X., Santos, F.J., Agulló, L., Gómez-Martínez, I., Allièse, F., Fernández-López de Pablo, J., 2015. The emergence of mesolithic cemeteries in SW europe: Insights from the El Collado (Oliva, Valencia, Spain) radiocarbon record. PLoS One 10. https://doi.org/10.1371/journal.pone.0115505

Glikson, A., 2013. Fire and human evolution: The deep-time blueprints of the Anthropocene. Anthropocene 3, 89–92. https://doi.org/10.1016/j.ancene.2014.02.002

González Sampériz, P., 1998. Estudio palinológico de la Cueva de En Pardo (Planes, Alicante). Primeros resultados. Cuaternario y Geomorfol. 12, 45–61.

GRASS Development Team, 2016. Geographic Resources Analysis Support System (GRASS) Software [WWW Document]. Open Source Geospatial Found.

Grayson, D.K., 2001. The Archaeological Record of Human Impacts on Animal Populations. J. World Prehistory 15, 1–68.

Gremillion, K.J., 2011. The Role of Plants in Southeastern Subsistence Economies, in:

Smith, B.D. (Bruce D. (Ed.), The Subsistence Economies of Indigenous North American Societies : A Handbook. Smithsonian Institution Scholarly Press, Washington D.C. ;Lanham Md., pp. 387–400.

Grimm, V., Revilla, E., Berger, U., Jeltsch, F., Mooij, W.M., Railsback, S.F., Thulke, H.-H., Weiner, J., Wiegand, T., DeAngelis, D.L., 2005. Pattern-Oriented Modeling of Agent-Based Complex Systems: Lessons from Ecology. Science (80-.). 310, 987–991. https://doi.org/10.1126/science.1116681

Guilaine, J., Manen, C., 2007a. From Mesolithic to Early Neolithic in the Western Mediterranean. Proc. Br. Acad. 144, 21–51.

Guilaine, J., Manen, C., 2007b. From Mesolithic to Early Neolithic in the Western Mediterranean, in: Whittle, A., Cummings, V. (Eds.), Going Over : The Mesolithic-Neolithic Transition in North-West Europe. Oxford University Press, Oxford, pp. 21–52.

Gunderson, L.H., Holling, C.S. (Eds.), 2002. Panarchy: Understanding Transformations in Human and Natural Systems. Island Press.

Higuera, P.E., Gavin, D.G., Bartlein, P.J., Hallett, D.J., 2010. Peak detection in sediment–charcoal records: impacts of alternative data analysis methods on fire-history interpretations. Int. J. Wildl. Fire 19, 996. https://doi.org/10.1071/WF09134

Higuera, P.E., Peters, M.E., Brubaker, L.B., Gavin, D.G., 2007. Understanding the origin and analysis of sediment-charcoal records with a simulation model. Quat. Sci. Rev. 26, 1790–1809. https://doi.org/10.1016/j.quascirev.2007.03.010

Holling, C., 1996. Engineering resilience versus ecological resilience, Engineering within ecological constraints. National Academy of Engineering.

Holling, C., 1973. Resilience and stability of ecological systems. Annu. Rev. Ecol. Syst. 4, 1–23.

Hughes, L., Alexander, D., 2017. Climate Change and the NSW / ACT Bushfire threat: Update 2016. Climate Council of Australia,. https://doi.org/10.1038/ismej.2013.34

Innes, J.B., Blackford, J.J., 2003. The ecology of Late Mesolithic woodland disturbances: Model testing with fungal spore assemblage data. J. Archaeol. Sci. 30, 185–194. https://doi.org/10.1006/jasc.2002.0832

Innes, J.B., Blackford, J.J., Rowley-Conwy, P.A., 2013. Late Mesolithic and early Neolithic forest disturbance: a high resolution palaeoecological test of human impact hypotheses. Quat. Sci. Rev. 77, 80–100. https://doi.org/10.1016/j.quascirev.2013.07.012

IVIA, 2015. Weather Station wind data from the Canal de Navarrés. Instituto Valenciano de Investigaciones Agrarias, Valencia, Spain.

Jackson, S.T., Hobbs, R.J., 2009. Ecological restoration in the light of ecological history. Science (80-.). 325, 567–569. https://doi.org/10.1126/science.1172977

Jalut, G., Esteban Amat, A., Bonnet, L., Gauquelin, T., Fontugne, M., 2000. Holocene climatic changes in the Western Mediterranean, from south-east France to south-east Spain. Palaeogeogr. Palaeoclimatol. Palaeoecol. 160, 255–290. https://doi.org/10.1016/S0031-0182(00)00075-4

Jensen, K., Lynch, E. a., Calcote, R., Hotchkiss, S.C., 2007. Interpretation of charcoal morphotypes in sediments from Ferry Lake, Wisconsin, USA: do different plant fuel sources produce distinctive charcoal morphotypes? The Holocene 17, 907–915. https://doi.org/10.1177/0959683607082405

Jiménez, E., 1935. Nueva estación parpallense. An. del Cent. Cult. Valencia. 144–153.

Jiménez Navarro, E., San Valero, J., 1943. Localidades con piedra tallada en la región de Buñol (Valencia). Empúries Rev. món clàssic i Antig. tardana 289–292.

Johansen, R.W., McNab, W.H., Hough, W.A., Edwards, B.M., 1976. Fuels, Fire, and Emissions, in: Southern Forestry Smoke Managment Guidebook. U.S. Department of Agriculture, Forest Service, Southeastern Forest Experiment Station, Asheville, NC.

Jones, C., Lawton, J., Shachak, M., 1997. Positive and Negative Effects of Organisms as Physical Ecosystem Engineers. Ecology 78, 1946–1957.

Jones, S.E., Burjachs, F., Ferrer-García, C., Giralt, S., Schulte, L., Fernández-López de Pablo, J., 2018. A multi-proxy approach to understanding complex responses of salt-lake catchments to climate variability and human pressure: A Late Quaternary case study from south-eastern, Spain. Quat. Sci. Rev. https://doi.org/10.1016/j.quascirev.2017.12.015

Juan Cabanilles, J., 1994. Estructuras de habitación en la Ereta del Pedregal (Navarrés, Valencia): Resultos de las campañas de 1980-1982 y 1990. SAGVNTVM. Papeles del Lab. Arqueol. Val. 27, 67–97.

Keeley, J.E., 2009. Fire intensity, fire severity and burn severity: A brief review and suggested usage. Int. J. Wildl. Fire 18, 116–126. https://doi.org/10.1071/WF07049

Keeley, J.E., Bond, W., Bradstock, R.A., Pauss, J.G., Rundel, P.W., 2012. Fire in Mediterranean Ecosystems: Ecology, Evolution and Management. Cambridge

University Press.

Kelly, R.F., Higuera, P.E., Barrett, C.M., Hu, F.S., 2011. A signal-to-noise index to quantify the potential for peak detection in sediment–charcoal records. Quat. Res. 75, 11–17. https://doi.org/10.1016/j.yqres.2010.07.011

Kendal, J., Tehrani, J.J., Odling-Smee, J., 2011. Human niche construction in interdisciplinary focus. Philos. Trans. R. Soc. Lond. B. Biol. Sci. 366, 785–792. https://doi.org/10.1098/rstb.2010.0306

Kirch, P.V., 1997. The Lapita peoples : ancestors of the oceanic world. Blackwell Publishers.

La Roca, N., Fumanal, M.P., Martínez Gallego, J., 1996. Evolución Cuaternaria del Drenaje en un Corredor Intramontano: La Canal de Navarrés (Valencia, Spain), in: IV Reunión de Geomorfología. pp. 445–455.

Laland, K., 1999. Evolutionary consequences of niche construction and their implications for ecology. Proc. Natl. Acad. Sci. 96, 10242–10247.

Laland, K.N., O'Brien, M.J., 2012. Cultural Niche Construction: An Introduction. Biol. Theory 6, 191–202. https://doi.org/10.1007/s13752-012-0026-6

Laland, K.N., O'Brien, M.J., 2010. Niche Construction Theory and Archaeology. J. Archaeol. Method Theory 17, 303–322. https://doi.org/10.1007/s10816-010-9096-6

Leigh, D.S., Gragson, T.L., Coughlan, M.R., 2015. Colluvial legacies of millennial landscape change on individual hillsides, place-based investigation in the western Pyrenees Mountains. Quat. Int. https://doi.org/10.1016/j.quaint.2015.08.031

Lemmen, C., Gronenborn, D., Wirtz, K.W., 2011. A simulation of the Neolithic transition in Western Eurasia. J. Archaeol. Sci. 38, 3459–3470. https://doi.org/10.1016/j.jas.2011.08.008

Lestienne, M., Aleman, J., Colombaroli, D., 2018. How Paleofire Research Can Better Inform Ecosystem Management. Eos (Washington. DC). 99. https://doi.org/10.1029/2018EO096613

Levin, M.J., Ayres, W.S., 2017. Managed agroforests, swiddening, and the introduction of pigs in Pohnpei, Micronesia: Phytolith evidence from an anthropogenic landscape. Quat. Int. 434, 70–77. https://doi.org/10.1016/j.quaint.2015.12.027

Leys, B., Brewer, S.C., McConaghy, S., Mueller, J., McLauchlan, K.K., 2015. Fire history reconstruction in grassland ecosystems: Amount of charcoal reflects local area burned. Environ. Res. Lett. 10, 114009. https://doi.org/10.1088/1748-

9326/10/11/114009

Liebmann, M.J., Farella, J., Roos, C.I., Stack, A., Martini, S., Swetnam, T.W., 2016. Native American depopulation, reforestation, and fire regimes in the Southwest United States, 1492–1900 CE. Proc. Natl. Acad. Sci. 113, E696–E704. https://doi.org/10.1073/pnas.1521744113

Llobera, M., Wilkinson, K.N., Weiss, M.C., Flaming, R.J., Marini, N.A.F., Mazet, S., 2010. Into the maquis: Methodological and interpretational challenges in surveying la Balagne, northwest Corsica. J. Mediterr. Archaeol. 23, 169–196. https://doi.org/10.1558/jmea.v23i2.169

Llobregat, M., Marti, B., Bernabeu Auban, J.M., Villaverde, V., Gallart, M.D., Perez, M., Acuna, J.D., Robles, F., 1981. Cova de les Cendres (Teulada, Alicante) Informe preliminar, in: Revista Del Instituto de Estudios Alicantinos. pp. 87–111.

López-Merino, L., López-Sáez, J. a., Alba-Sánchez, F., Pérez-Díaz, S., Carrión, J.S., 2009. 2000 years of pastoralism and fire shaping high-altitude vegetation of Sierra de Gredos in central Spain. Rev. Palaeobot. Palynol. 158, 42–51. https://doi.org/10.1016/j.revpalbo.2009.07.003

López-Sáez, J.A., López-Merino, L., Alba-Sánchez, F., Pérez-Díaz, S., Abel-Schaad, D., Carrión, J.S., 2009. Late Holocene ecological history of Pinus pinaster forests in the Sierra de Gredos of central Spain. Plant Ecol. 206, 195–209. https://doi.org/10.1007/s11258-009-9634-z

López de Pablo, J.F., Gómez Puche, M., 2009. Climate change and population dynamics during the late Mesolithic and the Neolithic transition in Iberia. Doc. Praehist. 36, 67. https://doi.org/10.4312/dp.36.4

Lynch, J.A., Clark, J.S., Stocks, B.J., 2004. Charcoal production, dispersal, and deposition from the Fort Providence experimental fire: interpreting fire regimes from charcoal records in boreal forests. Can. J. For. Res. 34, 1642–1656. https://doi.org/10.1139/x04-071

Malhi, Y., Doughty, C.E., Galetti, M., Smith, F.A., Svenning, J.-C., Terborgh, J.W., 2016. Megafauna and ecosystem function from the Pleistocene to the Anthropocene. Proc. Natl. Acad. Sci. 113, 838–846. https://doi.org/10.1073/pnas.1502540113

Mallol, C., Hernández, C.M., Machado, J., 2012. The significance of stratigraphic discontinuities in Iberian Middle-to-Upper Palaeolithic transitional sites. Quat. Int. 275, 4–13. https://doi.org/10.1016/j.quaint.2011.07.026

MAPA, 1989. Clave fotográfica para la identificación de modelos de combustible. Instituto para la Conservación de la Naturaleza (ICONA), Madrid.

Martí-Oliver, B., 2011. La Cova de l'Or, in: Las Primeras Producciones Cerámicas: El VI Milenio Cal AC En La Península Ibérica. UNIVERSITAT DE VALÈNCIA, Valencia, Spain, pp. 183–186.

Marti Oliver, B., 1988. Early Farming Communities in Spain. Berytus 36, 69–86.

Martí Oliver, B., Tortosa, J.E.A., Cabanilles, J.J., García Puchol, O., Fernández-López de Pablo, J., 2009. El Mesolítico geométrico de tipo "Cocina" en el País Valenciano, in: El Mesolítico Geométrico En La Península Ibérica. pp. 205–258.

Maxwell, A.L., 2004. Fire regimes in north-eastern Cambodian monsoonal forests, with a 9300-year sediment charcoal record. J. Biogeogr. 31, 225–239. https://doi.org/10.1046/j.0305-0270.2003.01015.x

McClure, S.B., 2004. Cultural Transmission of Ceramic Technology During the Consolidation of Agriculture in Valencia, Spain. University of California, Santa Barbara.

McClure, S.B., Barton, C.M., Jochim, M., 2009. Human behavioral ecology and climate change during the transition to agriculture in Valencia, Eastern Spain. J. Anthropol. Res. 65, 253–269.

McGlone, M., 2001. The origin of the indigenous grasslands of southeastern South Island in relation to pre-human woody ecosystems. N. Z. J. Ecol. 25, 1–15.

McKey, D., Rostain, S., Iriarte, J., Glaser, B., Birk, J.J., Holst, I., Renard, D., 2010. Pre-Columbian agricultural landscapes, ecosystem engineers, and self-organized patchiness in Amazonia. Proc. Natl. Acad. Sci. U. S. A. 107, 7823–7828. https://doi.org/10.1073/pnas.0908925107

McWethy, D.B., Whitlock, C., Wilmshurst, J.M., McGlone, M.S., Fromont, M., Li, X., Dieffenbacher-Krall, A., Hobbs, W.O., Fritz, S.C., Cook, E.R., 2010. Rapid landscape transformation in South Island, New Zealand, following initial Polynesian settlement. Proc. Natl. Acad. Sci. 107, 21343–21348. https://doi.org/10.1073/pnas.1011801107

McWethy, D.B., Whitlock, C., Wilmshurst, J.M., McGlone, M.S., Li, X., 2009. Rapid deforestation of South Island, New Zealand, by early Polynesian fires. The Holocene 19, 883–897. https://doi.org/10.1177/0959683609336563

Menéndez Amor, J., Florschütz, F., 1961. Resultado del análisis polínico de una serie de muestras de turba recogida en la Ereta del Pedregal (Navarrés, Valencia). Arch. Prehist. Levantina 9, 97–99.

Morehart, C.T., 2012. What If the Aztec Empire Never Existed? The Prerequisites of Empire and the Politics of Plausible Alternative Histories. Am. Anthropol. 114, 267–281. https://doi.org/10.1111/j.1548-1433.2012.01424.x

Moreno, J., Oechel, W., 1994. The role of fire in Mediterranean-type ecosystems, Ecological studies (USA). Springer; 1 edition.

NASA LP DAAC, 2011. Global Digital Elevation Model (GDEM). NASA EOSDIS Land Processes DAAC, USGS Earth Resources Observation and Science (EROS), Sioux Falls, South Dakota.

Nevle, R.J., Bird, D.K., Ruddiman, W.F., Dull, R.A., 2011. Neotropical human-landscape interactions, fire, and atmospheric CO2 during European conquest. The Holocene 21, 853–864. https://doi.org/10.1177/0959683611404578

O'Brien, M.J., Laland, K.N., 2012. Genes, Culture, and Agriculture. Curr. Anthropol. 53, 434–470. https://doi.org/10.1086/666585

Odling-Smee, F., Laland, K., Feldman, M., 2003. Niche construction: the neglected process in evolution. Princeton University Press.

Odling-Smee, F., Laland, K., Feldman, M., 1996. Niche Construction. Am. Nat. 147, 641–648.

Odling-Smee, J., Turner, J.S., 2011. Niche Construction Theory and Human Architecture. Biol. Theory 6, 283–289. https://doi.org/10.1007/s13752-012-0029-3

Ohlson, M., Tryterud, E., 2000. Interpretation of the charcoal record in forest soils: forest fires and their production and deposition of macroscopic charcoal. The Holocene 10, 519–525. https://doi.org/10.1191/095968300667442551

Oosterbeek, L., 2001. Re-thinking the Mesolithic-Neolithic transition in the Iberian peninsula: a view from the West. Doc. Praehistoria XXVIII, 75–84.

Ortman, S.G., 2016. Uniform Probability Density Analysis and Population History in the Northern Rio Grande. J. Archaeol. Method Theory 95–126. https://doi.org/10.1007/s10816-014-9227-6

Ortman, S.G., Varien, M.D., Gripp, T.L., 2007. Empirical Bayesian Methods for Archaeological Survey Data: An Application from the Mesa Verde Region. Am. Antiq. 72, 241–272. https://doi.org/10.2307/40035813

Pantaléon-Cano, J., Yll, E.-I., Pérez-Obiol, R., Roure, J.M., 2003. Palynological evidence for vegetational history in semi-arid areas of the western Mediterranean (Almería, Spain). The Holocene 13, 109–119. https://doi.org/10.1191/0959683603hl598rp

Pardo Gordó, S., Diez Castillo, A., Bernabeu Aubán, J., 2015. Prospecciones sistemáticas en la depressió de l'Alcoi (Alicante): Analizando las colecciones superficiales, in: V Congresso Do Neolítico Peninsular.

Pardo Gordó, S., Diez Castillo, A., Bernabeu Aubán, J., 2009. Áreas y suelos: El tamaño de los yacimientos de superficie. Una propuesta metodológica. Spal 18, 41–52. https://doi.org/10.12795/spal.2009.i18.03

Patterson, W., Edwards, K., Maguire, D., 1987. Microscopic Charcoal as a Fossil Indicator of Fire. Quat. Sci. Rev. 6, 3–23.

Pausas, J.G., 1999a. Response of plant functional types to changes in the fire regime in Mediterranean ecosystems : A simulation approach. J. Veg. Sci. 10, 717–722. https://doi.org/10.2307/3237086

Pausas, J.G., 1999b. Mediterranean vegetation dynamics: Modelling problems and functional types. Plant Ecol. 140, 27–39. https://doi.org/10.1023/A:1009752403216

Pausas, J.G., Fernández-Muñoz, S., 2012. Fire regime changes in the Western Mediterranean Basin: from fuel-limited to drought-driven fire regime. Clim. Change 110, 215–226. https://doi.org/10.1007/s10584-011-0060-6

Pausas, J.G., Keeley, J.E., 2009. A Burning Story: The Role of Fire in the History of Life. Bioscience 59, 593–601. https://doi.org/10.1525/bio.2009.59.7.10

Pausas, J.G., Paula, S., 2012. Fuel shapes the fire-climate relationship: evidence from Mediterranean ecosystems. Glob. Ecol. Biogeogr. 21, 1074–1082. https://doi.org/10.1111/j.1466-8238.2012.00769.x

Peters, M.E., Higuera, P.E., 2007. Quantifying the source area of macroscopic charcoal with a particle dispersal model. Quat. Res. 67, 304–310. https://doi.org/10.1016/j.yqres.2006.10.004

Pisaric, M.F.J., 2002. Long-distance transport of terrestrial plant material by convection resulting from forest fires. J. Paleolimnol. 28, 349–354. https://doi.org/10.1023/A:1021630017078

Pitkänen, A., Huttunen, P., 1999. A 1300-year forest-fire history at a site in eastern Finland based on charcoal and pollen records in laminated lake sediment. The Holocene 9, 311–320. https://doi.org/10.1191/095968399667329540

Pitkänen, A., Lehtonen, H., Huttunen, P., 1999. Comparison of sedimentary microscopic charcoal particle records in a small lake with dendrochronological data: evidence for the local origin of microscopic charcoal produced by forest fires of low intensity in

eastern Finland. The Holocene 9, 559–567. https://doi.org/10.1191/095968399670319510

Pla Ballester, E., Martí Oliver, B., Bernabeu Auban, J., 1983. La Ereta del Pedregal (Navarrés, Valencia) y los inicios de la Edad del Bronce, in: Crónica Del XVI Congreso Arqueológico Nacional. pp. 239–248.

Pyne, S., 2012. Fire: Nature and Culture, 1st Editio. ed. University of Chicago Press, Chicago.

Pyne, S.J., 1998. Forged in fire: history, land, and anthropogenic fire, in: Balée, W. (Ed.), Advances in Historical Ecology. Columbia University Press, pp. 62–103.

Pyne, S.J., 1997. Vestal fire : an environmental history, told through fire, of Europe and Europe's encounter with the world. University of Washington Press.

Pyne, S.J., Goldammer, J.G., 1997. The Culture of Fire: An Introduction to Anthropogenic Fire History, in: Clark, J.S., Cachier, H., Goldammer, J.G., Stocks, B. (Eds.), Sediment Records of Biomass Burning and Global Change. Springer Berlin Heidelberg, pp. 71–114.

Reidmiller, D.R., Avery, C.W., Easterling, D.R., Kunkel, K.E., Lewis, K.L.M., Maycock, T.K., Stewart, B.C. (Eds.), 2018. USGCRP, 2018: Impacts, Risks, and Adaptation in the United States: Fourth National Climate Assessment, Volume II: Report-in-Brief. U.S. Global Change Research Program, Washington, DC.

Riel-Salvatore, J., 2010. A Niche Construction Perspective on the Middle–Upper Paleolithic Transition in Italy. J. Archaeol. Method Theory 17, 323–355. https://doi.org/10.1007/s10816-010-9093-9

Riel-Salvatore, J., Barton, C.M., 2007. "Transitional" Upper Paleolithic industries: New questions, new methods. "Transitional" Up. Paleolit. Ind. New Quest. new methods 61–74.

Roebroeks, W., Villa, P., 2011. On the earliest evidence for habitual use of fire in Europe. Proc. Natl. Acad. Sci. 108, 5209–5214. https://doi.org/10.1073/pnas.1018116108

Roos, C.I., 2015. Western Apache Pyrogenic Placemaking in the Mountains of Eastern Arizona, in: Scheiber, L.L., Zedeño, M.. (Eds.), Engineering Mountain Landscapes: An Anthropology of Social Investment. University of Utah Press, Salt Lake City, pp. 116–125.

Roos, C.I., 2008. Fire, climate, and social-ecological systems in the ancient southwest: alluvial geoarchaeology and applied historical ecology. University of Arizona,

Tucson.

Roos, C.I., Bowman, D.M.J.S., Balch, J.K., Artaxo, P., Bond, W.J., Cochrane, M., D'Antonio, C.M., DeFries, R., Mack, M., Johnston, F.H., Krawchuk, M. a, Kull, C. a, Moritz, M. a, Pyne, S., Scott, a C., Swetnam, T.W., 2014. Pyrogeography, historical ecology, and the human dimensions of fire regimes. J. Biogeogr. 41, 833–836.

Roos, C.I., Field, J.S., Dudgeon, J. V., 2016. Anthropogenic Burning, Agricultural Intensification, and Landscape Transformation in Post-Lapita Fiji. J. Ethnobiol. 36, 535–553. https://doi.org/10.2993/0278-0771-36.3.535

Roos, C.I., Sullivan III, A.P., McNamee, C., 2010. Paleoecological Evidence for Systematic Indigenous Burning in the Upland Southwest, in: Dean, R.M. (Ed.), The Archaeology of Anthropogenic Environments. Southern Illinois University Carbondale, pp. 142–171.

Roos, C.I., Zedeño, M.N., Hollenback, K.L., Erlick, M.M.H., 2018. Indigenous impacts on North American Great Plains fire regimes of the last millennium I, 1–6. https://doi.org/10.1073/pnas.1805259115

San-Miguel-Ayanz, J., Durrant, T., Boca, R., Libertà, G., Branco, A., de Rigo, D., Ferrari, D., Maianti, P., Artés Vivancos, T., Costa, H., Lana, F., Löffler, P., Nuijten, D., Christofer Ahlgren, A., Leray, T., 2018. Forest Fires in Europe, Middle East and North Africa 2017. EUR 29318. https://doi.org/10.2760/663443

Sandom, C., Faurby, S., Sandel, B., Svenning, J.C., 2014. Global late Quaternary megafauna extinctions linked to humans, not climate change. Proc. R. Soc. B Biol. Sci. 281. https://doi.org/10.1098/rspb.2013.3254

Santana, V.M., Alday, J.G., Baeza, M.J., 2014. Effects of fire regime shift in Mediterranean Basin ecosystems: changes in soil seed bank composition among functional types. Plant Ecol. 215, 555–566. https://doi.org/10.1007/s11258-014-0323-1

Scherjon, F., Bakels, C., MacDonald, K., Roebroeks, W., 2015. Burning the Land:An Ethnographic Study of Off-Site Fire Use by Current and Historically Documented Foragers and Implications for the Interpretation of Past Fire Practices in the Landscape. Curr. Anthropol. 56, 299–326. https://doi.org/10.1086/681561

Schier, W., Ehrmann, O., Rösch, M., Bogenrieder, A., Hall, M., Herrmann, L., Schulz, E., 2013. The Economics of Neolithic Swidden Cultivation: Results of an Experimental Long-Term Project in Forchtenberg (Baden-Württemberg, Germany), in: Kerig, T., Zimmermann, A. (Eds.), Economic Archaeology: From Structure to Performance in European Archaeology. Universitätsforschungen zur prähistorischen

Archäologie, Bonn, pp. 97–106.

Schneider, C.A., Rasband, W.S., Eliceiri, K.W., 2012. NIH Image to ImageJ: 25 years of image analysis. Nat. Methods 9, 671–675. https://doi.org/10.1038/nmeth.2089

Scott, A.C., 2010. Charcoal recognition, taphonomy and uses in palaeoenvironmental analysis. Palaeogeogr. Palaeoclimatol. Palaeoecol. 291, 11–39. https://doi.org/10.1016/j.palaeo.2009.12.012

Scott, A.C., Chaloner, W.G., Belcher, C.M., Roos, C.I., 2016. The interaction of fire and mankind. Philos. Trans. R. Soc. B Biol. Sci. 371, 20160149. https://doi.org/10.1098/rstb.2016.0149

Scott, J.H., Burgan, R.E., 2005. Standard Fire Behavior Fuel Models : A Comprehensive Set for Use with Rothermel ' s Surface Fire Spread Model. Fort Collins, CO.

Servera-Vives, G., Riera, S., Picornell-Gelabert, L., Moffa-Sánchez, P., Llergo, Y., Molsosa, A.G., Mus-Amezquita, M., Álvarez, S.G., Trías, M.C., 2018. The onset of islandscapes in the Balearic Islands: A study-case of Addaia (northern Minorca, Spain). Palaeogeogr. Palaeoclimatol. Palaeoecol. #pagerange#. https://doi.org/10.1016/j.palaeo.2018.02.015

Sheridan, M., 2014. The Social Life of Landesque Capital and a Tanzanian Case Study, in: Landesque Capital: The Historical Ecology of Enduring Landcsape Modifications. Left Coast Press, Walnut Creek, CA, pp. 155–171.

Shimelmitz, R., Kuhn, S.L., Jelinek, A.J., Ronen, A., Clark, A.E., Weinstein-Evron, M., 2014. "Fire at will": The emergence of habitual fire use 350,000 years ago. J. Hum. Evol. 77, 196–203. https://doi.org/10.1016/j.jhevol.2014.07.005

Smith, B.D., 2015a. Documenting Human Niche Construction in the Archaeological Record. Method and Theory in Paleoethnobotany 355–370. https://doi.org/10.5876/9781607323167.c018

Smith, B.D., 2015b. A Comparison of Niche Construction Theory and Diet Breadth Models as Explanatory Frameworks for the Initial Domestication of Plants and Animals. J. Archaeol. Res. 215–262. https://doi.org/10.1007/s10814-015-9081-4

Smith, B.D., 2012. A Cultural Niche Construction Theory of Initial Domestication. Biol. Theory 6, 260–271. https://doi.org/10.1007/s13752-012-0028-4

Smith, B.D., 2011. General patterns of niche construction and the management of "wild" plant and animal resources by small-scale pre-industrial societies. Philos. Trans. R. Soc. Lond. B. Biol. Sci. 366, 836–48. https://doi.org/10.1098/rstb.2010.0253

Smith, B.D., 2007. Niche construction and the behavioral context of plant and animal domestication. Evol. Anthropol. Issues, News, Rev. 16, 188–199. https://doi.org/10.1002/evan.20135

Smith, B.D., Zeder, M. a., 2013. The onset of the Anthropocene. Anthropocene 4, 8–13. https://doi.org/10.1016/j.ancene.2013.05.001

Smith, E.A., 2001. Low-level food production. J. Archaeol. Res. 9, 1–43.

Snitker, G., 2018. Identifying natural and anthropogenic drivers of prehistoric fire regimes through simulated charcoal records. J. Archaeol. Sci. 95, 1–15. https://doi.org/10.1016/j.jas.2018.04.009

Snitker, G., Castillo, A.D., Barton, C.M., Aubán, J.B., Puchol, O.G., Pardo-Gordó, S., 2018a. Patch-based survey methods for studying prehistoric human land-use in agriculturally modified landscapes: A case study from the Canal de Navarrés, eastern Spain. Quat. Int. 483, 5–22. https://doi.org/10.1016/j.quaint.2018.01.034

Snitker, G., Diez-Castillo, A., Barton, C.M., Bernabeu Auban, J., García-Puchol, O., Pardo-Gordó, S., 2018b. Patch-based survey methods for studying prehistoric human land-use in agriculturally modified landscapes: A case study from the Canal de Navarrés, eastern Spain. Quat. Int. 483, 5–22. https://doi.org/https://doi.org/10.1016/j.quaint.2018.01.034

Sullivan, A.P., Berkebile, J.N., Forste, K.M., Washam, R.M., 2015. Disturbing Developments: An Archaeobotanical Perspective on Pinyon-Juniper Woodland Fire Ecology, Economic Resource Production, and Ecosystem History. J. Ethnobiol. 35, 37–59. https://doi.org/10.2993/0278-0771-35.1.37

Sullivan, A.P., Forste, K.M., 2014. Fire-reliant subsistence economies and anthropogenic coniferous ecosystems in the Pre-Columbian northern American Southwest. Veg. Hist. Archaeobot. 23, 135–151. https://doi.org/10.1007/s00334-014-0434-6

Swetnam, T.W., Farella, J., Roos, C.I., Liebmann, M.J., Falk, D.A., Allen, C.D., 2016. Multiscale perspectives of fire, climate and humans in western North America and the Jemez Mountains, USA. Philos. Trans. R. Soc. B Biol. Sci. 371, 20150168. https://doi.org/10.1098/rstb.2015.0168

Taylor, A.H., Trouet, V., Skinner, C.N., Stephens, S., 2016. Socioecological transitions trigger fire regime shifts and modulate fire–climate interactions in the Sierra Nevada, USA, 1600–2015 CE. Proc. Natl. Acad. Sci. 113, 13684–13689. https://doi.org/10.1073/pnas.1609775113

Tinner, W., Hofstetter, S., Zeugin, F., Conedera, M., Wohlgemuth, T., Zimmermann, L., Zweifel, R., 2006. Long-distance transport of macroscopic charcoal by an intensive

crown fire in the Swiss Alps - Implications for fire history reconstruction. The Holocene 16, 287–292. https://doi.org/10.1191/0959683606hl925rr

Trauernicht, C., Brook, B.W., Murphy, B.P., Williamson, G.J., Bowman, D.M.J.S., 2015. Local and global pyrogeographic evidence that indigenous fire management creates pyrodiversity. Ecol. Evol. 5, 1908–1918. https://doi.org/10.1002/ece3.1494

Umbanhowar Jr., C.E., McGrath, M.J., 1998. Experimental production and analysis of microscopic charcoal from wood, leaves and grasses. The Holocene 8, 341–346. https://doi.org/10.1191/095968398666496051

Vachula, R.S., Richter, N., 2018. Informing sedimentary charcoal-based fire reconstructions with a kinematic transport model. The Holocene 28, 173–178. https://doi.org/10.1177/0959683617715624

Valese, E., Conedera, M., Held, a. C., Ascoli, D., 2014. Fire, humans and landscape in the European Alpine region during the Holocene. Anthropocene 6, 63–74. https://doi.org/10.1016/j.ancene.2014.06.006

Van de Water, K.M., Safford, H.D., 2011. A Summary of Fire Frequency Estimates for California Vegetation before Euro-American Settlement. Fire Ecol. 7, 26–58. https://doi.org/10.4996/fireecology.0703026

Vannière, B., Colombaroli, D., Chapron, E., Leroux, A., Tinner, W., Magny, M., 2008. Climate versus human-driven fire regimes in Mediterranean landscapes: the Holocene record of Lago dell'Accesa (Tuscany, Italy). Quat. Sci. Rev. 27, 1181–1196. https://doi.org/10.1016/j.quascirev.2008.02.011

Vanniere, B., Power, M.J., Roberts, N., Tinner, W., Carrion, J., Magny, M., Bartlein, P., Colombaroli, D., Daniau, a. L., Finsinger, W., Gil-Romera, G., Kaltenrieder, P., Pini, R., Sadori, L., Turner, R., Valsecchi, V., Vescovi, E., 2011. Circum-Mediterranean fire activity and climate changes during the mid-Holocene environmental transition (8500-2500 cal. BP). The Holocene 21, 53–73. https://doi.org/10.1177/0959683610384164

Vigne, J.-D., Briois, F., Zazzo, A., Willcox, G., Cucchi, T., Thiebault, S., Carrere, I., Franel, Y., Touquet, R., Martin, C., Moreau, C., Comby, C., Guilaine, J., 2012. First wave of cultivators spread to Cyprus at least 10,600 y ago. Proc. Natl. Acad. Sci. 109, 8445–8449. https://doi.org/10.1073/pnas.1201693109

Villaverde Bonilla, V., Romána, D., Ripoll, M.P., Bergadà, M.M., Real, C., 2012. The end of the Upper Palaeolithic in the Mediterranean Basin of the Iberian Peninsula. Quat. Int. 272–273, 17–32. https://doi.org/10.1016/j.quaint.2012.04.025

Villaverde, V., Aura, J.E., Barton, C.M., 1998. The Upper Paleolithic in Mediterranean

Spain: A Review of Current Evidence. J. World Prehistory 12, 121–198. https://doi.org/10.1023/A:1022332217614

Walsh, M.K., Pearl, C.A., Whitlock, C., Bartlein, P.J., Worona, M.A., 2010. An 11 000-year-long record of fire and vegetation history at Beaver Lake, Oregon, central Willamette Valley. Quat. Sci. Rev. 29, 1093–1106. https://doi.org/10.1016/j.quascirev.2010.02.011

Wentworth, C.K., 1922. A Scale of Grade and Class Terms for Clastic Sediments. J. Geol. 30, 377–392. https://doi.org/10.1086/622910

Whelan, R., 1995. The ecology of fire. Cambridge University Press.

Whitlock, C., Anderson, R.S., 2003. Fire History Reconstructions Based on Sediment Records from Lakes and Wetlands, in: T. T. Veblen, W. L. Baker, G.M. and T.W.S. (Ed.), Fire and Climatic Change in Temperate Ecosystems of the Western Americas. Ecological Studies, Vol. 160, Springer, New York, pp. 3–31. https://doi.org/10.1007/0-387-21710-X_1

Whitlock, C., Higuera, P.E., McWethy, D.B., Briles, C.E., 2010. Paleoecological Perspectives on Fire Ecology : Revisiting the Fire-Regime Concept. Open Ecol. Journal, 3, 6–23.

Whitlock, C., Larsen, C., 2001. Charcoal as a fire proxy, in: Smol, J.P., Birks, H.J.B., Last, W.M., Bradley, R.S., Alverson, K. (Eds.), Tracking Environmental Change Using Lake Sediments: Vol 3 Terrestrial, Algal, and Siliceous Indicators. Springer Netherlands, pp. 75–97. https://doi.org/10.1007/0-306-47668-1_5

Whitlock, C., Millspaugh, S.H., 1996. Testing the assumptions of fire-history studies: an examination of modern charcoal accumulation in Yellowstone National Park, USA. The Holocene 6, 7–15. https://doi.org/10.1177/095968369600600102

Wilensky, U., 1999. Netlogo. Center for Connected Learning and Computer-Based Modeling, Northwestern University, Evanston, IL.

Yll, E.-I., Perez-Obiol, R., Pantaleon-Cano, J., Roure, J.M., 1997. Palynological Evidence for Climatic Change and Human Activity during the Holocene on Minorca (Balearic Islands). Quat. Res. 48, 339–347. https://doi.org/10.1006/qres.1997.1925

Zeder, M. a., 2011. The Origins of Agriculture in the Near East. Curr. Anthropol. 52, S221--S235. https://doi.org/10.1086/659307

Zeder, M.A., 2016. Domestication as a model system for niche construction theory. Evol. Ecol. 30, 325–348. https://doi.org/10.1007/s10682-015-9801-8

Zeder, M.A., 2008. Domestication and early agriculture in the Mediterranean Basin: Origins, diffusion, and impact. Proc. Natl. Acad. Sci. 105, 11597–11604. https://doi.org/10.1073/pnas.0801317105

Zilhão, J., 2001. Radiocarbon Evidence for Maritime Pioneer Colonization at the Origins of Farming in West Mediterranean Europe. Proc. Natl. Acad. Sci. U. S. A. 98, 14180–14185.

Zvelebil, M., 1994. Plant Use in the Mesolithic and its Role in the Transition to Farming. Proc. Prehist. Soc. 60, 35–74. https://doi.org/10.1017/S0079497X00003388

APPENDIX I

CHARCOAL LABORATORY PROCESSING METHODOLOGY

Charcoal Laboratory Processing Methodology

The methodology outlined below is based on the following published methods:

Rhodes, A.N., 1998. A method for the preparation and quantification of microscopic charcoal from terrestrial and lacustrine sediment cores. The Holocene 8, 113–117. https://doi.org/10.1191/095968398671104653

Roos, C.I., 2008. Fire, climate, and social-ecological systems in the ancient southwest: alluvial geoarchaeology and applied historical ecology. University of Arizona, Tucson.

Schlachter, K.J., Horn, S.P., 2010. Sample preparation methods and replicability in macroscopic charcoal analysis. J. Paleolimnol. 44, 701–708. https://doi.org/10.1007/s10933-009-9305-z

Whitlock, C., Anderson, R.S., 2003. Fire History Reconstructions Based on Sediment Records from Lakes and Wetlands, in: T. T. Veblen, W. L. Baker, G.M. and T.W.S. (Ed.), Fire and Climatic Change in Temperate Ecosystems of the Western Americas. Ecological Studies, Vol. 160, Springer, New York, pp. 3–31. https://doi.org/10.1007/0-387-21710-X_1

Exact steps:

1. Subsample 5cm3 of dry, loose sediment.
2. Transfer to 200ml beaker and add 100ml distilled water.
3. Add 25ml of diluted (6%) H_2O_2 to digest and lighten the color of unburned plant materials (Rhodes 1998).
4. Allow to react at room temperature for 48 hours.
5. Add 25ml of 10% Na-hexametaphosphate to diflocculate the sample.
6. Soak at room temperature for 6 hours.
7. Transfer sample into a set of nested sedimentology sieves (500μm and 125 μm).
8. “Using the spray nozzle attached to a faucet, gently spray the surface of the top sieve for 1.5 to 2 minutes so that the entire subsample is washed through the sieves” (2003:13).

9. “Separate the sieves, and then gently wash the sediment to one side of each sieve. Turn the sieve so that its surface is perpendicular to the counter top and the sediment is at the bottom (closest to the counter)” (2003:13).
10. Use a wash bottle to wash charcoal collected in each size category into a petri dish.
11. Allow sample to dry at 50° C until no more liquid remains (or under the fume hood).
12. Count black plant tissues using a binocular microscope at 5-25X magnification.
13. Collect large plant tissues for radiocarbon dating.
14. Calculate charcoal concentrations (pieces cm-3).

APPENDIX II

CHARTOOL: AN OPEN-ACCESS SOFTWARE FOR QUANTIFYING CHARCOAL FRAGMENT METRICS USING A SEMI-AUTOMATED PROCEDURE

Introduction

Human caused fires range broadly in terms of their scale, intensity, and the motivation behind them, which in turn results in a diverse set of depositional and taphonomic scenarios in which charcoal particles are preserved. Common archaeological approaches to paleo-charcoal focus on charcoal found in hearths and analyses include counting and taxonomically identifying macro-charcoal (<1000 μm) fragments to identify fuel use (Théry-Parisot and Chrzavzez, 2010). Paleoecological methods focus identifying anthropogenic contributions to fire regimes through micro-charcoal (>150 μm) samples derived from lacustrine cores and include counting the abundance of charcoal particles, classifying particles into size classes, and identifying charcoal particle morphologies (Enache and Cumming, 2006). Both methodological approaches rely on quantifying the abundance of charcoal fragments and recording some information about their metrics with the purpose of reconstruction human fire use in the past.

Current methods for quantifying charcoal counts and other metrics involve pre-treatments and extraction of charcoal particles, followed by time consuming visual counts and measures using microscopy. In the early 1990's, computerized image analysis was developed to increase the replicability and speed of traditional charcoal analysis (MacDonald et al., 1991). Although methods varied within research design and overall objectives, most early attempts at automated analysis involved high-cost microscope mounted cameras, proprietary imaging software, and multiple calibration trials to accurately isolate and quantify micro-charcoal fragments mounted on slides from lacustrine pollen cores. Current methods utilize greater computing power, higher

resolution digital images, and a wider array of image analysis software, but still rely on essentially the same series of methodological steps that were developed during the previous 25 years (Whitlock and Larsen, 2001:9). Most of the applications of automated charcoal analysis are still limited to paleoecological analysis of micro-charcoal and have not been applied to other depositional contexts, such as sedimentary charcoal or archaeological contexts.

This appendix describes the Charcoal Particle Measure Tool (CharTool), a customizable charcoal quantification tool designed for use as a macro plugin for ImageJ. CharTool overcomes many of the limitations of current image analysis techniques in charcoal analysis by offering advances in image capture, thresholding, calibration. Additionally, ImageJ is a free, java-based software program for image analysis available for download from the National Institutes of Health (Schneider et al. 2012), making CharTool an economical solution to quantifying charcoal. The following section describes the functions and operation of CharTool.

CharTool Design and Operation

CharTool is designed to operate as a plugin for ImageJ but can be customized by the user using ImageJ's macro language (see ImageJ developer information at https://imagej.nih.gov). CharTool uses the capability of ImageJ to interface with webcams and other USB-connected video sources to create a live video-microscope feed through which charcoal fragments can be identified and quantified. This approach offers many advantages over other image analysis techniques in that it allows for the contents of

the image to be adjusted and maneuvered in real time, giving the analyst more flexibility in isolating and analyzing charcoal. CharTool also relies on gray scale (0-255) color value thresholding to isolate charcoal fragments for quantification, with 0 representing black and 255 representing white. Many previous applications of charcoal image analysis use a fixed threshold value, which forms a binary classification of what is charcoal and what is not charcoal based on how dark the pixels in the digital image are (see Beaufort et al., 2003; Crawford and Belcher, 2014; Earle et al., 1996; Horn et al., 1992; MacDonald et al., 1991; Springer et al., 2012; Thevenon et al., 2003; Thevenon and Anselmetti, 2008; Umbanhowar and McGrath, 1998 for examples). Greyscale values are substantially influenced by lighting conditions and the difference between charcoal and the underlying sediment or other organic material also can change due to local conditions. Fixed thresholds can cause high rates of misidentification or make it impossible to extract charcoal from underlying material. CharTool addresses these issues by using an on-the-fly thresholding procedure that is adjustable for each charcoal particle and allows the user to select the best threshold for the conditions present.

The following section outlines the workflow for CharTool, as well as user adjustable features. CharTool is currently written for ImageJ version 1.50c4 but is both forward and backward compatible. In its current state, the plugin can be used with both Windows and Mac operating systems and is currently untested on Linux operating systems.

1. Open ImageJ and the CharTool start window will appear. The user may initiate a live video feed from the connected video microscope or exit CharTool and use ImageJ normally.

2. The ImageJ webcam interface will then appear. Select the digital microscope from the dropdown menu and select ok.
3. CharTool will then prompt a window for the user to install the remainder of the macros needed to run CharTool. The user may also at this point set the calibration measurements to quantify charcoal during the current session. This is an optional step an only needs to be performed once if the magnification settings are not going to change between sessions.
4. If measurements need to be set, select this option and click ok. CharTool will prompt the user to draw a line of a known length on the current video feed. Once the line is draw, click ok, then enter in the known length of the line and the units. Click ok. CharTool is now calibrated.
5. A final dialogue window will outline the keyboard shortcuts used in CharTool for selecting charcoal fragments in the video feed. They are as follows:
    a. [C] Selects the magic wand tool, which will use gray scale color values between 0 and 255 to isolate dark charcoal fragments.
    b. [X] Selects the freehand selection tool. This tool can be used to trace charcoal particles that cannot be isolated using the magic wand tool due to lighting conditions or other factors obscuring the fragment.
    c. [Z] Activates the measure tool, which first displays a threshold tolerance slider that can be used to make on-the-fly corrections to the threshold value selected by the magic wand tool. After pressing [OK], the measure tool then records 20 individual metrics on each fragment. See Table 17 for descriptions of the metrics collected by CharTool.

d. [D] Deletes the last measurement made.

6. Once all of the charcoal fragments in a sample have been quantified, the user closes the window containing a record of all the measurements. This will prompt a dialogue window asking the user to save the measurements. The measurements can be saved as a comma separated values file (.csv) or a Microsoft Excel file (.xlsx).

The CharTool macro script is available for download from the following DOI:

Snitker, Grant, 2018. *Charcoal Particle Measure Tool macro for ImageJ (CharTool): Version 2.0.* Retrievable from: DOI: http://doi.org/10.5281/zenodo.143447

Table 17: Metrics Collected by CharTool for Each Charcoal Fragment.

Metric	Description (adapted from ImageJ user manual)
Area	Area of selected pixels in calibrated units
Min	Minimum gray scale value
Max	Maximum gray scale value
Perimeter	Length of outside boundary of selected pixels in calibrated units
BX	X-coordinate of upper left corner of the smallest rectangle enclosing the selected pixels
BY	Y-coordinate of upper left corner of the smallest rectangle enclosing the selected pixels
Width	Width of smallest rectangle enclosing the selected pixels
Height	Height of smallest rectangle enclosing the selected pixels
Major	Length of the primary axis of the best fitting ellipse enclosing the selected pixels
Minor	Length of the secondary axis of the best fitting ellipse enclosing the selected pixels
Angle	Angle (0-180 degrees) of the primary axis of the best fitting ellipse enclosing the selected pixels
Circularity	Calculated as 4π*area/perimeter^2 ; A value of 1.0 indicates the selected pixels are a perfect circle; As values approach 0.0, the selected pixels are increasingly elongated
Feret	Feret's diameter of the selected pixels, which is the longest distance between any two points along the selection boundary
FeretX	Starting X-coordinate of the selected pixels Feret's diameter
FeretY	Starting Y-coordinate of the selected pixels Feret's diameter

Table 17: Continued.

FeretAngle	Angle (0-180 degrees) of the Feret's diameter of the selected pixels to a line parallel to the x-axis of the image
MinFeret	Minimum caliper diameter of the selected pixels
Aspect Ratio	Aspect ratio of selected pixels; calculated as the major (primary) axis / minor (secondary) axis of the best fitting ellipse
Round	Roundness of selected pixels; calculated as 4*area/(π*major (primary) axis^2)
Solidity	Solidity of selected pixels; calculated as area/convex area

References

Beaufort, L., De Garidel-Thoron, T., Linsley, B., Oppo, D., Buchet, N., 2003. Biomass burning and oceanic primary production estimates in the Sulu Sea area over the last 380 kyr and the East Asian monsoon dynamics, in: Marine Geology. pp. 53–65. https://doi.org/10.1016/S0025-3227(03)00208-1

Crawford, A.J., Belcher, C.M., 2014. Charcoal Morphometry for Paleoecological Analysis: The Effects of Fuel Type and Transportation on Morphological Parameters. Appl. Plant Sci. 2, 1400004. https://doi.org/10.3732/apps.1400004

Earle, C.J., Brubaker, L.B., Anderson, P.M., 1996. Charcoal in northcentral Alaskan lake sediments: relationships to fire and late-Quaternary vegetation history. Rev. Palaeobot. Palynol. 92, 83–95. https://doi.org/10.1016/0034-6667(95)00095-X

Enache, M.D., Cumming, B.F., 2006. Tracking recorded fires using charcoal morphology from the sedimentary sequence of Prosser Lake, British Columbia (Canada). Quat. Res. 65, 282–292. https://doi.org/10.1016/j.yqres.2005.09.003

Horn, S.P., Horn, R.D., Byrne, R., 1992. An automated charcoal scanner for paleoecological studies. Palynology 16, 7–12. https://doi.org/10.1080/01916122.1992.9989403

MacDonald, G., Larsen, C., 1991. The Reconstruction of Boreal Forest Fire History From Lake Sediments: A Comparison Of Charcoal, Pollen, Sedimentological, And Geochemical Indices. Quat. Sci. 10, 53–71.

Schneider, C.A., Rasband, W.S., Eliceiri, K.W., 2012. NIH Image to ImageJ: 25 years of image analysis. Nat. Methods 9, 671–675. https://doi.org/10.1038/nmeth.2089

Springer, G.S., Nivanthi Mihindukulasooriya, L., Matthew White, D., Rowe, H.D., 2012. Micro-charcoal abundances in stream sediments from buckeye Creek Cave, West Virginia, USA. J. Cave Karst Stud. 74, 58–64. https://doi.org/10.4311/2010AN0148R1

Théry-Parisot, I., Chabal, L., Chrzavzez, J., 2010. Anthracology and taphonomy, from wood gathering to charcoal analysis. A review of the taphonomic processes modifying charcoal assemblages, in archaeological contexts. Palaeogeogr. Palaeoclimatol. Palaeoecol. 291, 142–153. https://doi.org/10.1016/j.palaeo.2009.09.016

Thevenon, F., Anselmetti, F.S., 2007. Charcoal and fly-ash particles from Lake Lucerne sediments (Central Switzerland) characterized by image analysis: anthropologic, stratigraphic and environmental implications. Quat. Sci. Rev. 26, 2631–2643. https://doi.org/10.1016/j.quascirev.2007.05.007

Thevenon, F., Williamson, D., Vincens, A., Taieb, M., Merdaci, O., Decobert, M., Buchet, G., 2003. A late-Holocene charcoal record from Lake Masoko, SW Tanzania: climatic and anthropologic implications. The Holocene 13, 785–792. https://doi.org/10.1191/0959683603hl665rr

Umbanhowar Jr., C.E., McGrath, M.J., 1998. Experimental production and analysis of microscopic charcoal from wood, leaves and grasses. The Holocene 8, 341–346. https://doi.org/10.1191/095968398666496051

Whitlock, C., Larsen, C., 2001. Charcoal as a fire proxy, in: Smol, J.P., Birks, H.J.B., Last, W.M., Bradley, R.S., Alverson, K. (Eds.), Tracking Environmental Change Using Lake Sediments: Vol 3 Terrestrial, Algal, and Siliceous Indicators. Springer Netherlands, pp. 75–97. https://doi.org/10.1007/0-306-47668-1_5

APPENDIX III

K-NEAREST NEIGHBORS SUPERVISED CLASSIFICATION METHODS FOR ASSIGNING CHARCAL MORPHOLOGIES

Introduction

As discussed in Chapter IV, charcoal morphologies provide a reliable estimation of the intensity and types of fuels burned during a fire. The broad applicability of charcoal morphotype classifications are currently limited due to current method's reliance on expert opinion in classifying charcoal fragments, a focus on fuels from temperate North American ecosystems, and no consideration of taphonomic processes that may influence charcoal fragment morphology. The following sections provide details on a new methodological contribution to charcoal morphotype analysis that accommodates for these limitations. The procedure outline below is tailored to the interpretive challenges encountered in examining sedimentary charcoal from alluvial contexts in Mediterranean ecosystems in eastern Spain but can be adapted to meet the needs of any ecosystem or depositional context.

Experimental charcoal and mechanical weathering

To create an experimental charcoal assemblage against which to compare empirical charcoal data, a selection of woody and fine fuels was collected from the Canal de Navarrés study area during the 2016 and 2017 field seasons. The species collected are known to have been abundant vegetation types in all three study areas during the early and middle Holocene from regional pollen and anthracological sequences (Badal 2009; Carrión and Van Geel 1999; Dupré 1995). Table 18 indicates the species collected, but briefly woody fuels include pine, oak, wild pistachio, and juniper. Finer fuels include

Table 18: Species Used to Create Experimental Charcoal Assemblage.

Fuel Classification	Species	Morphotype
Woody Fuels	Pinus halepensis (wood/branches)	Geometric
	Juniperus oxycedrus (wood/branches)	Geometric
	Quercus coccifera (wood/branches)	Geometric
	Pistacia lentiscus (wood/branches)	Geometric
	Quercus ilex (wood/branches)	Geometric
Fine Fuels	Pinus halepensis (needles)	Elongated/Irregular
	Juniperus oxycedrus (leaves/needles)	Elongated/Irregular
	Quercus coccifera (leaves)	Irregular
	Pistacia lentiscus (leaves)	Irregular
	Quercus ilex (leaves)	Irregular
	Rosmarinus sp. (leaves/branches)	Irregular
	Erica arborea (leaves)	Irregular
	Cistus albidas (leaves/branches)	Elongated/Irregular
	Brachypodium retusum (stalk/leaves)	Elongated

leaves and needles form those species, as well as rosemary, rock rose, and tree heath (taxonomic names are listed here). This is not an exhaustive collection of fuels from this area but provides a selection of key species represent several vegetation communities.

All fuel samples were combusted to produce charcoal fragments. Combustion temperatures and duration varied with the ultimate goal to fully combust each fuel sample and achieve a carbonized state. Adapting Crawford and Belcher 2014 methodology, all charcoal fragments were then mechanically weathered in a beaker filled with 50ml of silicate gravel and water enough to cover the samples. The gravel and charcoal were stirred for two hours with a magnetic stir bar to simulated alluvial transport.

Training sets, building KNN classifier models, and classifier performance

After mechanical weathering, charcoal particles from each fuel type were measured using CharTool. A total of 100 charcoal fragments from each fuel type were measured to capture adequate variability, resulting in 1,400 measurements of known fuels. All measurements were then combined into a single dataset of known fuels. From this dataset, a random selection of 80% of the observations (n = 1120) were selected as a training set on which a K-nearest neighbor (KNN) algorithm was used to create classification models for geometric, irregular, and elongated charcoal morphotypes. The performance of the models will then be evaluated by classifying a testing dataset, which is composed of the remaining 20% of the observations (n = 280).

KNN is a supervised learning algorithm, meaning it is given a training set of labeled data and which it then uses to predict the classification of new, unknown data. This is done first assessing the relationship between all training labeled data through a distance measure. All new data is then classified by a majority vote of its neighbors, with the object being assigned to the class most common among its *k* nearest neighbors. KNN is non-parametric, meaning it no assumptions about the underlying data distribution, and is a lazy learning algorithm, meaning it relies mostly on the training datasets to make its classification predictions for new, unknown data. Because of its simplicity and flexibility, KNN has a range of applications from supervised classification in remote sensing to machine-learning such as recommendation services. It also performs well when visual clusters of similar data are not present, making it more advantageous for differentiated between groups than cluster analysis or other distance-based measures.

In initial trials using the KNN classifier to classify the testing dataset, morphotype categories were correct assigned at a low accuracy rate (approximately 50%). The solution for increasing the accuracy of the classifier models was to incorporate a staged classification strategy, which first classifies all of the charcoal fragments into two categories, geometric morphotypes and not geometric morphotypes. The algorithm then classifies the charcoal fragments that are not geometric in to irregular or elongated morphotypes.

The resulting KNN classifier performance was greatly improved. The performance of the classifier was evaluated using three measures. Sensitivity is the ability of the model to correctly identify the given morphotype (true positive rate), whereas specificity is the ability of the model to correctly identify all other charcoal fragments that are not the given morphotype (true negative rate). The most important performance measure here is balanced accuracy, which is the proportion of true results (both true positives and true negatives) among the total number of cases examined. Table 19 illustrates the performance of the KNN classifier using these three measures. Overall, this method performs well with a balance accuracy for all three morphotypes at almost 80%.

Table 19: KNN Classifier Performance

Morphotype	Sensitivity	Specificity	Balanced Accuracy
Geometric	0.71	0.86	0.79
Irregular	0.72	0.79	0.76
Elongated	0.65	0.93	0.79

Applying K-NN models to empirical data

The KNN classification models generated from the known fuels were then used to predict morphotype membership for the empirical data collected from watersheds throughout the three study areas analyzed in this dissertation. The predicted output is the probability that a charcoal fragment belongs to the geometric, irregular, or elongated morphotype classification. If morphotype probability for a fragment does not exceed 0.50 for a single category, it is then classified as indeterminate. The scripts needed to run the KNN classification procedure are written for R version 3.3 ("Frisbee Sailor") and available for download from the following DOI:

Snitker, Grant, 2018. *KNN classification procedure for categorizing sedimentary charcoal fragments from alluvial contexts into morphotypes*. R Script version 2.0. Retrievable from: Github, DOI: http://doi.org/10.5281/zenodo.1434430

References

Badal Garcia, E., 1995. La vegetación carbonizada. Resultados antracológicos del País Valenciano, in: El Cuaternario Del País Valenciano. Asociación Española para el Estudio del Cuaternario, Valencia, pp. 217–226.

Carrión, J.S., Van Geel, B., 1999. Fine-resolution Upper Weichselian and Holocene palynological record from Navarres (Valencia, Spain) and a discussion about factors of Mediterranean forest succession. Rev. Palaeobot. Palynol. 106, 209–236.

Carrión, J.S., Van Geel, B., 1999. Fine-resolution Upper Weichselian and Holocene palynological record from Navarres (Valencia, Spain) and a discussion about factors of Mediterranean forest succession. Rev. Palaeobot. Palynol. 106, 209–236.

Dupré, M., 1995. Cambios paleoambientales en el territoria Valenciano. La Palinología., in: El Cuaternario Del País Valenciano. Asociación Española para el Estudio del Cuaternario, pp. 205–216.

APPENDIX IV

CHARSOURCE: A COMPUTATIONAL MODEL OF CHARCOAL SOURCE AREA TRHOUGH PRIMARY DEPOSITION AND AERIAL DISPERSION

CharSource model design and description

CharSource is a mathematical and GIS-based model of charcoal deposition and dispersion processes that is used to model charcoal source areas for charcoal fragments sampled at a given location and can be used to estimate the spatial distribution of fires within the landscape that burned to create a given charcoal record. This model relies on the previously published models of charcoal dispersion and source areas, but also incorporates the contribution of secondary charcoal accumulation due to slope-wash into estimating final charcoals source areas (see Clark 1988; Higuera et al. 2007; Peters et al. 2007; and Snitker 2018 for examples of models of charcoal dispersion and Gaussian model). The model uses elevation, slope, prevailing winds, and charcoal fragment size to estimate how charcoal is transported following a fire and uses these conditions to identify where fires likely occurred. The model outputs a spatially explicit raster surface of fire locations within a series of confidence intervals.

Column samples collected at the bottom reaches of watersheds represent cumulative fire activity upstream. CharSource is used to calculate the potential source area for charcoal in each pixel within the watershed, the results of which are then aggregated to create a total charcoal source area for the entire watershed. The CharSource workflow is illustrated in Fig. 52 and is outlined below:

1. The CharSource model begins by creating all of the inputs needed to calculate the charcoal source area using a Gaussian model as demonstrated by Peters and

Higuera 2006. Needed inputs are divided into two categories: 1) constants related to gravity, turbulence, near ground, and other atmospheric parameters that are not adjusted, 2) user-configurable parameters and the derivatives thereof which are calculated from the specific landscape or conditions within a given study area.

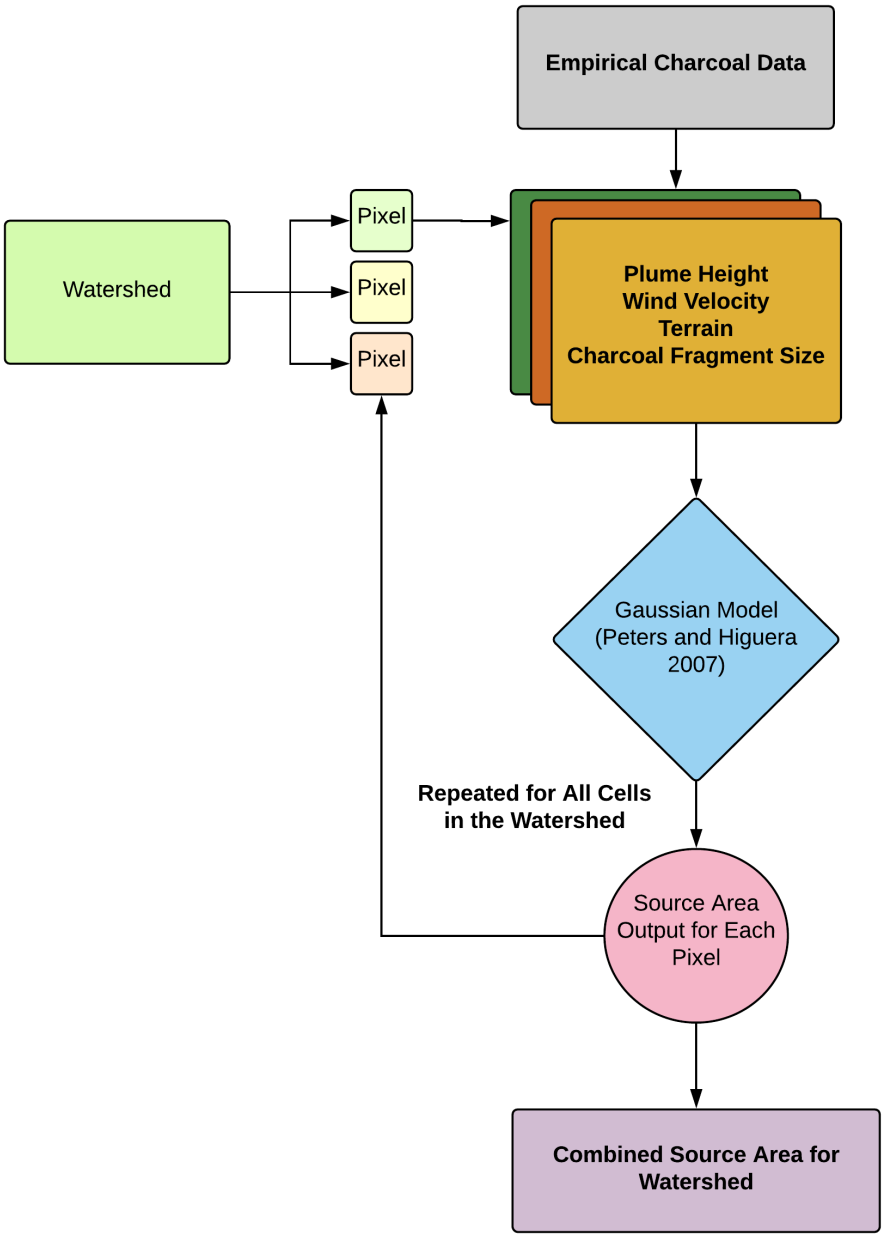

Fig. 52: Diagrammatic Representation of CharSource Modules and Data Inputs.

2. Constants and non-adjustable used by CharSource are located in Table 20. See Peters and Higuera 2006, Sutton 1947, and Chamberlin 1953 for information regarding these values.

Table 20: Constants and Non-adjustable Parameters in CharSource.

Parameter	Description
v_g	Deposition velocity (m s^{-1})
Q_0	Source strength (m^2 × 100)
u	Mean wind speed (see Sutton, 1947) (m s^{-1})
C_y, C_z	Diffusion constants (C_y = 0.21, C_z = 0.12; see Sutton, 1947) ($m^{1/8}$)
n	Measure of turbulence near ground (1/4; see Sutton, 1947) (dimensionless)
m	n/(4 - 2n) (dimensionless)
ξ	$h^2/(x^{2-n})$ (dimensionless)
(Γ (-m+1) - Γ_ξ (-m+1))	= -m t^{-m-1} dt (dimensionless)

3. The specific, user-configurable parameters needed to run CharSource are located in Table 21. These values include the plume height, regional average wind velocity and watershed attributes.

   A single plume height is used to approximate the size of a smoke plume generated form the combustion of fuels within a given landscape. Although, the diversity and arrangement of fuels within a landscape can influence combustion conditions such as convective uplift, plume heights for the study areas used in this

dissertation are illustrated in Table 22. Plume heights are estimated from previously published heat release rates (HRR) for fuel models (Anderson 1982) adapted to Mediterranean ecosystems.

Table 21: User-configurable Parameters in CharSource.

Parameter	Description
Starting plume height	100 m
Wind velocity	5.49 m/s
Charcoal fragment size	Depends on observed charcoal fragments; µm
Terrain	Digital elevation model (DEM) 30m resolution
Watershed	Watershed bounds for each column sample (ESRI Shapefile)

Table 22: Fuels, Ecosystem Types, and Resulting Plume Heights Used in This Dissertation.

Fuel Size	Ecosystem Type	Fuel Model (Anderson 1982)	Species represented	Height of Plume (m)
1-hour fuels				
	Grassland	1	*Brachypodium retusum*	134.0
	Mediterranean shrubs	4	*Ulex parviflorus, Cistus albidus, Rosmarinus officinalis, Quercus sp*	558.4
	Mediterranean pines	6	*Pinus sp., Quercus sp., Ulex parviflorus, Cistus albidus, Rosmarinus officinalis*	108.6
10-hour fuels				
	Grassland	1	*Brachypodium retusum*	134.0
	Mediterranean shrubs	4	*Ulex parviflorus, Cistus albidus, Rosmarinus officinalis, Quercus sp*	794.6
	Mediterranean pines	6	*Pinus sp., Quercus sp., Ulex parviflorus, Cistus albidus, Rosmarinus officinalis*	226.7

Regional average wind velocity is summarized from modern weather station data (IVIA 2015). These data are summarized from the last ten years of monthly average wind velocity data collected in each study region. Due to the somewhat

dispersed nature of meteorological weather stations in eastern Spain, the closest station and most topographically representative weather station was selected for each study area.

Finally, upstream watersheds for each column sample were calculated using GRASS GIS, a free and open-source GIS software suite. Drainage direction values are first calculated for each cell of a digital elevation model (DEM) within each study area using the GRASS module r.watershed. Using these values and the geographic location of each column sample, the spatial extent of the upstream watershed is calculated using the GRASS module r.water.outlet. The resulting raster watershed is converted into an ESRI shapefile format for later calculations. This workflow, plus the selection of an appropriate plume height and the regional average wind velocity, should be generated prior to running CharSource.

4. Once all of the needed constants and variable values have been assembled, CharSource begins by using the watershed shapefile to extract all of the cells within the study area DEM which are contained within it. The model then selects a single cell on which to perform all calculations, before moving on to the next cell, until all the cells within the watershed have been selected.

5. The first procedure performed on each cell is the calculation of an effective plume height, which accommodates for the influence of elevation on the dispersion of charcoal throughout the landscape. During this step, elevation of the selected cell is subtracted from all other cells within the landscape. This creates an adjustment value that accounts for differences in elevation between cells, so, for instance, a

cell is higher in elevation than the height of the plume will not receive charcoal deposition.

6. Second, CharSource imports and reads the empirical charcoal measurements collected from every sample within the column that is being analyzed. CharSource utilizes the parameters and plume adjustment values created in the previous steps to calculate a source area for each individual charcoal fragment from each sample within the column for each cell within the watershed. Each charcoal fragment's diameter, as quantified by CharTool (see Appendix II for details), provides the particle diameter variable needed to apply a Gaussian model to predict the locations within the surrounding landscape that would contribute that same size of charcoal fragment to the cell within the watershed that is being analyzed. The output is binary raster map of cells that would contribute charcoal (coded as 1) and those that would not (coded as 0).

7. The Gaussian model is applied to each cell within the watershed and with each individual fragment of charcoal collected from the column sample. The resulting maps are then aggregated to create a composite, total source area for the watershed. Since the material collected at the bottom of the watershed represent cumulative fire activities upstream, the exact origin of any particular charcoal fragment cannot be known. For this reason, modeling each charcoal fragment as though it could have originated at any point in the watershed is necessary to capture the full range of possible origin locations.

8. CharSource is run in R version 3.3 ("Frisbee Sailor") and the script is available for download from the following DOI:

Snitker, Grant, 2017. *GIS charcoal source area model for archaeological applications (CharSource)*. R Script version 2.0. Retrievable from: Github, DOI: http://doi.org/10.5281/zenodo.1434430

References

Anderson, H.E., 1982. Aids to Determining Fuel Models For Estimating Fire Behavior. Ogden, UT.

Chamberlain, A.C., 1953. Aspects of Travel and Deposition of Aerosol and Vapor Clouds. UK Atomic Energy Research Establishment Report, AERE-HP/R 1261, Harwell, Berkshire, UK.

Clark, J.S., 1988. Particle motion and the theory of charcoal analysis: Source area, transport, deposition, and sampling. Quat. Res. 30, 67–80. https://doi.org/10.1016/0033-5894(88)90088-9

Higuera, P.E., Peters, M.E., Brubaker, L.B., Gavin, D.G., 2007. Understanding the origin and analysis of sediment-charcoal records with a simulation model. Quat. Sci. Rev. 26, 1790–1809. https://doi.org/10.1016/j.quascirev.2007.03.010

Peters, M.E., Higuera, P.E., 2007. Quantifying the source area of macroscopic charcoal with a particle dispersal model. Quat. Res. 67, 304–310. https://doi.org/10.1016/j.yqres.2006.10.004

Snitker, G., 2018. Identifying natural and anthropogenic drivers of prehistoric fire regimes through simulated charcoal records Identifying natural and anthropogenic drivers of prehistoric fi re regimes through simulated charcoal records. J. Archaeol. Sci. 95, 1–15. https://doi.org/10.1016/j.jas.2018.04.009

Sutton, O., 1947. The Problem of Diffusion in the Lower Atmosphere. Q. J. R. Meteorol. Soc. 73, 257–281.

APPENDIX V

DATA AVAILABILITY AND SUMMARIZED CHARCOAL DATA

Data Availability

Charcoal data collected from watersheds in the Canal de Navarrés, Vall del Serpís, and Hoya de Buñol study areas, and which are used in this dissertation, are summarized below. Complete observations, charcoal morphology, charcoal source area size, and other data are curated through Arizona State University and Digital Antiquity's the Digital Archeological Record (tDAR) and can be located at the following DOI:

http://doi.org/10.6067/XCV8448329

Additionally, charcoal frequencies and total fragment areas are available for download through the Global Charcoal Database (www.paleofire.org/) via the following permanent link:

https://www.paleofire.org/index.php?p=CDA/site_view&site_id=1173

Table 23: Summarized Charcoal Data for the Canal de Navarrés Study Area.

Column	Sample	Period	Age BP	CMBS	Freq.	Skewness	Morphotype Percentages				Source Area	Local	Regional
							Geo.	Irr.	Elo.	Ind.	Ratio	Land-use	Land-use
SP.NV.2	01	BZ	3699	195 - 200	82	1.97	0.24	0.63	0.00	0.12	58.24	0.05	35.50
SP.NV.2	02	BZ	3550.5	190 - 195	59	1.29	0.37	0.47	0.02	0.14	56.69	0.10	35.50
SP.NV.2	03	BZ	3400.5	185 - 190	64	2.47	0.34	0.50	0.00	0.16	60.15	0.08	35.50
SP.NV.2	04	BZ	3265	180 - 185	15	1.36	0.07	0.60	0.00	0.33	61.38	0.00	35.50
SP.NV.2	05	BZ	3171	175 - 180	40	1.20	0.28	0.60	0.00	0.13	70.09	0.73	35.50
SP.NV.2	06	BZ	3076.5	170 - 175	5	0.06	0.00	1.00	0.00	0.00	58.97	0.00	35.50
SP.NV.2	07	BZ	2985.5	165 - 170	31	3.20	0.03	0.65	0.00	0.32	58.55	0.00	35.50
SP.NV.2	08	BZ	2902	160 - 165	86	1.38	0.07	0.70	0.00	0.23	60.82	0.00	35.50
SP.NV.2	09	BZ	2814.5	155 - 160	80	2.52	0.15	0.76	0.00	0.09	62.33	0.14	35.50
SP.NV.2	10	IB	2728	150 - 155	22	3.21	0.05	0.82	0.00	0.14	58.77	1.21	40.83
SP.NV.2	11	IB	2637.5	145 - 150	15	0.90	0.13	0.80	0.00	0.07	58.85	1.44	40.83
SP.NV.2	12	IB	2555.5	140 - 145	44	2.59	0.18	0.59	0.00	0.23	59.18	1.33	40.83
SP.NV.2	13	IB	2483	135 - 140	47	3.33	0.26	0.55	0.02	0.17	59.85	1.45	40.83
SP.NV.2	14	IB	2398	130 - 135	39	2.05	0.28	0.54	0.00	0.18	59.63	1.28	40.83
SP.NV.2	15	IB	2306.5	120 - 130	64	1.54	0.55	0.34	0.02	0.09	64.54	1.82	40.83
SP.NV.5	01	EN	7394	145 - 150	73	1.63	0.08	0.62	0.01	0.29	22.20	1.33	26.06
SP.NV.5	02	EN	7211.5	140 - 145	87	2.63	0.14	0.63	0.01	0.22	21.41	1.27	26.06
SP.NV.5	03	EN	6979	135 - 140	78	2.59	0.05	0.71	0.01	0.23	26.03	1.79	26.06
SP.NV.5	04	MN	6673.5	130 - 135	105	3.72	0.31	0.54	0.00	0.14	26.49	1.82	22.01
SP.NV.5	05	MN	6405.5	125 - 130	127	2.57	0.24	0.57	0.00	0.20	29.28	2.10	22.01
SP.NV.5	06	MN	6128	120 - 125	75	1.57	0.56	0.27	0.01	0.16	22.57	1.40	22.01
SP.NV.5	07	LN	5860	115 - 120	98	1.31	0.15	0.66	0.01	0.17	27.53	1.96	14.01
SP.NV.5	08	LN	5585.5	110 - 115	414	3.12	0.09	0.71	0.01	0.20	26.49	1.86	14.01
SP.NV.5	09	LN	5297	105 - 110	316	2.68	0.24	0.53	0.01	0.22	22.15	1.30	14.01
SP.NV.5	10	LN	5024.5	100 - 105	153	1.92	0.05	0.75	0.01	0.20	28.92	2.12	14.01
SP.NV.5	11	LN	4744	90 - 100	75	1.22	0.20	0.48	0.00	0.32	22.90	1.39	14.01
SP.NV.5	12	BB	4227.5	80 - 90	101	2.18	0.09	0.65	0.01	0.25	28.49	3.50	42.34
SP.NV.5	13	BZ	3742.5	70 - 80	147	2.33	0.12	0.65	0.01	0.22	33.61	1.03	35.50
SP.NV.5	14	BZ	3287	60 - 70	99	1.41	0.13	0.69	0.01	0.17	28.87	0.77	35.50
SP.NV.5	15	BZ	2821.5	50 - 60	78	1.49	0.15	0.62	0.00	0.23	29.08	0.82	35.50
SP.NV.5	16	IB	2362.5	40 - 50	51	1.40	0.18	0.57	0.00	0.25	34.34	1.96	40.83
SP.NV.7	01	LM	8366	230 - 235	48	3.11	0.35	0.52	0.00	0.13	12.63	1.54	5.88
SP.NV.7	02	LM	8108	225 - 230	33	1.92	0.33	0.58	0.00	0.09	17.02	1.90	5.88

Table 23: Continued

Column	Sample	Period	Age BP	CMBS	Freq.	Skewness	Morphotype Percentages				Source Area	Local	Regional
							Geo.	Irr.	Elo.	Ind.	Ratio	Land-use	Land-use
SP.NV.7	03	LM	7863	220 - 225	51	2.32	0.24	0.71	0.00	0.06	18.21	2.00	5.88
SP.NV.7	04	LM	7625	215 - 220	46	4.74	0.15	0.63	0.00	0.22	23.39	2.43	5.88
SP.NV.7	05	EN	7392	210 - 215	83	5.37	0.24	0.57	0.00	0.19	16.60	9.58	26.06
SP.NV.7	06	EN	7154.5	205 - 210	47	1.33	0.21	0.49	0.00	0.30	17.94	10.09	26.06
SP.NV.7	07	EN	6917	200 - 205	61	4.41	0.21	0.46	0.00	0.33	15.70	8.96	26.06
SP.NV.7	08	MN	6689.5	195 - 200	64	1.54	0.27	0.47	0.00	0.27	17.72	7.63	22.01
SP.NV.7	09	MN	6454	190 - 195	34	0.69	0.24	0.44	0.03	0.29	11.93	5.93	22.01
SP.NV.7	10	MN	6232	185 - 190	45	0.89	0.38	0.53	0.00	0.09	19.75	8.14	22.01
SP.NV.7	11	LN	5991	180 - 185	39	1.66	0.10	0.67	0.03	0.21	14.94	4.50	14.01
SP.NV.7	12	LN	5750.5	175 - 180	77	2.57	0.31	0.55	0.00	0.14	18.46	5.46	14.01
SP.NV.7	13	LN	5513.5	170 - 175	44	4.32	0.23	0.50	0.00	0.27	14.55	4.40	14.01
SP.NV.7	14	LN	5285.5	165 - 170	102	6.68	0.34	0.47	0.00	0.19	18.92	5.49	14.01
SP.NV.7	15	LN	5048.5	160 - 165	93	2.97	0.57	0.35	0.00	0.08	13.63	4.35	14.01
SP.NV.7	16	LN	4867	155 - 160	73	1.30	0.45	0.38	0.01	0.15	17.89	5.23	14.01
SP.NV.7	17	LN	4684	150 - 155	63	1.71	0.08	0.70	0.02	0.21	18.19	5.37	14.01
SP.NV.7	18	LN	4514.5	140 - 150	69	1.40	0.23	0.48	0.00	0.29	18.88	5.41	14.01
SP.NV.7	19	BB	4166.5	130 - 140	41	5.65	0.39	0.39	0.02	0.20	20.32	10.88	42.34
SP.NV.7	20	BB	3813.5	120 - 130	30	1.07	0.17	0.37	0.00	0.47	17.49	10.24	42.34
SP.NV.7	21	BZ	3482	110 - 120	16	1.41	0.63	0.31	0.00	0.06	15.14	0.88	35.50
SP.NV.7	22	BZ	3116.5	100 - 110	20	0.81	0.45	0.15	0.00	0.40	22.20	1.40	35.50
SP.NV.7	23	IB	2793	90 - 100	13	0.46	0.62	0.15	0.00	0.23	11.86	3.21	40.83
SP.NV.11	01	LM	7746.5	325 - 330	14	1.39	0.36	0.36	0.00	0.29	9.70	0.04	5.88
SP.NV.11	02	LM	7633.5	320 - 325	13	0.45	0.46	0.38	0.00	0.15	13.02	0.13	5.88
SP.NV.11	03	EN	7510	315 - 320	15	0.79	0.13	0.67	0.07	0.13	10.19	0.12	26.06
SP.NV.11	04	EN	7302	310 - 315	37	2.41	0.24	0.43	0.03	0.30	9.89	0.21	26.06
SP.NV.11	05	EN	7104	305 - 310	15	1.46	0.27	0.53	0.00	0.20	14.00	0.58	26.06
SP.NV.11	06	EN	6911	300 - 305	8	0.09	0.25	0.25	0.00	0.50	17.80	1.29	26.06
SP.NV.11	07	MN	6723	295 - 300	24	1.00	0.33	0.33	0.00	0.33	10.00	0.14	22.01
SP.NV.11	08	MN	6545	290 - 295	15	1.44	0.13	0.53	0.07	0.27	11.92	0.34	22.01
SP.NV.11	09	MN	6358	285 - 290	25	1.18	0.12	0.76	0.00	0.12	13.45	0.41	22.01
SP.NV.11	10	MN	6162.5	280 - 285	15	1.01	0.13	0.53	0.00	0.33	11.13	0.26	22.01
SP.NV.11	11	LN	5974.5	275 - 280	13	0.02	0.54	0.46	0.00	0.00	14.18	0.77	14.01
SP.NV.11	12	LN	5790	270 - 275	13	2.36	0.00	0.92	0.08	0.00	17.45	1.03	14.01

Table 23: Continued

Column	Sample	Period	Age BP	CMBS	Freq.	Skewness	Morphotype Percentages				Source Area Ratio	Local Land-use	Regional Land-use
							Geo.	Irr.	Elo.	Ind.			
SP.NV.11	13	LN	5605	265 - 270	9	0.55	0.33	0.56	0.00	0.11	8.38	0.00	14.01
SP.NV.11	14	LN	5416.5	260 - 265	10	-0.55	0.40	0.50	0.00	0.10	13.46	0.75	14.01
SP.NV.11	15	LN	5231.5	255 - 260	18	0.43	0.33	0.28	0.06	0.33	9.84	0.25	14.01
SP.NV.11	16	LN	5042.5	250 - 255	10	1.07	0.00	0.40	0.00	0.60	12.51	0.44	14.01
SP.NV.11	17	LN	4847.5	245 - 250	7	1.29	0.43	0.00	0.00	0.57	8.36	0.00	14.01
SP.NV.11	18	LN	4658	240 - 245	15	0.45	0.20	0.60	0.00	0.20	11.86	0.46	14.01
SP.NV.11	19	BB	4469	235 - 240	71	2.35	0.20	0.56	0.00	0.24	10.76	1.59	42.34
SP.NV.11	20	BB	4318.5	230 - 235	34	0.48	0.29	0.50	0.03	0.18	10.57	1.63	42.34
SP.NV.11	21	BB	4196.5	225 - 230	27	1.11	0.30	0.30	0.00	0.41	10.12	1.51	42.34
SP.NV.11	22	BB	4071	220 - 225	32	1.21	0.22	0.47	0.00	0.31	8.97	1.43	42.34
SP.NV.11	23	BB	3947.5	215 - 220	25	1.03	0.20	0.60	0.00	0.20	11.56	1.62	42.34
SP.NV.11	24	BB	3822.5	210 - 215	9	-0.31	0.33	0.44	0.00	0.22	8.33	1.43	42.34
SP.NV.11	25	BZ	3717.5	205 - 210	31	0.92	0.35	0.52	0.00	0.13	15.04	1.23	35.50

Table 24: Summarized Charcoal Data for the Hoya de Buñol Study Area.

Column	Sample	Period	Age BP	CMBS	Freq.	Skewness	Morphotype Percentages				Source Area Ratio	Local Land-use	Regional Land-use
							Geo.	Irr.	Elo.	Ind.			
SP.BN.1	01	None	NA	210 - 215	39	2.73	0.08	0.59	0.00	0.33	22.69	0.00	0.00
SP.BN.1	02	None	NA	205 - 210	18	0.84	0.00	0.83	0.00	0.17	23.93	0.00	0.00
SP.BN.1	03	None	NA	200 - 205	202	3.01	0.06	0.63	0.00	0.31	22.55	0.00	0.00
SP.BN.1	04	None	NA	195 - 200	100	2.36	0.09	0.65	0.01	0.25	23.14	0.00	0.00
SP.BN.1	05	None	NA	190 - 195	34	2.32	0.09	0.68	0.00	0.24	22.54	0.00	0.00
SP.BN.1	06	None	NA	185 - 190	29	1.94	0.24	0.55	0.00	0.21	22.97	0.00	0.00
SP.BN.1	07	None	NA	180 - 185	64	1.06	0.06	0.64	0.02	0.28	21.05	0.00	0.00
SP.BN.1	08	None	NA	175 - 180	74	4.75	0.03	0.66	0.04	0.27	20.77	0.00	0.00
SP.BN.1	09	None	NA	170 - 175	31	2.28	0.03	0.65	0.03	0.29	21.74	0.00	0.00
SP.BN.1	10	None	NA	165 - 170	40	3.15	0.08	0.68	0.00	0.25	22.19	0.00	0.00
SP.BN.1	11	None	NA	160 - 165	114	2.31	0.05	0.68	0.04	0.23	22.01	0.00	0.00
SP.BN.1	12	None	NA	155 - 160	47	2.36	0.00	0.64	0.00	0.36	19.85	0.00	0.00
SP.BN.1	13	None	NA	150 - 155	132	2.77	0.17	0.59	0.02	0.22	21.85	0.00	0.00
SP.BN.1	14	None	NA	145 - 150	52	2.09	0.04	0.58	0.04	0.35	20.33	0.00	0.00
SP.BN.1	15	None	NA	140 - 145	84	3.93	0.08	0.58	0.02	0.31	20.49	0.00	0.00
SP.BN.1	16	None	NA	135 - 140	133	1.84	0.02	0.59	0.07	0.32	19.74	0.00	0.00
SP.BN.1	17	None	NA	130 - 135	113	2.71	0.07	0.53	0.04	0.36	19.84	0.00	0.00
SP.BN.1	18	None	NA	125 - 130	191	3.02	0.02	0.57	0.01	0.40	20.22	0.00	0.00
SP.BN.1	19	None	NA	120 - 125	161	1.50	0.09	0.53	0.02	0.36	21.05	0.00	0.00
SP.BN.1	20	None	NA	110 - 120	137	3.89	0.06	0.69	0.01	0.24	20.79	0.00	0.00
SP.BN.1	21	None	NA	100 - 110	181	2.55	0.09	0.55	0.06	0.30	20.98	0.00	0.00
SP.BN.1	22	None	NA	90 - 100	51	2.43	0.06	0.59	0.06	0.29	20.56	0.00	0.00
SP.BN.1	23	None	NA	80 - 90	37	1.20	0.14	0.43	0.08	0.35	18.59	0.00	0.00

Table 24: Continued.

Column	Sample	Period	Age BP	CMBS	Freq.	Skewness	Morphotype Percentages				Source Area Ratio	Local Land-use	Regional Land-use
							Geo.	Irr.	Elo.	Ind.			
SP.BN.1	24	None	NA	70 - 80	120	2.68	0.20	0.60	0.02	0.18	21.92	0.00	0.00
SP.BN.1	25	None	NA	60 - 70	92	2.14	0.07	0.67	0.01	0.25	22.69	0.00	0.00
SP.BN.2	01	BZ	3196	225 - 230	8	1.47	0.13	0.50	0.13	0.25	10.61	1.50	0.38
SP.BN.2	02	BZ	3145.5	220 - 225	13	2.45	0.15	0.31	0.00	0.54	10.41	1.50	0.27
SP.BN.2	03	BZ	3093	215 - 220	16	0.37	0.13	0.88	0.00	0.00	10.35	1.50	0.19
SP.BN.2	04	BZ	3034.5	210 - 215	31	4.59	0.10	0.45	0.00	0.45	10.55	1.50	0.29
SP.BN.2	05	BZ	2976.5	205 - 210	103	1.34	0.17	0.66	0.01	0.17	10.35	1.50	0.22
SP.BN.2	06	BZ	2920.5	200 - 205	31	4.17	0.03	0.68	0.00	0.29	10.64	1.50	0.27
SP.BN.2	07	BZ	2861	195 - 200	19	1.31	0.05	0.74	0.00	0.21	10.58	1.50	0.29
SP.BN.2	08	BZ	2805	190 - 195	65	2.75	0.08	0.80	0.00	0.12	10.23	1.50	0.18
SP.BN.2	09	IB	2750.5	185 - 190	34	0.40	0.26	0.24	0.00	0.50	10.41	0.83	0.37
SP.BN.2	10	IB	2697.5	180 - 185	22	0.95	0.18	0.59	0.00	0.23	10.51	0.83	0.42
SP.BN.2	11	IB	2635.5	175 - 180	64	1.29	0.05	0.59	0.00	0.36	10.07	0.83	0.29
SP.BN.2	12	IB	2571.5	170 - 175	119	1.84	0.08	0.66	0.00	0.26	10.31	0.83	0.39
SP.BN.2	13	IB	2512	165 - 170	33	1.48	0.06	0.64	0.00	0.30	10.22	0.83	0.28
SP.BN.2	14	IB	2447	160 - 165	108	2.79	0.18	0.67	0.01	0.15	10.36	0.83	0.40
SP.BN.2	15	IB	2337	155 - 160	111	1.34	0.13	0.77	0.00	0.11	10.36	0.83	0.37

Table 25: Summarized Charcoal Data for the Vall del Serpís Study Area.

Column	Sample	Period	Age BP	CMBS	Freq.	Skewness	Morphotype Percentages				Source Area Ratio	Local Land-use	Regional Land-use
							Geo.	Irr.	Elo.	Ind.			
PB.RE	06	EN	7102.5	90 - 80	41	2.46	0.32	0.51	0.00	0.17	19.08	199.33	0.06
PB.RE	07	MN	6587	80 - 70	66	2.06	0.12	0.64	0.02	0.23	18.85	173.08	0.00
PB.RE	08	MN	6142.5	70 - 60	49	0.69	0.29	0.41	0.00	0.31	18.90	173.08	0.00
PB.RE	09	LN	5675.5	60 - 50	152	3.11	0.08	0.72	0.01	0.19	19.39	136.08	0.00
PB.RE	10	LN	4727.5	50 - 40	44	4.50	0.11	0.70	0.00	0.18	18.18	136.08	0.00
AC8.RE	01	None	NA	170 - 160	33	1.11	0.06	0.73	0.00	0.21	4.41	0.00	0.00
AC8.RE	02	None	NA	160 - 150	27	1.47	0.00	0.67	0.00	0.33	4.24	0.00	0.00
AC8.RE	03	None	NA	150 - 140	64	2.48	0.06	0.67	0.00	0.27	4.44	0.00	0.00
AC8.RE	04	None	NA	140 - 130	24	1.40	0.04	0.75	0.00	0.21	4.58	0.00	0.00
AC8.RE	05	None	NA	130 - 120	23	1.23	0.09	0.70	0.00	0.22	4.34	0.00	0.00
AC8.RE	06	None	NA	120 - 110	40	2.37	0.00	0.80	0.00	0.20	4.36	0.00	0.00
AC8.RE	07	None	NA	110 - 100	50	2.52	0.10	0.60	0.00	0.30	4.45	0.00	0.00
AC8.RE	08	None	NA	100 - 90	23	1.35	0.09	0.65	0.00	0.26	4.75	0.00	0.00
AC8.RE	09	None	NA	90 - 80	36	4.49	0.06	0.67	0.00	0.28	4.57	0.00	0.00
AC8.RE	10	None	NA	80 - 70	38	1.27	0.00	0.84	0.00	0.16	4.42	0.00	0.00
BF.RE	01	None	NA	370 - 360	14	0.57	0.07	0.71	0.00	0.21	4.51	0.00	0.00
BF.RE	02	None	NA	360 - 350	43	0.49	0.05	0.81	0.00	0.14	4.48	0.00	0.00
BF.RE	03	None	NA	350 - 340	14	1.86	0.00	0.79	0.00	0.21	4.50	0.00	0.00
BF.RE	04	None	NA	340 - 330	24	1.11	0.04	0.79	0.00	0.17	4.35	0.00	0.00
BF.RE	05	None	NA	330 - 320	25	3.44	0.16	0.64	0.00	0.20	4.51	0.00	0.00
BF.RE	06	None	NA	320 - 310	18	2.76	0.28	0.50	0.00	0.22	4.36	0.00	0.00
BF.RE	07	None	NA	310 - 300	25	2.29	0.08	0.56	0.00	0.36	4.22	0.00	0.00
BF.RE	08	None	NA	300 - 290	15	-0.40	0.00	0.87	0.00	0.13	4.57	0.00	0.00
BF.RE	09	None	NA	290 - 280	24	2.60	0.08	0.63	0.04	0.25	4.57	0.00	0.00
BF.RE	10	None	NA	280 - 270	30	0.92	0.27	0.60	0.00	0.13	4.44	0.00	0.00
BF.RE	11	None	NA	270 - 260	46	2.32	0.04	0.74	0.00	0.22	4.44	0.00	0.00
BF.RE	12	None	NA	260 - 250	108	1.40	0.15	0.65	0.00	0.20	4.62	0.00	0.00
BK5.RE	01	None	NA	200 - 190	13	2.33	0.00	0.85	0.00	0.15	6.32	0.00	0.00
BK5.RE	02	None	NA	190 - 180	5	0.07	0.40	0.60	0.00	0.00	6.09	0.00	0.00
BK5.RE	03	None	NA	180 - 170	11	2.14	0.27	0.45	0.00	0.27	6.37	0.00	0.00
BK5.RE	04	None	NA	170 - 160	7	1.16	0.14	0.71	0.00	0.14	5.96	0.00	0.00
BK5.RE	05	None	NA	160 - 150	8	-0.14	0.13	0.50	0.00	0.38	6.40	0.00	0.00

Table 25: Continued.

Column	Sample	Period	Age BP	CMBS	Freq.	Skewness	Morphotype Percentages				Source Area Ratio	Local Land-use	Regional Land-use
							Geo.	Irr.	Elo.	Ind.			
BK5.RE	06	None	NA	150 - 140	15	0.40	0.13	0.67	0.00	0.20	6.19	0.00	0.00
BK5.RE	07	None	NA	140 - 130	6	0.49	0.33	0.50	0.00	0.17	5.81	0.00	0.00
BK5.RE	08	None	NA	130 - 120	7	0.68	0.00	0.43	0.00	0.57	6.06	0.00	0.00
BK5.RE	09	None	NA	120 - 110	9	0.02	0.00	0.44	0.00	0.56	6.28	0.00	0.00
BK5.RE	10	None	NA	110 - 100	7	0.46	0.29	0.57	0.00	0.14	6.14	0.00	0.00
BK5.RE	11	None	NA	100 - 90	58	0.91	0.03	0.78	0.00	0.19	6.24	0.00	0.00
BK5.RE	12	None	NA	90 - 80	17	3.73	0.35	0.47	0.00	0.18	5.90	0.00	0.00
BK5.RE	13	None	NA	80 - 70	44	2.19	0.18	0.39	0.02	0.41	5.80	0.00	0.00
BK5.RE	14	None	NA	70 - 60	20	1.23	0.20	0.55	0.00	0.25	6.24	0.00	0.00
BK5.RE	15	None	NA	60 - 50	29	0.60	0.00	0.66	0.00	0.34	6.27	0.00	0.00
LP.RE	01	None	NA	400 - 390	15	2.91	0.20	0.73	0.00	0.07	47.91	0.00	0.00
LP.RE	02	None	NA	390 - 380	18	1.78	0.00	0.78	0.00	0.22	48.75	0.00	0.00
LP.RE	03	None	NA	380 - 370	27	1.43	0.04	0.70	0.00	0.26	53.63	0.00	0.00
LP.RE	04	None	NA	370 - 360	17	1.40	0.00	0.82	0.00	0.18	47.01	0.00	0.00
LP.RE	05	None	NA	360 - 350	28	1.49	0.11	0.57	0.00	0.32	49.67	0.00	0.00
LP.RE	06	None	NA	350 - 340	21	1.54	0.19	0.48	0.00	0.33	47.19	0.00	0.00
LP.RE	07	None	NA	340 - 330	14	1.23	0.07	0.50	0.00	0.43	49.74	0.00	0.00
LP.RE	08	None	NA	330 - 320	17	0.32	0.47	0.35	0.00	0.18	48.88	0.00	0.00
LP.RE	09	None	NA	320 - 310	72	1.11	0.14	0.69	0.00	0.17	48.49	0.00	0.00
LP.RE	10	None	NA	310 - 300	37	0.85	0.19	0.68	0.00	0.14	48.66	0.00	0.00
LP.RE	11	None	NA	300 - 290	107	1.46	0.23	0.49	0.01	0.27	49.78	0.00	0.00
LP.RE	12	None	NA	290 - 280	114	1.49	0.22	0.50	0.00	0.28	46.80	0.00	0.00
LP.RE	13	None	NA	280 - 270	41	2.38	0.12	0.46	0.00	0.41	48.98	0.00	0.00

APPENDIX VI

COLUMN SAMPLE PROFILE DRAWINGS AND AGE-DEPTH MODELS

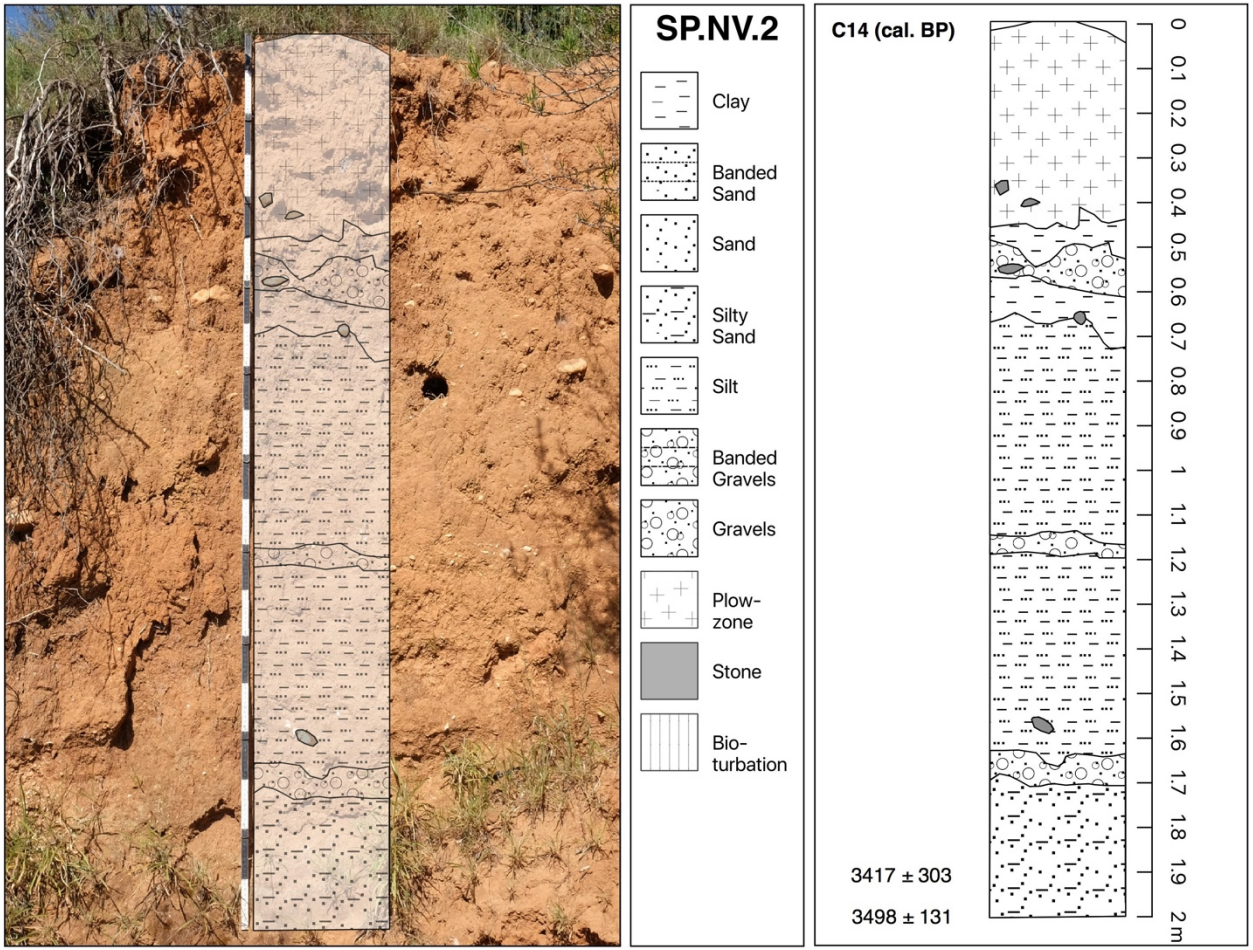

Fig. 53: SP.NV.2 Column Photograph and Profile Drawing.

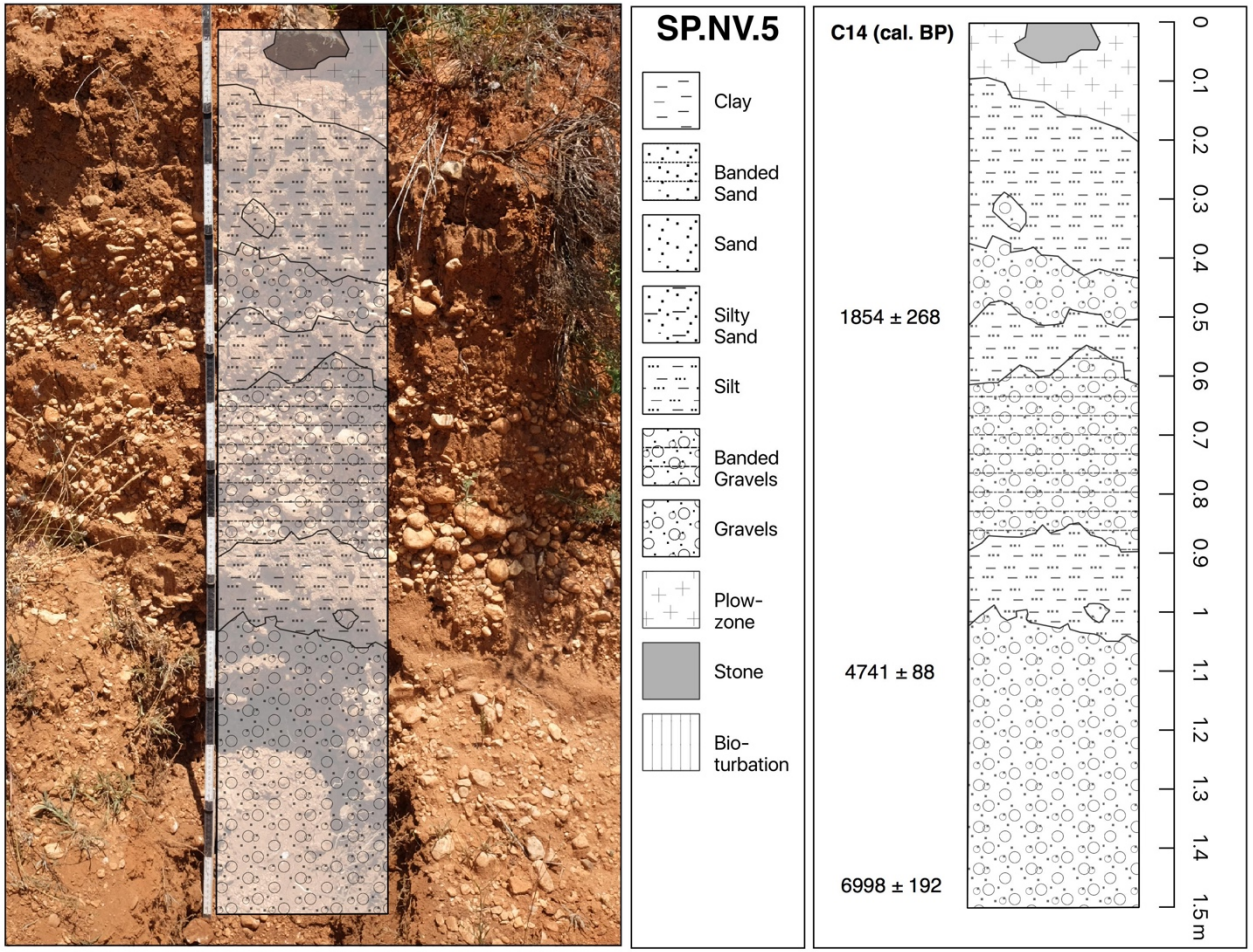

Fig. 54: SP.NV.5 Column Photograph and Profile Drawing.

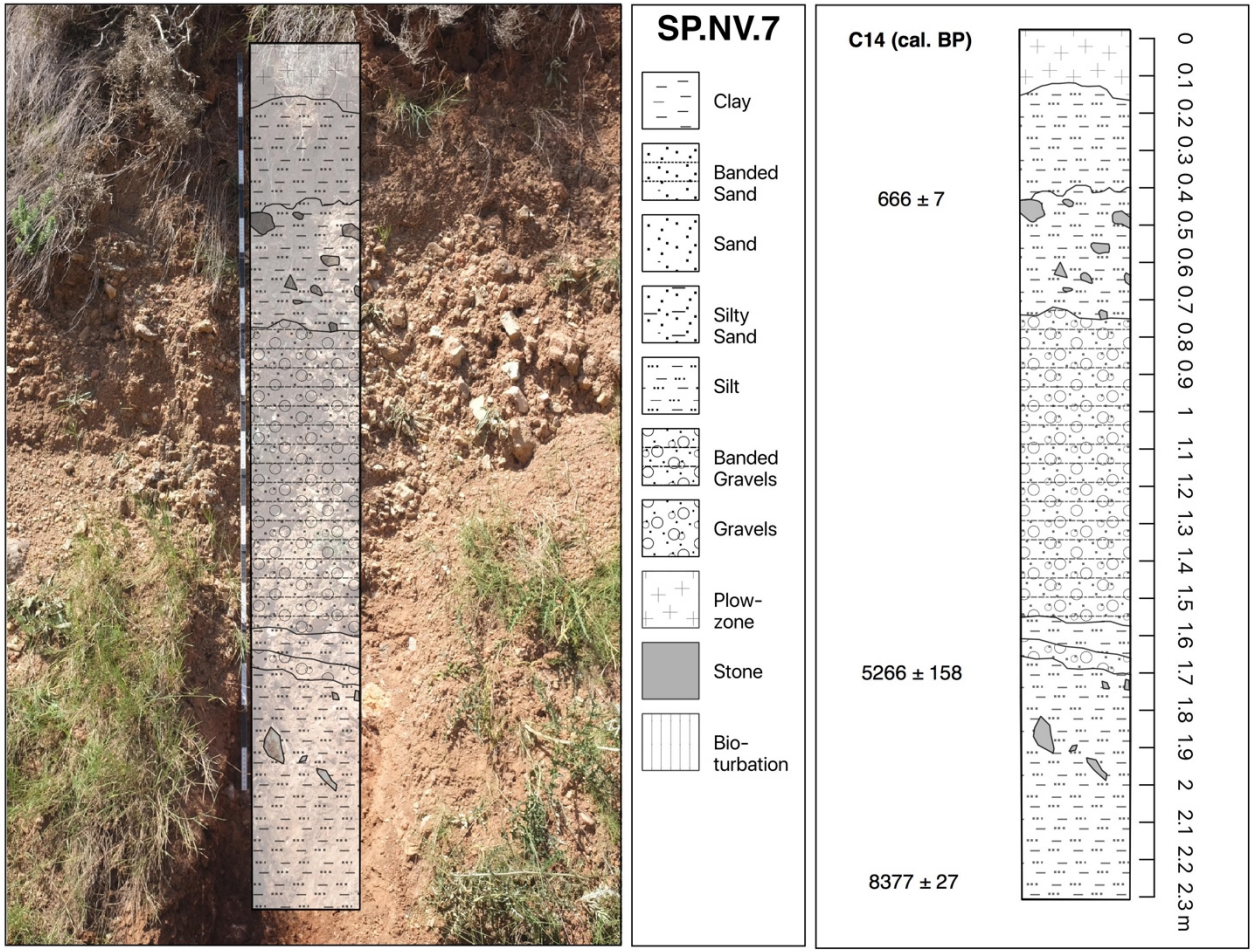

Fig. 55: SP.NV.7 Column Photograph and Profile Drawing.

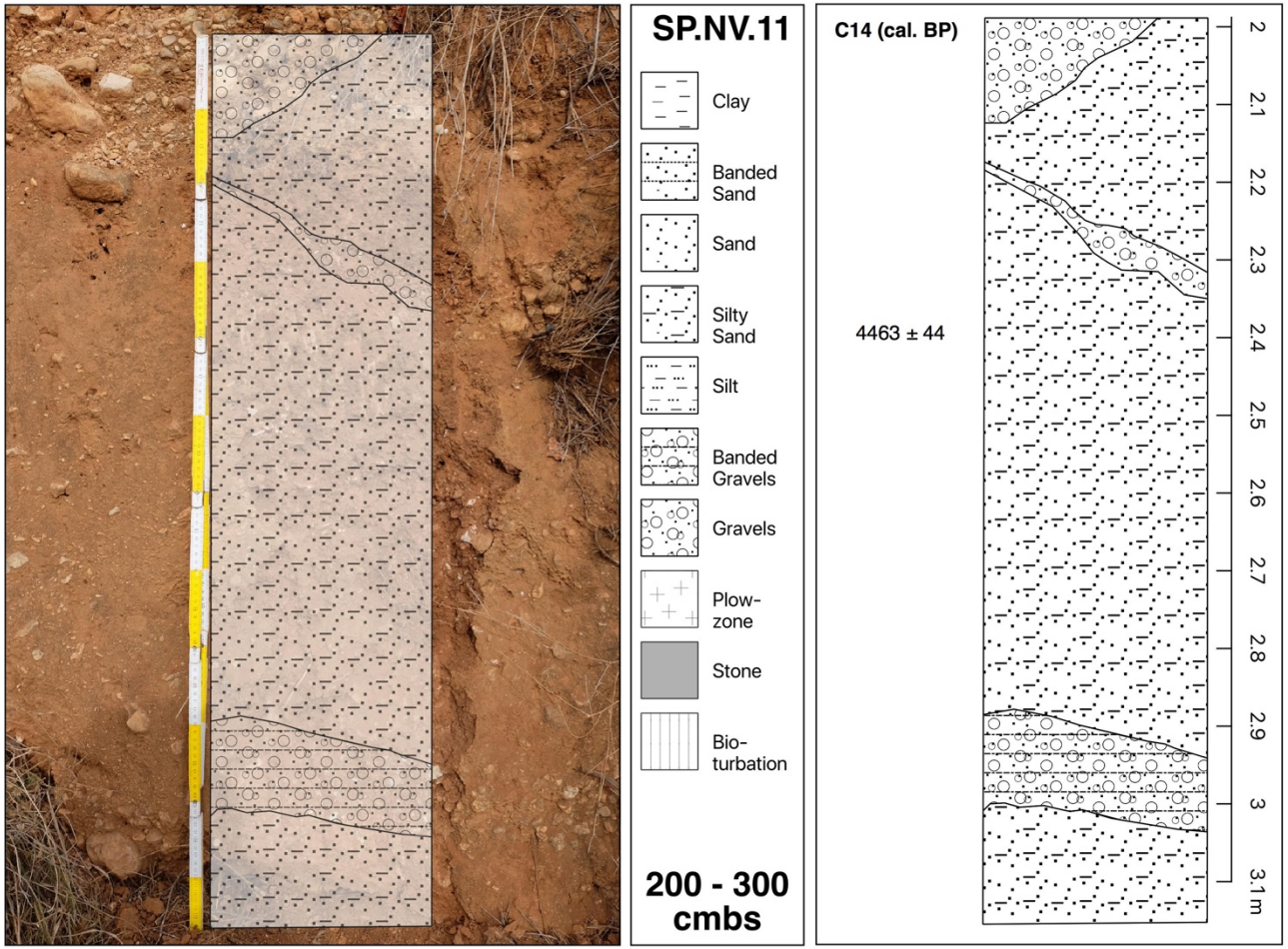

Fig. 56: SP.NV.11 (200-300 cmbs) Column Photograph and Profile Drawing.

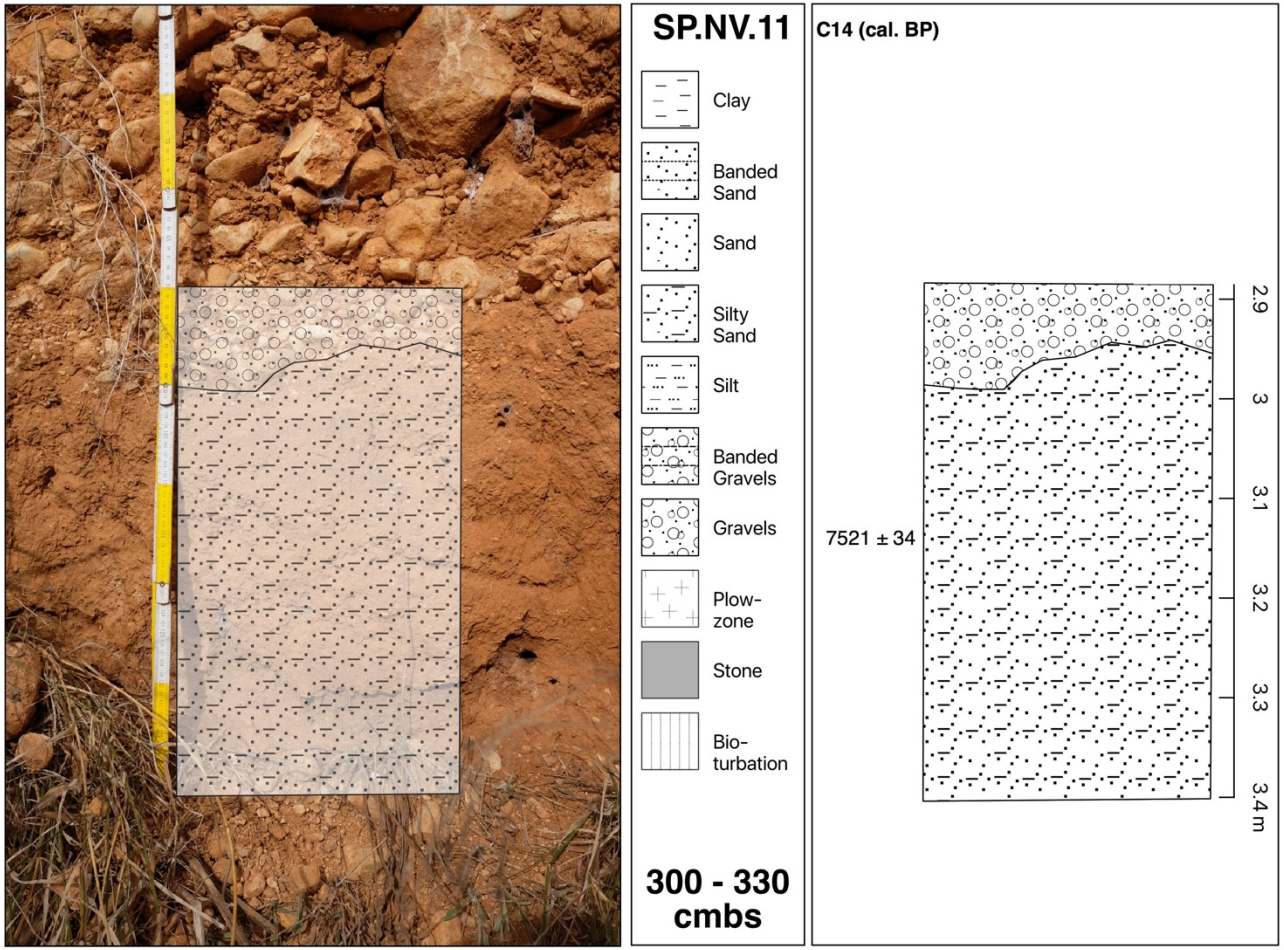

Fig. 57: SP.NV.11 (300-330 cmbs) Column Photograph and Profile Drawing.

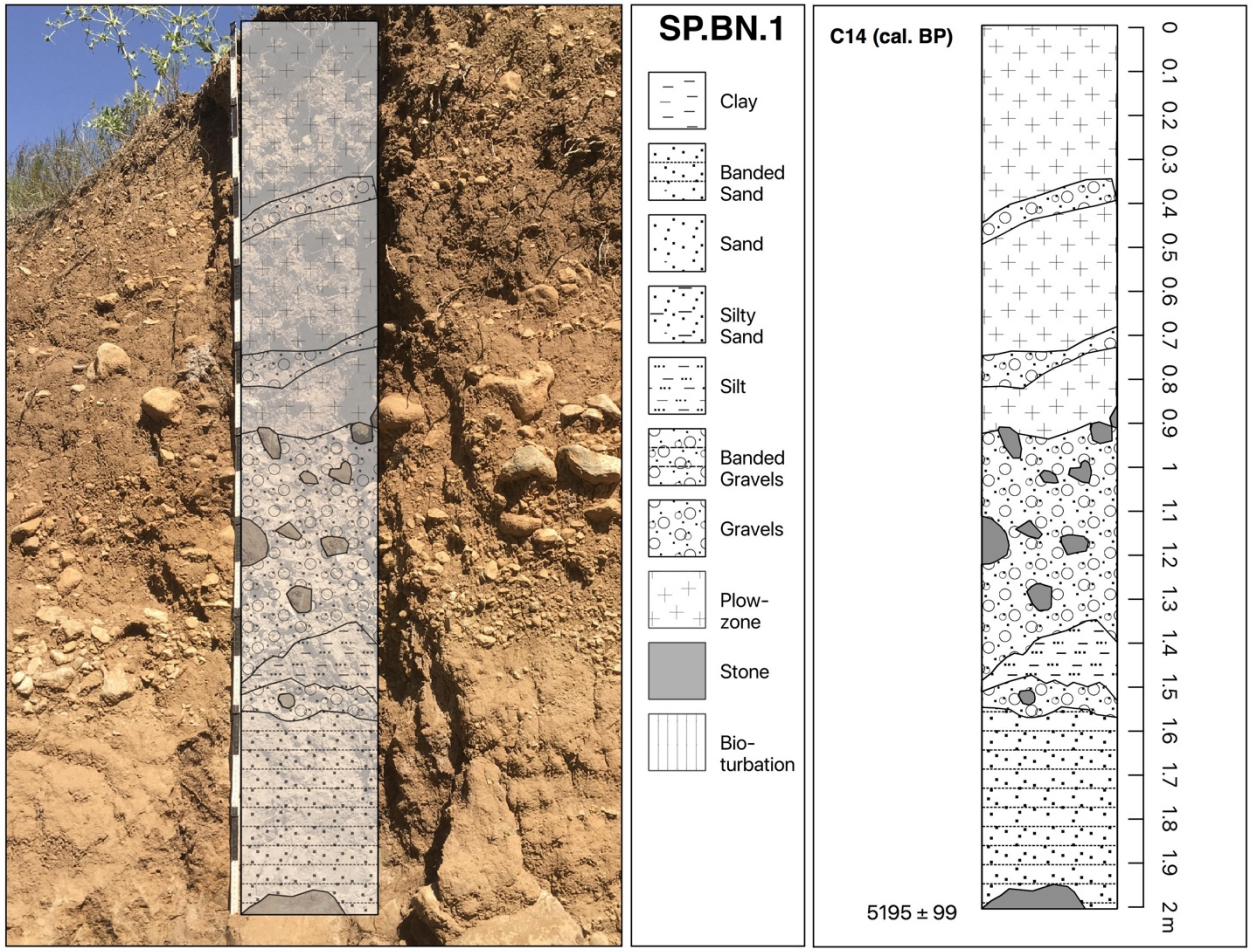

Fig. 58: SP.BN.1 Column Photograph and Profile Drawing.

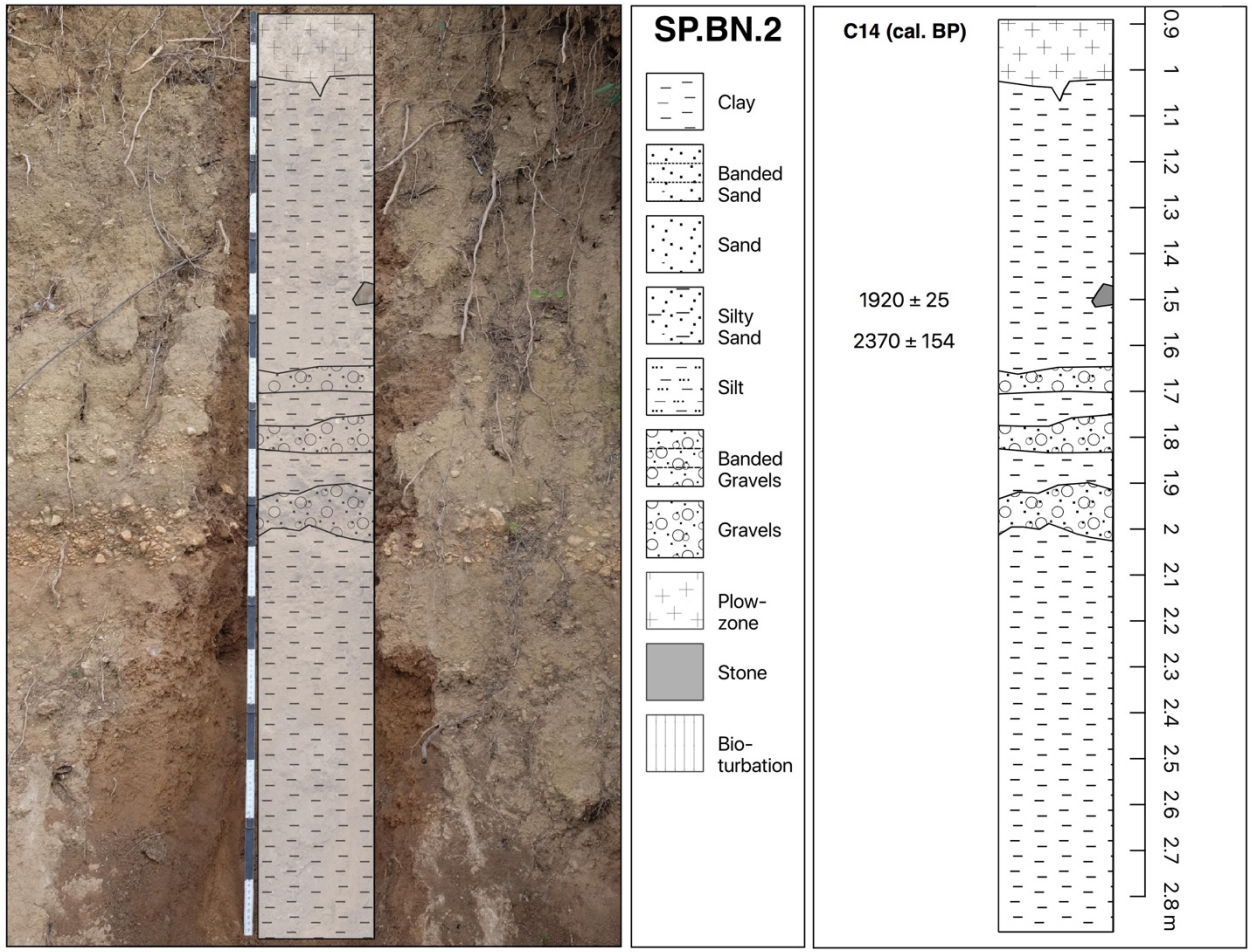

Fig. 59: SP.BN.2 Column Photograph and Profile Drawing.

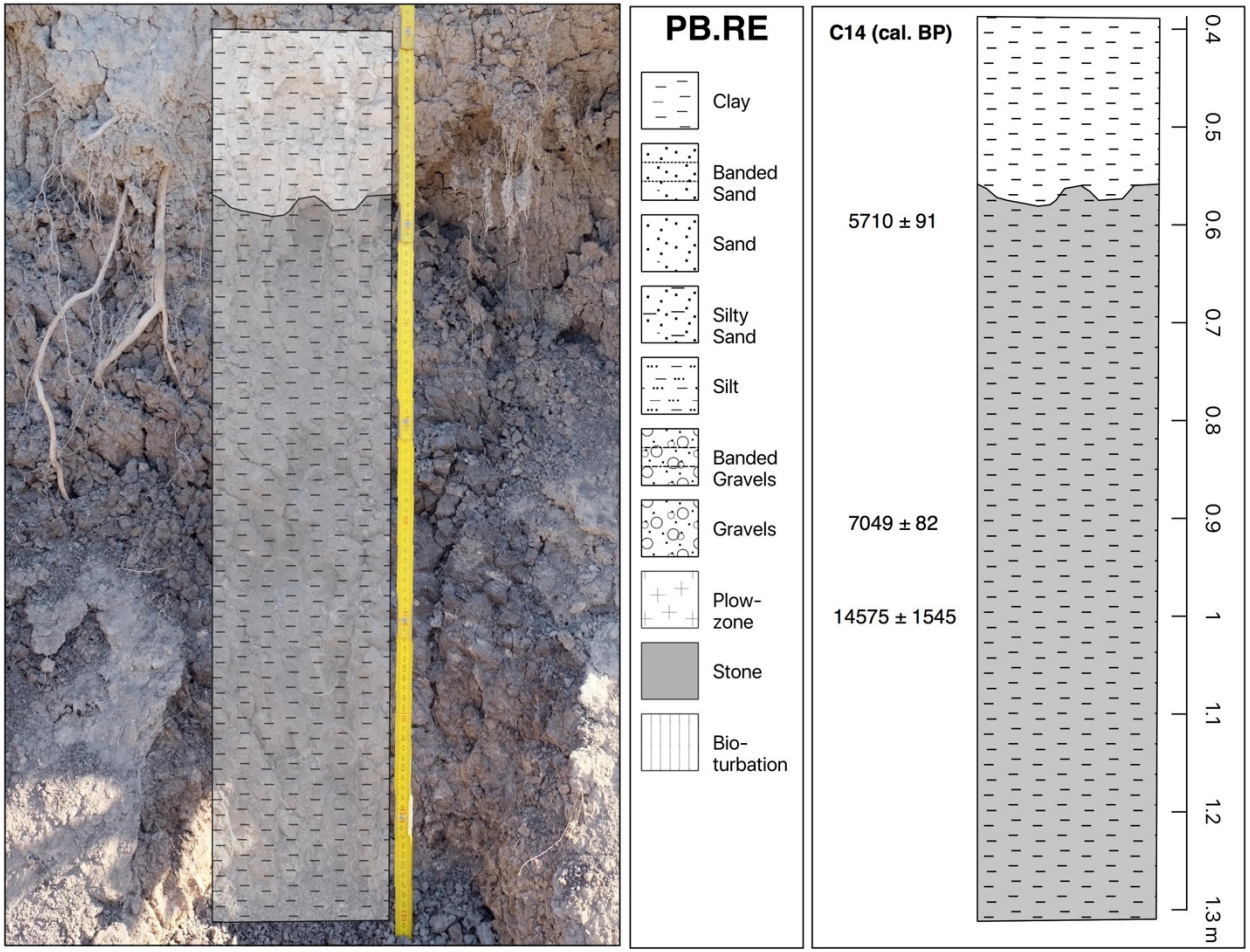

Fig. 60: PB.RE Column Photograph and Profile Drawing.

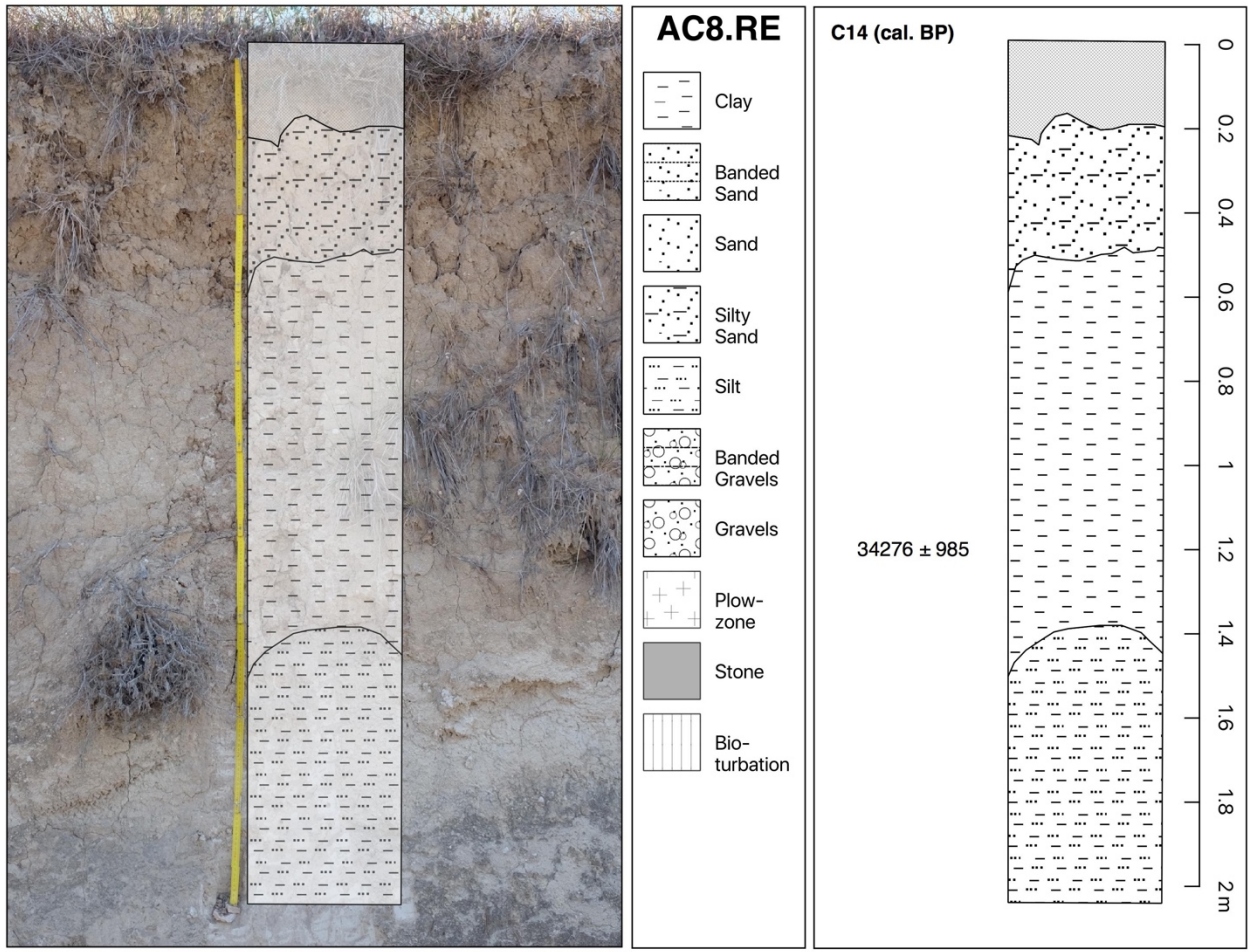

Fig. 61: AC8.RE Column Photograph and Profile Drawing.

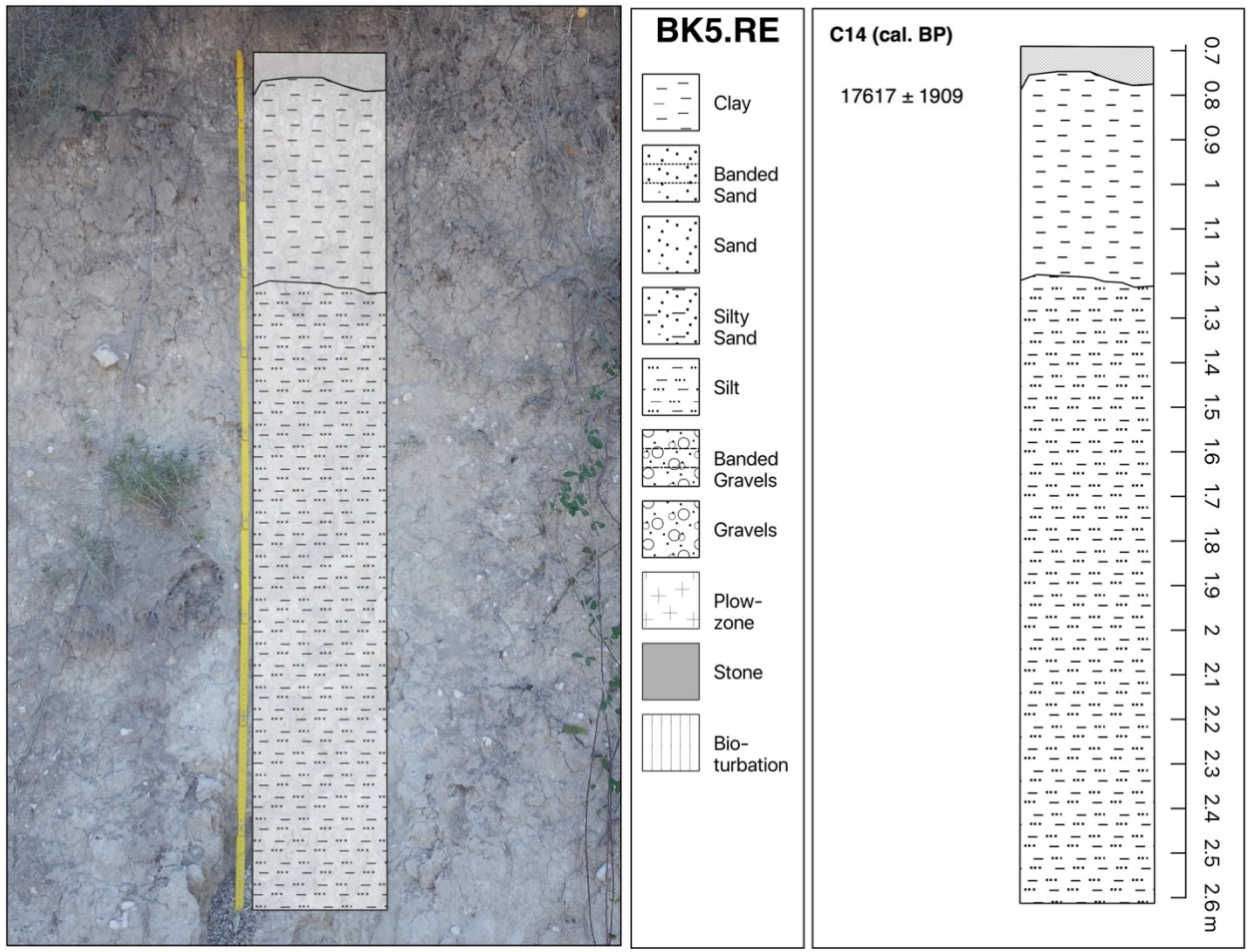

Fig. 62: BK5.RE Column Photograph and Profile Drawing.

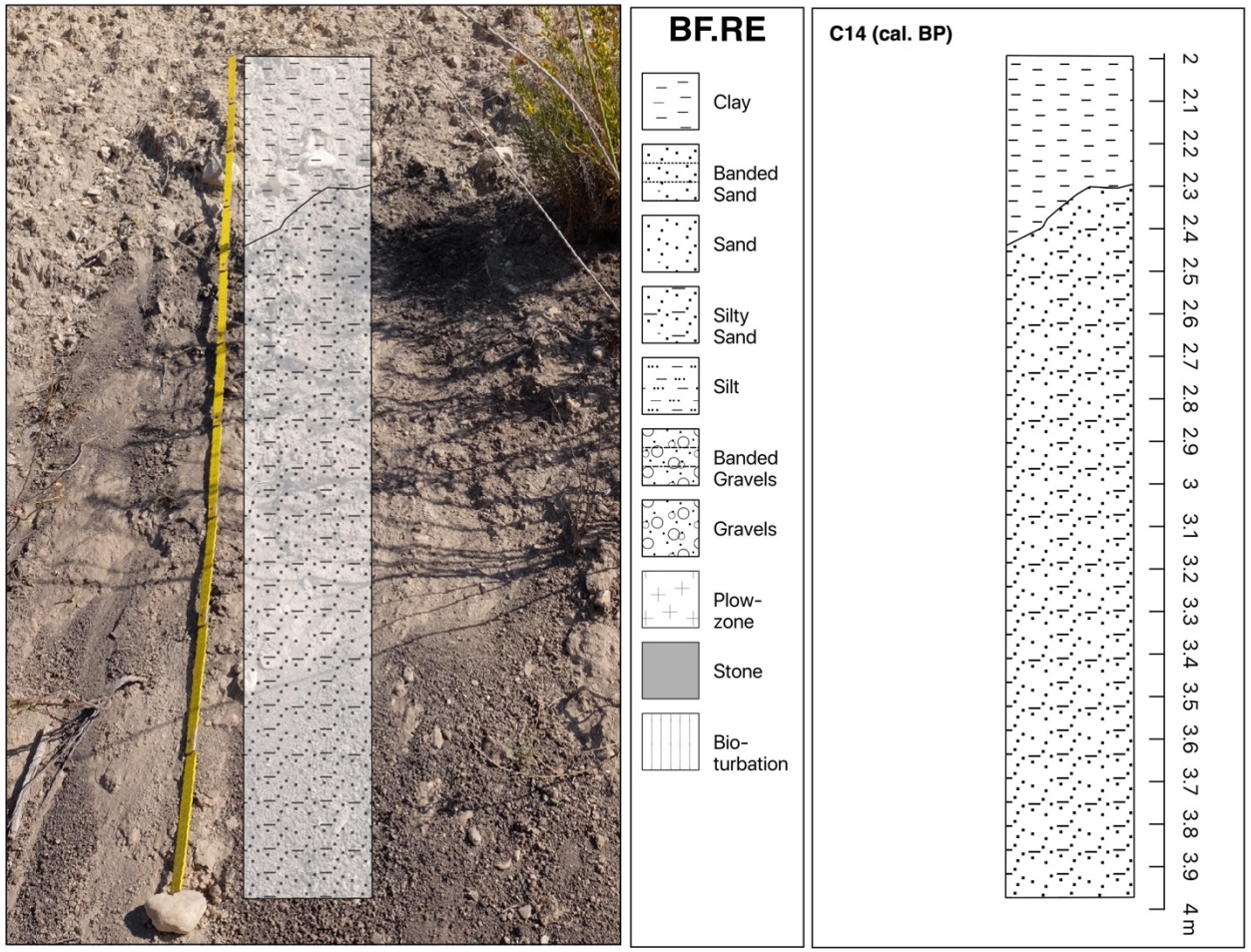

Fig. 63: BF.RE Column Photograph and Profile Drawing.

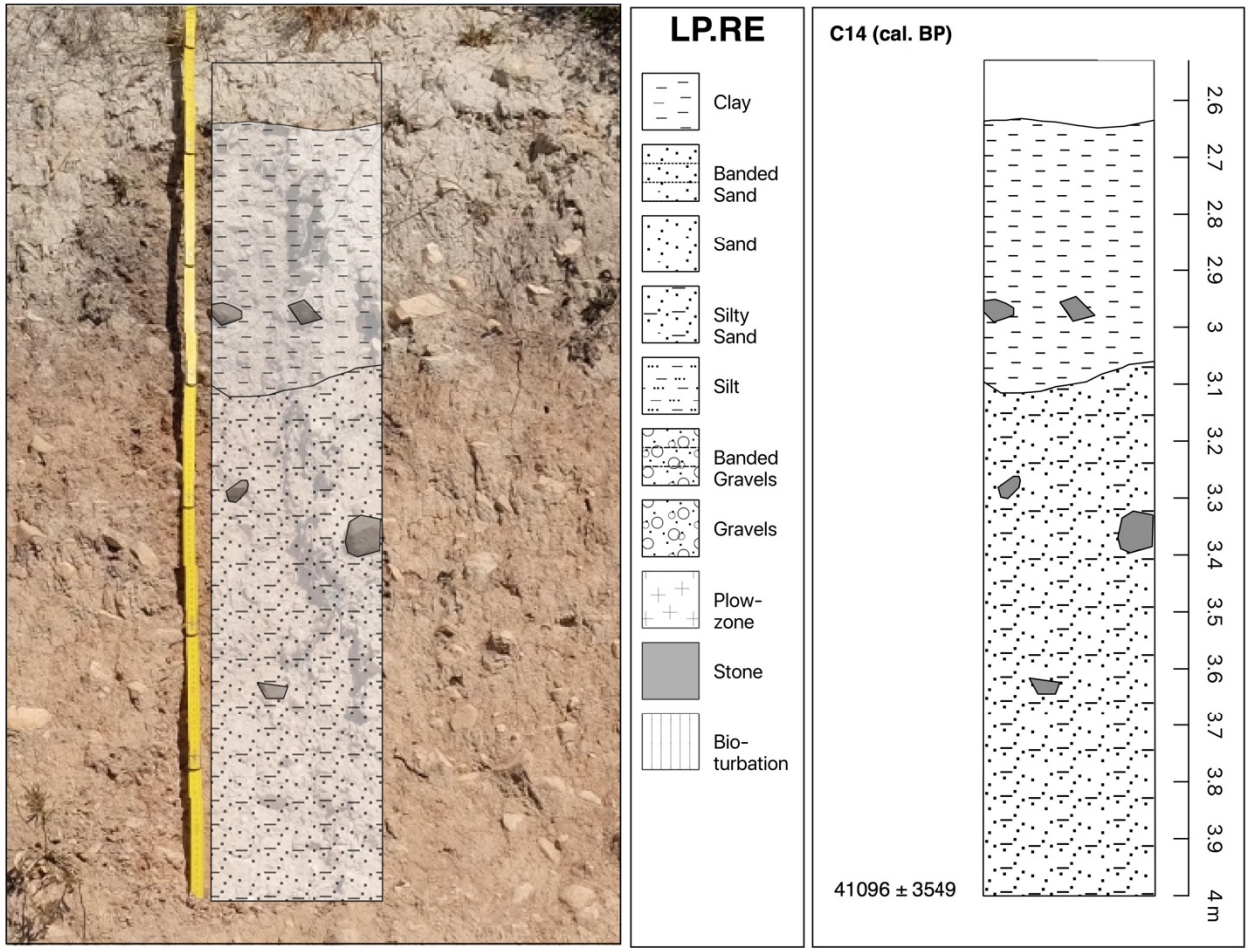

Fig. 64: LP.RE Column Photograph and Profile Drawing.

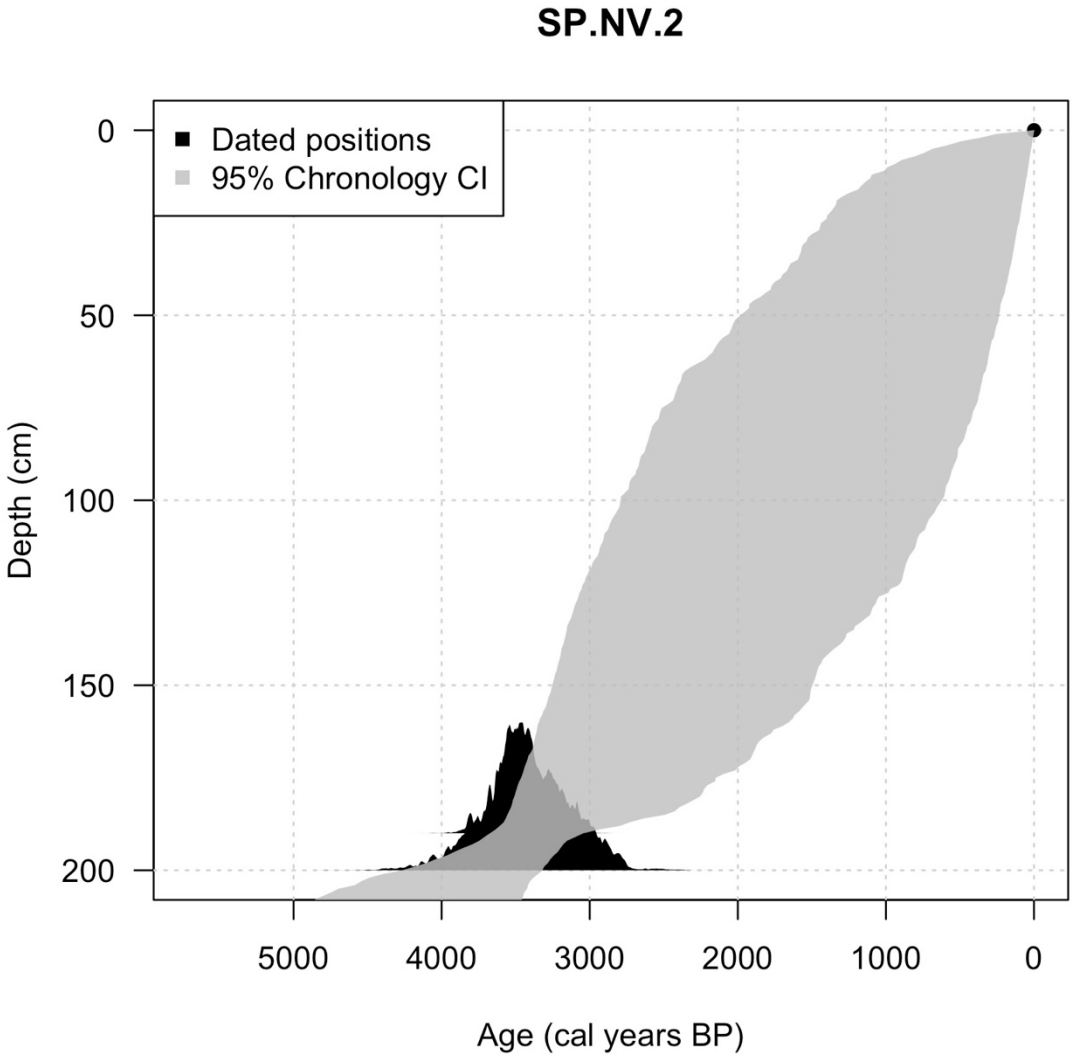

Fig. 65: Age-depth Model Generated by Bchron for Dates and Depths from SP.NV.2.

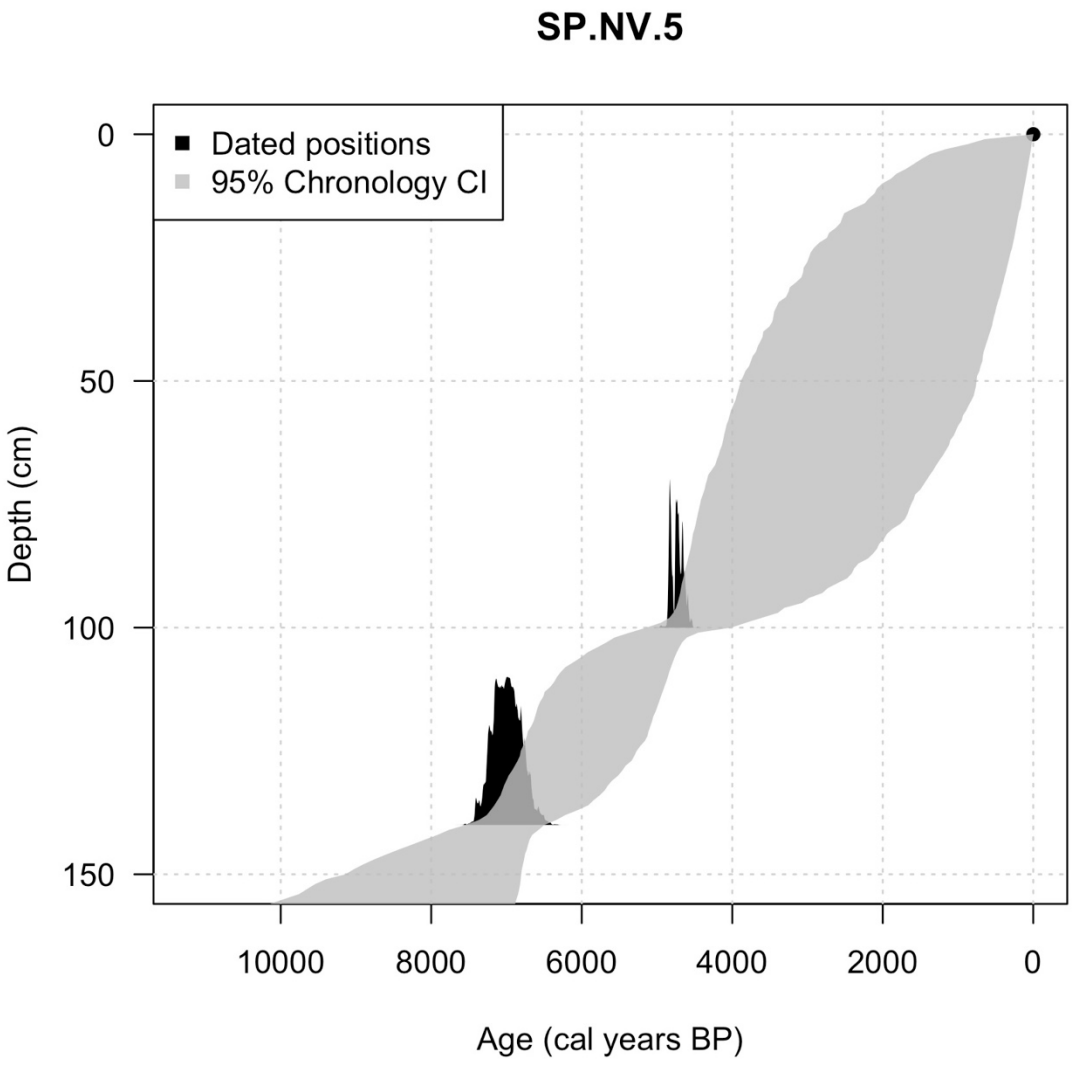

Fig. 66: Age-depth Model Generated by Bchron for Dates and Depths from SP.NV.5.

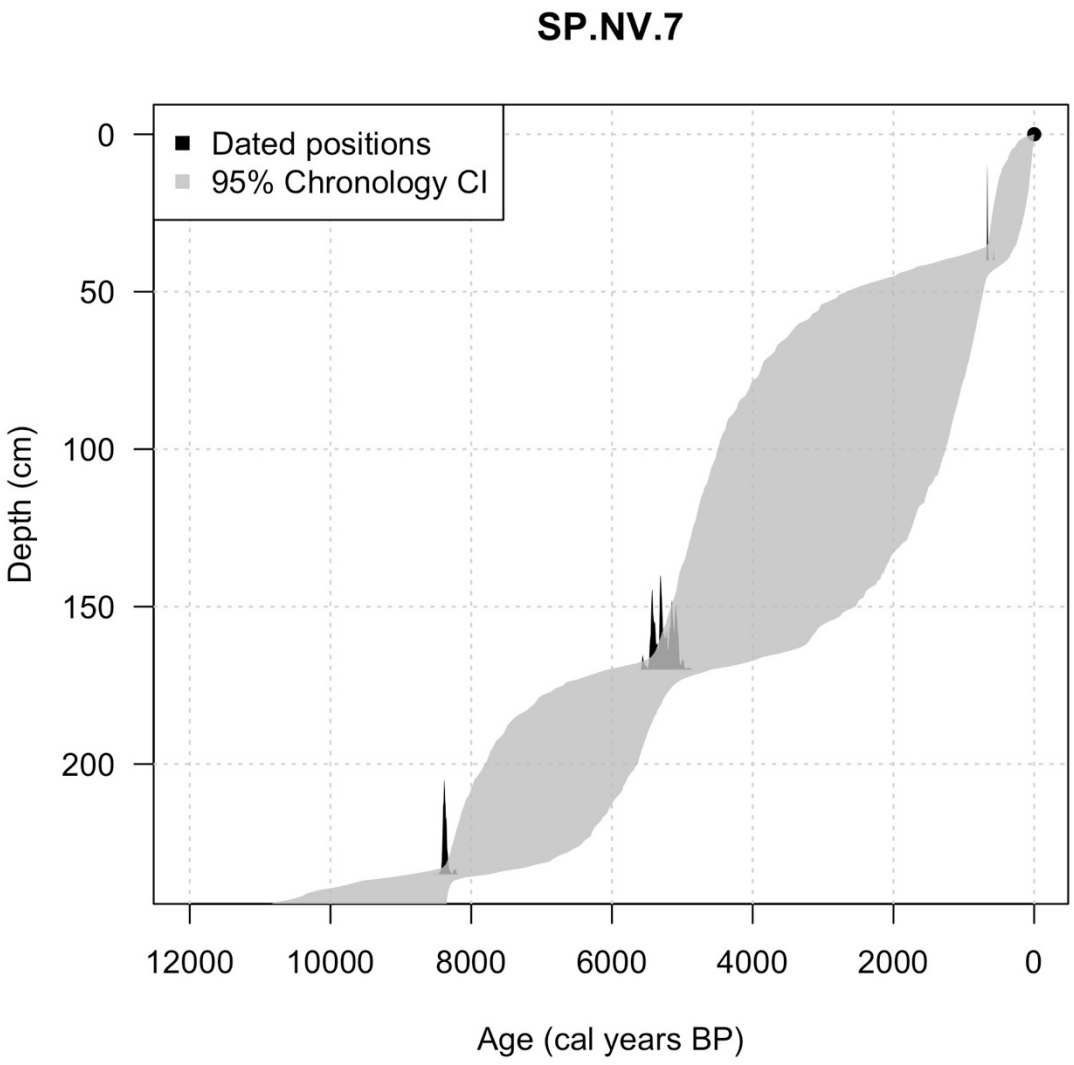

Fig. 67: Age-depth Model Generated by Bchron for Dates and Depths from SP.NV.7.

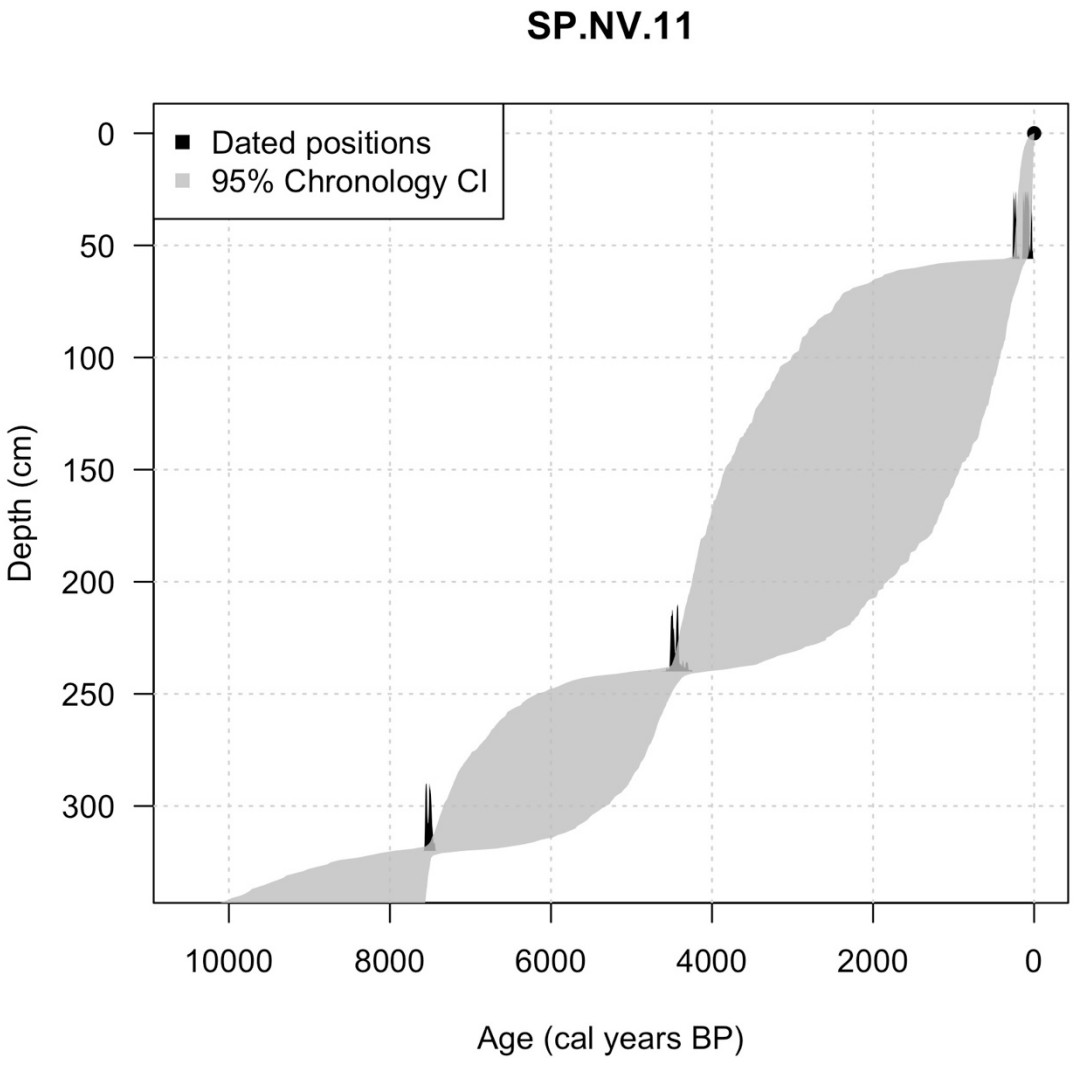

Fig. 68: Age-depth Model Generated by Bchron for Dates and Depths from SP.NV.11.

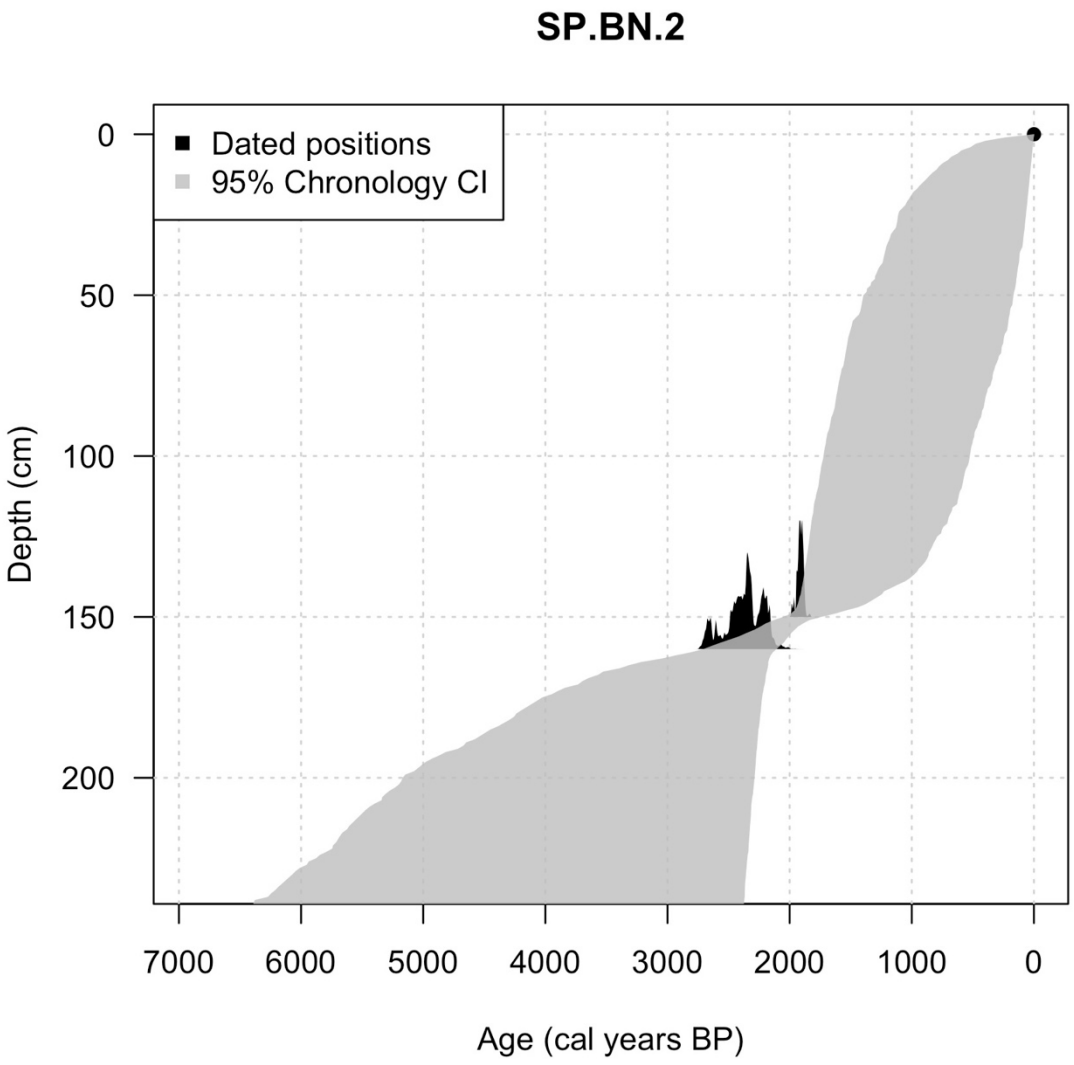

Fig. 69: Age-depth Model Generated by Bchron for Dates and Depths from SP.BN.2.

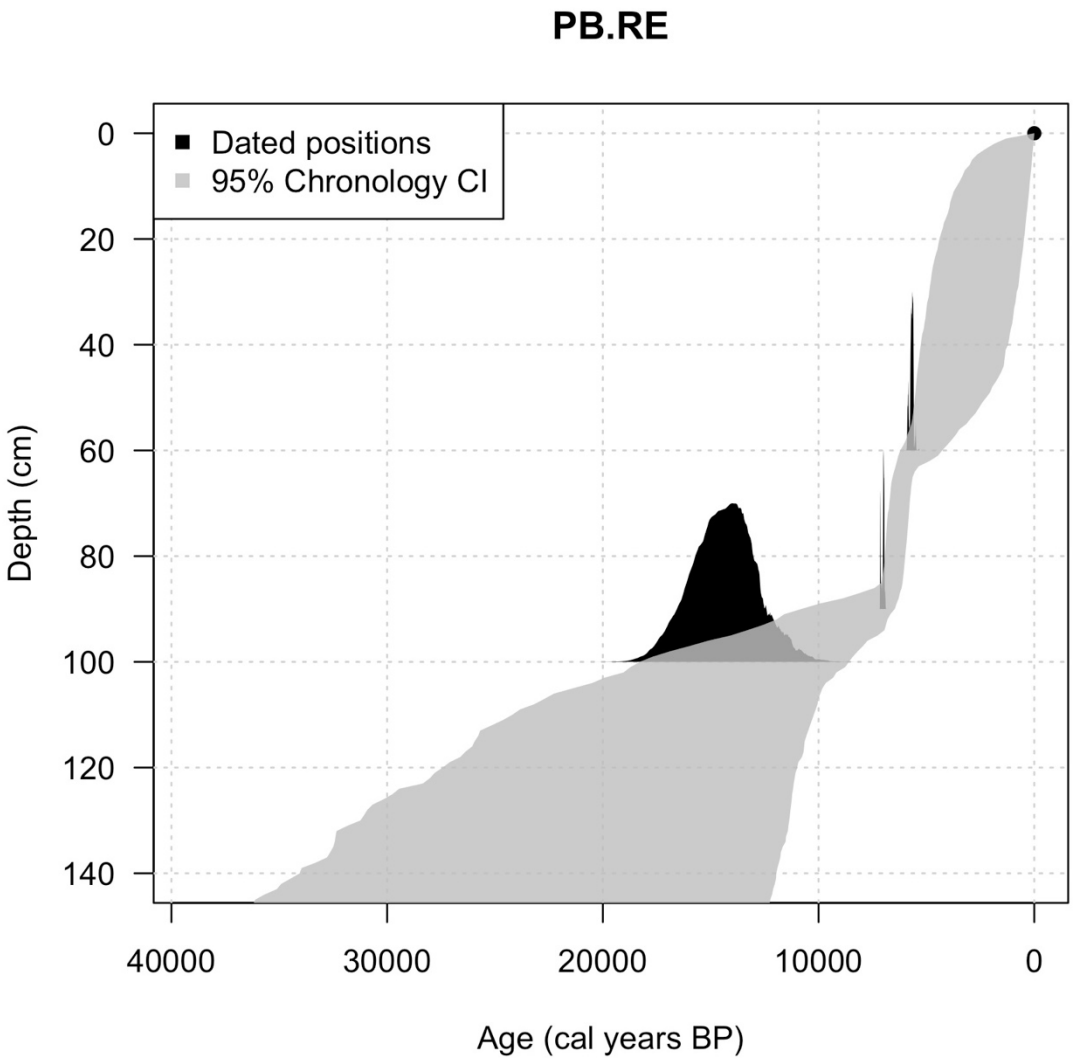

Fig. 70: Age-depth Model Generated by Bchron for Dates and Depths from PB.RE.

APPENDIX VII

STATEMENT OF PERMISISON FROM CO-AUTHORS AND DETAILS CONCERNING PREVIOUSLY PUBLISHED PORTIONS OF THIS DISSERTATION

Chapters II and III are published in peer-reviewed archaeology journals, while chapter IV remains unpublished. Chapter II is a single author publication and all of the authors listed as co-authors for chapter III have given their permission for the content of that article to be included in this dissertation. Below are the citations for chapters II and III:

Chapter II:

Snitker, G., Castillo, A.D., Barton, C.M., Aubán, J.B., Puchol, O.G., Pardo-Gordó, S., 2018. Patch-based survey methods for studying prehistoric human land-use in agriculturally modified landscapes: A case study from the Canal de Navarrés, eastern Spain. Quat. Int. 483, 5–22. https://doi.org/10.1016/j.quaint.2018.01.034

Chapter III:

Snitker, G., 2018. Identifying natural and anthropogenic drivers of prehistoric fire regimes through simulated charcoal records Identifying natural and anthropogenic drivers of prehistoric fi re regimes through simulated charcoal records. J. Archaeol. Sci. 95, 1–15. https://doi.org/10.1016/j.jas.2018.04.009